

2023-07

The Virus Resistance Mechanism of Abortive Infection K in *Lactococcus lactis*

Du, Amy

Du, A. (2023). The virus resistance mechanism of abortive infection K in *Lactococcus lactis* (Doctoral thesis, University of Calgary, Calgary, Canada). Retrieved from <https://prism.ucalgary.ca>.
<https://hdl.handle.net/1880/116749>

Downloaded from PRISM Repository, University of Calgary

UNIVERSITY OF CALGARY

The Virus Resistance Mechanism of Abortive Infection K in *Lactococcus lactis*

by

Amy Du

A THESIS

SUBMITTED TO THE FACULTY OF GRADUATE STUDIES
IN PARTIAL FULFILMENT OF THE REQUIREMENTS FOR THE
DEGREE OF DOCTOR OF PHILOSOPHY

GRADUATE PROGRAM IN BIOLOGICAL SCIENCES

CALGARY, ALBERTA

JULY, 2023

© Amy Du 2023

Abstract

In nature, there is a constant battle between viruses and their hosts known as the evolutionary arms race, where they both continuously evolve to attempt to gain an advantage over the other. This evolutionary arms race has resulted in many mechanistic inventions, such as abortive infection (Abi) mechanisms in bacteria. In Abi mechanisms, viruses inject their genetic material into cells, but bacteria block phage replication by preventing one of the steps of phage maturation, typically resulting in cell death. This study looks at the Abi mechanism called AbiK, which is controlled by a protein of the same name that was discovered on a plasmid in *Lactococcus lactis*.

A large portion of the study focuses on what happens *in vivo* during the AbiK mechanism. The normal wild-type infection, the abortive infection mediated by the AbiK protein, and the escape of the AbiK mechanism by a mutant phage are all studied for comparative analyses. Observations have shown that phage DNA replication is inhibited, and that transcription of the phage genes is delayed during the AbiK mechanism. The mutant phage can bypass these inhibitions, and successfully replicate its DNA and complete the phage lytic cycle. RNA-Sequencing experiments were conducted to narrow down the mechanism behind AbiK, and preliminary results indicate that AbiK depletes the nucleotide resources available in the cell, eventually resulting in cell death and inhibition of the phage replication cycle.

A second part of this study focuses on the biochemistry of the AbiK protein. The AbiK protein has a polymerase activity that polymerizes an untemplated long single-stranded DNA that is covalently attached to the AbiK protein. This study identified which amino acid is used as a primer, which is tyrosine 44 on the AbiK protein. The release of protein structure prediction databases allowed for the analysis of a generated model of the AbiK protein, allowing for the

elucidation of other biochemical functions the AbiK protein has. In addition to the polymerization activity, AbiK is hypothesized to bind to nucleotides or other proteins. The culmination of these studies allowed for insight on the AbiK mechanism, generating a hypothesis for future studies.

Preface

This thesis is original, unpublished, independent work by the author, Amy Du. RNA-Sequencing experiments were conducted with the help of Dr. Sean Workman, from Dr. Christopher Yost's group at the University of Regina.

Figure 1-8 is modified from Figure 3 and Figure 4 in Wang et al. (1). Figure 4-1 is copied from Figure 3.2.3 in B. Soufi's thesis, with permission (2). Figure 4-18 is modified from Figure 3 in Scaltriti et al., with permission from Blackwell Publishing Ltd. (3).

Acknowledgements

I would like to thank my supervisor Dr. Michael Hynes for adopting me into his lab. I am eternally thankful for his supervision and guidance during the last few years of my program. I am also extremely grateful for his compassion, consideration, and care towards his students. I would not have been able to complete my program without his kindness and understanding. He is truly an outstanding supervisor, and I will deeply miss my time in his lab. I would also like to thank Dr. Steven Zimmerly, whose lab I started my program in. I am very thankful for the potential he saw in me and for giving me the opportunity to explore my research questions. Through my experience in his lab, I was able to gain a lot of confidence and independence in my work, which helped shape me into the scientist I am now.

I am also thankful for my committee members Dr. Marie Fraser and Dr. Joe Harrison for their support, kindness, and generosity throughout my program. I am very grateful for their belief in my abilities, and their pressure which drove me towards the completion of my program. I am also thankful for Dr. Ken Ng, who initially served on my committee.

I am very thankful to current and former lab mates in both the Hynes and Zimmerly labs for their camaraderie, guidance, and friendship. I am very grateful to Dr. Ashley Jarding, Dr. Li Wu and Bahar Soufi, my mentors and friends, who taught me a lot of the basics in the lab and helped me learn to problem solve. I also appreciate the friendships I have formed in the Hynes lab, from Dr. Kasuni Hemananda, Dr. Augusta Schmidt, Lucia Nguyen, Termeh Tohidi, and Nicole Jervis, who made working in the lab very fun and whom I have had many meaningful conversations with. Notably when we made the lab a mess of pumpkin debris. Thank you to the many undergraduates I have trained, who provided me camaraderie in the lab.

I would like to acknowledge the many friends I have made throughout my program. It is impossible to list all of them here, but I truly value the conversations we have had, the coffee breaks and meals we shared, along with the support. I am especially thankful to Kayla Dias, Alex Paquette, Jordan Mattice, and Laura Sosa for the endless support and compassion during the roughest times of my program and helping me get back on my feet. I have made lifelong friendships in my program, and for that I am eternally grateful.

I am absolutely thankful to my family and friends. Despite asking me what I do, and me trying my best to explain, you all still believe I am studying cheese. Many thanks to my parents, Kien Du and Linh Tran, who have always been super supportive of my education and letting me stay a child as long as possible. I am extremely thankful to my closest friends: Crysty Ngo, Sherry Pham, and Diana Gallegos, who have listened to my concerns and complaints for many years and shown me plenty of compassion. I am also thankful to Kiki, Asi, and Matsu for being great distractions and being very helpful when I struggled with coding.

Finally, I would like to thank my partner, and the love of my life, Vinh Nguyen. He has been with me through some of the hardest points of my life and has been endlessly supportive of me. I am thankful for his patience and listening to me when I just wanted to ramble about my experiments and believing that I would be able to finish my program. I am thankful for his support, which applies to all aspects of our lives together. Thank you for keeping me grounded, taking care of me when I am not at my best, and for all our fun times together. I look forward to spending the rest of our lives together.

Table of Contents

Abstract.....	ii
Preface.....	iv
Acknowledgements	v
Table of Contents	vii
List of Tables	xi
List of Figures.....	xii
List of Symbols, Abbreviations and Nomenclature	xiv
Chapter 1 : Introduction	1
1.1 Viruses and Bacteriophages.....	1
1.1.1 Introduction	1
1.1.2 Bacteriophage Morphology and Taxonomy.....	2
1.1.3 Bacteriophage Replication Cycles.....	4
1.1.4 Applications of Bacteriophages	6
1.2 Lactococcal phages	7
1.3 Defense Mechanisms Against Bacteriophages	10
1.3.1 Defense Mechanisms	10
1.3.2 Abortive Infection Systems.....	13
1.4 Abortive Infection K.....	16
1.4.1 Discovery and Characterization.....	16
1.4.2 Enzymatic Activity of AbiK.....	18
1.4.3 Escape of AbiK: Sensitivity against AbiK.....	22
1.4.4 Proposed Mechanisms.....	23
1.5 Objectives of This Study.....	26
Chapter 2 : Phage Infection Dynamics and Kinetics of DNA Production.....	27
2.1 Introduction.....	27
2.2 Aims.....	28
2.3 Results and Discussion.....	29
2.3.1 Optimal Infection Conditions.....	29
2.3.1.1 <i>Lactococcus lactis</i> strains, plasmids, and bacteriophage selection.....	29
2.3.1.2 <i>Effect of AbiK expression on cell growth</i>	31
2.3.1.3 <i>Multiplicity of infection determination</i>	34
2.3.1.4 <i>Infection dynamics</i>	36
2.3.1.5 <i>Adsorption assays</i>	39
2.3.1.6 <i>One-step growth curves</i>	41
2.3.2 Viability Assay	44
2.3.3 DNA Kinetics of Phage Infection: Southern Blots.....	47
2.3.4 DNA Kinetics of Phage Infection: qPCR.....	53
2.3.5 Comparison to Literature	56
2.4 Conclusions.....	57
2.5 Methods and Materials.....	58
2.5.1 General Protocols	58
2.5.1.1 <i>Bacterial strains, plasmids, and growth conditions</i>	58
2.5.1.2 <i>Bacteriophage propagation</i>	58

2.5.1.3 DNA isolation and manipulation	61
2.5.1.4 Phage DNA isolation	61
2.5.1.5 Phenol extraction and ethanol precipitation	62
2.5.1.6 Restriction enzyme and PCR cloning.....	62
2.5.1.7 Tip-to-tail PCR cloning.....	63
2.5.2 Bacterial Growth Curves	64
2.5.3 Multiplicity of Infection Titrations	64
2.5.4 Bacteriophage Infection Curves	64
2.5.5 Adsorption Assays	65
2.5.6 One-step Growth Curves	65
2.5.7 Viability Assay – Cell Survivability Assay	66
2.5.8 Southern Hybridization	67
2.5.8.1 Sample collection and preparation.....	67
2.5.8.2 Preparation of radioactive RNA probe.....	68
2.5.8.3 Hybridization.....	69
2.5.8.4 Blot stripping.....	69
2.5.9 qPCR.....	69
2.5.9.1 Sample collection and preparation.....	69
2.5.9.2 Preparation of standards for qPCR.....	70
2.5.9.3 Primer design	70
2.5.9.4 qPCR.....	71
2.5.10 Plasmid Construction.....	71
2.5.10.1 Construction of pSRQ823-AbiKCut (p Δ AbiK)	71
2.5.10.2 Construction of phage genome plasmids	72
2.5.10.3 Construction of pTRKH2-Sak3.....	72
Chapter 3 : Kinetics of RNA Production.....	76
3.1 Introduction.....	76
3.2 Aims.....	77
3.3 Results and Discussion.....	78
3.3.1 RNA Kinetics During Phage Infection: RT-qPCR.....	78
3.3.2 RNA Kinetics During Phage Infection: RNA-Sequencing.....	85
3.3.2.1 RNA-Sequencing condition selection.....	85
3.3.2.2 No-phage controls	87
3.3.2.3 Gene expression post-infection.....	91
3.3.2.4 Differential gene expression analysis	102
3.3.2.5 Future transcriptomics studies	114
3.3.2.6 Author contributions.....	114
3.3.3 Comparison to Literature.....	114
3.4 Conclusions.....	116
3.5 Methods and Materials.....	118
3.5.1 General Protocols	118
3.5.2 RT-qPCR.....	118
3.5.2.1 Sample collection and preparation.....	118
3.5.2.2 Preparation of standards for RT-qPCR	119
3.5.2.3 Primer design	119
3.5.2.4 RT-qPCR	120

3.5.3 RNA-Sequencing.....	120
3.5.3.1 Sample collection and preparation.....	120
3.5.3.2 Preparation of samples for RNA-Sequencing	120
3.5.3.3 Analysis of RNA-Sequencing data	121
Chapter 4 : Biochemistry of AbiK.....	122
4.1 Introduction.....	122
4.2 Aims.....	124
4.3 Results and Discussion.....	125
4.3.1 Sequence Alignment of AbiK and Close Relatives	125
4.3.2 Making Y to F mutants of AbiK	126
4.3.2.1 <i>Escherichia coli</i> constructs.....	126
4.3.2.2 <i>Lactococcus lactis</i> constructs	126
4.3.3 Protein Purification of AbiK	129
4.3.4 Label-Chase Assay.....	132
4.3.5 <i>In vivo</i> effects of Y to F AbiK mutants	134
4.3.6 Structural Analysis of AbiK model.....	137
4.3.6.1 Analysis of AbiK domains.....	137
4.3.6.2 Analysis of AbiK's RT domain	137
4.3.6.3 Analysis of AbiK's carboxy terminal domain	141
4.3.6.4 Analysis of AbiK's active site and DNA attachment site	145
4.3.6.5 Comparison of AbiK model to published structures	147
4.3.7 Analysis of Sak3 model	150
4.4 Conclusions.....	153
4.5 Methods and Materials.....	155
4.5.1 General Protocols	155
4.5.1.1 Bacterial strains, plasmids, and growth conditions	155
4.5.1.2 DNA isolation and manipulation	155
4.5.1.3 Recombinant PCR.....	155
4.5.1.4 Quikchange lightning cloning.....	155
4.5.2 Sequence Alignment	158
4.5.3 Plasmid Construction	158
4.5.3.1 Construction of mutants in <i>E. coli</i>	158
4.5.3.2 Construction of mutants in <i>L. lactis</i>	158
4.5.4 Protein Purification	160
4.5.4.1 Protein purification protocol.....	160
4.5.4.2 <i>E. coli</i> denatured cell lysate preparation.....	161
4.5.4.3 SDS-PAGE gel electrophoresis and visualization	161
4.5.4.4 Western blot.....	162
4.5.5 Label-chase Assay.....	162
4.5.6 <i>In vivo</i> Effects of AbiK Mutants.....	163
4.5.7 Protein Model Generation and Analysis	163
Chapter 5 : Conclusions and Future Directions.....	164
5.1 Principal Conclusions of the Research.....	164
5.1.1 <i>In vivo</i> Effects of the AbiK Mechanism	165
5.1.2 <i>In vitro</i> Revelations about the AbiK Protein.....	166

5.2 Proposed Mechanism for AbiK	168
5.3 Future Directions	171
References	173
Appendices	179
Appendix A: Common Media and Buffers.....	179
Appendix B: Supplementary Data	181
Appendix C: Reuse Permissions.....	199

List of Tables

Table 1-1: Morphologies and genome sizes of lactococcal phage groups.....	8
Table 1-2: Intracellular effects of the AbiK system.....	17
Table 2-1: Strains and phages used in this study.	60
Table 2-2: Plasmids used in this study.....	60
Table 2-3: Primer sequences for qPCR.....	71
Table 2-4: Lactococcal phage p2 genome clones.	73
Table 2-5: Primers used in cloning.	73
Table 2-6: Primers used for sequencing.....	74
Table 3-1: Samples for RNA-Sequencing.	85
Table 3-2: Percentage of reads mapped in RNA-Sequencing.	86
Table 3-3: <i>L. lactis</i> gene counts organized in COG categories.....	88
Table 3-4: Differentially expressed genes in normal infection at 30 minutes vs. 10 minutes.....	95
Table 3-5: Differentially expressed genes in AbiK infection at 30 minutes vs. 10 minutes.	100
Table 3-6: Differentially expressed genes in the AbiK infection compared to the normal infection.	107
Table 3-7: Primer sequences for RT-qPCR.	119
Table 4-1: Summary of mutations found in pAbiK Y44F plasmids.....	136
Table 4-2: Strains and plasmids used in this study.....	156
Table 4-3: Primers used in cloning and sequencing.	159
Supplementary Table 1: Percentage of transcript counts in COG categories for RNA-Seq.	187

List of Figures

Figure 1-1: Phage classification based on morphology and genome type.....	3
Figure 1-2: Lytic and lysogenic life cycle of phages.....	5
Figure 1-3: Genome organization of lactococcal phages.....	9
Figure 1-4: Adsorption resistance mechanisms.....	12
Figure 1-5: Host defense systems.....	12
Figure 1-6: Abortive infection systems.....	15
Figure 1-7: AbiK protein sequence and structure.....	20
Figure 1-8: Label-Chase assay of AbiK.....	21
Figure 1-9: Proposed mechanisms for AbiK.....	25
Figure 2-1: Major experimental conditions of this study.....	30
Figure 2-2: Effect of AbiK expression on cell growth.....	32
Figure 2-3: Exponential growth rate of <i>L. lactis</i> cells.....	33
Figure 2-4: Multiplicity of infection titration.....	35
Figure 2-5: Lysis curves of <i>L. lactis</i> cells.....	38
Figure 2-6: Adsorption assay of lactococcal phage p2 infecting MG1363.....	40
Figure 2-7: One-step growth curves.....	43
Figure 2-8: Cell survivability assay.....	46
Figure 2-9: Lactococcal phage p2 genome.....	48
Figure 2-10: Southern blot with probe 3.....	51
Figure 2-11: Southern blot with probe 7-1.....	52
Figure 2-12: qPCR to detect DNA replication.....	55
Figure 2-13: Schematic of cloning methods.....	63
Figure 2-14: Lactococcal phage p2 genome clones.....	75
Figure 3-1: RT-qPCR of DNA Polymerase and HNH Endonuclease Genes.....	82
Figure 3-2: RT-qPCR of Capsid and Baseplate Genes.....	83
Figure 3-3: RT-qPCR of Sak3 Gene.....	84
Figure 3-4: Percentage of transcript counts in COG categories in uninfected cells.....	89
Figure 3-5: Percentage of transcript counts in COG categories in infected cells.....	92
Figure 3-6: Heat map of differentially expressed genes in normal infection at 30 minutes vs. 10 minutes.....	94
Figure 3-7: Gene expression of lactococcal phage p2 genes during normal infection.....	96
Figure 3-8: Heat map of differentially expressed genes in AbiK infection at 30 minutes vs. 10 minutes.....	99
Figure 3-9: Gene expression of lactococcal phage p2 genes during AbiK infection.....	101
Figure 3-10: Heat map of differentially expressed genes in <i>L. lactis</i> cells in the presence and absence of the AbiK protein.....	105
Figure 3-11: Heat map of differentially expressed genes during the AbiK infection compared to the normal infection.....	106
Figure 4-1: Label-chase assay for AbiK and mutant proteins.....	123
Figure 4-2: WebLogo of conserved tyrosines in the amino-terminal region of AbiK.....	125
Figure 4-3: Nucleotide sequence alignment of pGEX4T1-AbiK and tyrosine to phenylalanine AbiK mutants.....	127
Figure 4-4: Nucleotide sequence alignment of pSRQ823 and tyrosine to phenylalanine AbiK mutants.....	128

Figure 4-5: Silver stain of GST-AbiK and mutant purifications.	130
Figure 4-6: Western blot of GST-AbiK and mutant purifications.	131
Figure 4-7: Label-Chase Assay.	133
Figure 4-8: Effects of Y to F AbiK mutations in vivo.	135
Figure 4-9: Effects of Y44F AbiK mutations in vivo.	136
Figure 4-10: Ribbon diagram of AbiK model.	139
Figure 4-11: Superposition of AbiK model with group II intron reverse transcriptase.	139
Figure 4-12: Superposition of AbiK model active site with 6AR1.	140
Figure 4-13: Comparison of AbiK α Rep domain and other alpha helical repeat domains.	143
Figure 4-14: Superposition of AbiK model with pentatricopeptide repeat.	144
Figure 4-15: Active site of AbiK with proposed DNA attachment sites.	146
Figure 4-16: Comparison of AbiK model and the crystal structure.	148
Figure 4-17: Active site of AbiK.	149
Figure 4-18: Structure of Sak3.	152
Figure 4-19: Schematic of cloning methods.	157
Figure 5-1: AbiK in an uninfected cell.	168
Figure 5-2: AbiK mechanism during a phage infection.	170
Figure 5-3: Sak3 mutant phage's bypass of AbiK mechanism.	170
Supplementary Figure 1: Densitometry analysis of Southern blots with probe 7-1.	181
Supplementary Figure 2: Southern blot of samples pretreated at 65°C.	182
Supplementary Figure 3: PCR products of primers designed for RT-qPCR.	182
Supplementary Figure 4: RT-qPCR Products.	183
Supplementary Figure 5: DNA Control of Figure 3-1.	184
Supplementary Figure 6: DNA Control of Figure 3-2.	185
Supplementary Figure 7: DNA Control of Figure 3-3.	186
Supplementary Figure 8: WebLogo of AbiK and 16 related protein sequences.	188
Supplementary Figure 9: WebLogo of AbiK and 99 related protein sequences.	189
Supplementary Figure 10: Plasmid map for pGEX4T1-AbiK.	190
Supplementary Figure 11: Plasmid sizes of pAbiK Y44F.	191
Supplementary Figure 12: Alignment of the nucleotide sequences of AbiK mutants (1/7).	192

List of Symbols, Abbreviations and Nomenclature

Symbol	Definition
Abi	Abortive infection
AbiK	Abortive infection K
AIDS	Acquired immunodeficiency syndrome
Amp	Ampicillin
ATP	Adenosine triphosphate
BLAST	Basic local alignment search tool
BREX	Bacteriophage exclusion
Cas	CRISPR-associated genes
<i>cat</i>	Chloramphenicol acetyltransferase gene
CBASS	Cyclic oligonucleotide-based antiphage signaling systems
cDNA	Complementary DNA
CDS	Coding sequence
CFU	Colony forming units
Cm	Chloramphenicol
COBALT	Constraint-based Multiple Alignment Tool
COG	Clusters of orthologous groups
<i>cos</i>	Cohesive end site
COVID-19	Coronavirus diseases 2019
CRISPR	Clustered regularly interspaced short palindromic repeats
CTP	Cytidine triphosphate
DISARM	Defense island system associated with restriction-modification
DNA	Deoxyribonucleic acid
dsDNA	Double-stranded DNA
dsRNA	Double-stranded RNA
DTT	Dithiothreitol
<i>E. coli</i>	<i>Escherichia coli</i>
EDTA	Ethylenediaminetetraacetic Acid
EGTA	Ethylene glycol-bis(β -aminoethyl)-N,N,N',N'-tetraacetic acid
Ery	Erythromycin
FAD	Flavin adenine dinucleotide
FMN	Flavin mononucleotide
GM17	M17 medium supplemented with 0.5% glucose
GST	Glutathione S-transferase
GTP	Guanosine triphosphate
HEAT	Huntingtin, elongation factor 3, protein phosphatase 2A, yeast kinase tor1
HEPN	Higher eukaryotic and prokaryotic nucleotide-binding
HIV-1 and 2	Human immunodeficiency viruses
HRP	Horseradish peroxidase
ICTV	International Committee of Taxonomy of Viruses
IDT	Integrated DNA technologies
IPTG	Isopropyl β -D-1-thiogalactopyranoside
<i>L. lactis</i>	<i>Lactococcus lactis</i>
LB	Lysogeny broth

MALS/UV/RI	Multi-angle light scattering/UV/refractive index
MOI	Multiplicity of infection
mRNA	Messenger RNA
MWCO	Molecular weight cut-off
NTP	Nucleotide triphosphate
OD ₆₀₀	Optical density at 600 nm
ORF	Open reading frame
Ori	Origin of replication
PAGE	Polyacrylamide gel electrophoresis
PCR	Polymerase chain reaction
PES	Polyethersulphone
PFU	Plaque forming units
PMSF	Phenylmethylsulphonyl fluoride
qPCR	Quantitative PCR
RM	Restriction Modification
RMSD	Root-mean-square deviation
RNA	Ribonucleic acid
RNase	Ribonuclease
RNA-Seq	RNA Sequencing
rRNA	Ribosomal RNA
RT	Reverse transcriptase/Reverse transcription
RT-qPCR	Reverse transcription – quantitative PCR
Sak	Sensitivity against AbiK
Sak3	Sensitivity against AbiK 3
SARS-CoV-2	Severe acute respiratory syndrome coronavirus 2
SDS	Sodium dodecyl sulfate
SDS-PAGE	Sodium dodecyl sulfate polyacrylamide gel electrophoresis
SEM	Standard error of the mean
SSC	Saline sodium citrate
ssDNA	Single-stranded DNA
ssRNA	Single-stranded RNA
Str	Streptomycin
TAE	Tris-acetate-EDTA
TBE	Tris-borate-EDTA
TBS	Tris-buffered saline
TBS-T	Tris-buffered saline with tween
TE	Tris-EDTA
TMM	Trimmed mean of M values
tRNA	Transfer RNA
TTP	Thymidine triphosphate
UCSF	University of California San Francisco
UG	Unknown group
UTP	Uridine triphosphate
WT	Wild-type

Chapter 1 : Introduction

1.1 Viruses and Bacteriophages

1.1.1 Introduction

Throughout history, viruses have been the cause of many diseases that have had detrimental effects on human populations (4). Smallpox, caused by the variola virus, is estimated to have caused up to 400 million deaths in the 20th century before its eradication in 1978 (5). Acquired immunodeficiency syndrome (AIDS), which is caused by the human immunodeficiency viruses (HIV-1 and HIV-2), has caused 40.1 million deaths with 84.2 million infections since its discovery four decades ago (6, 7). Most recently, coronavirus disease 2019 (COVID-19) caused a global pandemic that is persisting due to emerging variants of the virus, severe acute respiratory syndrome coronavirus 2 (SARS-CoV-2) (8). Humans are not the sole targets of viruses, as viruses affect all domains of life (4). Avian influenza viruses can result in economic consequences when poultry are affected, and these viruses can also cross over to humans, causing diseases like the Spanish Flu pandemic (9, 10). Viruses are infectious parasites to their hosts, several of which have led to negative consequences for the world's economy, industry and health (4).

Bacteriophages, more popularly known as phages, are viruses that target and use bacteria as their hosts (11, 12). They are likely the most abundant biological entities on the planet, estimated to number up to 10^{31} , and are found in all ecosystems (11, 12). They can be found in all types of environments, including hot environments such as hot springs and the Sahara desert, or in cold environments like the depths of the Arctic Ocean (11, 12). Phages also play an important role in the animal microbiome, present mostly as lysogens, and play important roles in their host's metabolism (11). Phages vary widely, coming in many different shapes (polyhedral

or filamentous capsids), a large range of sizes (24 - 200 nm) and with a genome composed of either deoxyribonucleic acid (DNA) or ribonucleic acid (RNA) (11, 12). They play a vital role in microbial physiology and evolution as they interact with host bacteria, impact host populations and drive host evolution as hosts evolve for phage resistance (13).

1.1.2 Bacteriophage Morphology and Taxonomy

The taxonomic characterization of phages is a daunting task due to how numerous and diverse they are. The first approved taxonomic classification of phage particles was done in 1967 by David Bradley, who classified the phages based on their morphology, which was approved by the International Committee of Taxonomy of Viruses (ICTV) (12, 14, 15). Starting with six basic morphologies, this classification expanded as more phages were discovered and had their genome sequences determined; bacteriophages are now classified into one class and over 40 families, with new taxa being added regularly as new discoveries are made (11, 16–18). The phages are organized by their genome type (dsDNA, ssDNA, dsRNA and ssRNA), followed by their morphology, including the presence of a tail, their cubic symmetry, and if they are filamentous or pleomorphic (**Figure 1-1**) (14). In recent years, the ICTV has reworked the classification framework to be genome-based rather than morphology-based due to the expansion of known bacteriophages through metagenomic analysis (11). This has led to an upheaval and large changes in the taxonomic characterizations of bacteriophages in recent years (11).

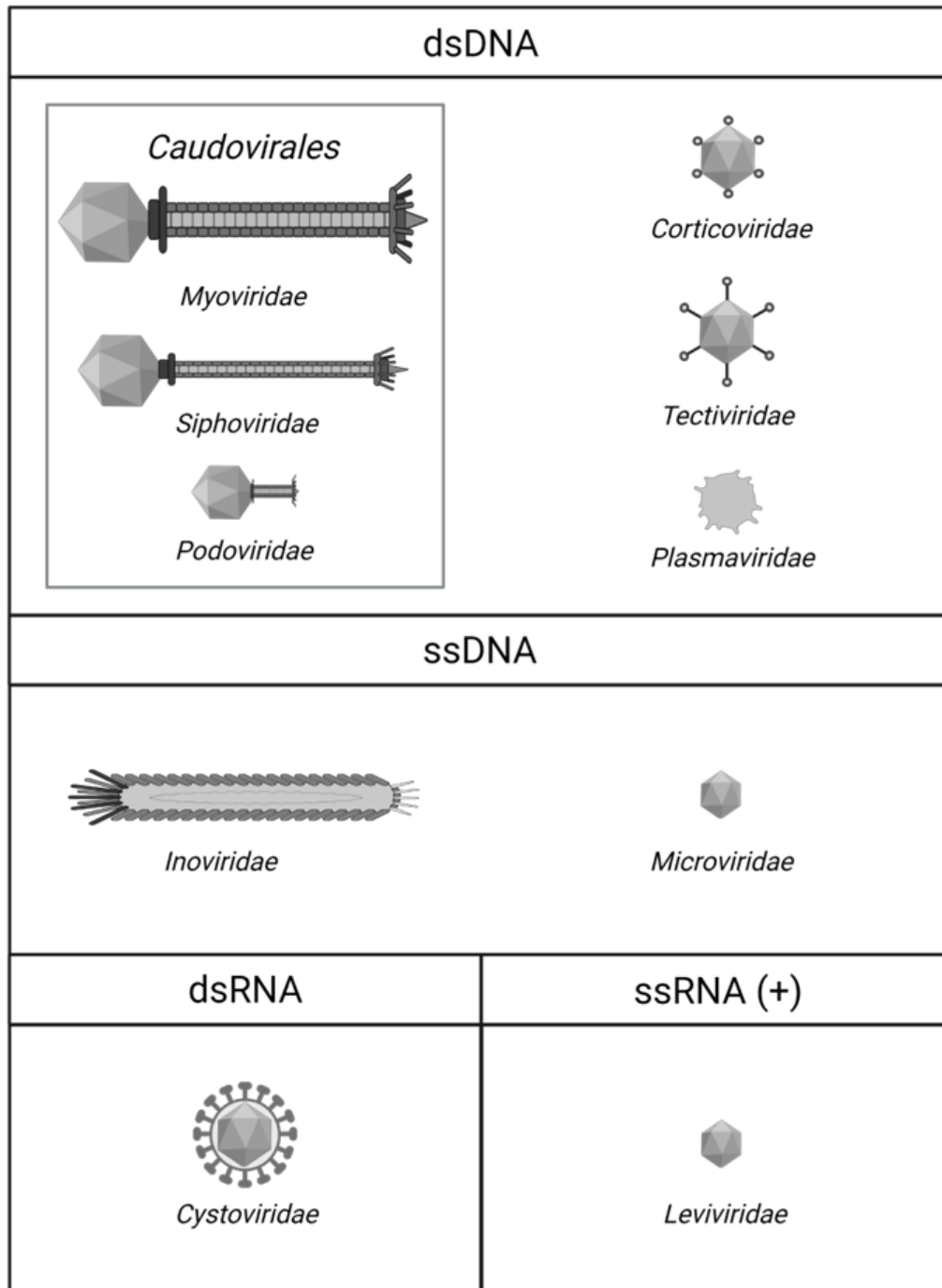


Figure 1-1: Phage classification based on morphology and genome type.

Schematic representations are shown for each morphology. Classifications are based on the 9th report of the International Committee on Taxonomy of Viruses (ICTV) from 2011 (16). The latest ICTV classification adds many families, notably within the Caudoviricetes class, which currently has 4 orders and over 40 families (17). The families within Caudoviricetes shown here are no longer recognized as families but continue to be used as morphological terms. Figure created with BioRender.com.

1.1.3 Bacteriophage Replication Cycles

There are two possible life cycles that a bacteriophage can undergo: the lytic cycle or the lysogenic cycle (**Figure 1-2**) (12). Virulent phages are those that invariably adopt the lytic cycle to produce new phage progeny in the infected cell, and temperate phages are those that can undergo either a lytic or a lysogenic cycle once they enter a host cell (12, 19). Both life cycles start with a phage interacting with receptors on the host cell, where it gets adsorbed, followed by injection of its genome into the host cell (12, 19). In the lytic cycle, this step is followed by the replication of the phage's genetic material along with the translation of phage proteins to make new phage progeny (12). In the later stages, the newly formed phage progeny exit the host cell, usually by breaking its cellular membrane and hydrolyzing the cell wall; this allows the new phage progeny to find new hosts to continue proliferating (12). In the lysogenic cycle, the injected viral genetic material becomes part of the bacterial genome either by integration into the chromosome or by becoming a plasmid-like entity; in either of these forms it is known as a prophage (12). The prophage continues to be replicated in the infected host as the host proliferates, with the prophage occasionally being excised under conditions of stress to initiate the lytic cycle in the host (12, 19).

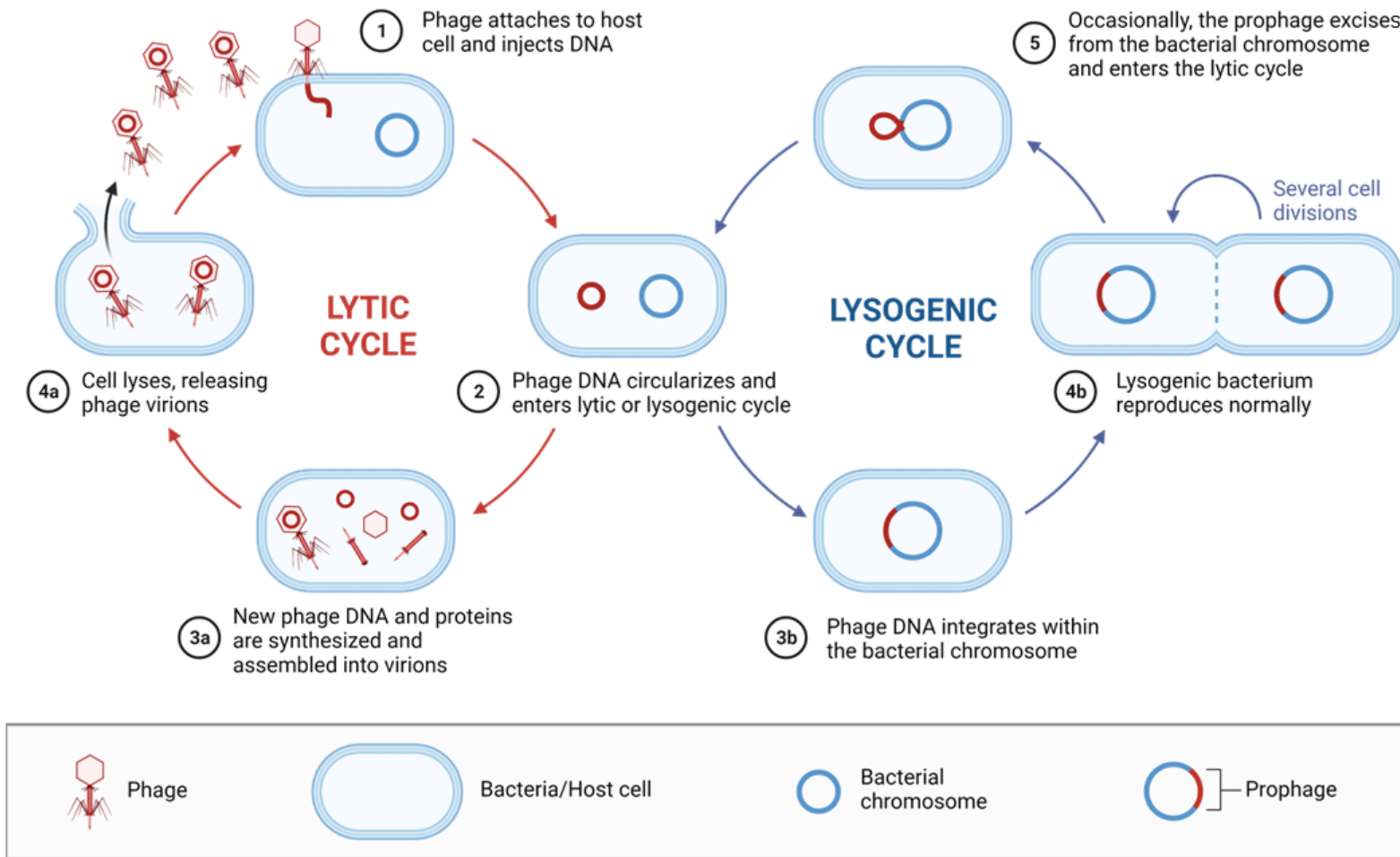


Figure 1-2: Lytic and lysogenic life cycle of phages.

A schematic representation of the lytic and lysogenic cycles of phages. The cycle starts with a phage attaching to the host cell and injecting its genetic material (1) followed by the circularization of its genome (2). In the lytic cycle, the genome is replicated, and new phage progeny are assembled (3a) before the release of the phage progeny with the lysis of the cell (4a). In the lysogenic cycle, the phage DNA is often integrated into the bacterial chromosome (3b) and remains in the cell as the host cell reproduces (4b). Under certain conditions, the prophage excises from the host's chromosome and continues the lytic cycle (5). Reprinted from Lytic and Lysogenic Cycle, by BioRender.com (2023).

1.1.4 Applications of Bacteriophages

Phages have been used in several different applications in biotechnology, medicine, and in the agriculture sector (12). In biotechnology, phages have been used as tools to detect pathogenic bacteria (12). This is done by expressing a display molecule on the surface of the phage with its coat protein, which can signal when the phage detects a pathogenic bacterium (19). In medicine, bacteriophage therapy was used to treat bacterial infections in the early 1920's until antibiotics were discovered and produced on an industrial scale (19). However, with the surge of antimicrobial resistant bacteria, phage therapy is re-emerging in popularity as a therapeutic option (20). Phages have also been used in the agriculture sector to combat bacterial contaminants in food, such as *Salmonella* and *Escherichia coli* (*E. coli*), and are also being used to optimize wastewater treatments (12, 21). Many molecular tools have been discovered from the evolutionary battle between phages and their hosts and applied in modern molecular biology, including restriction modification (RM) enzymes and replication enzymes (12). The CRISPR-Cas (clustered regularly interspaced short palindromic repeats and the CRISPR-associated (cas) genes) mechanism, initially discovered as a defense mechanism in bacteria and archaea to acquire immunity against phages, has also been used in molecular biology for gene editing (22). The impact of phages in biotechnology is immeasurable, and the exploitation of phage-based tools will continue to be extensive for many years to come (19).

1.2 Lactococcal phages

Lactococcus lactis (*L. lactis*) is a Gram-positive bacterium that is widely used in the dairy industry to produce yogurt, cheeses and other foods (23, 24). Cheese manufacturing and milk fermentation processes require large volumes of bacterial cultures, and fermentation by *L. lactis* represents 20% of the total economic value of fermented food worldwide (23). Since phage infections of *L. lactis* are the primary cause for fermentation failures, there is commercial relevance in studying phage infections of *L. lactis* (23). Bacteria in fermentation cultures are constantly under threat by phages in these non-aseptic conditions, causing the constant evolution of phage populations leading to a diverse number of phage isolates (25).

Lactococcal phages have historically been classified according to their morphology and DNA homology (26–28). It is important to note that these classifications are not indicative of ICTV's recent genome-based classifications, so terminology referring to the older families will be used. In 2006, the lactococcal phages were classified into a total of 10 different groups which are all part of the former *Caudovirales* order, having dsDNA genomes and noncontractile tails (26). The vast majority are classed into one of the three main groups, the 936, c2 and P335 groups of lactococcal phages (26, 29). 936-group phages are well-studied, due to their being the most problematic group of phages in fermentation facilities and being the most commonly isolated group (26). The c2-group phages stand out by having the broadest host-range of the lactococcal phages and extensive DNA homology between members of the group (29). The P335-group phages have significant genetic diversity within the group due to extensive recombination events between related phages, and no single feature is shared by all members of the group (29).

All three groups are morphologically classified as siphoviruses, having long noncontractile tails (26). There are small variations in morphology between the three groups, such as tail length, shape of the capsid, etc. (**Table 1-1**) (26). Phages from the 936-group and from the P335 group have small isometric heads, and phages from the c2 group have prolate heads (30). The three main groups of lactococcal phages are considered to be genetically distinct, based on DNA-DNA homology tests, which are done by Southern hybridization of a restriction digested genome of a queried phage by a genomic probe representative of the group (26, 27). Several members of each group have been sequenced, and the size ranges of the genomes along with the genome organization of the groups is shown (**Table 1-1** and **Figure 1-3**) (29, 31–33).

For their modes of replication, 936- and c2- phages are virulent and genetically similar to each other (34). The 936-group of phages in particular, have been known to have highly optimized genomes that lead to rapid propagation in large-scale milk fermentation (34). In contrast, P335-phages are temperate and considered a polythetic species (26, 29, 34). Many of the P335-phages (except phage P335, interestingly) contain a lysogeny module in their genome, and members of the group are prone to recombination (26, 32). Due to the diversity and persistence of lactococcal phages in dairy fermentation plants, studies of bacteriophages from these ecological niches have been fruitful to look at how they and their hosts evolve to outcompete one another.

Table 1-1: Morphologies and genome sizes of lactococcal phage groups.

Group	Capsid diameter, tail width, tail length*	Genome size (kb)**
936	50, 11, 126	26-32
P335	49, 7, 104	34-38
c2	54 x 41, 10, 95	20-22

* Sizes were reported in (26).

** Genome sizes were estimated based on restriction profiles of 137 phage isolates in (29).

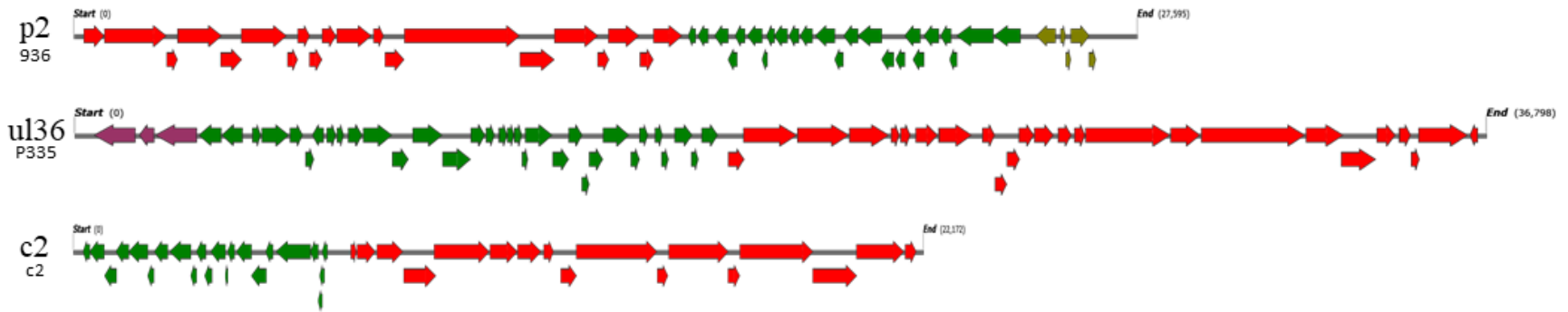


Figure 1-3: Genome organization of lactococcal phages.

Genome organization of representative lactococcal phages with the specific phage species and group labelled. Early genes are shown in green, middle genes are shown in olive, late genes are shown in red, and genes related to lysogeny are shown in burgundy. Start and end sites represent *cos* sites, where the genome circularizes. Genome maps were generated using Snapgene.

1.3 Defense Mechanisms Against Bacteriophages

1.3.1 Defense Mechanisms

There are many methods that bacteria can use to block infection by bacteriophages, including adsorption resistance, host defense systems, or phage-derived phage defense systems (35). It is currently unknown how many defense systems exist against bacteriophages, and many new defense systems have been uncovered in recent years due to increased interest in using phage therapies (35). The discovery of defense islands, regions in bacterial genomes that contain clusters of genes involved in defense systems, have allowed for the identification of new defense mechanisms (35–37). The identification of new defense mechanisms reveals a vast world of defense strategies that were previously unknown, expanding the known arsenal of anti-phage defense systems used by bacteria (36).

For a phage to bind to its host, it needs to bind to a receptor and adsorb to the cell before its genome can penetrate the host cell. Adsorption resistance is a type of defense mechanism that results in the host impeding the phage's ability to find and bind the receptor (**Figure 1-4**) (38). Mutations in the receptor itself can result in a modification or down-regulation in expression of the receptor (38). In fact, phage challenges to find resistant hosts often result in the identification of the receptor (38). There can also be an upregulation in the extracellular matrix or in masking proteins that can block the phage from binding to the receptor (35). Some bacteria are capable of releasing outer-membrane vesicles containing the receptor that the phage binds to, acting as decoys that can capture phages so the host cells do not become infected (35).

Bacteria have also adopted internal defense systems to combat phage infections, known as host defense systems (**Figure 1-5**) (35). A common way for bacteria to interfere with the phages is to directly interact with the phage's nucleic acids. Restriction modification systems can

act on phages with DNA genomes, targeting and cleaving phage DNA at recognition sites (35, 38). CRISPR-Cas systems also use adaptive immunity to recognize and target foreign genetic material for cleavage (22, 39). The exact mechanism for DISARM (defense island system associated with restriction-modification) and BREX (bacteriophage exclusion) systems remain unclear, but they have been shown to hamper the replication of phage DNA, blocking phage infection (40, 41). Chemical defense systems also exist, where bacteria produce secondary metabolites upon phage infection (35). These metabolites allow bacteria to proliferate even in the presence of phages, often by interacting with phage DNA to block phage replication (42). Abortive infections (Abi) are commonly used defense strategies that are adopted by bacterial cells, where the cell sacrifices itself before the phage can fully replicate, protecting the remainder of the population (35). This is further described in section **1.3.2**.

Superinfection exclusion is a phenomenon where infecting phages can provide bacteria with defense systems to protect against infection by the same or a closely related phage, also known as phage-derived phage defense systems (35). During a lytic phage's life cycle, the phage can produce proteins that get excreted and mask the receptors, preventing further infections (43). Membrane-associated proteins can also be used to target and block the entry of phage DNA by inhibiting the formation of the DNA entry channel (44). Prophages in bacteria are also able to express resistance mechanisms, even containing their own RM systems or Abi systems to prevent phage infections (44). There are many defense systems that have been identified in bioinformatic analysis that remain uncharacterized, including phage-derived defense systems (35). These unknown systems continue to be discovered and studied for their mechanisms of action and are generating considerable interest for their ability to protect bacteria used in

industrial processes from phages, but also because of their potential to undermine phage therapy approaches (20).

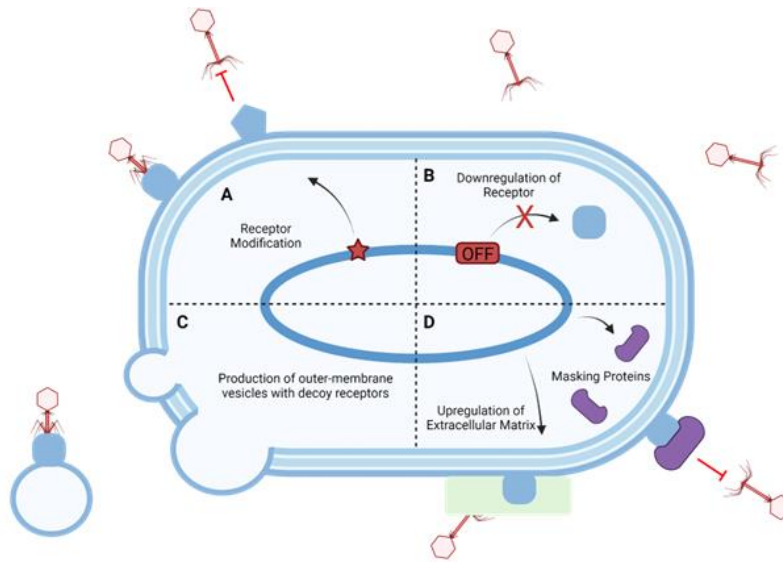


Figure 1-4: Adsorption resistance mechanisms.

A schematic representation of adsorption resistance mechanisms bacteria can adopt to combat phages. **A:** Receptor modification results in the phage being unable to recognize and bind the receptor. **B:** Downregulation of the receptor results in a decrease in the number of available receptors for the phage to bind. **C:** The release of outer-membrane vesicles containing the receptor can act as decoys to capture and inactivate phages. **D:** An upregulation of the extracellular matrix or of masking proteins can block the phage from binding to the receptor. Adopted from Egido et al. Created with BioRender.com.

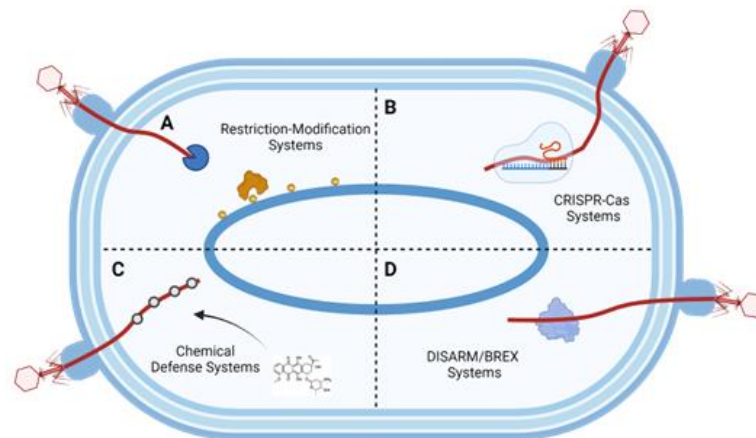


Figure 1-5: Host defense systems.

A schematic representation of host defense systems bacteria can adopt to combat phages. **A:** Restriction-Modification systems can degrade phage nucleic acids. **B:** CRISPR-Cas systems use adaptive immunity to target foreign genetic material. **C:** Chemical defense systems result in secondary metabolites that can interact and block phage genetic material. **D:** DISARM/BREX systems block phage infection by hampering the replication of phage genetic material. Adopted from Egido et al. Created with BioRender.com.

1.3.2 Abortive Infection Systems

Abortive infection defense mechanisms are suicidal systems, where the death of an infected cell ensures the survival of the remaining population (35, 45). Although bacteriophages are able to inject their genetic material, a key process is inhibited or a cell-killing module becomes activated, preventing the phage from maturing and causing the cell to die (**Figure 1-6**) (23, 45). Abi systems act as a last resort defense mechanism and are enacted when all other defense systems fail (45). Some Abi systems result in cell death by degrading the host membrane (45). Others target key cellular mechanisms, like DNA replication, transcription, or translation by degrading DNA or tRNAs or by proteolysis of key proteins involved in these processes (23, 45, 46). The blockage of an essential step can result in cell death, but it has been shown that a temporary growth arrest can occur to allow other defense mechanisms to inactivate the phage and prevent cell death (45). These mechanisms are widespread and have been found in many bacterial species including *E. coli* and *L. lactis* (23, 45). In fact, over 20 Abi systems have been characterized in *L. lactis* (dubbed AbiA to AbiZ) and almost all are found to be encoded on plasmids (23, 24, 45, 47).

It is difficult to determine how an Abi mechanism works. In *L. lactis*, Abi mechanisms are often mediated by one gene, but some Abi's are proposed to be encoded by two genes (23). Protein homology between Abi's and other proteins of known function is seldom found, making it difficult to predict their mode of action (23, 48). Only a minority of the Abi's discovered in *L. lactis* have known mechanisms of action (23, 45).

Some Abi systems work via a toxin-antitoxin mechanism, where a toxin and its antitoxin are expressed and bound within the cell (35, 45). Upon phage infection, the antitoxin gets suppressed and releases the toxin, causing the toxin to kill the bacterium (35, 45). One example

of this is the ToxIN system in *Pectobacterium atrosepticum* (analogous to AbiQ in *L. lactis*, which was actually discovered first) where the ToxN endoribonuclease interacts with ToxI, a noncoding RNA (45, 49, 50). When the phage infects the cell, ToxI releases ToxN, activating ToxN to cleave cellular and phage RNA, eventually leading to cell death (45). Cyclic oligonucleotide-based antiphage signaling systems (CBASS) belong to a new family of Abi systems recently discovered to protect against phage infection in *Vibrio cholerae* (45, 51, 52). In these systems, a phage-sensing protein produces a cyclic oligonucleotide secondary messenger that can activate the cell-killing effector protein (35, 45). Effector proteins can vary, including phospholipases, endonucleases, membrane-spanning ion channels, and other proteins of unknown function (45). Although not a ToxIN or CBASS system, AbiZ, discovered in *L. lactis*, is a protein that interacts with the phage's lysin and holin proteins to induce early cell lysis (45, 53). The first Abi system discovered in *L. lactis*, AbiA, is a reverse transcriptase fused to a HEPN (higher eukaryote and prokaryote nucleotide-binding) domain and is proposed to be involved in the degradation of phage and host RNA (54). An additional strategy that some Abi systems adopt is to deplete critical cellular resources, such as enzymatic cofactors and nucleotides (35).

Abi systems are abundant, with mechanisms that are equally as diverse. Despite the listed examples, many more were not mentioned including retrons and type III CRISPR-Cas systems (35, 45). Although genes involved in Abi systems can be identified, determining their functions remains difficult. Often, there are no known homologues with known functions. Escape mutants, which are phages that have mutated to resist a specific abortive infection mechanism, can be used to help determine the mechanism by identifying involved genes. However, in most cases, an escape mutant may not be found, and determining how an abortive infection mechanism works is

akin to finding a needle in a haystack due to the abundance of possible mechanisms. Cell suicide as an immunological strategy is widespread, and an effective last line of defense against phages as the overall population is protected (45).

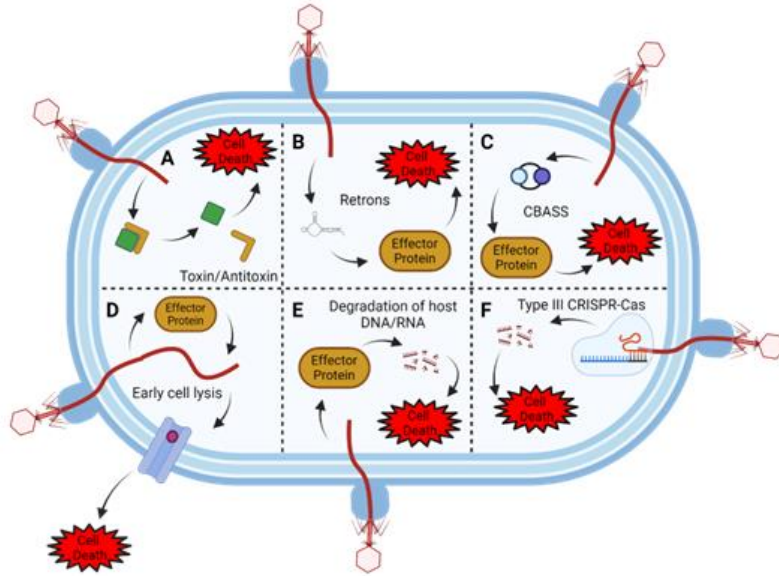


Figure 1-6: Abortive infection systems.

A schematic representation of Abi systems that bacteria can adopt to combat phages. Abi systems result in host cell death. **A:** Toxin-antitoxin system. Upon phage infection, the antitoxin releases the toxin which results in cell death. **B:** Retrons are activated upon phage infection, which activate effector proteins that lead to cell death. **C:** CBASS systems. Cyclic oligonucleotide secondary messengers activate effector proteins upon phage infection, leading to cell death. **D:** Upon phage infection, an effector protein (like AbiZ) is activated and can interact with holin/lysin proteins which results in early cell lysis, resulting in cell death. **E:** Upon phage infection, an effector protein is activated and results in nonspecific degradation of host nucleotides, resulting in cell death. **F:** In type III CRISPR-Cas systems, a nonspecific RNase indiscriminately cleaves phage and host RNA, resulting in cell death. Adopted from Egido et al. Created with BioRender.com.

1.4 Abortive Infection K

1.4.1 Discovery and Characterization

The AbiK mechanism was first reported in 1997, with the isolation of an industrial strain of *L. lactis* (Strain W1) that was found to be resistant to many lactococcal phages (24). Early work narrowed down the gene responsible for resistance against phages, and it was determined to be due to a single gene encoding a 599 amino acid protein on the natural plasmid, pSRQ800 (24). The phage resistance mechanism was found to be effective against three groups of genetically distinct lactococcal phages (936, c2 and P335), and was determined to be less effective at higher temperatures (38°C) (24). The protein is constitutively expressed in cells and was found to be more efficient at resisting phage infections when expressed on a high-copy-number plasmid (24). Upon phage infection, expression levels of the *abiK* gene are not affected (47).

Subsequent work went into characterizing the mechanism of AbiK to determine how it blocks phage infections. Adsorption resistance was ruled out as the phage resistance mechanism, as the phage adsorbed similarly on both sensitive and resistant cells (24). Restriction modification mechanisms were also ruled out when no endonucleolytic activity was observed on DNA extracted from resistant infected cells (24). Cell survival studies showed that cells containing the resistance mechanism died following phage infection, leading to the classification of the AbiK mechanism as an abortive infection system (24).

Studies were done to look at the intracellular effects of the AbiK system on the phage's life cycle in two different phage groups, the P335 phages and the 936 phages (**Table 1-2**). These studies looked at the overall replication of the phage, phage DNA replication, phage RNA production, and production of the major capsid protein. The replication of both phage groups was

found to be severely inhibited by the AbiK mechanism (24, 30). In the P335 group of phages, phage DNA replication does not occur, and late gene expression was not detected (24, 55). The production of the major capsid protein was monitored, and the capsid protein could not be detected in AbiK⁺ (AbiK-expressing) cells (24). AbiK was found to have little to no effect on the c2 group of phages (24).

For the 936 group of phages, including lactococcal phage p2 and phage P008, DNA replication of the phage was detected (24, 30). However, only immature forms of the phage DNA were detected, indicating that the phage DNA was not being processed for packaging (24, 30). Lactococcal phage p2's gene expression was not affected by AbiK, and phage genes were expressed normally (55). The lytic cycle of lactococcal phage p2 in AbiK⁺ cells was monitored via microscopy, and phages could be seen adsorbing and injecting their genetic material (30). Later on in the lytic cycle, capsid-like structures could be detected surrounding a DNA network, possibly showing an inability to package immature phage DNA into the capsids (30).

During the replication of P335 phages, AbiK seemingly acts before phage DNA replication, arresting downstream processes. On the contrary, for the 936 group of phages, the only change that could be detected is the phage's inability to process DNA for packaging, showing that AbiK could be acting in different manners depending on the species of the infecting phage. This property makes it difficult to ascertain AbiK's mechanism of action but shows a diverse ability to combat infecting phages.

Table 1-2: Intracellular effects of the AbiK system.

Phage Group	P335 Phages	936 Phages
DNA Replication	Not detected	Detected but immature forms of DNA
RNA Production	Not detected (Late genes)	Detected
Capsid Production	Not detected	Detected with immature DNA

1.4.2 Enzymatic Activity of AbiK

The amino terminal region of the AbiK protein was found to contain reverse transcriptase (RT) motifs (**Figure 1-7**) (47). Site-directed mutagenesis of five conserved amino acids in the motif abolishes phage resistance in cells, showing that the RT motif in AbiK is essential for phage resistance (47). Sequence alignment of AbiK to other reverse transcriptases shows that the finger and palm domains of the polymerase can be identified (1). Interestingly, prokaryotic reverse transcriptases across many different lineages have been found to be key components of different phage defense mechanisms (54). This includes reverse transcriptases in group II introns, retrons, diversity-generating retroelements, CRISPR-Cas, Abi systems and many more (54).

The carboxy terminal region of AbiK is suggested to have a more Abi-specific role, and when the last 42 amino acids are removed, the Abi phenotype is abolished, showing that it is critical for phage resistance (1, 24). However, the removal of the last 42 amino acids resulted in the incorporation of additional non-AbiK codons preceding a stop codon, which could result in the abolishment of the phenotype due to a non-functional protein with the non-AbiK amino acids (24). Historically, the carboxy terminal region of AbiK did not have any sequence similarity with proteins of known functions, making it difficult to predict its role in the AbiK mechanism (1). Recent studies have revealed that domains similar to AbiK's carboxy terminal region have been found across reverse transcriptases associated with defense functions (54). Proteins containing this domain, dubbed α Rep, make up the largest group of defense associated reverse transcriptases and were classed as Class 1 UG (Unknown Group)/Abi RT's (54). This domain's function remains unknown, but the domain is proposed to have an accessory role as opposed to a catalytic function (54).

AbiK has been biochemically assayed, but does not possess activities expected for typical reverse transcriptases, which polymerize complementary DNA (cDNA) molecules using an RNA template (1). AbiK does have polymerase activity and is able to synthesize a long single-stranded DNA (1). Unlike common polymerases, incorporation of deoxyribonucleotides occurred even without the presence of a template, and bases are incorporated without sequence specificity (**Figure 1-8**) (1). This activity is analogous to terminal transferases, which can catalyze the incorporation of nucleotides onto a nucleotide initiator without copying a template (56). Interestingly, the polymerized DNA was found to be attached covalently to AbiK as AbiK uses an internal amino acid as a primer (1). After over a decade of work to identify this priming site, the structure for AbiK was solved and the priming site was shown to be on tyrosine 44 of the AbiK protein (**Figure 1-7**) (57). Uncharacteristic of polymerases, AbiK's structure also revealed a hexameric configuration which is required for its activity (57). More detail about AbiK's solved structure is presented in Chapter 4.

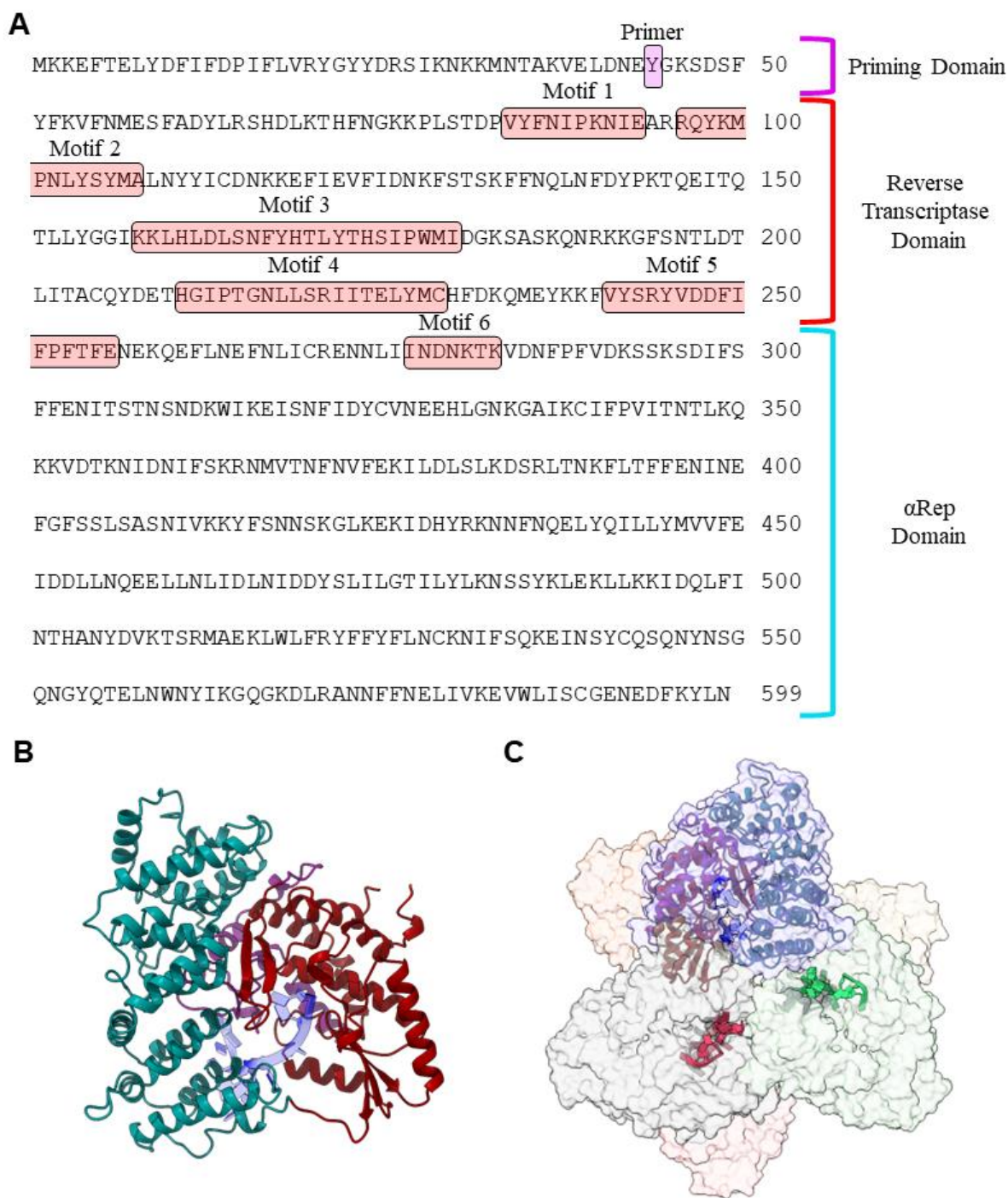
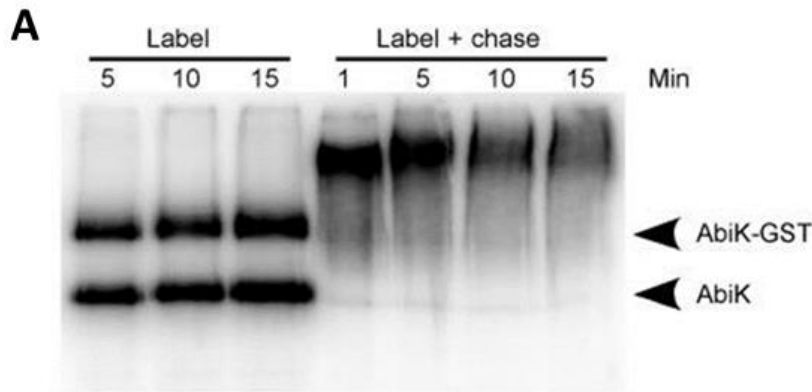


Figure 1-7: AbiK protein sequence and structure.

A: AbiK's amino acid sequence with labeled domains. The priming residue is indicated along with conserved reverse transcriptase motifs. **B:** Ribbon diagram of monomeric AbiK structure (7R06) (57). The priming domain is coloured in violet, with the reverse transcriptase domains in red and the carboxy terminal (α Rep) domain in turquoise. The covalently bound ssDNA is coloured in blue. **C:** Space filling model of AbiK's hexameric structure (7R06), with one monomer shown as a ribbon (57). DNA strands are shown as blue, green and red in protomers. Figure made using UCSF Chimera X (58).



B AbiK + dNTPs

5' GTCTATCGCATGGGGCCTGCGTAGAATGGATGGGAGCCGATAACCGA
 CAGTCCGGGAGGAGGAAATCGCAGTGCTCTTGAGCGTAGAACTAAACTAC
 GAAAAAGAATTGGAGCTGGTGTTCACCTCTAACTGAGACGTGACGAGTG
 CTTGTCAGTAAGGATGTCCTACGGA 3'

5' TATCCCGGAAGAGATTATCTGACTGCCCAAAGTAGTACCGCTGATT
 GCCCACCGTGGGATTGAGAGAAAACCCGAGGCTACGCGTTAGCCGTTGA
 AGGACAAGATCAGATACACGTACTTATGACTCTTAGACGCCGAGAGAGAA
 TGGCGAACAGACGCTATCTTGATAGTAAGA 3'

C AbiK + dATP, dCTP, dGTP

5' AGAAAGCCAGAAAGGAAAAAGAGCAAAGAGCAGCAGCGGAGAACGGA
 GAAGGGCCAAACAGAGAAAAAGAGCACGACAGCCCGAAGCCACAGA 3'

5' AAGAGAGAAAGAGAGAGACCAGAACAGAAAAAAAAACGACGAAACAA
 CCGCAGAAAAGAGAAAAAAAAACAGCA 3'

D AbiK + dATP, dGTP, dTTP

5' ATGATTGGAAAAAATAATGATTGGTGGTATTAAATGAGGAAGAAA
 AGTGAATGTGGGAATAGGGTATGTATATAA 3'

5' AGAGAGTGTTTTGGAAAGATAGTGATAATGTTATAGGTGATGTTAGGA
 AGTTGATAAGAATGAGGTAGGATATAGATTGGAAGAATAATAAAAAAAG
 ATGTTGTA 3'

Figure 1-8: Label-Chase assay of AbiK.

A: Label-chase assay showing the biochemical activity of AbiK. Upon incubation with a radioactive deoxyribonucleotide, a band is present at the same size as AbiK, indicating a self-priming activity. Upon incubation with additional deoxyribonucleotides, this band migrates more slowly, showing incorporation of the deoxyribonucleotides to the growing strand. **B-D:** Sequencing of the DNAs polymerized by AbiK shows non-templated polymerization as none of the sequenced DNA have similarity to each other. Figures taken from Wang et al. (1).

1.4.3 Escape of AbiK: Sensitivity against AbiK

To help determine Abi protein functions, resistant phages can be isolated and genes aiding with resistance can be identified (24). Emond et al. were able to identify some escape mutant phages of AbiK and have shown that they have a slower maturation period than the wild-type phage (24). These mutant phages were found to have single amino acid mutations on *sak* (sensitivity against AbiK) genes, found in four different phages (*sak* in phage ul36, *sak2* in phage P335, *sak3* in phage p2, *sak4* in phage f31) (1, 3, 59). A mutation in the *sak* gene allows the phage to no longer be susceptible to the AbiK mechanism and bypass it to produce phage progeny. *Sak* genes encode single-strand annealing proteins that form rings with multiple subunits and are known to have roles in genome circularization after infection, in DNA replication, as well as roles in processing DNA concatemers (3, 60, 61).

In lactococcal phage p2, a single amino acid mutation (V16A, M90I, or S144Y) in *sak3* (ORF35) was found to give the phages resistance to the AbiK mechanism (3, 59). Sak3 is conserved among the phages in the 936 group (3). When Sak3 is expressed with AbiK, the efficacy of AbiK is increased, showing that it is involved in the phage defense mechanism (59). Sak3 has been found to exhibit an oligomeric structure that forms a doughnut-like shape (3). Biochemical studies show that the amino terminal portion of Sak3 can bind both single-stranded DNA (ssDNA) and double-stranded DNA (dsDNA) but has been shown to bind ssDNA with a stronger affinity (3). Sak3 was also tested for its capacity to anneal complementary nucleotides and can anneal short complementary DNA sequences, which is notable as the ends of the phage p2 genome are single-stranded and complementary (11 nucleotides long) (3). In addition, Sak3 has ATPase activity and can stimulate *E. coli* RecA-mediated homologous recombination, implying a role in recombination-dependent replication (3).

The Sak3 protein has many activities that can indicate its possible biological roles. Although its exact role in phage replication is not confirmed, based on its activities and what is known about single strand annealing proteins, Sak3 is hypothesized to be involved in phage genome circularization upon host entry. In addition, Sak3 may have a role in DNA replication and in processing DNA concatemers into mature forms of DNA that can be packaged into phage capsids. By looking at the biological role of the gene involved in escape of defense systems, hypotheses on how the Abi mechanisms disrupt the phage's replication cycle can be inferred. Unfortunately, where the AbiK mechanism acts in phage replication remains inconclusive as Sak3 has many potential unconfirmed biological roles.

1.4.4 Proposed Mechanisms

Over the years, many mechanisms for AbiK have been proposed (**Figure 1-9**). The AbiK mechanism is believed to act before DNA replication and has a different mode of action depending on the infecting phage as DNA replication is not detected in P335 phages but is detected in 936 phages (24, 30). The blockage of protein synthesis by AbiK has also been proposed (47). AbiK has also been hypothesized to produce a cDNA using an unknown template and unknown primer that is cleaved by endonucleases in cells (55). Upon phage infection, the Sak protein binds and protects this cDNA, which is then used to sequester phage mRNA and prevent phage protein production (55). This hypothesis has since been disproven, as AbiK is now known to have untemplated polymerization, so the produced cDNA cannot effectively target a phage RNA (1).

Further studies hypothesized a nuclease activity that is present in the carboxy terminal region of the AbiK protein. This hypothesis stems from polymerases commonly containing endonuclease domains, such as DNA polymerases containing nuclease domains for proofreading

and group II intron proteins containing nuclease domains (62). In addition, RNA cleavages mediated by type III CRISPR-Cas systems, the ToxIN system, the AbiA, and the AbiQ systems result in cell death, showing that indiscriminate RNA cleavage is an effective Abi mechanism (45, 49, 50). Studies looking for RNase activity in the AbiK protein showed a potential carboxy terminal RNase activity (3' - 5') and an odd slow migrating band that was formed on an RNA substrate when a portion (residues 359 – 599) of AbiK's carboxy terminal region was produced and incubated with an RNA substrate (2). These studies remained inconclusive, and AbiK's crystal structure revealed that the carboxy terminal region of AbiK likely has an accessory role rather than a catalytic function, providing evidence against this theory (57).

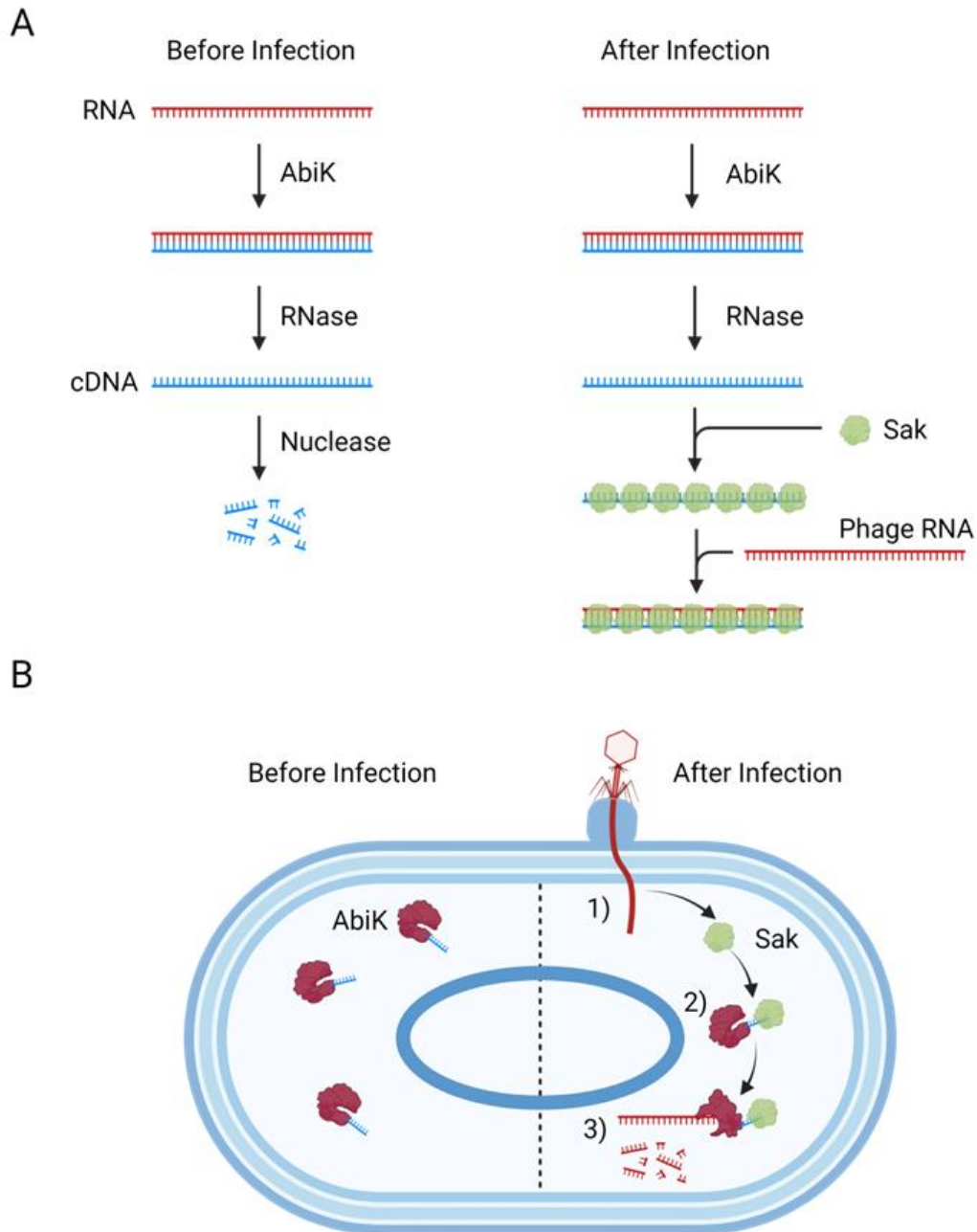


Figure 1-9: Proposed mechanisms for AbiK.

A: Proposed mechanism of AbiK by Bouchard et al. in 2004 (55). Before infection, AbiK uses an RNA template to make a strand of cDNA. The template RNA is degraded by an RNase and the cDNA is degraded by cellular nucleases. After phage infection, Sak binds to the cDNA preventing nuclease digestion, allowing the cDNA to be used to sequester phage RNA and prevent transcription of phage genes. **B:** Proposed mechanism of AbiK by Soufi in 2019 (2). Before infection, AbiK is constitutively expressed in cells, covalently attached to a self-polymerized ssDNA. After phage infection (1), the produced Sak phage protein binds to the ssDNA on AbiK (2), causing a conformational change in the AbiK protein (3). This conformational change reveals a nuclease activity, allowing for nonspecific degradation of phage and host RNA, resulting in cell death. Created with BioRender.com.

1.5 Objectives of This Study

It remains inconclusive how the AbiK mechanism is inhibiting phage replication. As more Abi systems are discovered, there is a plethora of possible mechanisms leading to Abi. Despite years of studies on AbiK and Sak proteins, the exact mechanism leading to the arrest of phage replication remains unclear. My thesis has two main objectives:

1. Uncover what happens during the AbiK mechanism at the cellular level and identify what step(s) AbiK is interfering with during the phage's life cycle. Experiments were done to:
 - a. Analyze overall phage propagation during these systems.
 - b. Detect if phage DNA replication is occurring.
 - c. Look at phage and global gene transcription during these systems.

Based on previous studies, phage DNA replication as well as phage gene transcription are expected to be detected during this study, which uses lactococcal phage p2 (a 936-group phage) to infect *L. lactis* (30, 59).

2. Analyze the AbiK protein biochemically, to determine the priming site of AbiK, and to also conduct protein modeling using protein structure prediction programs to make a hypothesis for possible functions of the protein.

Based on previous studies, the priming site for AbiK is hypothesized to be in the amino-terminal portion of the protein, and the carboxy-terminal domain of the AbiK protein is hypothesized to have nucleolytic activity (2).

Experiments described in chapters 2 and 3 cover the first objective, and experiments described in chapter 4 cover the second objective. Based on resulting data, a hypothesis for the AbiK mechanism can be formulated.

Chapter 2 : Phage Infection Dynamics and Kinetics of DNA Production

2.1 Introduction

Abortive infection defense mechanisms are frequently suicidal systems, where the death of an infected cell ensures the survival of the remaining population. It can be difficult to determine how an abortive infection mechanism works, as the mechanism causing cell death can be difficult to discern. The abortive infection K (AbiK) mechanism is one such defense mechanism, and despite being discovered in 1997, studies have not resolved the mechanism of cell death (24). During the AbiK mechanism, DNA replication was shown using Southern blotting to not occur in lactococcal phage ϕ 36 or phage P335 (both of the P335 species of phages), although there was evidence for DNA replication in lactococcal phage p2 and phage P008 (both of the 936 species of phages) (24, 30).

One hypothesis on the mechanism of cell death resulting from AbiK is that the AbiK protein can reverse transcribe viral RNA and block protein synthesis in the cell through an unknown mechanism, resulting in cell death (47). However, AbiK was demonstrated to possess polymerization activity that is atypical for a reverse transcriptase, and instead polymerizes a non-templated single-stranded DNA molecule, presumably using its own amino acid as a primer (1). This unique biochemical activity conflicts with the proposed hypothesis, leaving AbiK's mode of action unknown.

This chapter serves as the foundation for examining the events that occur within infected cells during a wild-type infection of *Lactococcus lactis* (*L. lactis*) by lactococcal phage p2 and what changes during the AbiK mechanism. The infection of AbiK⁺ cells by the mutant *sak3* (M90I) phage is also examined to see how the mutant phage can overcome and bypass the AbiK mechanism. Initial experiments aim to optimize infection conditions for downstream

experiments, which involve analyzing phage DNA replication during these conditions. In examining the infection dynamics and whether or not phage DNA replication occurs during these infections, clues can be obtained to narrow down the AbiK mechanism's mode of action to prevent phage propagation.

2.2 Aims

The goal of the experiments described in this chapter was to determine the infection dynamics for the infection of *L. lactis* by lactococcal phage p2 (p2) as well as to examine the DNA kinetics during infection. Preliminary experiments were done to look at which strain of *L. lactis* should be used, the effect of the AbiK protein on bacterial cell growth, and the optimal temperatures and multiplicity of infections (MOI) to use during infection. Following this work, adsorption assays were conducted to determine how long it took for phages to adsorb to cells. One-step growth curves were then done for both p2 and the *sak3* mutant (M90I) of p2 to determine how long the infection cycle takes. Once all this information was obtained, the DNA kinetics during infection were analyzed to see if DNA replication was occurring under three different conditions: normal wild-type infection, the AbiK infection and the escape of the AbiK infection mediated by the *sak3* mutant phage. Viability assays were also done to confirm if AbiK is truly an abortive infection system resulting in cell death. Collectively, these data give information into the infection dynamics of lactococcal phage p2 and what changes occur to the infection dynamics during the AbiK mechanism and when escape of the AbiK infection is mediated by the *sak3* mutant phage.

2.3 Results and Discussion

2.3.1 Optimal Infection Conditions

2.3.1.1 *Lactococcus lactis* strains, plasmids, and bacteriophage selection

Two different strains of *L. lactis* were available to use in studies looking at the AbiK mechanism. *L. lactis* strain LM0230 was used to host the pSRQ800 plasmid, the native plasmid where AbiK was discovered (**Figure 2-1A**) (24). Other open reading frames found in pSRQ800 were found to affect the transcription of *abiK*, and many inverted repeats were detected in *abiK*'s promoter region, suggesting regulation of the operon, making the plasmid valuable to study (24).

However, the AbiK mechanism is more effective when expressed in a high-copy number vector (24). *L. lactis* strain MG1363 was used to host the pSRQ823 (pAbiK) plasmid, where *abiK* was cloned into the high-copy number vector pNZ123, which has a 10-fold higher copy number than the pSRQ800 plasmid (**Figure 2-1A**) (24). *L. lactis* strain MG1363 was chosen for the *in vivo* studies due to its complete genome sequence being available (Accession number NC_009004). Downstream experiments involved RNA-Sequencing (RNA-Seq), so the availability of the complete genome was an asset to readily identify hits. An empty plasmid was constructed, named pΔAbiK, is used as a negative control where *abiK* was deleted from the pSRQ823 plasmid (**Figure 2-1A**).

Lactococcal phage p2 was selected for *in vivo* experiments because it can infect *L. lactis* strains LM0230 and MG1363. In addition to the wild-type (WT) lactococcal phage p2, a mutant form of the phage, containing a mutation in the *sak3* gene (M90I) was used to examine how the mutant phage can bypass the AbiK mechanism. An overview of the systems studied in this chapter and their respective phenotypes is shown (**Figure 2-1B**).

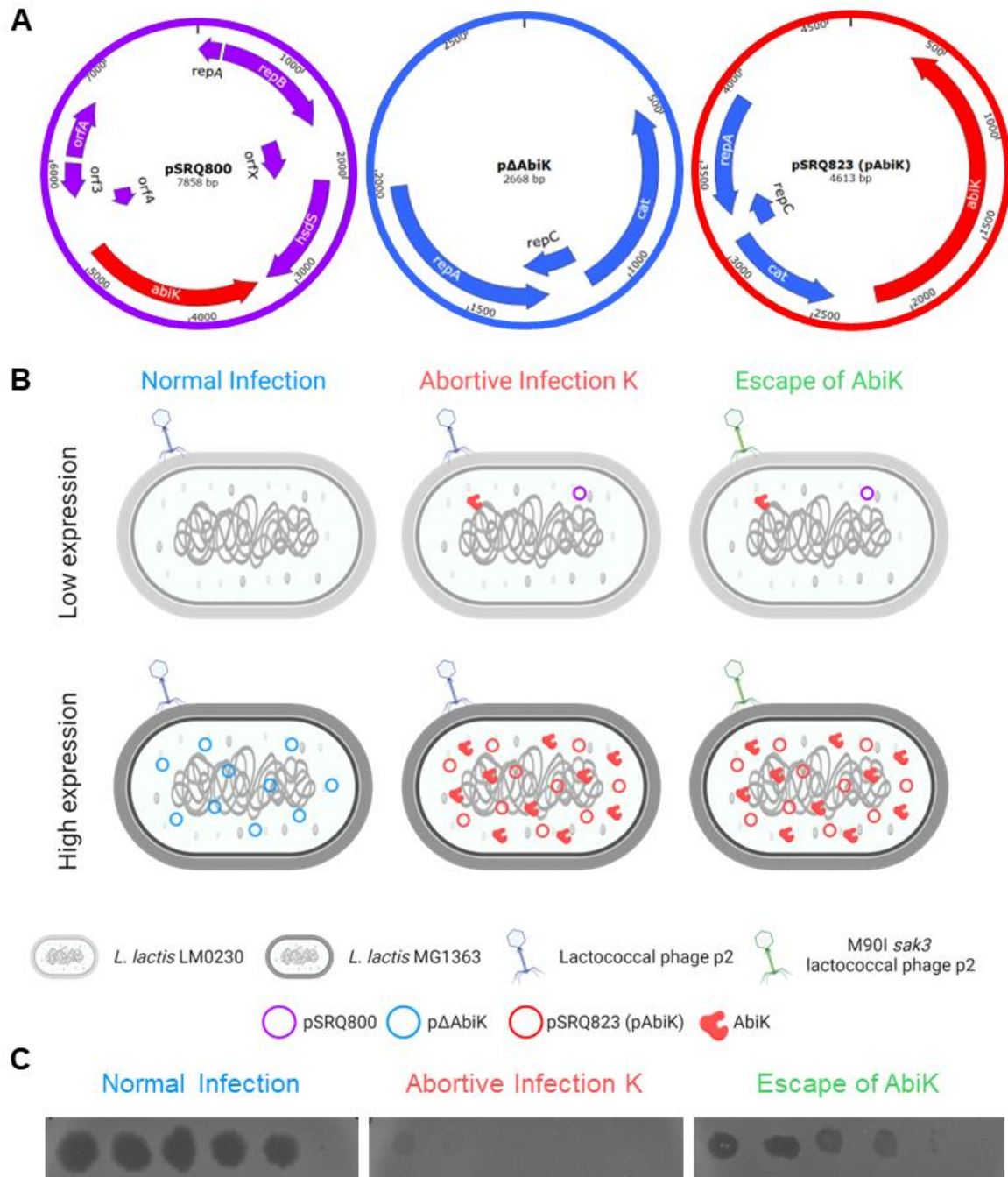


Figure 2-1: Major experimental conditions of this study.

A: Plasmid maps for pSRQ800, pΔAbiK and pSRQ823 (pAbiK). The *abiK* gene is coloured red, with pSRQ800-specific genes coloured purple and pNZ123-specific genes coloured in blue. Plasmid maps were generated using Snapgene. **B:** Schematic representing the experimental conditions used in this study, including cell strains, phages, and plasmids involved in each condition. Created with BioRender.com. **C:** Phage spot assay showing the observed phenotypes of the experimental conditions used in this study. Ten-fold serial dilutions of lactococcal phage p2 (stock titer = 1×10^9 PFU/mL) were spotted on bacterial lawns of *L. lactis* strain MG1363 pΔAbiK (AbiK⁻ cells) or MG1363 pAbiK (AbiK⁺ cells) for the normal infection and abortive infection K condition, respectively. Serial dilutions of mutant M90I *sak3* lactococcal phage p2 (stock titer = 1×10^8 PFU/mL) were spotted on bacterial lawns of *L. lactis* strain MG1363 pAbiK (AbiK⁺ cells) for the escape of AbiK condition.

2.3.1.2 Effect of *AbiK* expression on cell growth

For both the pSRQ800 plasmid and the pSRQ823 (pAbiK) plasmid, the *abiK* gene is expressed constitutively (24). The difference between the two plasmids is that pSRQ800, being a low-copy plasmid, would result in a lower expression of *abiK* than the high-copy pAbiK plasmid. In addition, inverted repeats that may be involved in transcriptional control of the *abiK* gene in the pSRQ800 plasmid are absent in the pAbiK construct, resulting in a lower expression of *abiK* in the pSRQ800 plasmid (24). It was of interest to see if expression of the *abiK* gene would affect cell growth, so the optical density at 600 nm (OD₆₀₀) of the cells was analyzed over time with and without the *abiK* gene, in addition to comparing the low and high expression number vectors. This experiment was done at two different temperatures, 30°C for *L. lactis*' optimum cell growth, and 25°C to see how a lower temperature would further affect cells.

In the low expression system using LM0230 cells, AbiK⁺ cells grew slower than AbiK⁻ cells during the logarithmic phase at both 30°C and 25°C (**Figure 2-2**). Although significant (**Figure 2-3**), this slowed growth was minimal, and both AbiK⁺ cells and AbiK⁻ cells reached the stationary phase at the same time. In the high expression system using MG1363 cells, AbiK⁺ cells lag significantly in their growth compared to AbiK⁻ cells during the logarithmic phase, ultimately reaching the stationary phase three hours after AbiK⁻ cells at 30°C (**Figure 2-2**). However, this lag in growth is not significant during the exponential phase of growth (**Figure 2-3**). At 25°C, this effect is more evident, with AbiK⁺ cells not reaching the stationary phase within the allotted experiment time of 16 hours (**Figure 2-2**).

In the low expression system, *abiK* gene expression in cells is not consequential for cells. There is a slight delayed growth in AbiK⁺ cells, but this can be explained by the presence of the plasmid in cells. When *abiK* is highly expressed, AbiK⁺ cells grow much slower than the AbiK⁻

counterpart. One explanation is that cells are focusing on protein production of AbiK rather than cell growth. Alternatively, high quantities of the AbiK protein in cells could lead to toxicity, leading to the delayed growth.

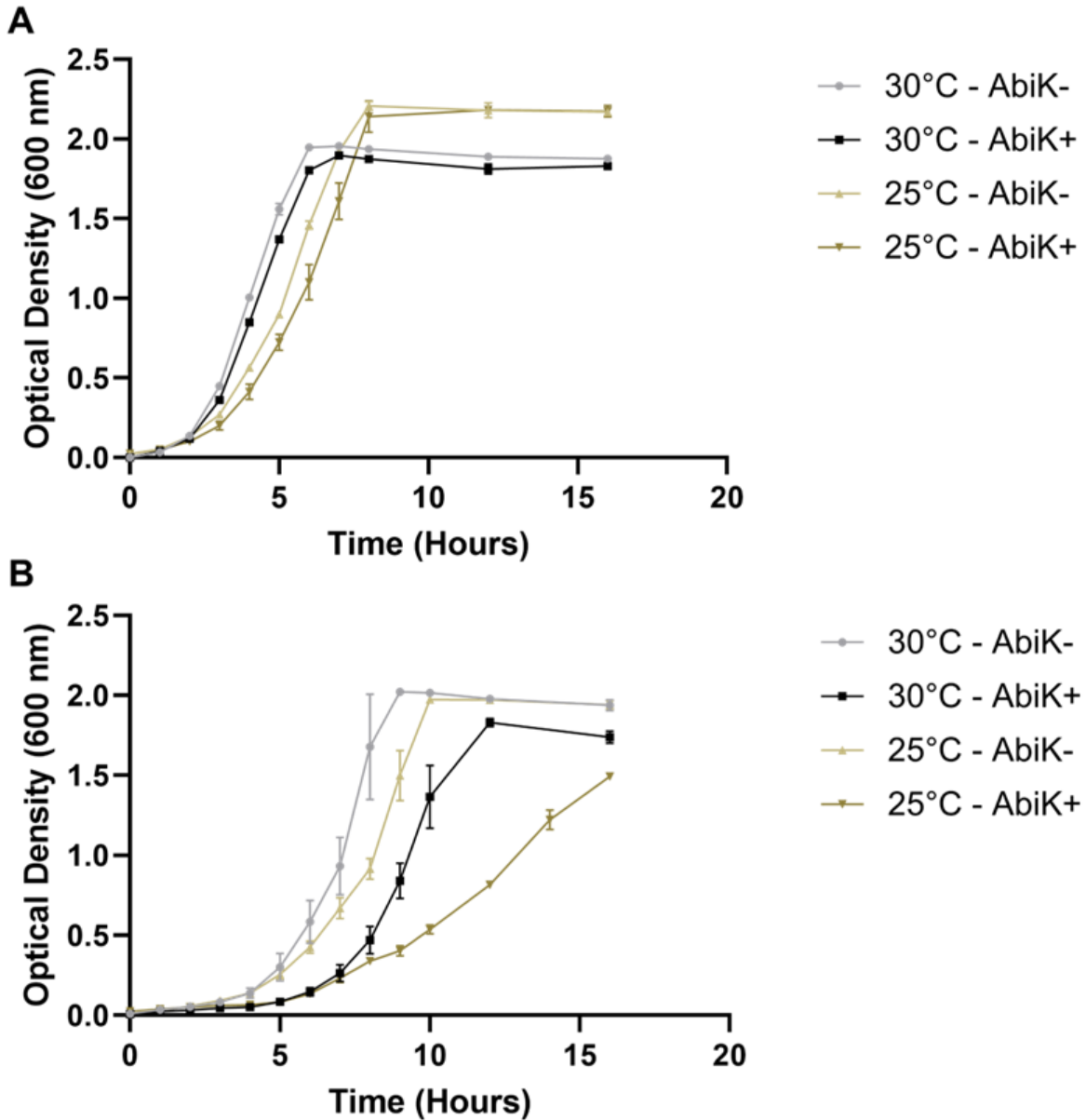


Figure 2-2: Effect of AbiK expression on cell growth.

Optical density (600nm) measurements of *L. lactis* strain LM0230 (A) and *L. lactis* strain MG1363 (B) with and without the presence of the *abiK* gene at two different temperatures. Cells were grown at 30°C in GM17 – 10 mM CaCl₂, and with 25 µg/mL chloramphenicol (Cm) for MG1363 cells. Values are the means of three replicates and error bars represent standard error of the mean (SEM). Missing error bars are due to small SEM values.

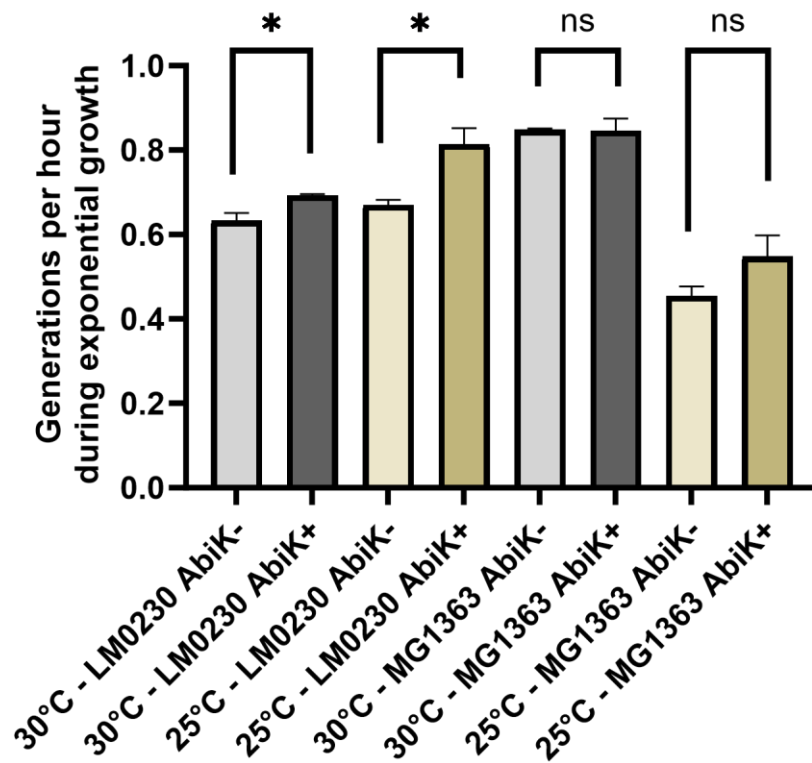


Figure 2-3: Exponential growth rate of *L. lactis* cells.

Growth rates during the exponential phase of growth were calculated for the effect of AbiK expression on cell growth using the equation $N = N_0 \times 2^n$. Values are the means of three replicates and error bars represent standard error of the mean (SEM). The t-test was used to determine significance at $p = 0.05$.

2.3.1.3 Multiplicity of infection determination

In nature, the chance of a viral infection starting is very rare as it depends on the probability of a virus being able to find and properly attach to its host (63). In a laboratory environment, the probability of a virus finding its host is increased by manipulating the ratio of viruses to hosts. The MOI refers to the ratio of viruses to hosts that are successfully adsorbed, attached, and infecting the host cells. Determining the MOI allows standardization, ensuring consistency between replicates and among experiments.

Titration experiments using different MOIs of lactococcal phage p2 were done with sensitive AbiK⁻ cells of both *L. lactis* strain LM0230 and *L. lactis* strain MG1363 pΔAbiK to determine which MOI could be used in downstream experiments to allow all cells to be infected and lysed synchronously. The chosen MOI was determined by the minimal MOI that resulted in the quickest lysing of host cells, measured by taking OD₆₀₀ measurements over time.

For both *L. lactis* strains LM0230 and MG1363, the minimal MOI that led to the quickest clarification of the lysate was 20 (**Figure 2-4**). With lower MOIs, such as 10, there was a lag in the clarification of the lysate, showing that not all cells were infected from the initial inoculation of the phage (**Figure 2-4**). For LM0230, it took one hour for the lysate to clarify. For MG1363 pΔAbiK, it took 1.5 hours for the lysate to clarify. The MOI of 20 that was obtained from the titration experiments is very high in comparison to literature, where MOIs range from 3 to 6 (24, 59). It is likely that the phages were not given enough time to adsorb onto cells, causing a much higher MOI in these experiments compared to the literature.

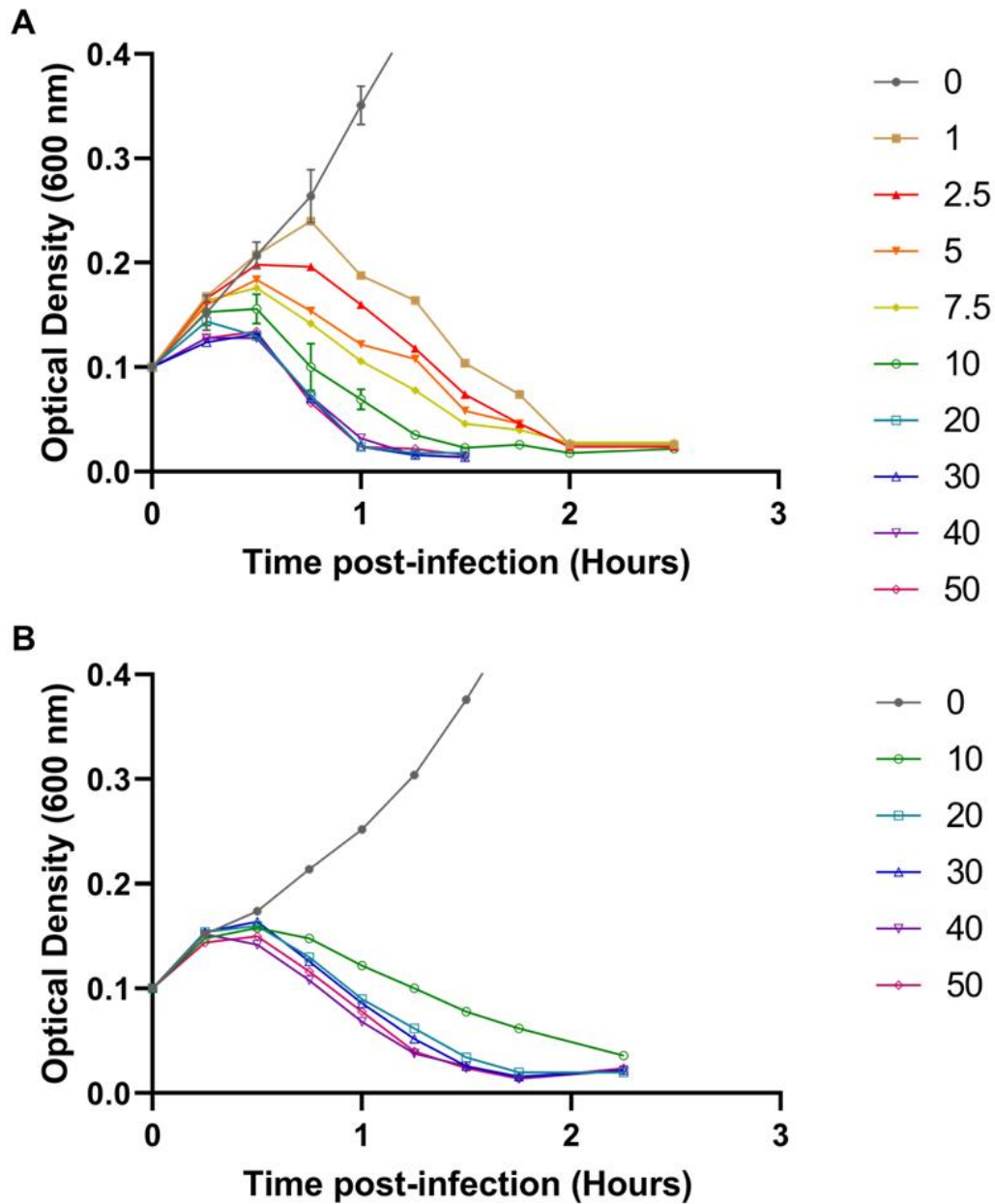


Figure 2-4: Multiplicity of infection titration.

Multiplicity of infection (MOI) titration of lactococcal phage p2 infecting (A) *L. lactis* strain LM0230 and (B) *L. lactis* strain MG1363 pΔAblK. Cells were infected with varying concentrations of lactococcal phage p2 to yield different MOIs, and values are optical density (600 nm) measurements taken post-infection. Cells were grown at 30°C in GM17 – 10 mM CaCl₂, and with 25 μg/mL chloramphenicol for MG1363 pΔAblK cells. Negative controls without phage (MOI=0) were also performed. Values are from single replicates, other than MOI 0 and 10 of lactococcal phage p2 infecting *L. lactis* strain LM0230, where the values are the means of two replicates and error bars represent standard error of the mean (SEM).

2.3.1.4 Infection dynamics

The infection dynamics during a normal infection, during abortive infection K, and during the escape of abortive infection K were studied. Lysis curves were done by measuring the OD₆₀₀ post-infection for the three different conditions. This was done with both the low and high expression systems in *L. lactis* strain LM0230 and *L. lactis* strain MG1363, respectively. Cells were infected by phage at an MOI of 7.5 for the low-expression system (due to human error), or an MOI of 20 for the high-expression system. Controls without phages infecting the system were done as well, to confirm normal cell growth in the absence of the phages. The results for both the low- and high- expression systems are shown in **Figure 2-5**.

For the low-expression system, the optical density decreases 15 minutes post-infection, with a complete clarification of the culture 1-hour post-infection during the normal infection. The same was seen with the escape of AbiK infection. Interestingly, during the AbiK infection, the OD₆₀₀ stopped changing 30 minutes post-infection, staying stagnant for nearly 3 hours post-infection before increasing again. Unexpectedly, the OD₆₀₀ started decreasing 6 hours post-infection, possibly due to phages mutating in real time and overcoming the AbiK mechanism over the course of the experiment. The controls with no phages added to the culture grew normally, hitting their stationary phase 5 hours post-infection time.

The same patterns were seen in the high-expression system. For both the normal infection and the escape of AbiK infection, the optical density started to decrease 30 minutes post-infection with a complete clarification 2.5 hours post-infection. For the AbiK infection, rather than seeing an arrest in change of the optical density, the cells continue to grow at a slow pace. The cells continue to grow slowly for 6 hours post-infection, before hitting their exponential

growth and then reaching the stationary phase 11 hours post-infection. The controls with no phages added hit their stationary phases 5 hours post-infection.

During the AbiK mechanism, cell growth is either arrested or host cells are dying at a similar rate to that at which uninfected cells are growing. Both outcomes would lead to the trend seen on the lysis curves. With the high MOI used in experiments, it is expected that all cells are infected at the addition of the phage. If cells die because of the abortive infection mechanism, a clarification of the lysate is expected when all cells are infected. It is possible that not all cells became infected when the phage was added, as it was known from adsorption assay experiments that the phages do not instantly adsorb to cells (2.3.1.5), so the remaining uninfected population could continue to thrive and grow at the same rate that infected cells were dying. If all cells are infected at the addition of the phage, however, then the trend seen could be explained by an arrest of cell growth as infected cells combat the phage infection. This would imply that AbiK is not an abortive infection mechanism, but another form of phage defense that arrests cell growth. To clarify what is occurring during the abortive infection mechanism, viability assays were performed to uncover if cells die because of the AbiK mechanism (2.3.2).

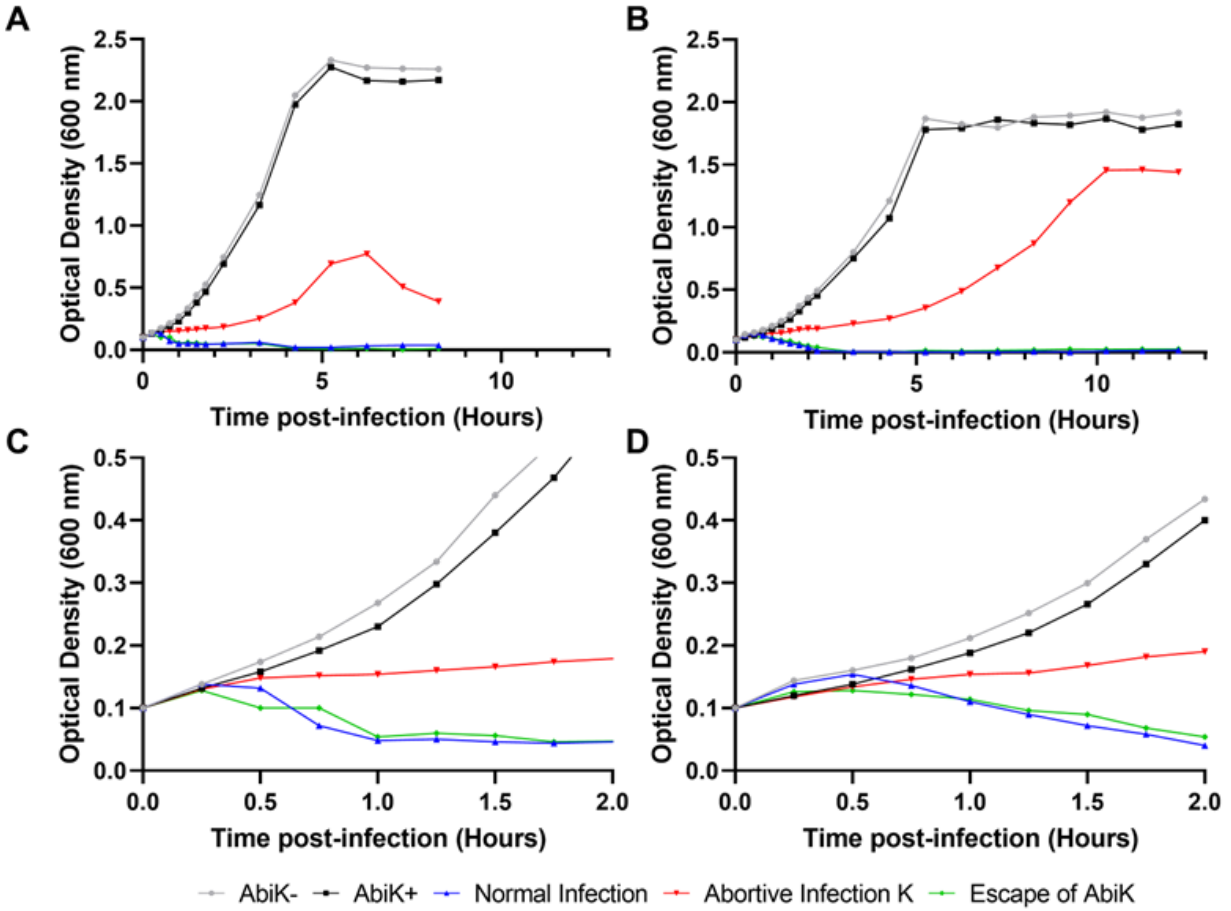


Figure 2-5: Lysis curves of *L. lactis* cells.

Lysis curves during the (A) low-expression system and the (B) high-expression system. The first two hours post-infection is enlarged for the (C) low- and (D) high- expression systems. LM0230 cells were infected with an MOI of 7.5 and MG1363 cells were infected with an MOI of 20 of either lactococcal phage p2 or M90I *sak3* lactococcal phage p2. Negative controls without phages (AbiK- and AbiK+) were performed. For the normal infection, lactococcal phage p2 infected AbiK- cells. For abortive infection K, lactococcal phage p2 infected AbiK+ cells. For the escape of AbiK, mutant M90I *sak3* lactococcal phage p2 infected AbiK+ cells. Values are optical density (600 nm) measurements taken post-infection. Cells were grown at 30°C in GM17 – 10 mM CaCl₂, and with 25 µg/mL chloramphenicol for MG1363 cells. Values are from single replicates.

2.3.1.5 Adsorption assays

As part of the first step of a virus's life cycle, it must find and adsorb to the host cell (63). Viruses must bind to their host receptors, and the affinity of the virus attachment protein to its receptor on the host cell dictates how quickly this can occur (64). Due to the MOI titration yielding an MOI much higher than that used in literature (**2.3.1.3**), it was of interest to see how long it took for phages to adsorb to the bacterial cell. Poor adsorption of the phage results in a high MOI during titration, as only a small percentage of phages start the infection when added to the culture. With additional time for adsorption, more host cells are infected when time points are taken for experiments.

The amount of extracellular infectious phages was measured for 20 minutes post-inoculation. At specific time points post-inoculation, aliquots of infected cells were treated with chloroform, allowing only extracellular phages to be measured, as chloroform disrupts bacterial membranes and kills them via lysis. Treated aliquots were titered to quantify the amount of extracellular phage at each time point, with the reduction in extracellular phage reflecting phages that adsorbed and infected cells.

From the adsorption assay, the amount of extracellular phage drops below 10% at 12.5 minutes post-infection (**Figure 2-6**). At 15 minutes, the amount of free phage starts to increase, corresponding to phage progeny that are released by lysed cells (**Figure 2-6**). For downstream experiments, phages were allowed to adsorb for 10 minutes post-inoculation, ensuring 80% of phages are infecting cells and unadsorbed phages were washed away, synchronizing the infection. Giving time for phages to adsorb also reduces the number of phages that need to be added at infection. An MOI of 0.001 – 0.002 was used for adsorption, one-step growth curve, qPCR, and RT-qPCR experiments, to ensure infected bacteria are infected with only a single

phage. It is important to note that downstream experiments (one-step growth curve, qPCR, RT-qPCR and RNA-Seq experiments) dictate 0 minutes post-infection as the first measurement taken. This measurement occurs after adsorption is allowed and cells are spun down, so it is truly 15-20 minutes post-infection. The adsorption rate constant, k , of lactococcal phage p2 to its MG1363 host was calculated to be 1.36×10^{-9} mL/min according to calculations and methods determined in Chapter 15 of Bacteriophages Methods and Protocols (65).

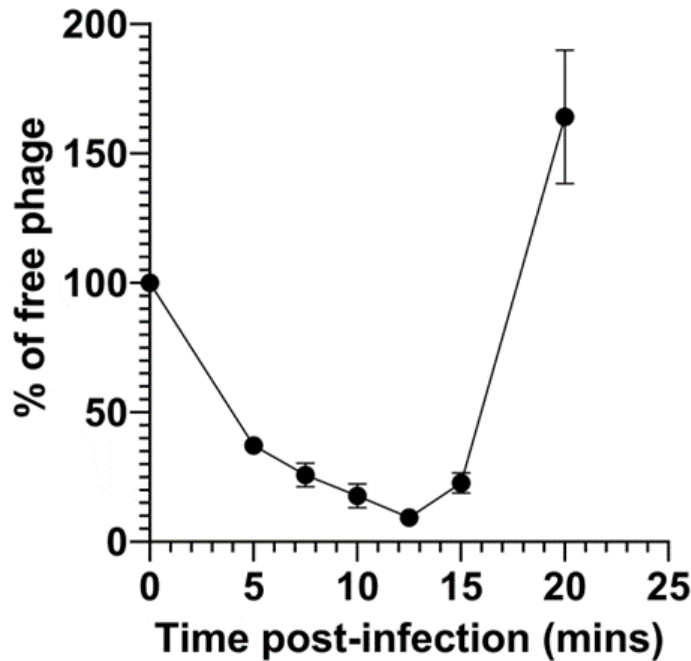


Figure 2-6: Adsorption assay of lactococcal phage p2 infecting MG1363.

Adsorption assay of lactococcal phage p2 infecting *L. lactis* strain MG1363. Values are the percentage of free phage, calculated by dividing the PFU/mL of extracellular phages at each time point by the PFU/mL at the time of infection (time = 0 minutes). Cells were grown at 30°C in GM17 – 10 mM CaCl₂, and then infected by lactococcal phage p2 at an MOI of 0.001 – 0.002. Values are the means of three replicates, and error bars represent standard error of the mean (SEM). Missing error bars are due to small SEM values.

2.3.1.6 One-step growth curves

From the adsorption assays, phage progeny can be seen being released as early as 15 minutes after the initial inoculation (**Figure 2-6**). It is important to know the total timing of the infection and how long it takes for phage progeny to be released, and more detailed information can be obtained using a one-step growth curve. From one-step growth curves, one can obtain the eclipse and latent periods of the phage, which is the time from infection to mature virus being made and the time from infection to mature virus being released, respectively (65). In addition, one can obtain the burst number, which is the number of phages released per infected cell (65). Obtaining this information is vital for understanding the timing of the phage's life cycle.

For the one-step growth curves, phages were allowed to adsorb for 10 minutes following inoculation at an MOI of 0.001, before unadsorbed phages were washed away by centrifugation. This was done to ensure one synchronous infection, as unadsorbed phages were prevented from infecting later. Post-infection, two aliquots were removed at set time points, with one aliquot being treated with chloroform to analyze the extracellular phages and one aliquot left untreated to analyze the total number of phages. Three sets of one-step growth curves were analyzed. The first set was the infection by wild-type lactococcal phage p2 of the sensitive MG1363 host. The second set was the infection by *sak3* mutant (M90I) lactococcal phage p2 of the sensitive MG1363 host to see if the mutant phage was less efficient at producing phage progeny. The last set was the infection by *sak3* mutant (M90I) lactococcal phage p2 of AbiK⁺ MG1363 cells, also known as the escape of AbiK, to see if any further changes in the mutant phage's infection cycle occurred due to the AbiK mechanism.

The primary set of one-step growth curves looked at the wild-type infection by wild-type lactococcal phage p2 of the sensitive MG1363 host. From this, the eclipse period was determined

to be 0-10 minutes, as an increase in intracellular phage after 10 minutes post-infection is seen (**Figure 2-7A**). The latent period ranges from 10-25 minutes, as extracellular phages are detected as early as 10 minutes post-infection, and the burst per infected cell was 123 ± 43 phages (**Figure 2-7A**). The burst size was calculated by dividing the total number of phages at 40 minutes post-infection by the total number of phages at 0 minutes.

The *sak3* mutant (M90I) lactococcal phage p2 was less efficient at making phage progeny, as it takes 30 minutes before there is an increase in intracellular phages (**Figure 2-7B**). Extracellular phages can be seen as early as 20 minutes post-infection, continuing to increase for 40 minutes post-infection (**Figure 2-7B**). Only 60% (73 ± 9 phages) of phage progeny are released compared to the wild-type infection, showing a smaller burst size (**Figure 2-7B**). During the escape of the AbiK mechanism by the mutant phage, the efficiency of the mutant phage in making progeny is unchanged. However, far fewer (18 ± 19 phages) phage progeny are released per infected cell, showing a 7-fold decrease in released progeny (**Figure 2-7C**). Even though the mutant phage can bypass the AbiK mechanism, the AbiK mechanism continues to drastically inhibit the mutant phage's ability to make viable progeny.

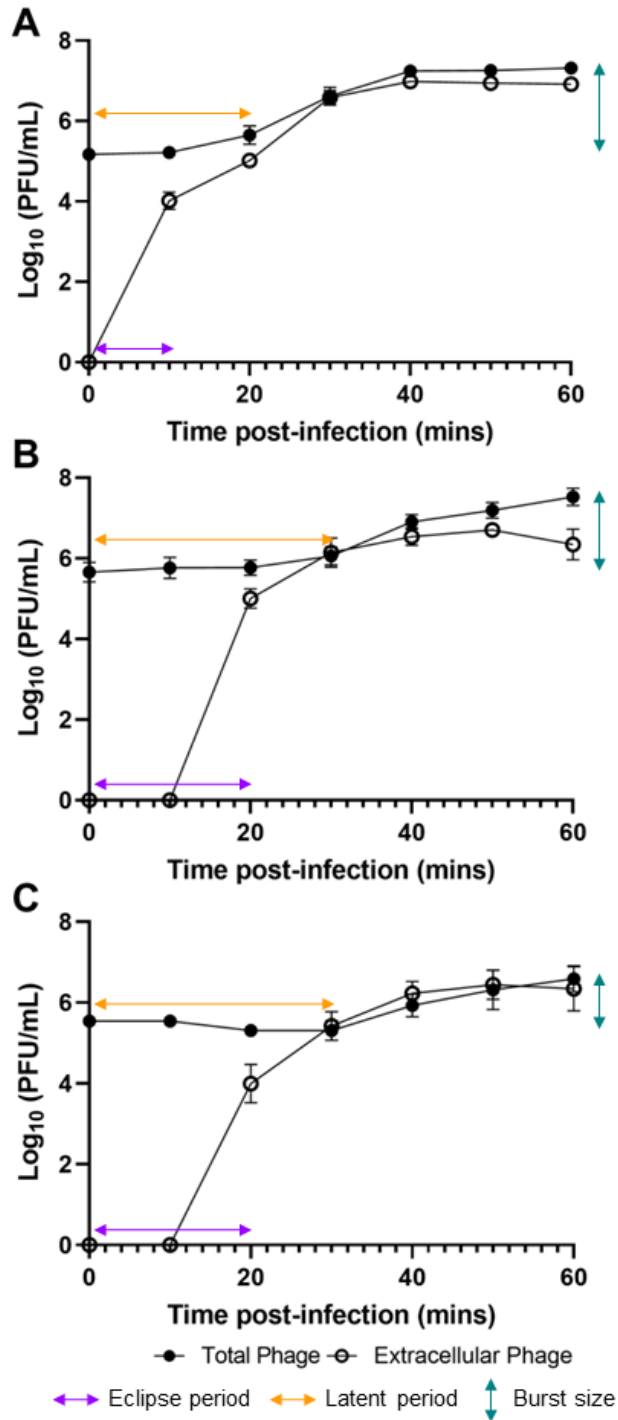


Figure 2-7: One-step growth curves.

One-step growth curves of lactococcal phage p2 infecting *L. lactis* strain MG1363 (A), mutant *sak3* (M90I) lactococcal phage p2 infecting *L. lactis* strain MG1363 (B), and mutant *sak3* (M90I) lactococcal phage p2 infecting *L. lactis* strain MG1363 pAbiK (C). Values are the log₁₀(PFU/mL) at different time points. Cells were grown at 30°C in GM17 – 10 mM CaCl₂, and with 25 µg/mL chloramphenicol for MG1363 pAbiK cells and then infected by phage at an MOI of 0.001 – 0.010. Values are the means of three biological replicates and error bars represent standard error of the mean (SEM). Missing error bars are due to small SEM values.

2.3.2 Viability Assay

During the AbiK mechanism, the OD₆₀₀ of infected cells stopped changing 30 minutes post-infection, staying stagnant for nearly 3 hours post-infection (**Figure 2-5**). It is unknown if the cell growth is arrested or if host cells are dying at a similar rate to that at which uninfected cells are growing, as both would result in the optical density staying stagnant. A cell survivability assay was performed, where infected and uninfected cells were enumerated at different time points post-infection, to detect if cells were dying due to the abortive infection K mechanism. From this assay, there was no growth of infected cells at any time points post-infection, which matches previous results (**Figure 2-8**) (24). Although cells containing the AbiK protein do not produce phage progeny post-infection, the mechanism results in cell death.

The AbiK mechanism resulting in cell death remains uncertain, because it is plausible that mutant phage progeny that are resistant to the AbiK mechanism could remain in samples and kill cells during enumeration. To eliminate the possibility of phage infection by mutant resistant phages being the cause of cell death, attempts were made to control when phages could adsorb to cells and therefore infect cells. Lactococcal phage p2 requires calcium to be able to adsorb to cells and when calcium is not present, it is not able to adsorb to the host cell and start the infection (66). Knowing this, attempts were made to control the calcium concentration in the culture by using ethylene glycol-bis(β -aminoethyl)-N,N,N',N'-tetraacetic acid (EGTA), which can chelate calcium ions and prevent the phage from using it to adsorb. However, these experiments added another level of complexity as calcium is required for the *L. lactis* cells to grow properly and EGTA was found to inhibit growth of the cells, so these experiments were halted (67).

The AbiK protein is known to be constitutively expressed in cells, but it is unknown how the AbiK mechanism that results in cell death is activated. The Sak3 protein is known to be involved in this mechanism, so it has been hypothesized that the Sak3 protein activates the AbiK protein which can then lead to cell death (1). Based on this hypothesis, the AbiK and Sak3 proteins can be coexpressed in cells to see if cells are viable when both proteins are present. This has previously been done, and the initial presence of Sak3 has improved the efficacy of the AbiK mechanism upon phage infection, rather than causing cell death (55). Experiments were commenced to confirm or deny these previous findings.

The AbiK protein is constitutively expressed using the pSRQ823 plasmid, so cloning *sak3* under the control of an inducible promoter was conducted. An inducible promoter allows for control of the expression of *sak3*, and thereby controlled activation of the AbiK mechanism. Attempts were made to clone the *sak3* gene into the pTRKH2 vector, which is a shuttle cloning vector that allows the cloning to be performed in *Escherichia coli* (*E. coli*) before being shuttled to *L. lactis*. Despite several attempts, the *sak3* gene cloned into the pTRKH2 vector was unable to produce colonies containing the correct construct in *E. coli*. Cloning attempts were then done directly in *L. lactis* instead, and one potential colony was formed. Cultures from this colony grew three times slower than *L. lactis* containing the empty vector but attempts to confirm if the correct construct was made were not successful, so it is unknown if the clone was obtained.

Experiments were unable to check if Sak3 was activating the AbiK mechanism in cells, and if the AbiK mechanism causes cell death in the absence of a phage infection. Future experiments could involve imaging of cells post-infection to see what cells look like and compare with AbiK⁻ cells that die from phage infection. This would allow for phenotypic differences to be directly observed visually, rather than enumerating viable cells.

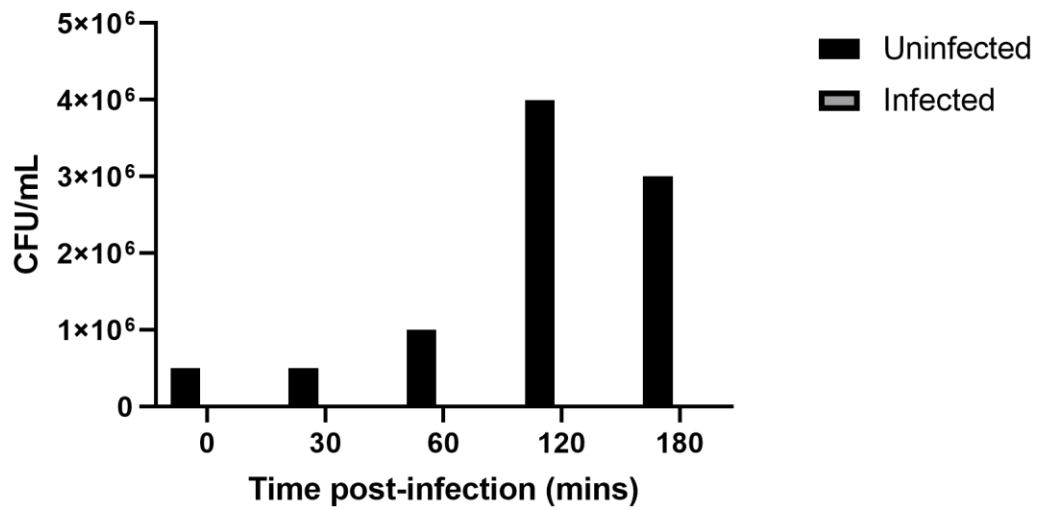


Figure 2-8: Cell survivability assay.

Cell survivability assay of lactococcal phage p2 infecting *L. lactis* strain MG1363 pAbiK. Values are the CFU/mL at different time points post-infection. Cells were grown at 30°C in GM17 – 10 mM CaCl₂ with 25 µg/mL chloramphenicol and then infected by phage at an MOI of 20. No colonies were recovered from infected cells, as explained in the text above. Values are from single replicates.

2.3.3 DNA Kinetics of Phage Infection: Southern Blots

The DNA kinetics during a wild-type infection, abortive infection K, and during the escape of abortive infection K were analyzed. Based on the infection dynamics (2.3.1.4) and the MOI titrations (2.3.1.3), experiments were designed to analyze how the quantities of phage DNA changed for 3 hours post-infection with an MOI of 20. The high expression system was studied using two biological replicates, and samples were analyzed using Southern blots. Southern blots are advantageous as the entire digested genome can be analyzed on one blot with multiple probes, in addition to estimations of the quantities of the genome (68). DNA extracted samples were digested by restriction enzymes EcoRI and HindIII, producing discrete bands to be detected on an agarose gel, and then via probes on a membrane (**Figure 2-9**). Two probes were used for the analysis, one spanning open reading frames (ORF) 15-17 on the phage genome, called probe 3, which was used to analyze overall quantities of phage DNA (**Figure 2-10**). The other probe spans the *cos* site and ORF 1 of the phage genome, called probe 7-1, and was chosen to detect circular immature forms of the DNA generated during replication as well as linear mature forms of the DNA that are ready for DNA packaging into the phage (**Figure 2-11**). Probes targeting regions of the phage genome were made by cloning fragments of the phage genome into a commercial vector, pBluescript KS II+, which possesses a T7 promoter that is used by T7 RNA polymerase to make radioactive RNA probes by incorporating [α -³²P] UTPs (2.5.10.2).

Blots were probed with probe 3, which spans the late gene ORF's 15-17. This probe only binds to one digestion product of the phage genome, allowing for simple quantification of phage DNA at the different time points (**Figure 2-10**). Relative DNA quantities, obtained by dividing the intensity of the band by the average of all the band intensities, were plotted as a bar graph

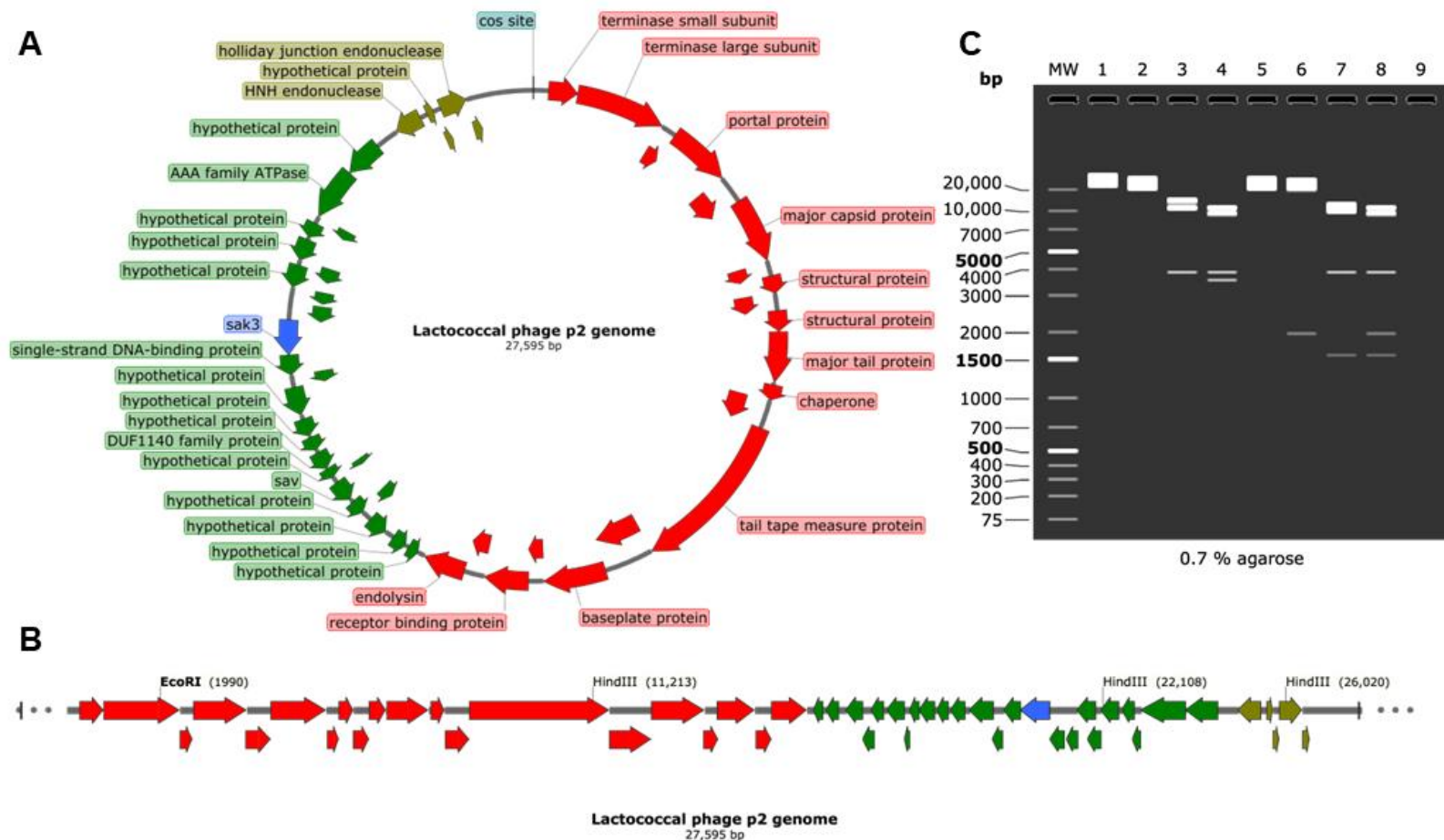


Figure 2-9: Lactococcal phage p2 genome.

Circular (A) and linear (B) schematics of the lactococcal phage p2 genome. Early genes are coloured in green, middle genes are coloured in olive, late genes are coloured in red, and the *sak3* gene is coloured in blue. The *cos* site and genes are labeled (A). Restriction enzyme sites used in Southern experiments are shown (B). C: A simulated agarose gel of digestion of lactococcal phage p2 genome in circular immature (lanes 1-4) and linear mature (lanes 5-8) forms is shown. Lanes contain undigested DNA (lanes 1 and 5), digestion with EcoRI (lanes 2 and 6), digestion with HindIII (lanes 3 and 7), and double digestion with EcoRI and HindIII (lanes 4 and 8). Genome maps and the simulated agarose gel were generated using Snapgene.

(**Figure 2-10**). In the normal infection, DNA quantities increase at 45 minutes post-infection and stay high for the remainder of the experiment (**Figure 2-10**). This is also seen in the escape of AbiK condition, but DNA quantities increase later at 90 minutes post-infection (**Figure 2-10**). Interestingly, DNA is not seen to accumulate during the AbiK condition, as quantities of DNA stay stable throughout the course of the experiment (**Figure 2-10**).

During the phage replication cycle, DNA gets injected into host cells in a linear form, before it is circularized and undergoes DNA replication (13). DNA replication products are circular when undergoing DNA replication, representing immature phage DNA (13). When phage progeny are assembled, the concatemeric and circular DNA then gets cleaved into mature linear products which are then packaged into the phage capsids (13). Mature and immature forms of phage DNA were analyzed using a probe that would span the *cos*, or circularization, site of the phage genome, called probe 7-1 (**Figure 2-11**). This probe bound to three digestion products: the slowest migrating band representing the immature circular form of the phage DNA where the *cos* site is annealed, and two fragments representing the mature linear form of the phage DNA when the *cos* site isn't annealed. Theoretically, during the normal infection, quantities of the immature form of phage DNA should be seen accumulating and then decreasing as the DNA is processed into its mature form. This was not the case as all three forms could be detected at all time points, with no indication of the immature or mature forms being favoured (**Figure 2-11**). Further densitometry analysis also did not yield the expected results, and the data remained unclear (**Supplementary Figure 1**). *Cos* sites are known to spontaneously bind, so another experiment was done where samples were treated at 65°C to melt the *cos* sites before running samples on a gel, and the same result was achieved (**Supplementary Figure 2**).

Compared to the normal infection, the mutant phage in the escape of AbiK condition accumulates DNA more slowly, indicating that the presence of AbiK or the mutant Sak3 protein affects DNA replication of the phage genome. Further evidence is the lack of phage DNA accumulation over the course of the AbiK infection, which leads to speculation that AbiK could be arresting DNA replication. However, the Southern blot experiments analyzed DNA quantities over the course of 3 hours and DNA in the normal infection was not seen to increase until 45 minutes post-infection (**Figure 2-10**), which contradicts the knowledge that phage progeny are formed within 10 minutes post-infection (**2.3.1.6**). Although early time points post-infection were taken, the infection was not synchronous as unadsorbed phages remained in the culture, continuing to infect more host cells. The increase in DNA quantities that is seen is likely a result of the second or even third iteration of phage infections mediated by progeny that were released after previous infections. In addition, Southern blotting as a method to detect DNA quantities was not accurate enough to discern what was occurring at these early time points. Lastly, due to the method of sample collection, total DNA in the culture is extracted, making it hard to discern what was occurring within cells and what form the phage DNA adopted throughout the course of infection.

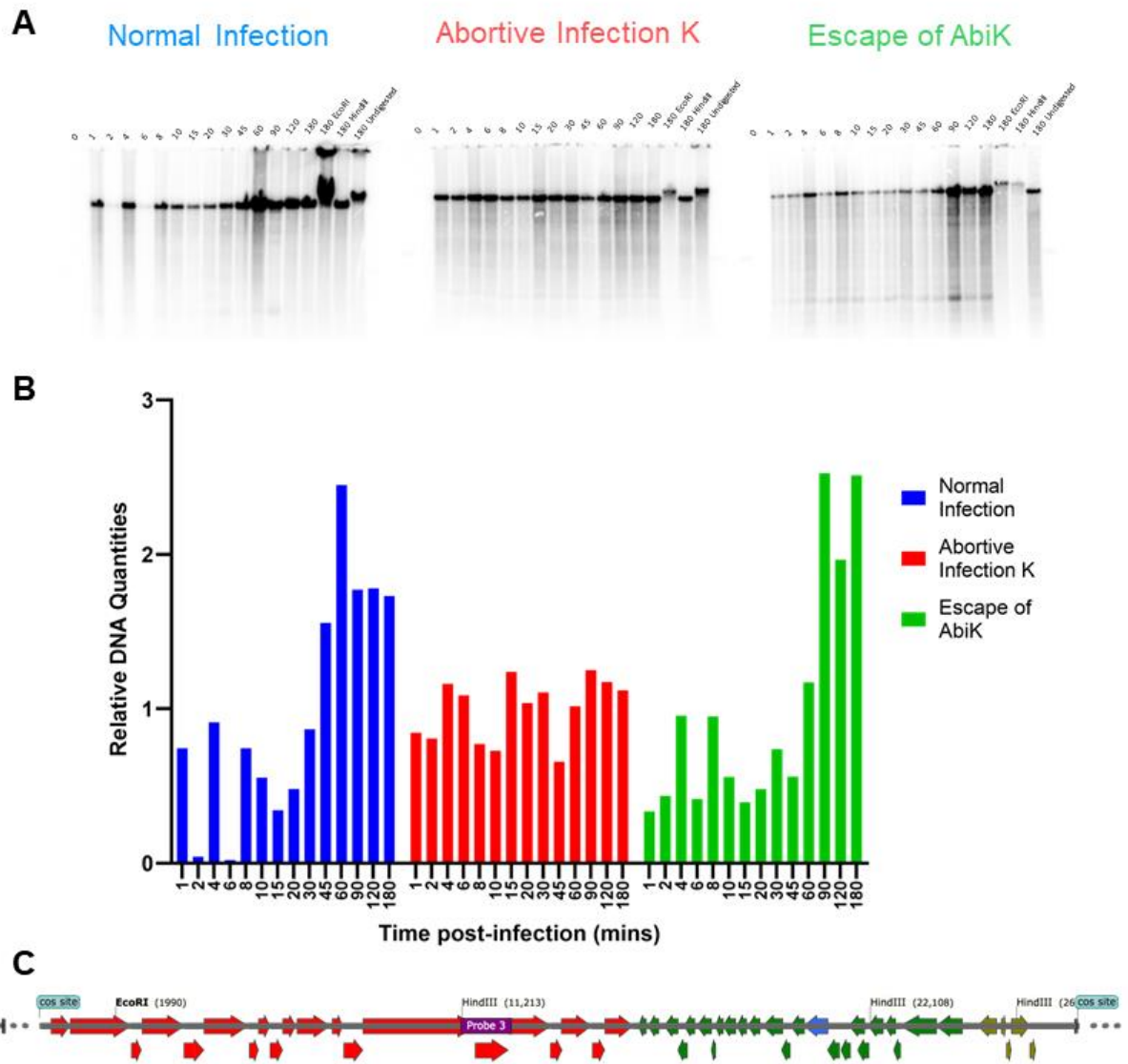


Figure 2-10: Southern blot with probe 3.

A: Southern blot hybridization of DNA extracted from time points post-infection. DNA samples were double digested with EcoRI and HindIII restriction enzymes before electrophoresis and transfer to a Hybond-XL (Amersham) membrane, followed by hybridization by probe 3. For the normal infection, lactococcal phage p2 infected AbiK⁻ cells. For abortive infection K, lactococcal phage p2 infected AbiK⁺ cells. For the escape of AbiK, mutant *sak3* (M90I) lactococcal phage p2 infected AbiK⁺ cells. Negative controls without phages (time = 0 minutes) were performed. Undigested and single digestion (EcoRI and HindIII) controls were performed. **B:** Bar graph of the relative DNA quantities from time points post-infection. Values were obtained by densitometry analysis of Southern blots, where the band intensity was divided by the average of all band intensities. **C:** A linear schematic of the lactococcal phage p2 genome showing restriction enzyme sites used in Southern experiments and where probe 3 (purple) binds. Genome map was generated using Snapgene.

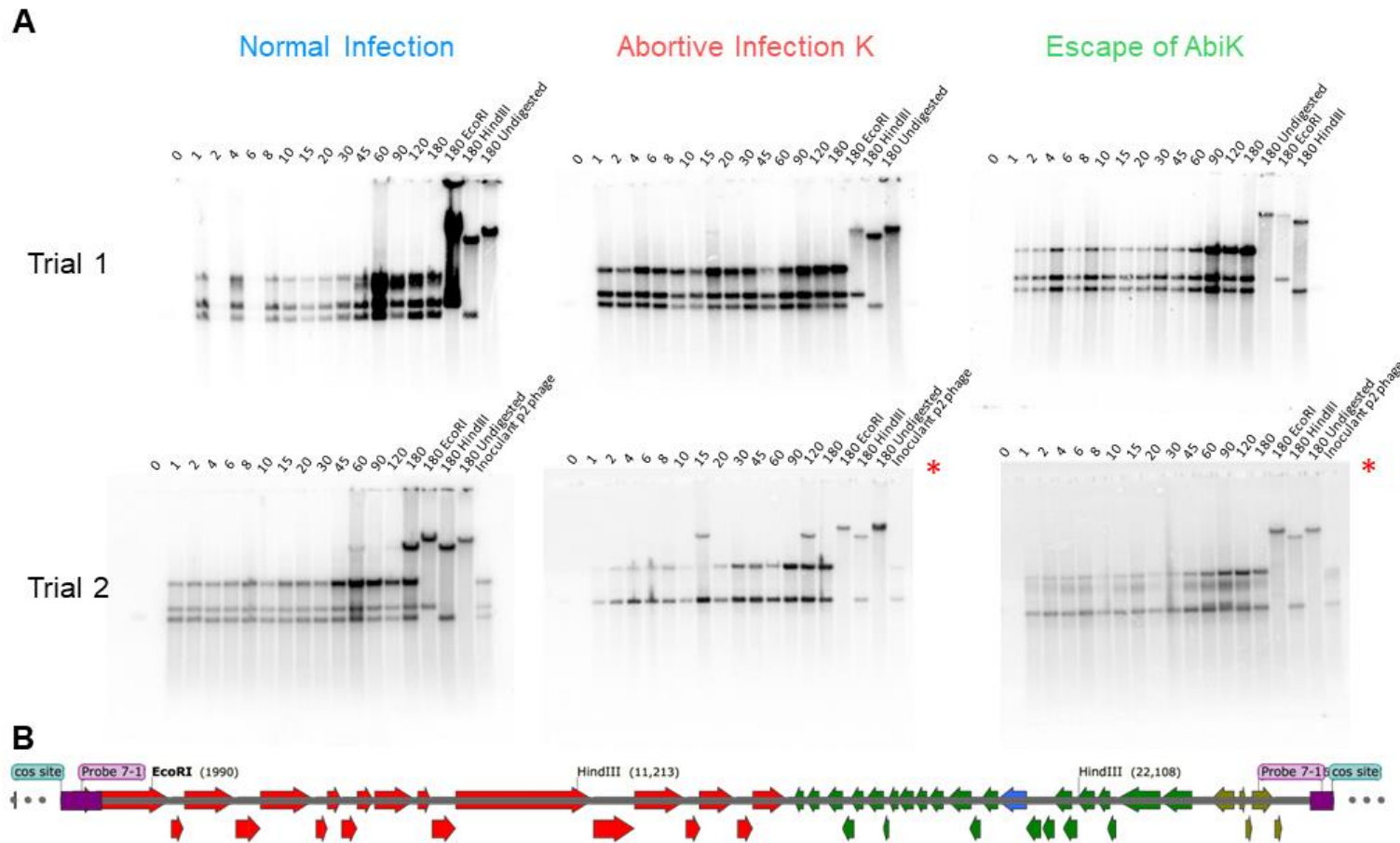


Figure 2-11: Southern blot with probe 7-1.

A: Southern blot hybridization of DNA extracted from time points post-infection. DNA samples were double digested with EcoRI and HindIII restriction enzymes before electrophoresis and transfer to a Hybond-XL (Amersham) membrane, followed by hybridization by probe 7-1. For the normal infection, lactococcal phage p2 infected AbiK⁻ cells. For abortive infection K, lactococcal phage p2 infected AbiK⁺ cells. For the escape of AbiK, mutant *sak3* (M90I) lactococcal phage p2 infected AbiK⁺ cells. Negative controls without phages (time = 0 minutes) were performed. Control using inoculant phage was performed in trial 2. Undigested and single digestion (EcoRI and HindIII) controls were performed. Blots marked with a red star had incomplete EcoRI digestion. **B:** A linear schematic of the lactococcal phage p2 genome showing restriction enzyme sites used in Southern experiments and where probe 7-1 (purple) binds. Genome map was generated using Snapgene

2.3.4 DNA Kinetics of Phage Infection: qPCR

To obtain a more accurate view of DNA quantities during the phage infection, DNA was analyzed using qPCR, or quantitative PCR. qPCR is a high-throughput and sensitive method that can detect gene copies in an entire sample, using DNA-binding fluorophores (69). As the template is amplified with primers, the amount of DNA in the reaction is quantified, allowing the user to calculate the gene copy number in the original sample (69). Primers were designed to target 2 genes in the lactococcal phage p2 genome, the capsid, and the baseplate (**Figure 2-12**). The primers produced PCR products around 100 base pairs in length and were checked for amplification in a PCR reaction (**Supplementary Figure 3**). To allow for a synchronous infection, phages were allowed to adsorb onto host cells for 10 minutes before unadsorbed cells were washed away, and due to the nature of how samples were collected, only intracellular DNA was collected and analyzed.

Genome copies of phage DNA were detected using capsid primers (**Figure 2-12**). During the normal infection, phage DNA was seen to start accumulating immediately post-infection, peaking at 25 minutes, and then decreasing until 35 minutes post-infection before increasing again (**Figure 2-12**). The accumulation of DNA in samples shows that the phage is undergoing DNA replication, and the decrease corresponds to DNA that was packaged and released in new phage progeny. This data correlates with data obtained from the one-step growth curves, where new phage progeny are released between 10-25 minutes post-infection (**2.3.1.6**). The increase in DNA quantities 40 minutes post-infection corresponds to the next wave of phage infection.

For the escape of AbiK condition, DNA quantities increase immediately post-infection (**Figure 2-12**). However, DNA quantities do not decrease with a release of phage progeny. Instead, DNA quantities peak at 25 minutes, staying stagnant until they increase again 40

minutes post-infection (**Figure 2-12**). This is explained by the one-step growth curves, that show an 11-fold decrease in phage progeny being released compared to the wild-type infection (**2.3.1.6**). Since the *sak3* mutant phage is less efficient at making progeny compared to its wild-type counterpart, DNA is accumulating in cells and not being packaged into phage progeny. DNA quantities were not seen to accumulate during the AbiK infection, showing that the phage is unable to replicate its DNA during the AbiK mechanism (**Figure 2-12**). The same conclusions can be made when the quantities of DNA were detected using the baseplate primers (**Figure 2-12**).

Analysis from both Southern blots and qPCR have shown that phage DNA is not replicating during the AbiK mechanism, suggesting that the AbiK mechanism is disrupting the phage's ability to replicate its DNA. The *sak3* mutant (M90I) phage can bypass this, and allow for DNA replication to continue, although DNA packaging is less efficient than in the wild-type phage.

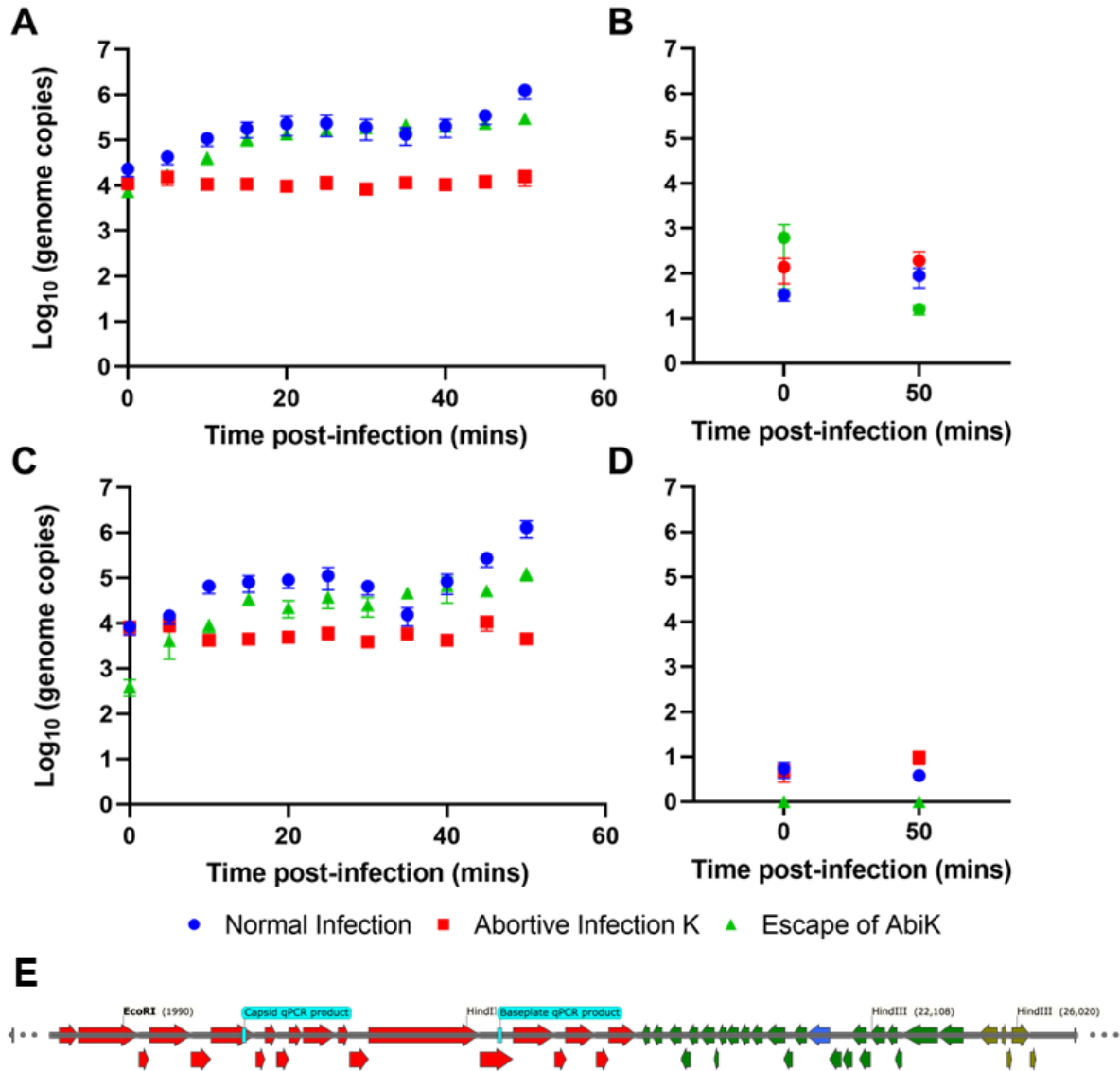


Figure 2-12: qPCR to detect DNA replication.

Log of genome copies of DNA extracted from time points post-infection analyzed by qPCR primers targeting the capsid gene (A) and primers targeting the baseplate gene (C) For the normal infection, lactococcal phage p2 infected AbiK⁻ cells. For abortive infection K, lactococcal phage p2 infected AbiK⁺ cells. For the escape of AbiK, mutant *sak3* (M90I) lactococcal phage p2 infected AbiK⁺ cells. Negative controls without phages were performed at time points 0 minutes and 50 minutes using primers targeting the capsid gene (B) and primers targeting the baseplate gene (D). Genome copy number was per 5 μ L of DNA extract. Values are the means of three biological replicates with two technical replicates each, and error bars represent standard error of the mean (SEM). Missing error bars are due to small SEM values. E: A linear schematic of the lactococcal phage p2 genome with the qPCR primer targets (cyan). Genome map was generated using Snappgene.

2.3.5 Comparison to Literature

A one-step growth curve for lactococcal phage p2 using *L. lactis* strain MG1363 as a host was previously done (70). In their findings, lactococcal phage p2 has a latent period of 35.5 minutes and a burst size of 129 ± 17 phages, whereas this study found the latent period to range from 10 to 25 minutes with a burst size of 123 ± 43 phages; these numbers were quite similar to the published values when the adsorption times are taken into account (70). Emond et al. also showed mutant phages have a longer latent period of 50 minutes and a reduced burst size by 15-fold, similar to the findings in this study (24).

A cell survivability assay was previously done to see if the abortive infection K mechanism resulted in cell death. Emond et al. showed that post-infection, only 2% of infected cells survived the AbiK mechanism (24). A 0% survivability rate of infected cells was found here, as no viable cells were detected at any time point taken post-infection. Although this study was able to replicate previous studies, it remains unclear how accurate the method is to detect cell survivability, as mutant phages could remain in the culture, killing cells.

Phage DNA replication was not detected during the abortive infection K mechanism from either Southern blot analysis and qPCR analysis. Previous studies have shown that during the AbiK mechanism, DNA replication was not occurring for P335 phages but does occur for 936 phages (24, 30). The results from this study directly go against what was shown previously, as DNA replication is not seen from lactococcal phage p2, a 936 phage. As replication of the phage DNA has been shown to both occur and not occur in previous studies, it is possible that the AbiK mechanism does not target DNA replication but instead a different step of phage replication. However, many trials were done in this study, confirming that phage DNA replication does not

occur during the AbiK mechanism implying that AbiK has a role in inhibiting phage DNA replication.

2.4 Conclusions

Although the mechanism of cell death due to the AbiK mechanism remains elusive, information about what happens within cells during the mechanism has been revealed. Timings of the phage infection for both the wild-type lactococcal phage p2 and the *sak3* mutant lactococcal phage p2 were settled using the one-step growth curve, and the mutant phage was seen to be less efficient at making phage progeny, in addition to having a drastically reduced burst size when the AbiK protein is present. During the AbiK mechanism, DNA replication of the phage DNA could not be detected from either Southern blot hybridization experiments and qPCR experiments, making the arrest of phage DNA synthesis a possible mode of action for the AbiK mechanism. The exact mechanism remains unknown, but it is known that phage DNA replication is restored when the *sak3* gene in the phage genome is mutated. One preliminary hypothesis is that AbiK disrupts a method of phage DNA replication involving the Sak3 protein, and when the Sak3 protein is non-functional due to a mutation, then the phage uses a different mode of DNA replication that AbiK cannot disrupt – bypassing the system. A viability assay was performed to see if cells truly die because of the AbiK mechanism. Cells did die, but as phages, and possibly mutant phages, were still present during the assay, it is difficult to ascertain that the reason for cell death was due to the AbiK mechanism.

2.5 Methods and Materials

2.5.1 General Protocols

2.5.1.1 Bacterial strains, plasmids, and growth conditions

Bacterial strains of *L. lactis* and *E. coli* used in this study are listed (**Table 2-1**). *E. coli* strains used for cloning were grown in lysogeny broth medium (LB) at 37°C with shaking and on LB-agar as streak plates at 37°C. *L. lactis* strains were grown in M17 broth medium supplemented with 0.5% (w/v) glucose (GM17) at 30°C and on GM17-agar as streak plates at 30°C (71). Compositions of each medium are included in **Appendix A**. For phage infections, GM17 medium was supplemented with 10 mM CaCl₂ to allow phages to adsorb to host cells (66, 72). Concentrations of antibiotics used to grow resistant strains of *E. coli* were 100 µg/mL for ampicillin (Amp) and 25 µg/mL for chloramphenicol (Cm). Concentrations of antibiotics used to grow resistant strains of *L. lactis* were 5 µg/mL for erythromycin (Ery) and 25 µg/mL for chloramphenicol (Cm). OD₆₀₀ of *E. coli* at 1.0 is 8×10^8 CFU/mL and OD₆₀₀ of *L. lactis* at 1.0 is 1×10^8 CFU/mL. Chemical competent and electrocompetent cells of *E. coli* were prepared as previously described (73). Electrocompetent cells of *L. lactis* were prepared as previously described (74).

2.5.1.2 Bacteriophage propagation

One lytic bacteriophage, lactococcal phage p2, was used in this study along with a *sak3* mutant form of the phage (59). Propagation of the phage was performed using previously described methods, with some modifications (75). An overnight culture of the sensitive host strain, *L. lactis* strain MG1363, was inoculated 1:100 into GM17 broth supplemented with 10 mM CaCl₂. Phage was inoculated into the culture at 1:200, either from a previous phage propagation or a phage stock treated with a few drops of chloroform. The infected culture was

incubated at 30°C until clarification of the lysate and was then filtered through a 0.45 µm Supor® PES filter and stored at 4°C, concluding the first propagation. The following day, an overnight culture of the sensitive host strain was inoculated 1:100 into fresh GM17 broth supplemented with 10 mM CaCl₂ and allowed to grow at 30°C to an OD₆₀₀ of 0.100. Once the culture reached the correct optical density, a 1:200 inoculation of the phage from the first propagation was added and the culture was incubated at 30°C. After full lysis, the culture was centrifuged at 12 000 x g for 10 minutes at 4°C to remove cellular debris, then filtered through a 0.45 µm Supor® PES filter and stored at 4°C for future use. Phages were titered by plaque assays using the agar double-layer technique, usually yielding 1 x 10⁹ PFUs/mL (76).

To obtain higher phage titers, phage lysate was filtered through Vivaspın® 20, 100 kDa MWCO PES Amicon filters. Aliquots of phage lysate were added to the filters, and the samples were spun at 3 400 x g for 90 minutes at 4°C, before removing the filtrate and adding another aliquot of lysate. Bacteriophage remains in the filtrate, concentrating the sample. This process was repeated until all phage lysate was filtered, and the total volume was one tenth of the original volume. The filtrate was then washed with four times the volume of phage buffer (20 mM Tris-HCl pH 7.4, 100 mM NaCl and 10 mM MgSO₄) and then collected before being filtered through a 0.45 µm Supor® PES filter and stored at 4°C. Phages were titered by plaque assays using the agar double-layer technique to confirm higher phage titers, usually yielding 1 x 10¹⁰ PFUs/mL (76).

Table 2-1: Strains and phages used in this study.

Strain, Plasmid, or Phage	Relevant Characteristics *	Source
<i>E. coli</i>		
DH5 α	<i>lacZ</i> Δ M15 <i>recA1 endA1 hsdR17</i>	Invitrogen
DH10b	<i>lacZ</i> Δ M15 <i>recA1 endA1 Str</i> ^R	Invitrogen
<i>L. lactis</i>		
LM0230	Plasmid-free host for phage p2	(47)
MG1363	Plasmid-free host for phage p2	(47)
LM0230 AbiK ⁺	LM0230 (pSRQ800), AbiK ⁺	(47)
MG1363 AbiK ⁻	MG1363 (p Δ AbiK), Cm ^R , AbiK ⁻	This study
MG1363 AbiK ⁺	MG1363 (pAbiK), Cm ^R , AbiK ⁺	This study
Bacteriophages		
Lactococcal phage p2	Phage with LM0230 and MG1363 hosts	(24)
Lactococcal phage p2 – M90I <i>sak3</i> mutant	Phage with LM0230 and MG1363 hosts, mutation in <i>sak3</i> gene (M90I)	(59)

* *lacZ* Δ M15, partial deletion of *lacZ* that allows α -complementation; *recA1*, mutation in recombination gene; *endA1*, mutation in endonuclease gene; *hsdR17*, mutation in methylation and restriction system genes; Str^R, streptomycin resistance; Cm^R, chloramphenicol resistance; Amp^R, ampicillin resistance; Ery^R, erythromycin resistance; AbiK⁻, lacking AbiK gene; AbiK⁺, AbiK gene present.

Table 2-2: Plasmids used in this study.

Strain, Plasmid, or Phage	Relevant Characteristics *	Source
Plasmids		
pSRQ800	Natural <i>L. lactis</i> plasmid encoding AbiK, AbiK ⁺	(24)
pSRQ823 (pAbiK)	<i>abiK</i> encoded in pNZ123, Cm ^R , AbiK ⁺	(1)
pSRQ823-AbiKCut (p Δ AbiK)	pSRQ823 with <i>abiK</i> deletion, Cm ^R , AbiK ⁻	This study
pTRKH2	Cloning vector, Ery ^R , Sak3 ⁻	Addgene (77)
pTRKH2- <i>sak3</i>	<i>sak3</i> gene in pTRKH2, Ery ^R , Sak3 ⁺	This study
pTRKH2-M90I <i>sak3</i>	Mutant <i>sak3</i> (M90I) gene in pTRKH2, Ery ^R , Sak3 ^{M90I+}	This study
pBluescript KS II (+)	Cloning vector, Amp ^R	Stratagene
Late 1-1	p2 ORF 1 in pBluescript KS II (+), Amp ^R	This study
Late 1-2	p2 ORFs 2-3 in pBluescript KS II (+), Amp ^R	This study
Late 2	p2 ORFs 3-10 in pBluescript KS II (+), Amp ^R	This study
Late 3	p2 ORFs 11-14 in pBluescript KS II (+), Amp ^R	This study
Late 4	p2 ORFs 15-17 in pBluescript KS II (+), Amp ^R	This study
Late 5	p2 ORFs 18-20 in pBluescript KS II (+), Amp ^R	This study
Early 1-1	p2 ORFs 21-24 in pBluescript KS II (+), Amp ^R	This study
Early 2-1	p2 ORFs 35-39 in pBluescript KS II (+), Amp ^R	This study
Middle 1	p2 ORFs 45-47 in pBluescript KS II (+), Amp ^R	This study

* Cm^R, chloramphenicol resistance; Amp^R, ampicillin resistance; Ery^R, erythromycin resistance; AbiK⁻, lacking AbiK mechanism; AbiK⁺, AbiK mechanism present; Sak3⁻, lacking *sak3* gene; Sak3⁺, *sak3* gene present; Sak3^{M90I+}, mutant *sak3* gene present.

2.5.1.3 DNA isolation and manipulation

Bacterial genomic DNA was extracted using EZ-10 Spin Column Genomic DNA Miniprep Kit, Bacteria (BioBasic) according to the manufacturer's protocol (78). Plasmid DNA was extracted using the EZ-10 Spin Column Plasmid DNA Miniprep Kit (BioBasic) or the High-Speed Plasmid Mini Kit (Geneaid Biotech Ltd.) according to the manufacturer's protocols (79, 80). Enzymes used for phosphorylation, PCR, restriction enzyme digestion and ligations were purchased from Invitrogen or New England Biolabs and were used according to the manufacturer's protocols. PCR reactions, digestion reactions, and ligation reactions were cleaned using the EZ-10 Spin Column PCR Products Purification Kit (BioBasic) when necessary (79). PCR products that were gel extracted were done using the EZ-10 Spin Column DNA Gel Extraction Kit (BioBasic) according to the manufacturer's protocol (79). Transformations of plasmid DNA into competent cells were performed as previously described (73). Agarose gel electrophoresis was performed as previously described using 0.7 - 1.1% (w/v) of agarose (Invitrogen) and gels were electrophoresed using either 1 x TAE or 1 x TBE buffer (**Appendix A**) (73). Sequencing of DNA samples was done by the University of Calgary Core DNA Services.

2.5.1.4 Phage DNA isolation

Phages were propagated according to the protocol in section **2.5.1.2**, before incubation with 0.25 mg of RNase A and 0.05 mg of DNase I for 1 hour at 37°C. Samples were then ultracentrifuged at 30 000 rpm for 2 hours at 4°C in the 45 Ti rotor in the Optima 100K ultracentrifuge (Beckman Coulter) to pellet phage particles. Pellets were then resuspended in 1 mL 0.05 M Tris-HCl pH 7.5 before phage DNA was isolated using the Phage DNA Isolation Kit (Norgen Biotek) according to the manufacturer's protocol (81).

2.5.1.5 Phenol extraction and ethanol precipitation

A 1/10 volume of 3 M sodium acetate pH 5.2 was added to samples for DNA extraction and an equal volume of 8 M ammonium acetate was added to samples for RNA extractions. UltraPure™ glycogen (1 µL of 20 µg/µL, Invitrogen) can be optionally added to act as a carrier for nucleic acids in ethanol. An equal volume of phenol:chloroform:isoamyl alcohol (25:24:1, v/v) was added to samples, which were then vortexed for 30 seconds. Samples were centrifuged at 14 000 x g for 10 minutes at room temperature, and then the aqueous layer was extracted to a new tube. The phenol extraction was repeated 1-2 more times depending on the purity of the sample, based on the lack of a protein interface. Three volumes of ice-cold 100% ethanol were added to samples, and samples were incubated at -70°C for a minimum of 20 minutes. Samples were centrifuged at 14 000 x g for 10 minutes at 4°C, and the supernatant was removed. One volume of ice-cold 70% ethanol was then added to the pellet before samples were centrifuged at 14 000 x g for 10 minutes at 4°C, and the supernatant was removed. Pellets were air-dried before being dissolved in Tris buffer (10 mM Tris-HCl pH 7.5) or TE buffer (10 mM Tris-HCl pH 7.5, 1mM EDTA).

2.5.1.6 Restriction enzyme and PCR cloning

In restriction enzyme subcloning, a plasmid and the target insert (either from PCR or through the source) have restriction enzyme sites that are cleaved and then ligated together by T4 DNA ligase (**Figure 2-13A**). Ligation products are then transformed into competent cells and screened for desired products. Desired inserts are analyzed for restriction enzyme sites compatible with the target plasmid. If no compatible restriction enzyme sites are available, primers with compatible restriction enzyme sites are designed to amplify the desired insert.

2.5.1.7 Tip-to-tail PCR cloning

Tip-to-tail PCR can be used to make deletions in plasmids by generating primers that amplify the entire plasmid around the desired deletion (**Figure 2-13B**). Before PCR, primers were phosphorylated using T4 DNA kinase according to the manufacturer's protocol. Primers were then used in PCR reactions, whose products were purified by gel extraction before ligation. Ligation products were then transformed into competent cells and screened for desired products.

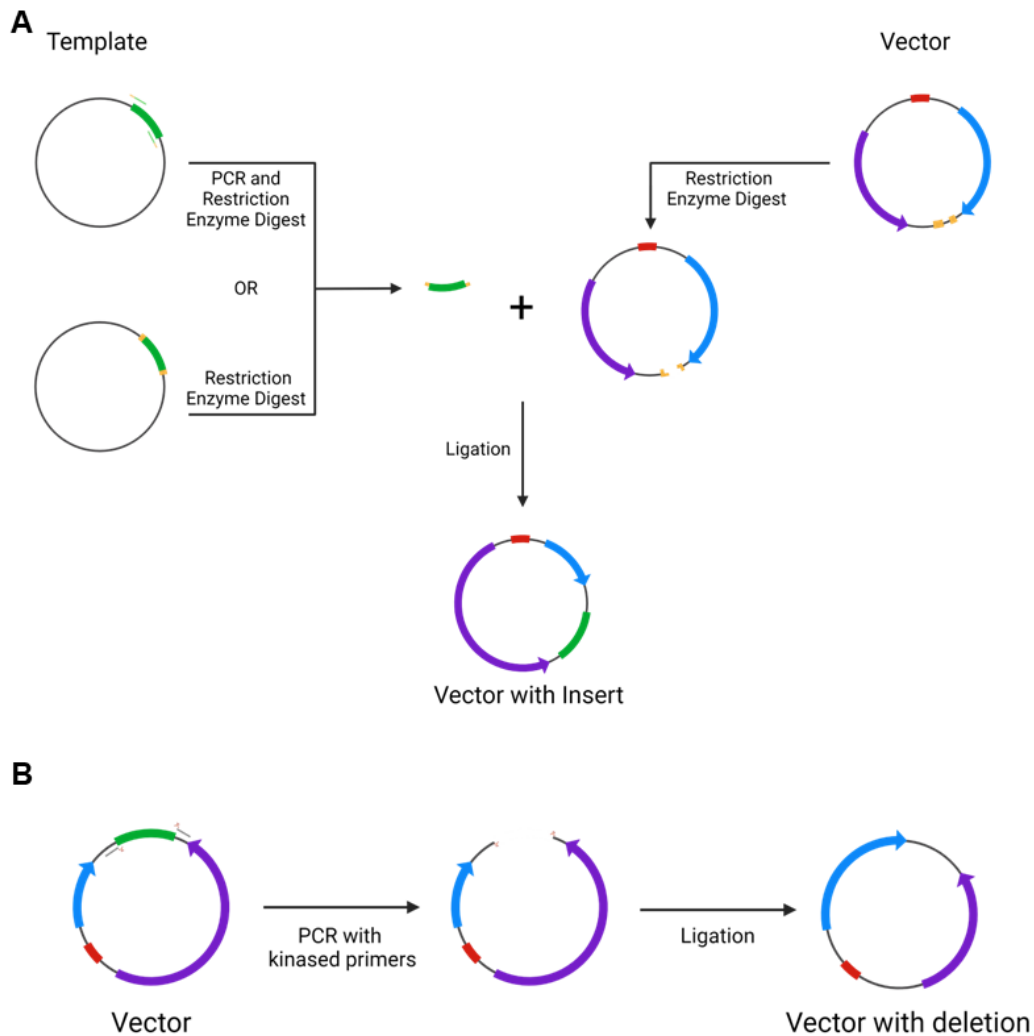


Figure 2-13: Schematic of cloning methods.

A: A schematic representation of restriction enzyme and PCR cloning. **B:** A schematic representation of tip-to-tail PCR cloning. Created with BioRender.com.

2.5.2 Bacterial Growth Curves

Overnight cultures made from single colonies of *L. lactis* were inoculated 1:100 into GM17 supplemented with 10 mM CaCl₂. Medium was supplemented with chloramphenicol (Cm) at 25 µg/mL when necessary. Cultures were grown at either 30°C or 25°C. Samples were withdrawn at hourly intervals for 8-10 hours, then every 2 hours until 16 hours post-inoculation. Optical density (600 nm, OD₆₀₀) measurements were recorded to observe the growth of bacterial cultures. Growth rates during the exponential phase of growth were calculated for the effect of AbiK expression on cell growth using the equation $N = N_0 \times 2^n$. The t-test was used to determine significant differences between growth rates at $p = 0.05$.

2.5.3 Multiplicity of Infection Titrations

L. lactis strains MG1363 and LM0230 were titered for colony forming units (CFU) per mL of culture at an OD₆₀₀ of 0.100 by counting colonies on agar plates with serial dilutions of culture samples. Quantities of phage required to obtain MOIs of 0, 1, 2.5, 5, 7.5, 10, 20, 30, 40 and 50 were calculated using plaque forming units (PFU) per mL of phages and CFU/mL of host cells. Overnight cultures made from single colonies of *L. lactis* were inoculated 1:100 into GM17 supplemented with 10 mM CaCl₂. Medium was supplemented with Cm at 25 µg/mL when necessary. Cultures were grown at 30°C until an OD₆₀₀ over 0.100 was achieved. Phages were diluted in fresh medium before being added to the culture, diluting the culture's OD₆₀₀ to 0.100. Samples were withdrawn every 15 minutes, and OD₆₀₀ measurements were taken until full lysis.

2.5.4 Bacteriophage Infection Curves

Overnight cultures made from single colonies of *L. lactis* were inoculated 1:100 into GM17 supplemented with 10 mM CaCl₂. Medium was supplemented with Cm at 25 µg/mL when necessary. Cultures were grown at 30°C until an OD₆₀₀ over 0.100 was achieved. Phages

were diluted in fresh medium for an MOI of 7.5 for the low expression system using strain LM0230 or an MOI of 20 for the high expression system using strain MG1363, then added to the culture. Samples were withdrawn every 15 minutes and OD₆₀₀ measurements were taken until full lysis, after which samples were withdrawn at hourly intervals for 8-12 hours post-infection.

2.5.5 Adsorption Assays

An overnight culture made from a single colony of *L. lactis* strain MG1363 was inoculated 1:100 into GM17 supplemented with 10 mM CaCl₂. Cultures were grown at 30°C until an OD₆₀₀ of 0.100 - 0.200 was achieved. An aliquot of culture was removed to obtain bacterial cell counts by plating serial dilutions of the culture onto GM17 agar plates.

Phages were diluted in fresh medium to a titer of 1×10^5 PFU/mL. 1 mL was added to a flask containing 9 mL of bacterial culture and 1 mL was added to a flask containing 9 mL of fresh medium. Both flasks were thoroughly mixed before being incubated in a water bath at 30°C. Samples (1 mL) were withdrawn at 5-, 7.5-, 10-, 12.5-, 15- and 20- minutes post-infection and added to fresh medium containing chloroform. Samples were vortexed for 10 seconds and then left on ice until all time points were collected. Samples were appropriately diluted and titered by plaque assays using the agar double-layer technique, and control samples from phages added to fresh medium were used to obtain titer counts pre-infection (76). The MOI for the adsorption assays ranged from 0.001 - 0.002. Three biological replicates were conducted.

2.5.6 One-step Growth Curves

Overnight cultures made from single colonies of *L. lactis* were inoculated 1:100 into GM17 supplemented with 10 mM CaCl₂. Medium was supplemented with Cm at 25 µg/mL when necessary. Cultures were grown at 30°C until an OD₆₀₀ of 0.150 was achieved in 10 mL of culture. The culture was centrifuged at 5 000 x g for 5 minutes at 4°C, and the pellet resuspended

in 9 mL of fresh medium. Phages were diluted in fresh medium to a titer of 1×10^5 PFU/mL and added to the culture, mixed gently, and then incubated at 30°C for 10 minutes to allow phages to adsorb to host cells. Cultures were centrifuged at 5 000 x g for 5 minutes at 4°C to remove unadsorbed phages, and pellets washed by resuspension in 1 mL of fresh medium. Samples were then centrifuged in a tabletop centrifuge at 14 000 rpm for 4 minutes at room temperature and pellets washed by resuspension in 1 mL of fresh medium. The wash step was performed one additional time, for a total of three washes. The pellet was resuspended in 1 mL of fresh medium and added to a flask containing 19 mL of fresh medium and incubated at 30°C. Samples of 200 μ L were withdrawn every 10 minutes for a total of 60 minutes. 100 μ L of the sample was appropriately diluted and titered by plaque assays using the agar double-layer technique (76). The other 100 μ L of the sample was treated with chloroform before being appropriately diluted and titered by plaque assays to obtain titers of extracellular phages. The MOI for the one-step growth curves ranged from 0.001 to 0.002. Three biological replicates were conducted.

2.5.7 Viability Assay – Cell Survivability Assay

Overnight cultures made from single colonies of *L. lactis* strain MG1363 AbiK⁺ were inoculated 1:100 into GM17 supplemented with 10 mM CaCl₂. Medium was supplemented with Cm at 25 μ g/mL. Cultures were grown at 30°C until an OD₆₀₀ of 0.150 was achieved. Phages were diluted in fresh medium for an MOI of 20 and added to the culture. Samples were withdrawn at 0-, 30-, 60-, 120- and 180- minutes post-infection for OD₆₀₀ measurements and cell counts were enumerated by plating serial dilutions of the culture onto GM17 agar plates. For tests to chelate calcium, 15 mM EGTA was added to either the culture, the inoculating phage, or to plates.

2.5.8 Southern Hybridization

2.5.8.1 Sample collection and preparation

Overnight cultures made from single colonies of *L. lactis* strain MG1363 AbiK+ or AbiK- were inoculated 1:100 into GM17 supplemented with 10 mM CaCl₂. Medium was supplemented with Cm at 25 µg/mL. Cultures were grown at 30°C until an OD₆₀₀ of 0.400 was achieved. An aliquot of culture was removed as a no phage infection control. Phages were diluted in fresh medium for an MOI of 20 and added to the culture. Samples were withdrawn at 1-, 2-, 4-, 6-, 8-, 10-, 15-, 20-, 30-, 45-, 60-, 90-, 120- and 180- minutes post-infection and added to two volumes of RNeasy Protect[®] Bacteria Reagent and treated according to the manufacturer's protocol (82). Samples were centrifuged for 10 minutes at 13 000 x g at 4°C, and pellets were snap frozen in liquid nitrogen before being stored at -70°C.

Samples were lysed according to the manufacturer's protocol with some modifications (82). Pellets were thawed and resuspended in lysis buffer (30 mM Tris-HCl, 1 mM EDTA pH 8.0, 15 mg/mL lysozyme and 2 mg/mL Proteinase K), vortexed for 10 seconds and then incubated at room temperature for 10 minutes with vortexing every 2 minutes for 10 seconds. An appropriate volume (350 µL) of Buffer RLT was added to samples, which were vortexed vigorously before being centrifuged for 2 minutes at 14 000 x g, and the supernatant (450 µL) was kept for the subsequent steps. Samples then underwent phenol extraction and ethanol precipitation according to the methods outlined in General Protocols (2.5.1.5).

An aliquot of each sample was incubated at 65°C overnight to inactivate any residual proteins, then samples were treated with RNase A (2 U per sample) at 37°C for 2 hours to remove RNAs in the sample. RNase A was then deactivated by the addition of Proteinase K (1 µL of 20 mg/mL) with incubation at 65°C for 20 minutes before phenol extraction and ethanol

precipitation according to the methods outlined in General Protocols (2.5.1.5). Samples were then digested with EcoRI and HindIII according to the manufacturer's protocol at 37°C overnight before a final phenol extraction and ethanol precipitation according to the methods outlined in General Protocols (2.5.1.5).

2.5.8.2 Preparation of radioactive RNA probe

Templates were linearized by digestion of plasmid DNA according to the manufacturer's protocol. Restriction enzymes used for template linearization were chosen based on restriction sites roughly 1 400 bp downstream of the T7 promoter to produce RNA transcription products of that size. Plasmids used as templates to generate RNA probes are described in Plasmid Construction (2.5.10.2). Digestion products were phenol extracted and ethanol precipitated according to the methods outlined in General Protocols (2.5.1.5).

Radioactive RNA probes were transcribed by 50 U of T7 RNA polymerase (NEB) in transcription buffer (40 mM Tris pH 8.0, 20 mM MgCl₂, 2 mM spermidine, 50 mM NaCl, and 5 mM DTT) with 0.5 mM ATP, 0.5 mM GTP, 0.5 mM CTP, 0.025 mM UTP, 5 µL [α -³²P] UTP (Perkin-Elmer, 3 000 Ci/mmol), and 4 µL of linearized plasmid template in a total reaction volume of 20 µL. Reactions were incubated at 37°C for 1 hour and then diluted in STE buffer (10 mM Tris-HCl pH 7.5, 1 mM EDTA and 100 mM NaCl) before being put through a Sephadex G-50 column to remove unincorporated NTPs. Elutions were further purified by phenol extraction and ethanol precipitation according to the methods outlined in General Protocols (2.5.1.5) before storage at -20°C. 1 µL of the radioactive transcript was measured for ionizing radiation by scintillation counting.

2.5.8.3 Hybridization

Samples were electrophoresed on a 0.7% (w/v) agarose gel using 1xTBE buffer (**Appendix A**) and were imaged after staining with ethidium bromide. Gels were then prepared according to the manufacturer's protocols, and DNA was transferred to a Hybond-XL membrane (Amersham) using capillary blotting overnight (83). The DNA was crosslinked to the membrane using UV crosslinking (70 000 $\mu\text{J}/\text{cm}^2$) before hybridization, and hybridization in tubes was performed overnight according to the manufacturer's protocols (83). Blots were washed according to the manufacturer's protocols (83). Blots were then exposed to phosphor plates, and the autoradiograms were imaged using ImageQuant software and quantified using ImageJ software (84).

2.5.8.4 Blot stripping

Probes were stripped from blots, which was done according to the manufacturer's protocols with modifications (83). Blots were rinsed with 2xSSC solution (**Appendix A**) and then washed twice with 0.2 M NaOH at 42°C for 10 minutes each. NaOH was removed and boiling 0.1% SDS solution was poured onto blots and allowed to cool for 20 minutes. This process was repeated once. Blots were finally rinsed in 2xSSC solution and checked for removal of the probe from exposure to phosphor plates and imaging of the autoradiograms before hybridization with a different probe.

2.5.9 qPCR

2.5.9.1 Sample collection and preparation

Overnight cultures made from single colonies of *L. lactis* were inoculated 1:100 into GM17 supplemented with 10 mM CaCl_2 . Medium was supplemented with Cm at 25 $\mu\text{g}/\text{mL}$. Cultures were grown at 30°C until an OD_{600} of 0.150 was achieved in 10 mL of culture. The

culture was centrifuged at 5 000 x g for 5 minutes at 4°C, and the pellet resuspended in 9 mL of fresh medium. Phages were diluted in fresh medium to a titer of 1×10^5 PFU/mL and added to the culture, mixed gently, and then incubated at 30°C for 10 minutes to allow phages to adsorb to host cells. Cultures were centrifuged at 5 000 x g for 5 minutes at 4°C to remove unadsorbed phages, and pellets were resuspended in 1 mL of fresh medium then added to a flask containing 19 mL of fresh medium where the 20 mL sample was separated into 1 mL aliquots. Aliquots were incubated at 30°C, with one aliquot removed and placed on ice every 5 minutes for a total of 50 minutes. Control cultures where sterile medium was added instead of phage to mimic a phage infection were withdrawn at initial and final time points. Samples were kept on ice until DNA extraction using the EZ-10 Spin Column Genomic DNA Miniprep Kit, Bacteria (BioBasic) (78). DNA was extracted according to the manufacturer's protocols with minor modifications, including incubating the tube at 50°C during the RNase A digest and eluting with 30 µL of water obtained from a Millipore filtration system at the elution step. The MOI ranged from 0.001 - 0.002.

2.5.9.2 Preparation of standards for qPCR

Standards were prepared from genomic DNA extracted from lactococcal phage p2 (2.5.1.4). DNA was quantified using the Nanodrop 2000 (Thermoscientific). The number of genome copies in each sample was calculated, and samples were diluted to create a series of standards with different genome copy numbers (30, 300, 3 000, 30 000, and 300 000). Ct values ranged from 11 – 31 for standards during qPCR reactions.

2.5.9.3 Primer design

Two genes were targeted for qPCR analysis: the capsid and the baseplate gene. All genes in the lactococcal phage p2 genome are present as single copies in the genome, so genome copy

numbers obtained from analysis would be equal to the number of copies of the genome. Primer sets were designed using the PrimerQuest™ tool from IDT™ (Integrated DNA Technologies) with a desired amplicon length between 75 - 150 bp, GC content between 40 - 60%, and an optimal primer melting temperature of 62°C. Primers were between 18 and 25 bp long (**Table 2-3**).

Table 2-3: Primer sequences for qPCR.

Primer	Sequence (5' - 3') *	Length (bp)	Size of amplicon (bp)
Capsid_F	TGACTTTGTTTCGCCCTACTG	20	109
Capsid_R	GCGAACGTTAGCATTTGCAG	20	
Baseplate_F	TATGGAGGAACCGCACCA	18	96
Baseplate_R	ATCCCAACGGCTTAAACG	18	

* Compatible primers are named as F (forward) and R (reverse). Primers purchased from IDT™.

2.5.9.4 qPCR

qPCR was performed on the Qiagen Rotor-Gene Q platform with either the Rotor-Gene SYBR Green PCR Kit or the Quantinova SYBR Green PCR Kit according to the manufacturer's protocol (85, 86). Each sample was performed in duplicate with 5 µL of the DNA extraction used as the template. A melt-curve analysis was also performed on the machine to check for nonspecific amplifications. Ct values for measured samples fell within ranges of the standard samples.

2.5.10 Plasmid Construction

2.5.10.1 Construction of pSRQ823-*AbiK*Δ (*p*Δ*AbiK*)

A plasmid without the *abiK* gene was required for use as a control in experiments. The pSRQ823 plasmid was sequenced before use. Using pSRQ823 as a template, the *abiK* gene was deleted using tip-to-tail PCR as described (2.5.1.7). The deletion was confirmed via gel electrophoresis and DNA sequencing.

2.5.10.2 Construction of phage genome plasmids

Probes of the lactococcal phage p2 genome were required for Southern blots (**Figure 2-13**). Fragments of the entire lactococcal phage p2 genome were cloned into pBluescript II KS(+) (Stratagene) using restriction enzyme and PCR cloning as described (**2.5.1.6**). Cloning was done in *E. coli*. Cloning strategies are described (**Table 2-4**). Inserts were confirmed via gel electrophoresis and DNA sequencing.

2.5.10.3 Construction of pTRKH2-Sak3

The *sak3* gene and mutant *sak3* gene were amplified from the respective phages with primers containing restriction enzyme sites for insertion into the pTRKH2 vector. This was done as described (**2.5.1.6**).

Table 2-4: Lactococcal phage p2 genome clones.

Name	Probe Name	ORFs	Cloning method	Obtained? (Y/N)
Late 1-1	Probe 7-1	1	PCR	Y
Late 1-2		2-3	PCR	Y
Late 2		3-10	Restriction cloning	Y
Late 3		11-14	PCR	Y
Late 4	Probe 3	15-17	Restriction cloning	Y
Late 5		18-20	PCR	Y
Early 1-1		21-24	PCR	Y
Early 1-2		25-34	PCR	N
Early 2-1		35-39	PCR	Y
Early 2-2		40-44	PCR	N
Middle 1		45-47	PCR	Y
Middle 2-1		47-49	PCR	N
Middle 2-2		Non-coding	PCR	N

Table 2-5: Primers used in cloning.

Primer	Sequence (5' - 3') *
AbiKCut_S	CCTTAAATCTTAGAGTCACTATTGTATGG
AbiKCut_AS	GTCAATATAAATGACAAGACACAGC
Late 1-1_S	GGGGG AAGCTT GTTAGCAGTATAGTCTAATGG
Late 1-1_AS	GGGGG GTCGACT CTGAATAGTCTTGC
Late 1-2_S	GGGGG AAGCTT AGCAATGATGGTTGC
Late 1-2_AS	GGGGG GTCGAC ACTCCAATTGAG
Late 3_S	GGGGG GAATTC GGCGCTAATTATGC
Late 3_AS	GGGGG ATCGAT CTAAATTAGAGGGCTGG
Late 5_S	GGGGG GAATTC GCTCTTGTACG
Late 5_AS	GGGGG AAGCTT GTTGACAGAATCG
Early 1-1_S	GGGGG GAATTC CACTTAATTGTGGGG
Early 1-1_AS	GGGGG AAGCTT GGCAAGAAAGAGG
Early 1-2_S	GGGGG GAATTC TGAGCCTTACAGC
Early 1-2_AS	GGGGG AAGCTT AAAGCAACAGAGGG
Early 2-1_S	GGGGG GAATTC TAATTGAATGAAGTCAGG
Early 2-1_AS	GGGGG ATCGAT GTTATGAAGTTATTGAACC
Early 2-2_S	GGGGG GAATTC TCTGTTATCATCAGG
Early 2-2_AS	GGGGG ATCGAT TTCTTGTGTTGATTGATTGG
Middle 1_S	GGGGG GAATTC AAGAATAAAAATATTGTTCCGG
Middle 1_AS	GGGGG ATCGAT AAGGATTACGAAATGC
Middle 2-1_S	GGGGG GAATTC GATTAATCTTGATACAGC
Middle 2-1_AS	GGGGG ATCGAT TATAACATTTAAGCACCG
Middle 2-2_S	GGGGG GAATTC TATTGGTAGTGGCTGG
Middle 2-2_AS	GGGGG ATCGAT CAATGCTATGCTCCGG
Sak3_S	TTTAA CTCGAG ATGAGCGTATTTGAACAG
Sak3_AS	AAATTT GGATCCT TATTTTCCCTCTGTTGC

* Compatible primers are named as S (sense) and AS (antisense). Restriction enzyme sites in red. Primers purchased from IDT™.

Table 2-6: Primers used for sequencing.

Primer *	Sequence (5' - 3')
M13_pUC_forward	CCCAGTCACGACGTTGTAAAACG
M13_pUC_reverse	GTGAGCGGATAACAATTTTCACACAGG
T7	GTAATACGACTCACTATAGGGCG
T3	AATTAACCCTCACTAAAGGG
pBluescript SK	CGCTCTAGAACTAGTGGATCC
pBluescript KS	TCGAGGTCGACGGTATC
pNZ123 (219-F)	TAACGGGGCAGGTTAGTGAC
pNZ123 (1229-F)	CCCCTAAGGCGAATAAAAAGC
pNZ123 (2128-F)	CGATTGAAAAACCCCTCAAA
pNZ123 (354-R)	GGTTATCATGCAGGATTGTT
pNZ123 (1114-R)	TGCAAAGGTTCTTGATGCTG
pNZ123 (1832-R)	CTCGCGTTTTTAGAAGGATA
AbiK (251-F)	AATTTTTCTGCCATACGAGA
AbiK (1023-F)	GCTTTTCATTCTCAAAGTA
AbiK (1689-F)	CTTTTGCAGTATTCATTTTT
AbiK (464-R)	TGGTTGTCTTTGAAATAGATGA
AbiK (1514-R)	GACAATATAAGATGCCCAATTT
pNZ123 (AD)	GCATATTCTTCTATAGCTAACGCCGCAACCGC

* Primers purchased from IDT™.

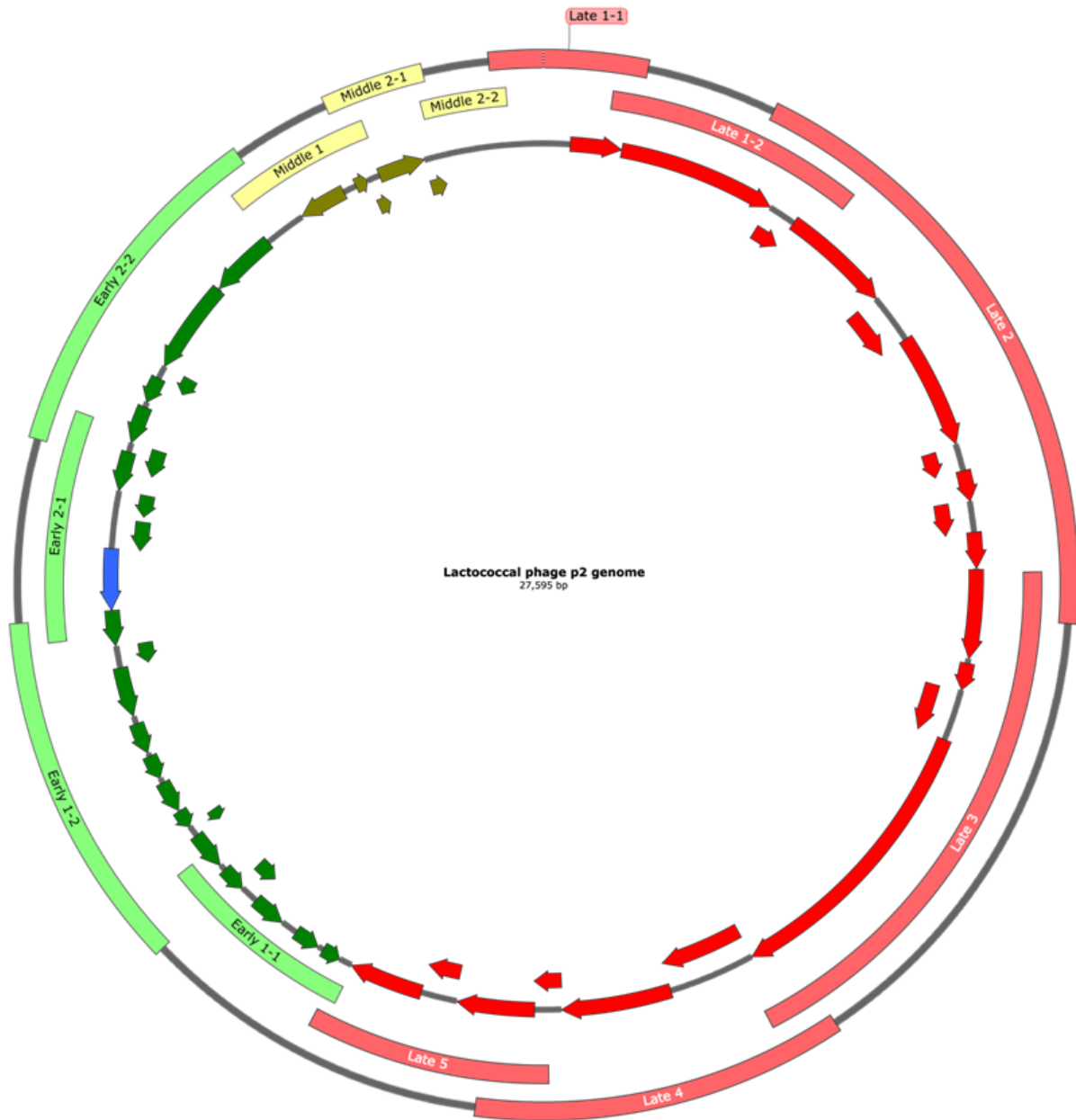


Figure 2-14: Lactococcal phage p2 genome clones.

Circular schematic of the lactococcal phage p2 genome with open reading frames (inner circle) and fragments of the phage genome cloned into the pBluescript KS II+ vector (outer circle) shown. Early genes are coloured in green, middle genes are coloured in yellow, late genes are coloured in red, and the *sak3* gene is coloured in blue. Names of phage genome clones are labeled. Genome map was generated using Snapgene.

Chapter 3 : Kinetics of RNA Production

3.1 Introduction

Several hypotheses have been proposed for the mechanism of AbiK that have been disproven. AbiK was proposed to block protein synthesis by aiding with sequestering viral RNA and to also have a nuclease activity that indiscriminately cleaves RNA within infected cells (2, 55). Both proposed hypotheses have been disproven, and the mechanism of AbiK remains unclear. To help reveal clues about the AbiK mechanism, transcriptome studies can be performed as a non-biased method to look at the differential gene expression between infected cells with and without AbiK to see what global changes occur during the mechanism.

RNA-Seq is a tool for transcriptome-wide analysis, allowing for the analysis of differential gene expression (87). Through technological advancements, RNA-Seq allows for a richer and less biased view of the transcriptome in comparison to microarray systems that were previously used to analyze the transcriptome (87). Many studies have been released in recent years analyzing the transcriptome of phage-infected cells to look at the phage-host interactions and the differential gene expression of the host resulting from the infection. Here, RNA-Seq is used to analyze how the transcriptome of an infected cell changes during the AbiK mechanism in comparison to a normal wild-type infection; this could reveal clues on how the AbiK mechanism functions and ultimately results in cell death.

3.2 Aims

The aim of this research was to look at the transcriptome of phage-infected cells. Experiments using RT-qPCR, looking at five phage genes (capsid, baseplate, sak3, DNA polymerase, and HNH endonuclease) were done to look at how the expression of these genes change because of the AbiK mechanism and when there is an escape of the AbiK mechanism. The five genes were chosen to encompass the three large gene modules on lactococcal phage p2, to get an overview of when these genes normally express. With the timings of phage gene expression, time points of interest were selected for further analysis using RNA-Seq. Collectively, these data give information into the differential gene expression of phage-infected cells during the normal infection, the AbiK infection and during the escape of the AbiK infection mediated by the *sak3* mutant phage. These data reveal how the cell is combatting the phage infection and what genes and RNA are involved in the AbiK mechanism.

3.3 Results and Discussion

3.3.1 RNA Kinetics During Phage Infection: RT-qPCR

RT-qPCR was performed to analyze the gene expression of five phage genes post-infection. Like qPCR, RT-qPCR is a high-throughput and sensitive method that can detect gene copies in a sample (69). Starting with a reverse transcriptase step, RNAs in the sample are used as templates to make cDNA, which can then be quantified using qPCR (69). Primers were designed to target five genes from lactococcal phage p2: capsid, baseplate, *sak3*, DNA polymerase, and HNH endonuclease. The expression of these genes was quantified and analyzed post-infection for the normal wild-type infection, the AbiK infection, and the escape of the AbiK infection mediated by the *sak3* mutant phage.

Lactococcal phage p2's whole genome has been sequenced twice, first in 2010 (Accession number GQ979703.1) and the latest in 2023 (NC_042024.1) with identical sequences. Lactococcal phage p2 has 49 annotated ORFs in addition to one unannotated ORF (33) (**Figure 2-8**). Its genes are clustered into three large modules, known as the early, middle and late genes, which are chronologically transcribed upon infection (33). The early and middle gene modules contain non-structural proteins that are responsible for hijacking the cellular machinery, including the *sak3* gene, the DNA polymerase gene, and the HNH endonuclease gene (33). The late expressed gene module codes for structural proteins that form the virion structure, like the capsid and the baseplate (33). Due to the knowledge of lactococcal phage p2's gene modules, the order in which the genes are expressed is known and was used as a reference for RT-qPCR experiments.

ORF 43 of lactococcal phage p2 is an early-expressed gene that was originally annotated as a DNA polymerase subunit, which has been labeled as an AAA family ATPase in the updated

sequence in 2023. ORF 45 is annotated as one of the two HNH endonuclease in the genome, as a middle-expressed gene. Both genes are hypothesized to be involved in hijacking the cellular machinery and are expected to have their highest expression levels early in the infection cycle. They were seen to start with a high expression level at 0 minutes post-infection, which then decreased at 5 minutes before peaking at 15 minutes, then stayed stagnant (**Figure 3-1**). This is not expected during a normal phage infection, but it is important to note that the earliest time point (0 minutes) was taken 20 minutes after phages were added, as the phages were allowed to adsorb onto the cell for 10 minutes, followed by centrifuge spins, before measurements were taken. The highest expression of an early gene is likely not collected or measured in this experiment.

During the AbiK mechanism, expression of the HNH endonuclease gene mimicked the expression levels of the normal infection at early time points, then decreased over the course of the infection before rapidly increasing and then decreasing between 20-30 minutes post-infection (**Figure 3-1**). For the escape of AbiK mechanism, the HNH endonuclease gene expression started at similar levels to the normal infection, decreased until 20 minutes post-infection before increasing again (**Figure 3-1**). Expression of the DNA polymerase gene was not detected in the AbiK and escape of AbiK mechanisms. Further analysis showed non-specific amplification with the primers, as amplification was seen in no-phage controls, indicating that the primers were not targeting the desired gene and instead amplifying an unknown template, making measurement unreliable (**Supplementary Figure 4**).

The capsid and baseplate genes encode structural proteins that form the virion structure, which are expressed later in the infection cycle as virions are produced. During the normal wild-type phage infection, RNAs from the capsid gene increased over the course of the experiment,

peaking at 15 minutes post-infection before decreasing (**Figure 3-2**). The same pattern was seen for the baseplate gene. The capsid gene expression was high even at early time points, indicating that the expression of the capsid gene starts at an early stage and continues until virion assembly. During the AbiK mechanism, the gene expression of the capsid and baseplate genes were the same at early time points, but the gene expression peaked later, at 25 minutes post-infection, showing a delay in the expression of late genes. During the escape of the AbiK infection mediated by the *sak3* mutant phage, the gene expression pattern of the late genes mimicked the normal wild-type phage infection until 15 minutes post-infection, when gene expression declines.

Sak3 was chosen as a gene of interest due to its involvement in the AbiK mechanism. It is encoded on the early gene module, and although its exact role in phage replication is not known, it is hypothesized to be involved in phage genome circularization, phage DNA replication, and in processing DNA concatemers. During the normal wild-type infection, the *sak3* gene followed the same pattern as the capsid and baseplate genes, peaking in expression at 15 minutes post-infection (**Figure 3-3**). Although the *sak3* gene shares the same module as the DNA polymerase gene, its gene copy numbers were also much higher during the normal infection, at similar counts to the baseplate gene. It is interesting that despite being an early gene, the *sak3* gene followed the expression pattern of a late gene, implying that the protein also has a role later in the phage's replication cycle. During the AbiK mechanism, the *sak3* gene was highly expressed for the duration of the experiment. During the escape of the AbiK mechanism, where the mutant *sak3* gene is detected, the expression levels mimicked those of the capsid and baseplate genes where expression levels matched the normal wild-type phage infection before expression decreased 15 minutes post-infection.

The AbiK mechanism does not prevent the expression of four of the five genes tested in the RT-qPCR experiment but is seen to cause a lag in the expression of three of the genes tested (capsid, baseplate, and HNH endonuclease). The expression of *sak3* was high throughout the course of the AbiK infection, which is not surprising as Sak3 is known to be involved in the AbiK mechanism. Infection by the mutant phage restores normal gene expression levels even with the AbiK protein present. The only anomaly was a decrease of gene expression 15 minutes post-infection, possibly due to experimental error (**Figure 3-3**).

All genes across the three conditions showed a secondary peak between 40- and 50-minutes post-infection that was larger than the initial peak. This is likely due to a second infection cycle from the first produced progeny, as even though an MOI of 1 was used for infection, uninfected host cells may remain in the host culture. This corresponds well with the data from Chapter 2, as the phage is known to finish its lytic cycle 10-25 minutes post-infection, and DNA replication of the phage can be seen to ramp up 40 minutes post-infection.

The results shown here act as a preliminary experiment, showing the expression of only select phage genes, and giving the timings of phage gene expression for genes in different modules. These results indicate that downstream experiments involving RNA-Seq should not surpass 30 minutes post-infection, with the risk of a second infection cycle. Although the AbiK mechanism delays the expression of a few of the phage genes tested, this timing for RNA-Seq experiments includes that consideration, and downstream experiments will give a detailed view of the global gene expression during the phage infections.

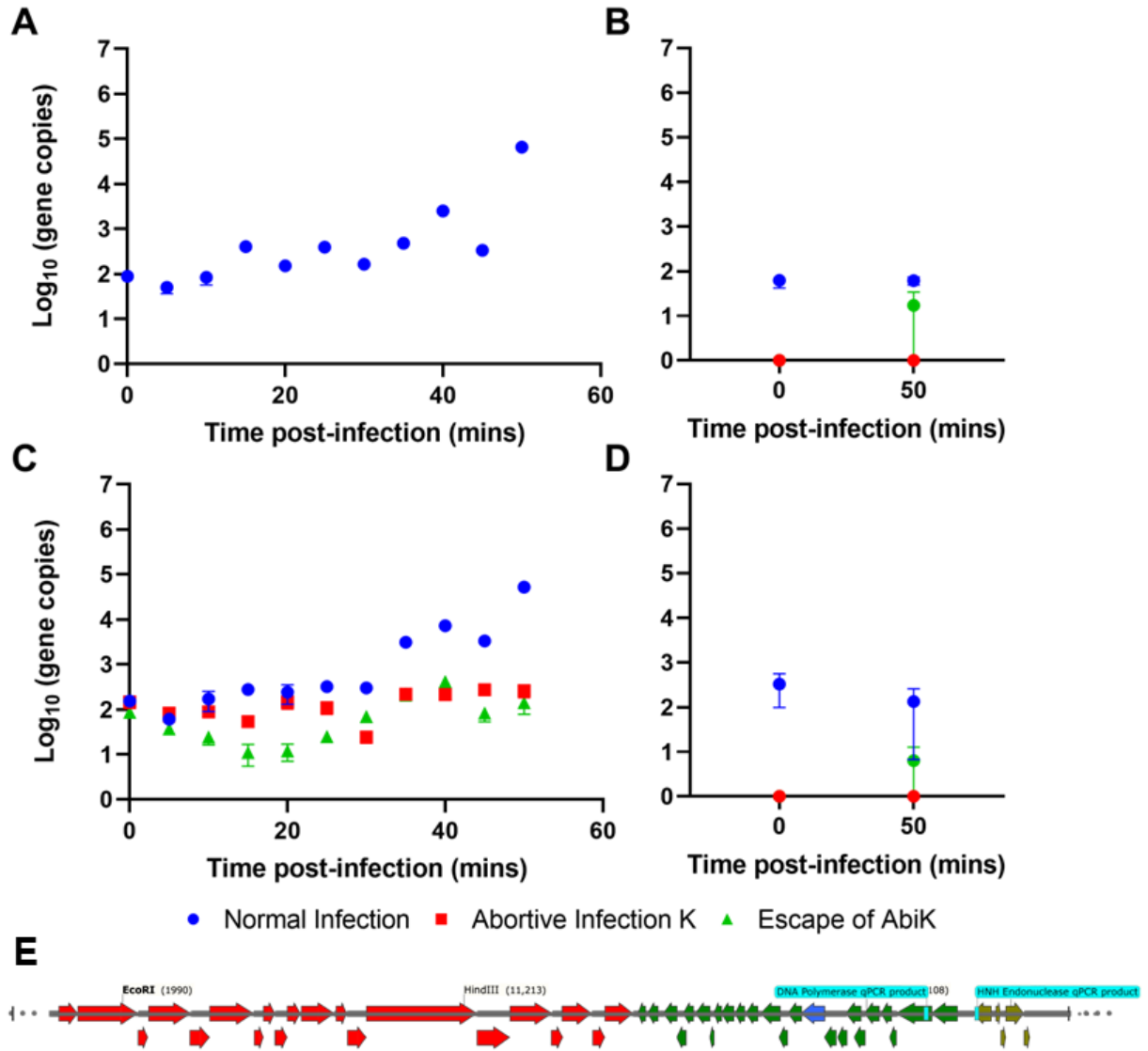


Figure 3-1: RT-qPCR of DNA Polymerase and HNH Endonuclease Genes.

Log of genome copies of RNA extracted from time points post-infection analyzed by RT-qPCR primers targeting the DNA polymerase gene (A) and primers targeting the HNH endonuclease gene (C). For the normal infection, lactococcal phage p2 infected AbiK⁻ cells. For abortive infection K, lactococcal phage p2 infected AbiK⁺ cells. For the escape of AbiK, mutant *sak3* (M90I) lactococcal phage p2 infected AbiK⁺ cells. Negative controls without phages were performed at time points 0 minutes and 50 minutes using primers targeting the DNA polymerase gene (B) and primers targeting the HNH endonuclease gene (D). Genome copy number was per 1 μ L of RNA extract. Values are the means of three technical replicates, and error bars represent standard error of the mean (SEM). Missing error bars are due to small SEM values. E: A linear schematic of the lactococcal phage p2 genome with the RT-qPCR primer targets (cyan). Genome map was generated using Snapgene.

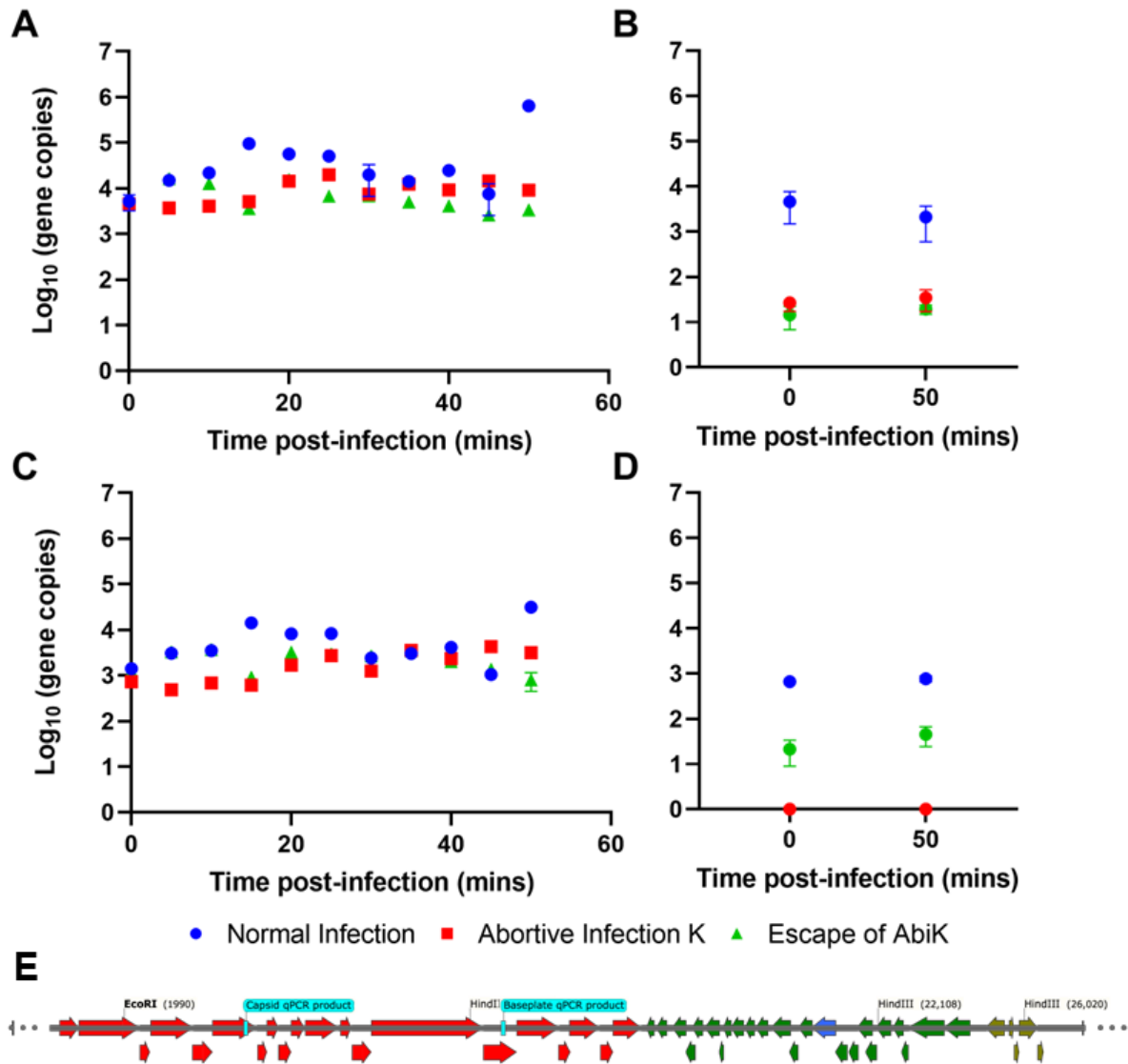


Figure 3-2: RT-qPCR of Capsid and Baseplate Genes.

Log of genome copies of RNA extracted from time points post-infection analyzed by RT-qPCR primers targeting the capsid gene (A) and primers targeting the baseplate gene (C). For the normal infection, lactococcal phage p2 infected AbiK⁻ cells. For abortive infection K, lactococcal phage p2 infected AbiK⁺ cells. For the escape of AbiK, mutant *sak3* (M90I) lactococcal phage p2 infected AbiK⁺ cells. Negative controls without phages were performed at time points 0 minutes and 50 minutes using primers targeting the capsid gene (B) and primers targeting the baseplate gene (D). Genome copy number was per 1 μ L of RNA extract. Values are the means of three technical replicates, and error bars represent standard error of the mean (SEM). Missing error bars are due to small SEM values. **E**: A linear schematic of the lactococcal phage p2 genome with the RT-qPCR primer targets (cyan). Genome map was generated using Snapgene.

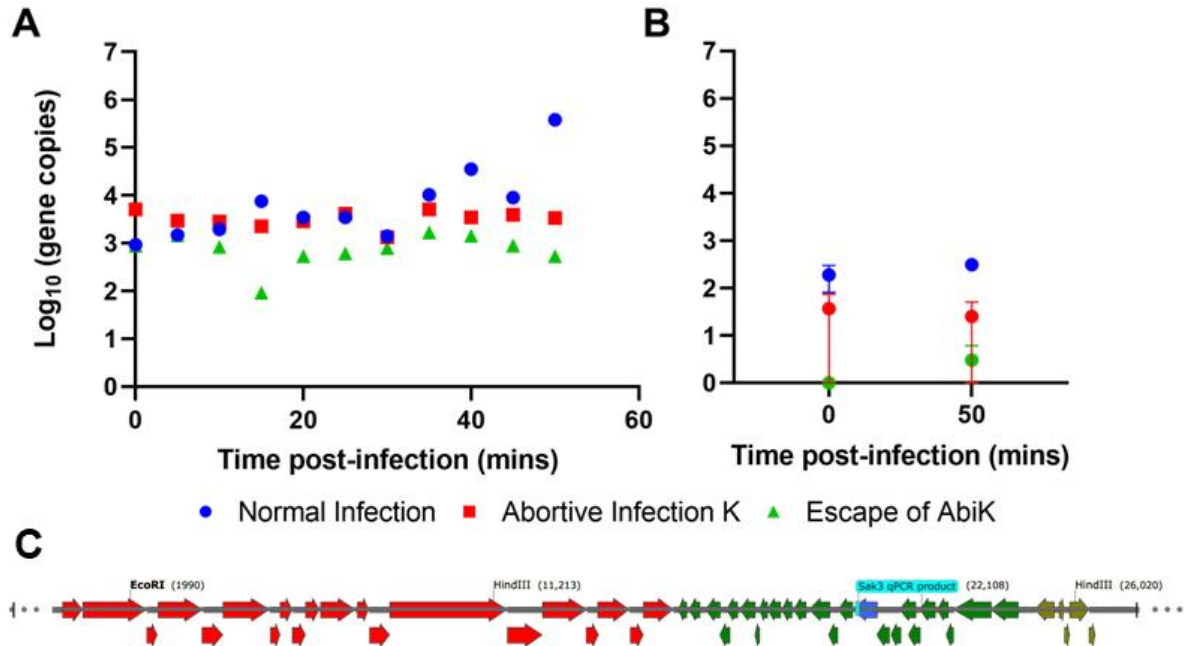


Figure 3-3: RT-qPCR of Sak3 Gene.

Log of genome copies of RNA extracted from time points post-infection analyzed by RT-qPCR primers targeting the *sak3* gene (A). For the normal infection, lactococcal phage p2 infected AbiK⁻ cells. For abortive infection K, lactococcal phage p2 infected AbiK⁺ cells. For the escape of AbiK, mutant *sak3* (M90I) lactococcal phage p2 infected AbiK⁺ cells. Negative controls without phages were performed at time points 0 minutes and 50 minutes using primers targeting the *sak3* gene (B). Genome copy number was per 1 μ L of RNA extract. Values are the means of three technical replicates, and error bars represent standard error of the mean (SEM). Missing error bars are due to small SEM values. C: A linear schematic of the lactococcal phage p2 genome with the RT-qPCR primer targets (cyan). Genome map was generated using Snapgene.

3.3.2 RNA Kinetics During Phage Infection: RNA-Sequencing

3.3.2.1 RNA-Sequencing condition selection

Like the RT-qPCR experiments, RNA was extracted for the normal wild-type infection, the AbiK infection, and the escape of the AbiK infection mediated by the *sak3* mutant phage for quantification and analysis of genes 0-, 10-, 20- and 30-minutes post-infection (**Table 3-1**). Controls were also performed without phages to analyze how the cell grows without the stress of a phage infection and to see how the presence of AbiK affects gene expression of the cell (**Table 3-1**). It is important to note that although the earliest time point is denoted at 0 minutes post-infection, due to the experimental method of allowing the phage to adsorb to cells and further centrifuge spins, 0 minutes post-infection is truly 20 minutes after the initial inoculation of phage to host cells. With three biological replicates per sample, a total of 54 RNA samples were prepared and sent to collaborators at the University of Regina (Dr. Christopher Yost's laboratory) for further processing of the samples prior to RNA-Seq. Due to the large number of samples, only a subset of the samples (10 in total) was further processed and sent for RNA-Seq for preliminary analysis. These samples include no-phage controls, samples at 0-, 10-, and 30-minutes post-infection for a single replicate of the wild-type infection and the AbiK infection (**Table 3-1**). Due to the lack of replicates in this initial analysis, the following results were cautiously interpreted.

Table 3-1: Samples for RNA-Sequencing.

	Normal Infection	Abortive Infection K	Escape of AbiK
Control T=0	WT_C0*	AbiK_C0*	Sak3_C0
Control T=30	WT_C30*	AbiK_C30*	Sak3_C30
Sample T=0	WT_0*	AbiK_0*	Sak3_0
Sample T=10	WT_10*	AbiK_10*	Sak3_10
Sample T=20	WT_20	AbiK_20	Sak3_20
Sample T=30	WT_30*	AbiK_30*	Sak3_30

* Samples sent for RNA-Seq preliminary analysis

RNA-seq data of the no-phage controls revealed expression of 2 587 genes across the *L. lactis* strain MG1363 genome and 5 genes on the plasmid used to express the *abiK* gene (pSRQ823). RNA-seq data of the phage infection samples included the 49 lactococcal phage p2 genes on top of the *L. lactis* and plasmid genes. The *L. lactis* genome includes 6 copies of the 16S rRNA gene, 6 copies of the 23S rRNA gene, 7 copies of the 5S rRNA gene, 64 tRNA genes, 3 small RNA genes and 2 501 protein coding genes (CDS). All plasmid and lactococcal phage p2 genes are protein coding genes. For the no-phage controls, roughly 99% of all reads map to the *L. lactis* genome, with roughly 1% mapping to the plasmid (**Table 3-2**). For the phage infection samples, early time points have roughly 1% of the reads mapping to the phage whereas the later time points have roughly 15% of the reads mapping to the phage, showing the phage's takeover of the transcription machinery for transcription of phage genes (**Table 3-2**). Roughly 0.1% of reads in all conditions were unmapped (**Table 3-2**). A more detailed table of the read percentages is shown below (**Table 3-2**).

Table 3-2: Percentage of reads mapped in RNA-Sequencing.

	<i>L. Lactis</i> Reads (%)	pSRQ823 Reads (%)	p2 Phage Reads (%)	Unmapped Reads (%)	Total Read Count
WT_C0	98.9	1.0	0.0	0.1	16494835.0
WT_C30	98.7	1.2	0.0	0.1	16830087.0
AbiK_C0	99.2	0.7	0.0	0.1	18365938.0
AbiK_C30	99.2	0.7	0.0	0.1	18644588.0
WT_0	97.2	0.9	1.7	0.1	16605184.0
WT_10	90.7	0.7	8.5	0.1	13740470.0
WT_30	84.9	0.7	14.3	0.2	16456469.0
AbiK_0	98.2	0.6	1.1	0.1	15514474.0
AbiK_10	94.7	0.6	4.6	0.1	22388762.0
AbiK_30	83.4	0.5	16.0	0.1	16011121.0

3.3.2.2 No-phage controls

The no-phage controls act as a baseline to see how *L. lactis* cells grow under the same conditions, without the stress of a phage infection. Controls were taken at the earliest time point (0 minutes) and the latest time point (30 minutes) for all conditions. The *L. lactis* cells are undergoing the exponential phase of growth at this stage, and the expected OD₆₀₀ of cells ranges from 0.2 - 0.4 over the course of the measurements. During the exponential phase of bacterial cell growth, cells are rapidly dividing and using the nutrients available in the medium (88). The metabolic activity is high; DNA replication, transcription, and translation of proteins are readily occurring to produce new cells, and this is what we expect to see in the RNA-seq data for the no-phage controls (88).

All the genes in the *L. lactis* genome were classified into clusters of orthologous groups (COGs) by querying the genes against the COG database (89). As a result, 78% of the protein sequences were sorted into COG functional categories. Furthermore, 3% of genes were labeled as RNA genes (rRNA, tRNA, etc.). The remaining genes were categorized into the COGs manually, with the majority being hypothetical proteins with unknown functions. The lactococcal phage p2 genes were added to the list as numbers, in addition to the genes encoded on the plasmid, producing a table with each gene in the experiment categorized by function (**Table 3-3**). The number of normalized transcript counts for each category was summed up and shown as the percentage of transcripts in the sample as a pie chart (**Figure 3-4**) and in a table (**Supplementary Table 1**).

Table 3-3: *L. lactis* gene counts organized in COG categories.

COG Letter	Description	Counts
A	RNA processing and modification	0
B	Chromatin structure and dynamics	0
C	Energy production and conversion	79
D	Cell cycle control, cell division, chromosome partitioning	36
E	Amino acid transport and metabolism	176
F	Nucleotide transport and metabolism	91
G	Carbohydrate transport and metabolism	177
H	Coenzyme transport and metabolism	103
I	Lipid transport and metabolism	60
J	Translation, ribosomal structure, and biogenesis	209
K	Transcription	165
L	Replication, recombination, and repair	108
M	Cell wall/membrane/envelope biogenesis	122
N	Cell motility	12
O	Posttranslational modification, protein turnover, chaperones	60
P	Inorganic ion transport and metabolism	91
Q	Secondary metabolites biosynthesis, transport, and catabolism	17
R	General function prediction only	144
S	Function unknown	567
T	Signal transduction mechanisms	67
U	Intracellular trafficking, secretion, and vesicular transport	15
V	Defense mechanisms	74
W	Extracellular structures	0
X	Mobilome: prophages, transposons	128
Y	Nuclear structure	0
Z	Cytoskeleton	0
1	rRNA	19
2	tRNA	64
3	Other RNA	3
4	Lactococcal phage p2 early genes	24
5	Lactococcal phage p2 middle genes	5
6	Lactococcal phage p2 late genes	20
7	Plasmid genes (pAbiK or pΔAbiK)	5

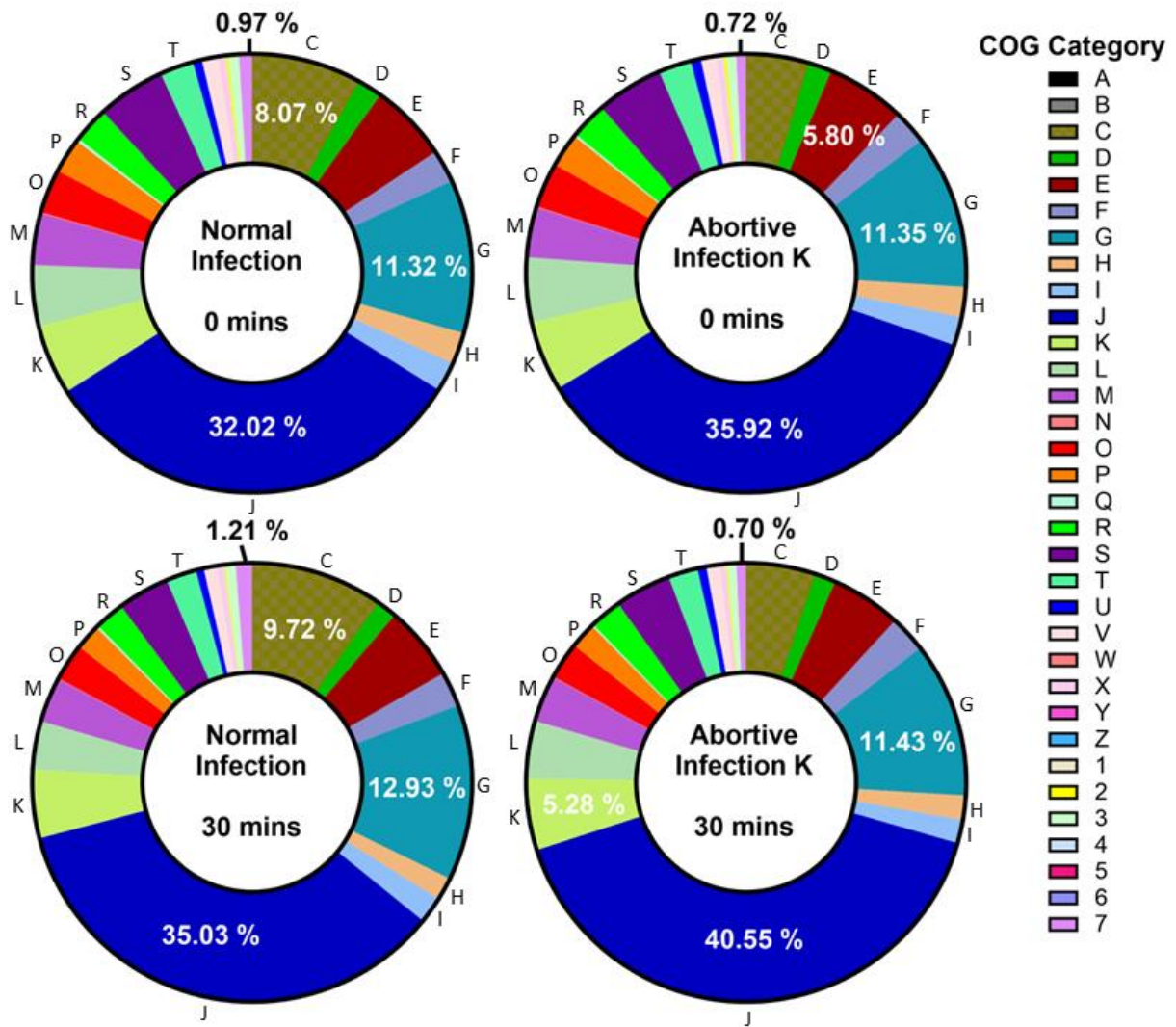


Figure 3-4: Percentage of transcript counts in COG categories in uninfected cells.

Pie charts representing the percentage of transcript counts for each COG category in uninfected cells. Condition and time point are specified in the center of the pie charts. The three most abundant COG categories are indicated with their percentage values. Percentage of plasmid transcripts is indicated. Missing COG categories are due to no or low transcript amounts in that category.

When cells are growing normally without the stress of a phage infection, 32.02% of transcripts are dedicated to protein translation, with 11.32% dedicated to carbohydrate transport and metabolism and 8.07% dedicated to energy production and conversion (**Figure 3-4**). Over time, the percentage of transcripts dedicated to these functions increases (35.03%, 12.93% and 9.72% respectively) as the *L. lactis* cells proliferate, matching what is expected during the exponential phase of bacterial cell growth (**Figure 3-4**). In addition, 0.97% of the transcripts come from the plasmid, with an increase to 1.21% at 30 minutes. Most transcripts made from the plasmid are derived from the *cat* gene (chloramphenicol acetyltransferase), which gives the cells resistance to the chloramphenicol antibiotic that is present in these experiments.

With the introduction of the *abiK* gene on the plasmid, the most abundant set of transcripts is dedicated to protein translation at 35.92% with an increase to 40.55% at 30 minutes (**Figure 3-4**). The second most abundant set of transcripts is dedicated to carbohydrate metabolism at 11.35% with a small increase at 30 minutes to 11.43% (**Figure 3-4**). The third most abundant set of transcripts is dedicated to amino acid transport and metabolism (5.80%) as opposed to energy production and conversion in cells without the *abiK* gene (**Figure 3-4**). At 30 minutes, this changes again as cells are more dedicated to transcription (5.28%) (**Figure 3-4**). With just the introduction of the *abiK* gene without a phage infection, the *abiK* gene changes the transcriptome of a cell. The cell is less dedicated to producing energy, and more dedicated to protein production with the increase in amino acid production and the increase in transcripts dedicated to protein translation, aligning with the increased production of the AbiK protein. A more detailed analysis on the differential gene expression between the normal infection and abortive infection K controls is explained later in this chapter (**3.3.2.4**).

3.3.2.3 Gene expression post-infection

Normal Infection

During a typical phage infection against a sensitive host, the phage hijacks the host's metabolic machinery and uses it to proliferate (12). DNA phages, like the lactococcal phage p2, can immediately hijack the transcription machinery to make mRNA which can then direct the ribosomes to make its corresponding proteins (12). Early genes, transcribed immediately after infection, generally encode proteins involved in RNA transcription, DNA replication and for host takeover (90). This is followed by the middle genes, which encode similar proteins (90). The late genes are encoded last, and typically encode the phage assembly and structural proteins (90). For the host cell, upon phage infection, defense mechanisms can be activated to combat the infecting phage, but for sensitive cells, the metabolic machinery is taken over and phage products dominate (90).

For the course of this experiment, RNA transcripts at 0 minutes, 10 minutes, and 30 minutes post-transcription were analyzed. Pie charts were used to analyze the percentage of transcripts dedicated to COG functional categories. For the normal infection, a majority of the transcripts were dedicated to protein translation, carbohydrate transport and metabolism and energy production and conversion in the first 10 minutes post-infection (**Figure 3-5**). However, at 30 minutes post-infection, the phage late genes become the third most abundant transcript category at 11.74% of global transcripts, signifying a takeover of the cellular machinery and the development of phage progeny (**Figure 3-5**).

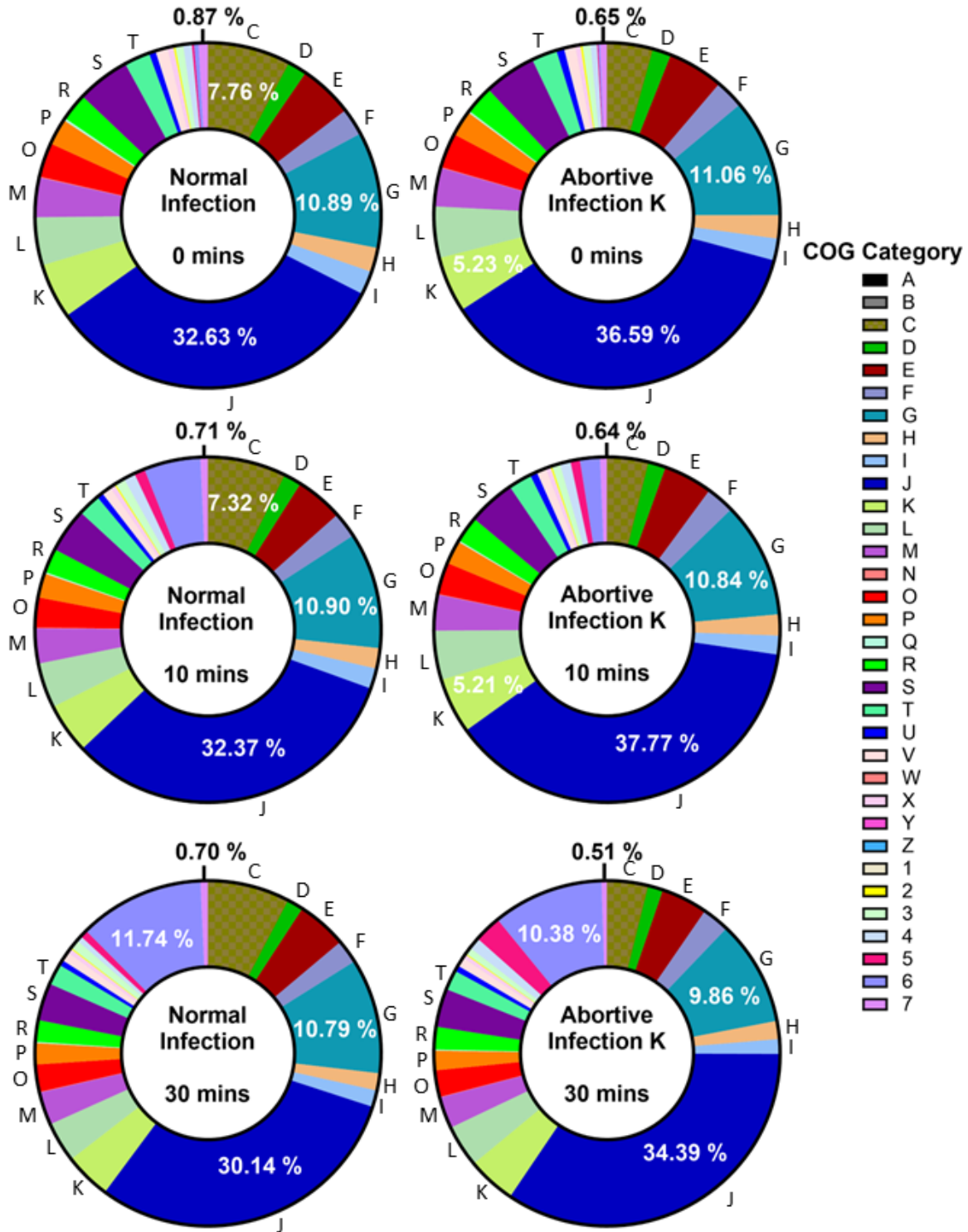


Figure 3-5: Percentage of transcript counts in COG categories in infected cells.

Pie charts representing the percentage of transcript counts for each COG category in infected cells. Condition and time point are specified in the center of the pie charts. The three most abundant COG categories are indicated with their percentage values. Percentage of plasmid transcripts is indicated. Missing COG categories are due to no or low transcript amounts in that category.

Unfortunately, the pie charts make it difficult to discern how *L. lactis* cells are reacting to the phage infection. A differential gene analysis was done for 10 minutes vs. 0 minutes post-infection, and again for 30 minutes vs. 10 minutes post-infection. Genes were filtered based on having a probability of over 95% to be differentially expressed for further analysis. From 0 to 10 minutes post-infection, only phage genes had over a 95% probability of being differentially expressed (not shown). From 10 to 30 minutes post-infection, in addition to phage genes, there are ten *L. lactis* genes that have over a 95% probability of being differentially expressed, which were further analyzed (**Figure 3-6** and **Table 3-4**).

There is a decrease in expression of two genes involved in nucleotide transport and metabolism, notably a decrease in the pyrimidine operon attenuation protein, and an increase in four genes involved in riboflavin biosynthesis. In addition, there is an increase in transcription for two phage shock proteins (proteins that respond to extracytoplasmic stress that can then change the energy status of the cell) along with an uncharacterized protein believed to be involved in stress (91). Lastly, there is an increase in a hypothetical protein with an unknown function. With this evidence, the *L. lactis* cells are trying to combat the phage with increased expression of the phage shock proteins, but it ultimately fails as phage progeny are formed. Notably, a decrease in the pyrimidine operon attenuation protein implies an increase in the production of pyrimidine molecules. An increase in the production of pyrimidine ribonucleotide synthesis has been previously linked to the phage successfully hijacking the machinery to replicate itself (33). Interestingly, there is also an increase in gene expression of riboflavin biosynthesis genes, where the pathway for the biosynthesis of riboflavin uses GTP, a nucleotide, as a precursor.

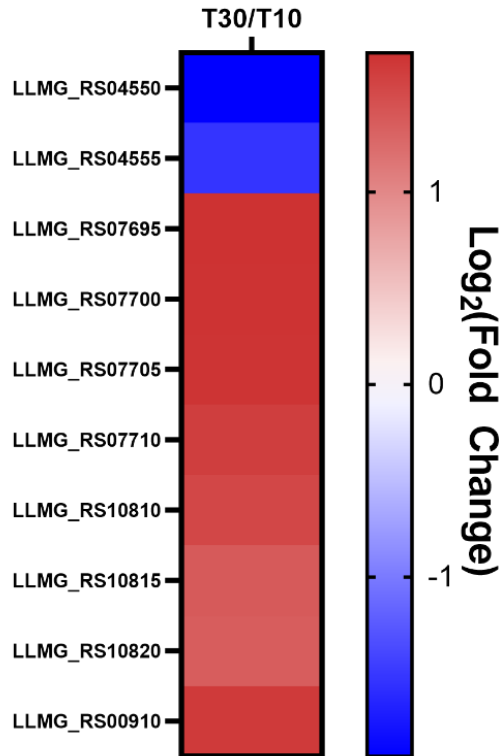


Figure 3-6: Heat map of differentially expressed genes in normal infection at 30 minutes vs. 10 minutes.

Heat map showing the $\log_2(\text{fold-change})$ of genes that have a 95% probability of being differentially expressed in the normal infection at 30 minutes vs. 10 minutes post-infection. Values >1 (red) indicate a higher expression at 30 minutes post-infection, and values < -1 (blue) indicate a lower expression at 30 minutes post-infection. Locus tags of genes are indicated.

Table 3-4: Differentially expressed genes in normal infection at 30 minutes vs. 10 minutes.

Locus Tag	Protein Name	Product	Function	COG Category	Log ₂ (Fold Change)
LLMG_RS04550	PyrR	Pyrimidine operon attenuation protein PyrR/uracil phosphoribosyltransferase	Regulator protein, regulates the transcription of pyr mRNA	F	-1.93
LLMG_RS04555	UraA	Xanthine/uracil permease	Transport protein that uptakes xanthine or uracil	F	-1.54
LLMG_RS07695	RibE	6,7-dimethyl-8-ribityllumazine synthase (Riboflavin synthase beta chain)	Involved in riboflavin biosynthesis	H	1.72
LLMG_RS07700	RibB	3,4-dihydroxy-2-butanone 4-phosphate synthase	Involved in riboflavin biosynthesis	H	1.71
LLMG_RS07705	RibC	Riboflavin synthase alpha chain	Involved in riboflavin biosynthesis	H	1.70
LLMG_RS07710	RibD	Pyrimidine reductase, riboflavin biosynthesis	Involved in riboflavin biosynthesis	H	1.62
LLMG_RS10810	PspC	Phage shock protein PspC (stress-responsive transcriptional regulator)	Controls transcription when a phage infection is sensed	K	1.54
LLMG_RS10815	PspC	Phage shock protein PspC (stress-responsive transcriptional regulator)	Controls transcription when a phage infection is sensed	K	1.38
LLMG_RS10820	YvlB	Uncharacterized conserved protein YvlB, contains DUF4097 and DUF4098 domains	A stress-related protein	S	1.35
LLMG_RS00910		Hypothetical protein	Unknown function	S	1.65

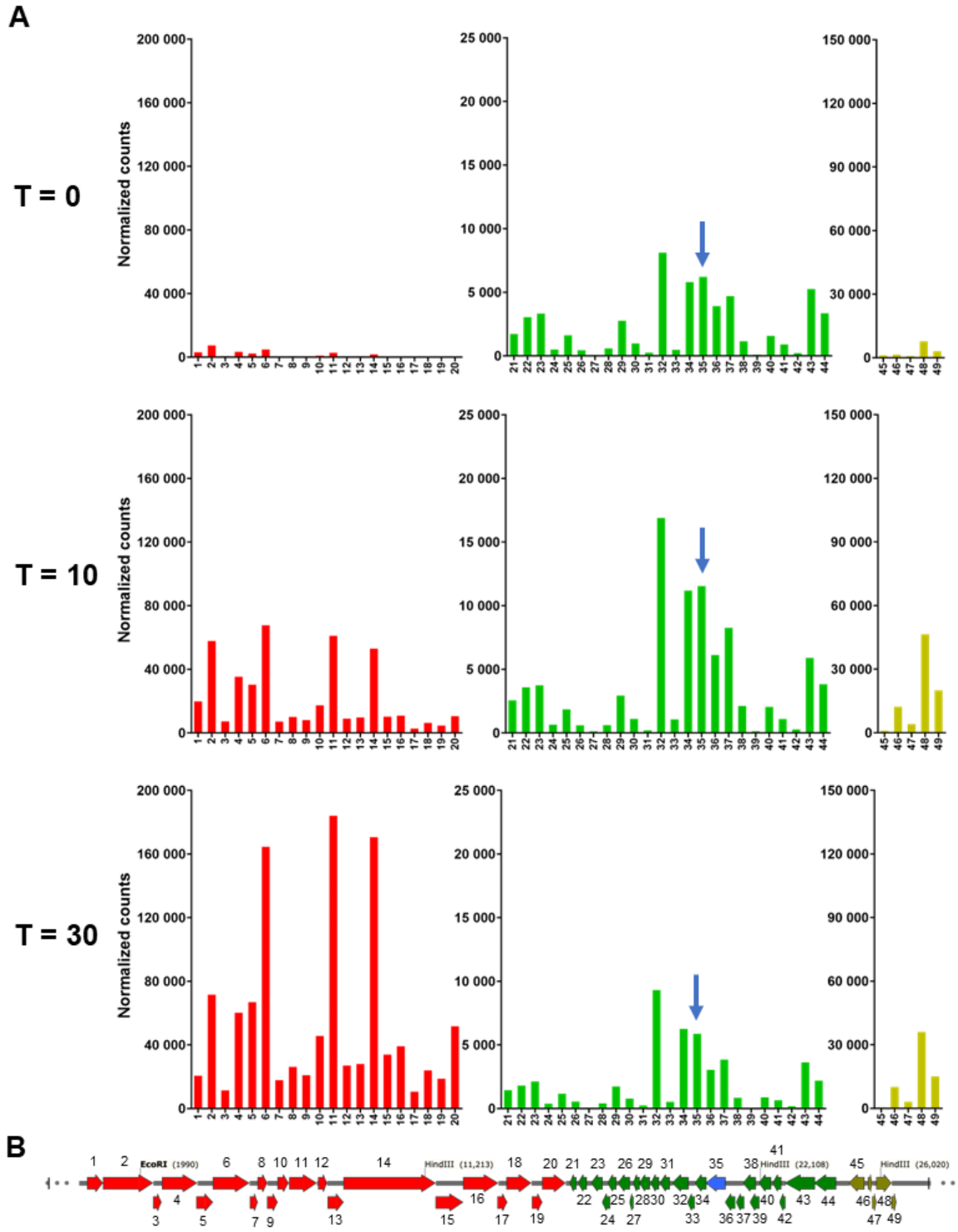


Figure 3-7: Gene expression of lactococcal phage p2 genes during normal infection.

Normalized counts of transcripts of lactococcal phage p2 genes during normal infection at three time points (0-, 10-, and 30-minutes) (A). *Sak3* is indicated by an arrow (blue). Linear schematic of lactococcal phage p2 genome (B). Early genes are coloured in green, middle genes are coloured in yellow, late genes are coloured in red, and the *sak3* gene is coloured in blue. Genome map was generated using Snapgene.

To analyze the changes in gene expression over time, the transcripts were split into early, middle, and late genes with the normalized counts plotted on a chart (**Figure 3-7**). The early phage genes have their highest expression at 10 minutes post-infection, before dropping to their lowest expression at 30 minutes-post infection. The same pattern can be seen with the middle genes. The late genes gradually increase with expression, peaking at 30 minutes post-infection. These patterns match what is expected based on what is known about phage gene transcription. Interestingly, the *sak3* gene encoded on the phage genome, is the second most highly expressed early gene of the phage, implying an important role in the phage's replication (**Figure 3-7**).

Abortive Infection K

From previous evidence gathered about the AbiK mechanism, DNA replication of the phage is inhibited, and late gene transcription is delayed. Although the phage is still able to hijack the transcriptional machinery of the host cell and transcribe its genes, this mechanism is slowed in the presence of the AbiK protein. The percentage of transcripts dedicated to nucleotide transport and metabolism (Category F) and transcripts dedicated to DNA replication, recombination, and repair (Category L) do not have a drastic change compared to the normal infection (**Figure 3-5** and **Supplementary Table 1**). The majority of transcribed genes are dedicated to protein translation (Category J), carbohydrate metabolism (Category G), and transcription (Category K) (**Figure 3-5**). At 30 minutes post-infection, the phage late genes become the 3rd most abundant set of transcripts, showing that the phage can still successfully hijack the transcriptional machinery during the AbiK mechanism (**Figure 3-5**).

Similar to the normal infection, only phage genes were detected with a 95% chance of being differentially expressed between 0- and 10-minutes post-infection (not shown). When comparing the changes from 10 minutes to 30 minutes post-infection, 14 genes were detected as

having over a 95% probability of being differentially expressed (**Figure 3-8** and **Table 3-5**). Most of the genes that were detected have lower expression at 30 minutes, including two enzymes involved in energy production and conversion, along with seven genes involved in pyrimidine biosynthesis (**Table 3-5**). For two genes, including an uncharacterized stress protein detected in the normal infection, expression was higher at 30 minutes (**Figure 3-8**). The decrease in expression for genes involved in pyrimidine biosynthesis is notable; as well those involved in riboflavin biosynthesis, which uses the GTP nucleotide as a precursor, have higher expression during the normal infection, indicating a change in a vital metabolic pathway for the development of phage progeny.

When looking at the gene expression of phage genes during the AbiK mechanism, the gene expression patterns match the normal infection at early time points, with overall lower counts (**Figure 3-9**). Interestingly, gene expression for all three sets of phage genes increases at 10 minutes post-infection, and further increases at 30 minutes post-infection (**Figure 3-9**). This is different from the normal infection, where early and middle phage gene transcription slows at later time points. During the AbiK condition, all phage genes are continuously transcribed throughout the course of the experiment. The mechanism that slows the transcription of early and middle genes in lactococcal phage p2 remains unknown, but it is likely that signalling involved in this mechanism is hindered during the AbiK mechanism. Although phage gene transcription is delayed in the AbiK infection compared to the normal infection, phage gene transcription occurs continuously with no arrest.

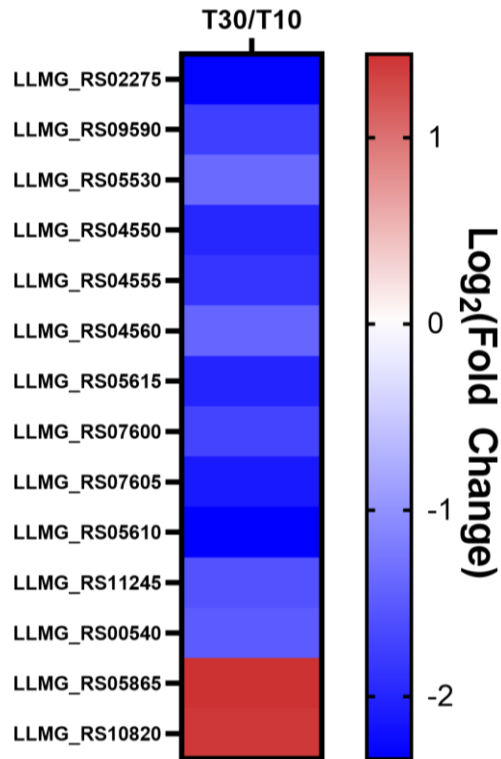


Figure 3-8: Heat map of differentially expressed genes in AbiK infection at 30 minutes vs. 10 minutes.

Heat map showing the $\log_2(\text{fold-change})$ of genes that have a 95% probability of being differentially expressed in the AbiK infection at 30 minutes vs. 10 minutes post-infection. Values >1 (red) indicate a higher expression at 30 minutes post-infection, and values < -1 (blue) indicate a lower expression at 30 minutes post-infection. Locus tags of genes are indicated.

Table 3-5: Differentially expressed genes in AbiK infection at 30 minutes vs. 10 minutes.

Locus Tag	Protein Name	Product	Function	COG Category	Log ₂ (Fold Change)
LLMG_RS02275	PorA	Pyruvate:ferredoxin oxidoreductase, alpha subunit	A key enzyme in anaerobic metabolism	C	-2.32
LLMG_RS09590	LutB	L-lactate utilization protein LutB, contains a ferredoxin-type domain	Likely an electron transporter, allows cells to use lactate as a carbon source	C	-1.77
LLMG_RS05530	CarB	Carbamoylphosphate synthase large subunit	Catalyzes the first committed step in pyrimidine/arginine biosynthesis	E	-1.37
LLMG_RS04550	PyrR	Pyrimidine operon attenuation protein PyrR/uracil phosphoribosyltransferase	Regulator protein, regulates the transcription of pyr mRNA	F	-1.99
LLMG_RS04555	UraA	Xanthine/uracil permease	Transport protein that uptakes xanthine or uracil	F	-1.85
LLMG_RS04560	PyrB	Aspartate carbamoyltransferase, catalytic subunit	Catalyzes the first step in the pyrimidine biosynthetic pathway	F	-1.41
LLMG_RS05615	PyrD	Dihydroorotate dehydrogenase	Catalyzes a reaction in pyrimidine biosynthesis	F	-2.01
LLMG_RS07600	AlIB	Dihydroorotase or related cyclic amidohydrolase	Catalyzes a reaction in pyrimidine biosynthesis	F	-1.72
LLMG_RS07605	PyrE	Orotate phosphoribosyltransferase	Catalyzes a reaction in pyrimidine biosynthesis	F	-2.11
LLMG_RS05610	Mcr1	NAD(P)H-flavin reductase	Catalyzes the reduction of flavin using NAD(P)H	H	-2.34
LLMG_RS11245	RlhA	23S rRNA C2501 and tRNA U34 5'-hydroxylation protein RlhA/YrrN/YrrO	RNA modification enzyme	J	-1.58
LLMG_RS00540	ZntA	Cation-transporting P-type ATPase	Transporter of cations	P	-1.51
LLMG_RS05865	ArsC	Arsenate reductase or related protein, glutaredoxin family	Catalyzes the reduction of arsenate	P	1.45
LLMG_RS10820	YvlB	Uncharacterized conserved protein YvlB	A stress-related protein	S	1.40

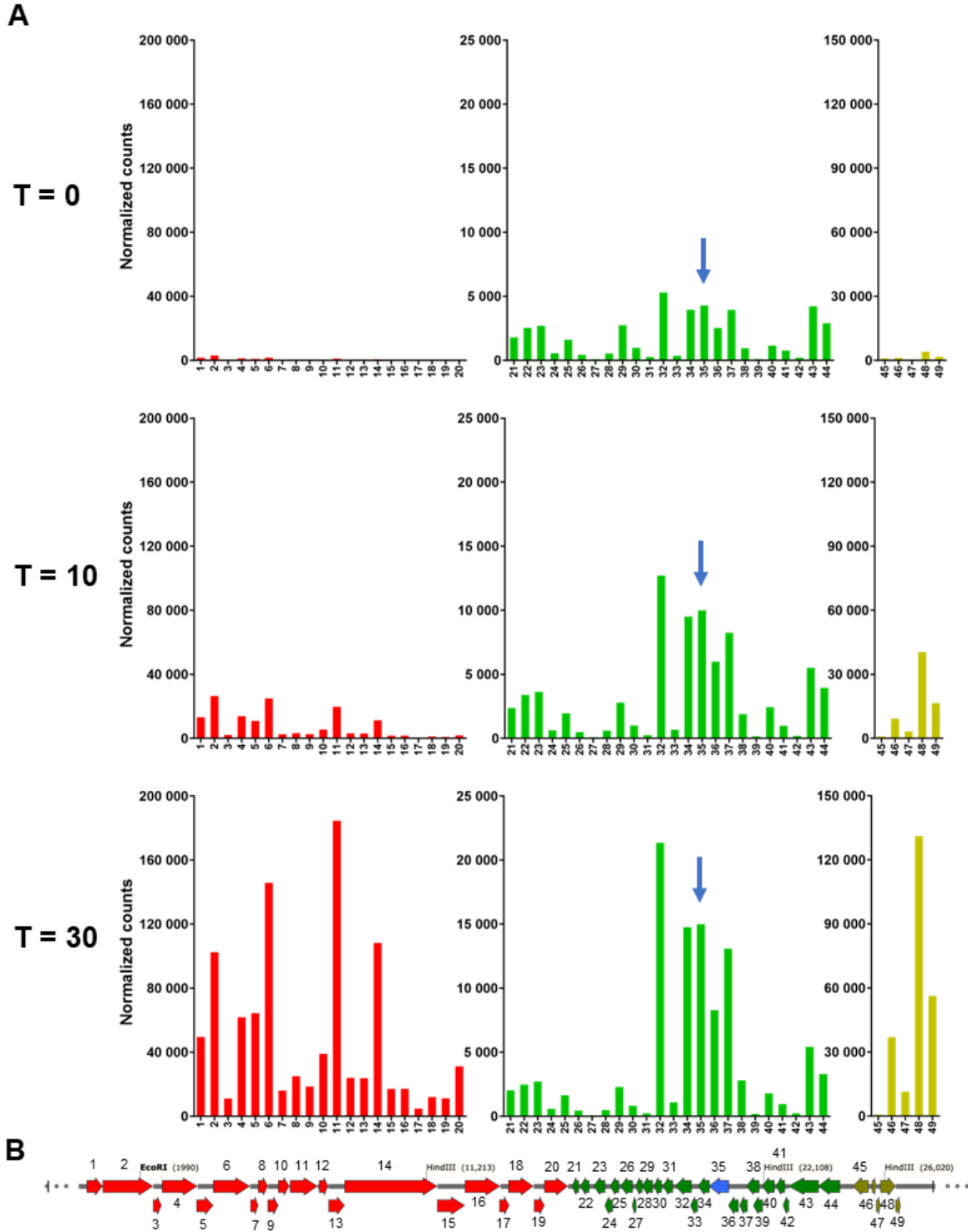


Figure 3-9: Gene expression of lactococcal phage p2 genes during AbiK infection.

Normalized counts of transcripts of lactococcal phage p2 genes during the AbiK infection at three time points (0-, 10-, and 30-minutes) (A). *Sak3* is indicated by an arrow (blue). Linear schematic of lactococcal phage p2 genome (B). Early genes are coloured in green, middle genes are coloured in yellow, late genes are coloured in red, and the *sak3* gene is coloured in blue. Genome map was generated using Snapgene.

3.3.2.4 Differential gene expression analysis

To analyze the differential gene expression between the normal infection and the AbiK mechanism, a pairwise analysis was done comparing each time point between the two conditions. A compilation of the genes that have a 95% probability of being differentially expressed was made and used to generate heat maps (**Figure 3-10** and **Figure 3-11**).

The differences in gene expression caused by the presence of the AbiK protein can be detected using the pairwise analysis of the no-phage controls: wild-type cells vs. cells with AbiK (**Figure 3-10**). Unsurprisingly, the most overexpressed gene is *abiK*. The most notable set of genes that are overexpressed is genes involved in nucleotide transport and metabolism (Category F) (**Figure 3-10**). More specifically, three of these genes are involved in the synthesis of deoxyribonucleotides and one is involved in the breakdown of a nucleotide to its sugar-phosphate and a free base (**Table 3-6**). In addition, three RNA modification enzymes are overexpressed (Category J). These changes are unsurprising, as the AbiK protein uses deoxyribonucleotides as a substrate for its polymerization activity, so the cell must increase production to increase the concentration of these substrates.

The majority of the differentially expressed genes are underexpressed in the presence of the AbiK protein, including enzymes involved in energy production and conversion (Category C), enzymes involved in carbohydrate transport and metabolism (Category G), enzymes involved in defense mechanisms (Category V), and genes involved in the mobilome (Category X). The most underexpressed gene is a putative translation factor (Category J). Notably, there is an underexpression of genes involved in riboflavin biosynthesis (Category H) at early time points post-infection, which reverts to normal levels of gene expression at 30 minutes post-infection

(**Figure 3-10**). This effect is likely seen due to the overexpression of riboflavin biosynthesis genes in the normal infection, which is not occurring during the AbiK infection (**Figure 3-6**).

A potential effect of the AbiK mechanism could be a global slowdown of the cell's metabolism. Interestingly, riboflavin biosynthesis is also decreased during the AbiK mechanism. Riboflavin, also known as vitamin B2, is a precursor to flavin adenine dinucleotide (FAD) and flavin mononucleotide (FMN), which participate in many important processes for cell survival such as electron transport and metabolism of lipids (92). In many cases, the inhibition of key enzymes in the riboflavin biosynthesis pathway often results in cell death due to the shutdown of these key processes (92). A decrease in riboflavin synthesis in the cell, which could be explained by AbiK consuming its substrates, can cause a global slowdown of the cell's metabolism.

One observation is a change in expression of the 23S rRNA (COG category 1, **Figure 3-10**). There are six copies of the 23S rRNA in the *L. lactis* genome, and all six were detected to have changes in expression, both overexpressed and underexpressed, depending on the time point. However, this observation is not reliable, as part of the experimental method of preparing samples for RNA-Seq involves a depletion of rRNA. In addition, five of the six copies have identical sequences, and, in these cases, the program randomly assigns the transcript to one of the copies, so it is best to analyze this as an overall quantity of the rRNA transcripts as opposed to individual copies. It is likely that the depletion was incomplete, leaving residual rRNA in the sample. Even between the control samples and experimental samples, the direction of change in expression is not consistent, making these findings unreliable and likely an artifact of the experiment.

When looking at the experimental samples, the same genes were found to be differentially expressed in the infection samples compared to the controls, indicating that the

introduction of the phage does not cause further changes to the expression of the *L. lactis* genome, and all changes due to the AbiK protein are already present in the cell before phage infection (**Figure 3-11**). An analysis of the phage transcriptome during the AbiK infection compared to the normal infection, shows that during early time points post-infection, there is an underexpression of almost all phage genes, notably the late genes (**Figure 3-11**). This is reversed in the later time points, where late gene expression catches up to the levels in the normal infection, but early and middle gene expression continues. These observations match what was observed in the previous section (**3.3.2.3**).

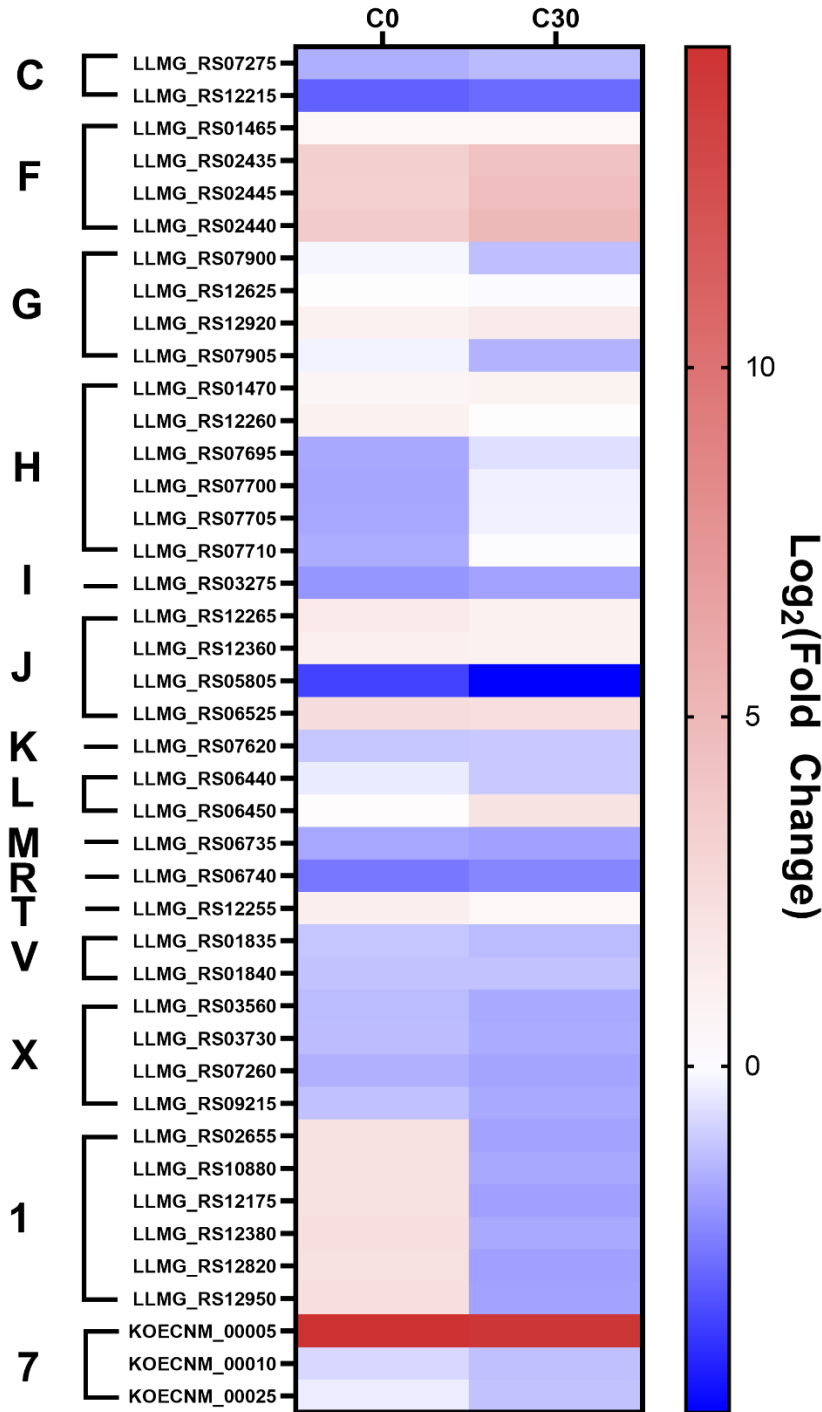


Figure 3-10: Heat map of differentially expressed genes in *L. lactis* cells in the presence and absence of the AbiK protein.

Heat map showing the log₂(fold-change) of genes that have a 95% probability of being differentially expressed in the presence of the AbiK protein compared to cells in the absence of the AbiK protein at 0 minutes and 30 minutes. Values >1 (red) indicate a higher expression in AbiK-containing cells, and values < -1 (blue) indicate a lower expression in AbiK containing cells. Locus tags of genes are indicated.

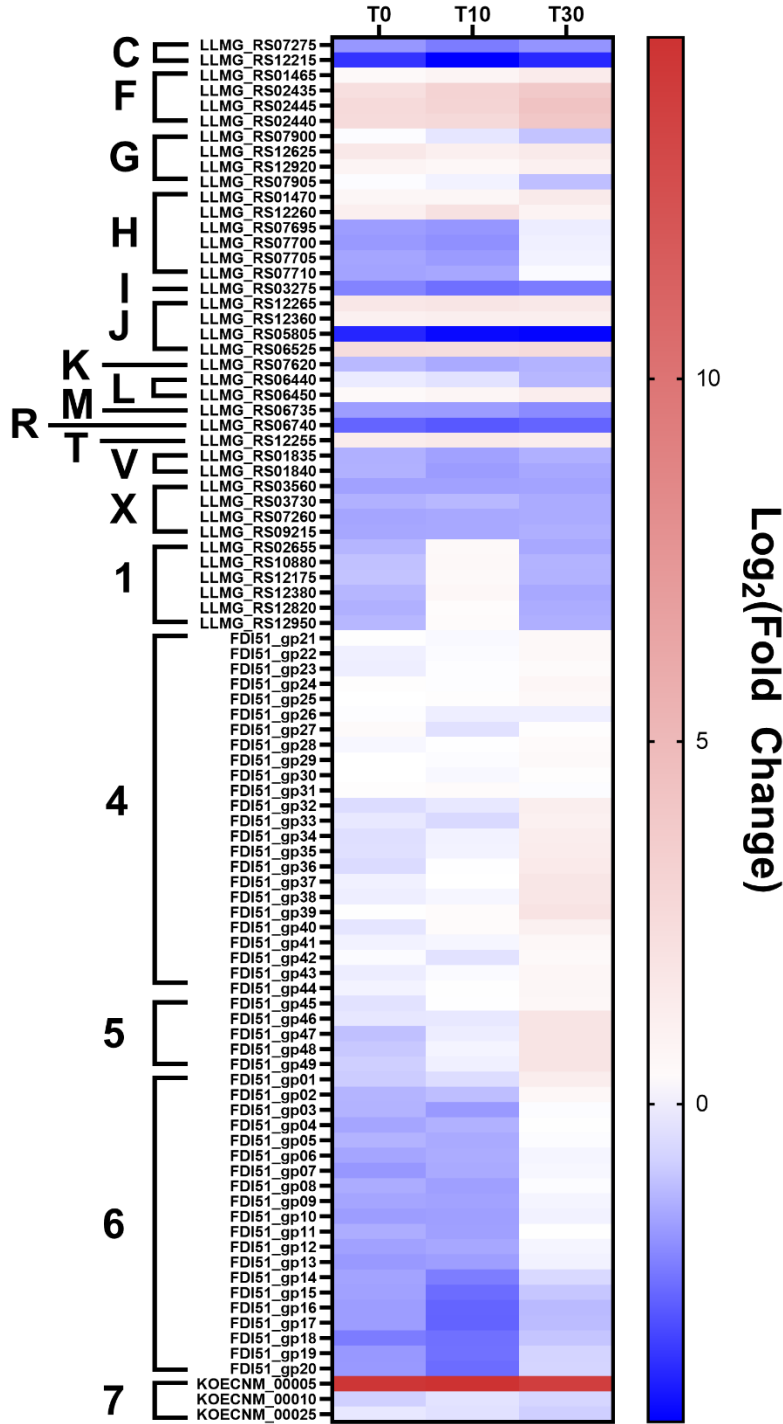


Figure 3-11: Heat map of differentially expressed genes during the AbiK infection compared to the normal infection.

Heat map showing the log₂(fold-change) of genes that have a 95% probability of being differentially expressed in the AbiK infection compared to the normal infection at 0 minutes, 10 minutes, and 30 minutes post-infection. Values >1 (red) indicate a higher expression during the AbiK infection, and values < -1 (blue) indicate a lower expression during the AbiK infection. Locus tags of genes are indicated.

Table 3-6: Differentially expressed genes in the AbiK infection compared to the normal infection.

Locus Tag	Protein Name	Product	Function	COG Category	Log ₂ (Fold Change) 0 minutes	Log ₂ (Fold Change) 10 minutes	Log ₂ (Fold Change) 30 minutes
LLMG_RS07275	SdhA	Succinate dehydrogenase/fumarate reductase, flavoprotein subunit	Central enzyme in respiratory chain in sulfur-oxidizing bacteria	C	-1.79	-2.26	-1.84
LLMG_RS12215	EutG	Alcohol dehydrogenase, class IV	Protein involved in alcohol metabolism	C	-3.52	-4.38	-3.70
LLMG_RS01465	NrdD	Anaerobic ribonucleoside-triphosphate reductase	Catalyzes the reduction of ribonucleotides to deoxyribonucleotides	F	0.41	0.73	1.36
LLMG_RS02435	RCL	Nucleoside 2-deoxyribosyltransferase	Catalyzes cleavage of deoxyribonucleoside's glycosidic bond and then transfers the deoxyribosyl to an acceptor purine or pyrimidine	F	2.27	3.11	3.84
LLMG_RS02445	Dck	Deoxyadenosine/deoxycytidine kinase	Catalyzes the attachment of a monophosphate to a deoxynucleoside	F	2.61	3.03	4.24
LLMG_RS02440	PpnN	Nucleotide monophosphate nucleosidase PpnN/YdgH, Lonely Guy (LOG) family	Catalyzes the hydrolysis of pyrimidine and purine nucleotides to form ribose 5-phosphate and a free base	F	2.55	2.66	4.00

LLMG_RS07900	FrwC	Phosphotransferase system, fructose specific IIC component	Transporter that intakes fructose	G	-0.05	-0.44	-1.03
LLMG_RS12625	AraJ	Predicted arabinose efflux permease AraJ, MFS family	Transporter that expels arabinose	G	1.63	1.10	1.48
LLMG_RS12920	GlcU	Glucose uptake protein GlcU	Transporter that intakes glucose	G	0.78	0.54	1.05
LLMG_RS07905	FruK	1-phosphofructokinase or 6-phosphofructokinase II	Regulatory enzyme in glycolysis, catalyzes the 'committed step' of glycolysis	G	-0.06	-0.22	-1.11
LLMG_RS01470	QueE	Organic radical activating enzyme NrdG/QueE	Activator of NrdD, the anaerobic ribonucleoside-triphosphate reductase	H	0.60	0.61	1.50
LLMG_RS12260	CoaD	Phosphopantetheine adenylyltransferase	Catalyzes the penultimate step of CoA synthesis	H	1.11	2.15	0.79
LLMG_RS07695	RibE	6,7-dimethyl-8-ribityllumazine synthase (Riboflavin synthase beta chain)	Involved in riboflavin biosynthesis	H	-1.69	-1.81	-0.31
LLMG_RS07700	RibB	3,4-dihydroxy-2-butanone 4-phosphate synthase	Involved in riboflavin biosynthesis	H	-1.75	-1.91	-0.26
LLMG_RS07705	RibC	Riboflavin synthase alpha chain	Involved in riboflavin biosynthesis	H	-1.55	-1.73	-0.23
LLMG_RS07710	RibD	Pyrimidine reductase, riboflavin biosynthesis	Involved in riboflavin biosynthesis	H	-1.58	-1.51	-0.09
LLMG_RS03275	Acs	Acyl-coenzyme A synthetase/AMP-(fatty) acid ligase	Catalyzes the synthesis of acetyl-CoA	I	-2.14	-2.48	-2.27

LLMG_RS12265	RsmD	16S rRNA G966 N2-methylase RsmD	RNA modification enzyme	J	1.70	1.82	1.62
LLMG_RS12360	TrmA	tRNA/tmRNA/rRNA uracil-C5-methylase, TrmA/RlmC/RlmD family	RNA modification enzyme	J	1.04	1.17	1.18
LLMG_RS05805	aMBF1	Archaeal ribosome-binding protein aMBF1, putative translation factor, contains Zn-ribbon and HTH domains	Putative translation factor	J	-3.74	-4.23	-4.31
LLMG_RS06525	TrhO	tRNA U34 5'-hydroxylase TrhO, rhodanese family	RNA modification enzyme	J	2.42	2.35	2.52
LLMG_RS07620	Rex	NADH/NAD ratio-sensing transcriptional regulator Rex	Transcriptional regulator that senses redox state of the cell	K	-1.20	-1.46	-1.31
LLMG_RS06440	XerD	Site-specific recombinase XerD	DNA repair protein	L	-0.34	-0.51	-1.25
LLMG_RS06450	TopA	DNA topoisomerase IA	Releases tension during DNA replication and transcription	L	0.38	0.67	1.25
LLMG_RS06735	MurB	UDP-N-acetylenolpyruvoylglucosamine reductase	Involved in synthesis of the cell wall	M	-1.68	-1.70	-2.00
LLMG_RS06740	NiaX	niacin ECF transporter S component NiaX	Vitamin transporter	R	-2.66	-2.87	-2.66
LLMG_RS12255	SdrC	Predicted secreted protein YlbL, contains PDZ domain	Secreted protease	T	1.33	1.56	1.28

LLMG_RS01835	AhpC	Alkyl hydroperoxide reductase subunit AhpC (peroxiredoxin)	Detoxifies reactive oxygen species under stress	V	-1.36	-1.61	-1.36
LLMG_RS01840	AhpF	Alkyl hydroperoxide reductase subunit AhpF	Transfers electrons from pyridines to AhpC	V	-1.34	-1.71	-1.52
LLMG_RS03560	Tra5	Transposase InsO and inactivated derivatives	Transposase protein involved in DNA transposition and recombination	X	-1.62	-1.61	-1.58
LLMG_RS03730	Tra5	Transposase InsO and inactivated derivatives	Transposase protein involved in DNA transposition and recombination	X	-1.35	-1.23	-1.45
LLMG_RS07260	Tra5	Transposase InsO and inactivated derivatives	Transposase protein involved in DNA transposition and recombination	X	-1.55	-1.49	-1.44
LLMG_RS09215	Tra5	Transposase InsO and inactivated derivatives	Transposase protein involved in DNA transposition and recombination	X	-1.52	-1.50	-1.37
LLMG_RS02655		23S ribosomal RNA	Component of the large ribosomal subunit (50S)	1	-1.27	0.37	-1.50
LLMG_RS10880		23S ribosomal RNA	Component of the large ribosomal subunit (50S)	1	-1.07	0.45	-1.32
LLMG_RS12175		23S ribosomal RNA	Component of the large ribosomal subunit (50S)	1	-1.03	0.38	-1.34
LLMG_RS12380		23S ribosomal RNA	Component of the large ribosomal subunit (50S)	1	-1.25	0.55	-1.49
LLMG_RS12820		23S ribosomal RNA	Component of the large ribosomal subunit (50S)	1	-1.36	0.18	-1.43
LLMG_RS12950		23S ribosomal RNA	Component of the large ribosomal subunit (50S)	1	-1.24	0.25	-1.38

FDI51_GP21	Transglycosylase	Transforms one glycoside to another	4	0.05	-0.10	0.49
FDI51_GP22	Hypothetical protein	Unknown function	4	-0.26	-0.08	0.45
FDI51_GP23	Hypothetical protein	Unknown function	4	-0.30	-0.04	0.35
FDI51_GP24	Hypothetical protein	Unknown function	4	0.12	-0.04	0.58
FDI51_GP25	Hypothetical protein	Unknown function	4	-0.01	0.08	0.49
FDI51_GP26	DUF3310 domain-containing protein	SaV protein	4	-0.04	-0.30	-0.28
FDI51_GP27	Hypothetical protein	Unknown function	4	0.35	-0.52	0.13
FDI51_GP28	Hypothetical protein	Unknown function	4	-0.13	-0.03	0.29
FDI51_GP29	DUF1140 domain-containing protein	Unknown function	4	-0.01	-0.06	0.40
FDI51_GP30	DNA methyltransferase	Transfers a methyl group to DNA	4	-0.01	-0.13	0.08
FDI51_GP31	Hypothetical protein	Unknown function	4	0.10	0.24	-0.05
FDI51_GP32	Hypothetical protein	Unknown function	4	-0.61	-0.41	1.19
FDI51_GP33	Hypothetical protein	Unknown function	4	-0.40	-0.65	1.04
FDI51_GP34	Single strand DNA binding protein	DNA that binds to ssDNA	4	-0.55	-0.23	1.23
FDI51_GP35	Sak3 protein	Protein involved in sensitivity against the AbiK mechanism	4	-0.53	-0.20	1.35
FDI51_GP36	Hypothetical protein	Unknown function	4	-0.63	-0.03	1.44
FDI51_GP37	Hypothetical protein	Unknown function	4	-0.25	-0.00	1.76
FDI51_GP38	Hypothetical protein	Unknown function	4	-0.30	-0.16	1.73
FDI51_GP39	Hypothetical protein	Unknown function	4	0.04	0.27	1.93
FDI51_GP40	Hypothetical protein	Unknown function	4	-0.45	0.25	1.02
FDI51_GP41	Hypothetical protein	Unknown function	4	-0.23	-0.15	0.52
FDI51_GP42	Hypothetical protein	Unknown function	4	-0.07	-0.49	0.40
FDI51_GP43	AAA family ATPase	ATPase with diverse cellular activities, has also been hypothesized to be a DNA polymerase	4	-0.31	-0.09	0.57

FDI51_GP44	Hypothetical protein	Unknown function	4	-0.21	0.03	0.59
FDI51_GP45	HNH endonuclease	Nuclease	5	-0.50	-0.02	0.51
FDI51_GP46	Hypothetical protein	Unknown function	5	-0.41	-0.40	1.87
FDI51_GP47	Hypothetical protein	Unknown function	5	-1.08	-0.31	1.87
FDI51_GP48	Holliday junction resolvase	Induces structural changes to Holliday junctions, involved in recombination	5	-0.95	-0.20	1.86
FDI51_GP49	Hypothetical protein	Unknown function	5	-0.82	-0.27	1.90
FDI51_GP01	Terminase small subunit	Component of DNA packaging machinery	6	-0.88	-0.59	1.26
FDI51_GP02	Terminase large subunit	Component of DNA packaging machinery	6	-1.29	-1.12	0.51
FDI51_GP03	HNH endonuclease	Nuclease	6	-1.32	-1.76	-0.05
FDI51_GP04	Portal protein	Form a channel for packaging of phage DNA	6	-1.55	-1.34	0.03
FDI51_GP05	HK97 family prohead protease	Protease	6	-1.31	-1.46	-0.05
FDI51_GP06	Capsid, minor head protein	Component of phage structure	6	-1.55	-1.44	-0.17
FDI51_GP07	Head-tail connector protein	Component of phage structure	6	-1.79	-1.46	-0.14
FDI51_GP08	Virion structural protein	Component of phage structure	6	-1.43	-1.65	-0.06
FDI51_GP09	Virion structural protein	Component of phage structure	6	-1.55	-1.61	-0.18
FDI51_GP10	Virion structural protein	Component of phage structure	6	-1.68	-1.65	-0.22
FDI51_GP11	Major tail protein	Component of phage structure	6	-1.41	-1.63	0.00
FDI51_GP12	Virion structural protein	Component of phage structure	6	-1.63	-1.51	-0.17

FDI51_GP13		Virion structural protein	Component of phage structure	6	-1.76	-1.67	-0.23
FDI51_GP14		Tail tape measure protein	Component of phage structure	6	-1.59	-2.23	-0.65
FDI51_GP15		Tail protein	Component of phage structure	6	-1.62	-2.54	-0.99
FDI51_GP16		Tail associated lysin	Hydrolase that lyses bacterial cell wall - associated with the phage tail	6	-1.68	-2.66	-1.19
FDI51_GP17		Hypothetical protein	Unknown function	6	-1.68	-2.69	-1.15
FDI51_GP18		Receptor binding tail protein	Component of phage structure	6	-2.26	-2.46	-0.99
FDI51_GP19		Holin	Triggers and controls the degradation of the host cell wall	6	-1.78	-2.44	-0.74
FDI51_GP20		Endolysin	Hydrolase that lyses bacterial cell wall	6	-1.75	-2.53	-0.73
KOECNM_00005	AbiK	Abortive infection K protein	Protein of interest in this study	7	14.41	14.70	13.81
KOECNM_00010	Cat	Chloramphenicol acetyltransferase	Resistance to chloramphenicol antibiotic	7	-0.82	-0.48	-0.71
KOECNM_00025		Plasmid vector sequence	Cloning vector sequence	7	-0.39	-0.51	-0.82

3.3.2.5 Future transcriptomics studies

The analyses here represent a preliminary RNA-seq analysis, with conclusions formed by generating simulated RNA-Seq replicates. For more meaningful analyses with more concrete evidence on differentially expressed genes, a total of 3 replicates should be used for RNA-Seq analyses at each time point. In addition, samples from only the normal infection and the AbiK infection were sent for RNA-Seq. It is known that the *sak3* gene encoded on the phage genome is involved in the AbiK mechanism, however the differential gene expression for *sak3* did not stand out in these analyses. It would be interesting to see how the global transcriptome changes during an infection with the *sak3* mutant phage, to give clues on how the mutant phage bypasses the AbiK mechanism and produces its phage progeny.

3.3.2.6 Author contributions

Processing of RNA samples for RNA-seq along with quality control was conducted by Dr. Sean Workman at the University of Regina (Dr. Christopher Yost's laboratory), and sequencing was done at the BC Genome Science Centre on a NovaSeq instrument. Processing of RNA-seq reads and aligning reads to the genome, followed by generating simulated RNA-Seq replicates using the NOIseq R package and normalizing reads between conditions using edgeR and the TMM method of normalization were conducted by Dr. Sean Workman. Furthermore, a query of genes in the RNA-seq experiment and assignment of COG categories to genes was done by Dr. Sean Workman. All other experiments and analyses of RNA-seq data were performed by me.

3.3.3 Comparison to Literature

From the RT-qPCR analysis, the AbiK mechanism was concluded to delay late phage gene transcription. Further evidence was obtained from the RNA-Seq analysis, which showed

that late gene transcription is delayed, and early/middle gene transcription persisted over the course of the AbiK infection. This is in agreement with previous studies where early and middle gene transcription of phage ϕ 36 (of the P335 species of phages) was unaffected, but gene expression of the structural proteins and the lysis module (late genes) was perturbed (55). These studies did the analyses using northern blot hybridization using the *sak* gene to represent early genes, and a late gene ORF to represent late genes (55).

Proteomic analysis of the normal infection of lactococcal phage p2 to *L. lactis* MG1363 has been reported (33). This proteomic analysis was able to detect 1 412 proteins from *L. lactis* and 38 lactococcal phage p2 proteins (33). When looking at the phage proteins detected during time-course infections, the detection of phage proteins matches the gene expression levels in this study, where genes with lower expression were not detected at the proteomics level (33). They were able to detect a significant host response to the phage infection with notable changes in protein abundance upon phage infection (33). The authors specifically note an abundance of proteins associated with pyrimidine ribonucleotide biosynthesis, which matches what is seen in this study, and indicates the phage overtaking the host machinery to rapidly replicate its genomic DNA (33). Other metabolic changes that the authors note are reductions in restriction-modification proteins and build-ups of proteins involved in ribosomal protein synthesis, representing the phage's hijacking of the cellular machinery (33). Unfortunately, these changes were not detected with the transcriptome analysis in this study, but it is important to note that no replicates were done in the RNA-Seq analysis and further replicates will lead to more meaningful analyses.

3.4 Conclusions

RNA-Seq was employed to determine what changes occur during the AbiK mechanism to allow *L. lactis* to abort infection from the phage. Although experiments were done to see how cell growth is affected and whether DNA replication is occurring, these did not reveal what the AbiK protein is doing within cells to combat the phage. Transcriptomics analysis can find the differences in gene expression on a global level and narrow down where AbiK is acting. One limitation is determining whether a change is directly due to the AbiK mechanism or a downstream effect of it.

Late phage gene transcription was seen to be delayed during the AbiK infection from the RT-qPCR and the RNA-Seq analysis. In addition, early and middle gene transcription persists and does not slow down as seen in the normal infection. Some phages, such as the T7 phage, arrest early/middle gene transcription by modifying and inhibiting the host RNA polymerase and use their own RNA polymerase for late gene transcription (90). Unfortunately, the mechanism of how lactococcal phage p2 arrests its early/middle gene transcription is unknown, so it is unknown why transcription of these genes persists. Lastly, despite many decades of research on lactococcal phage p2, the functions for many of its early/middle genes remain unknown, and questions remain on the exact mechanisms it uses to hijack the cellular machinery and propagate.

Many genes were detected as being differentially expressed between the normal infection and the abortive infection, but the most notable change is a decrease in genes involved in riboflavin biosynthesis in the AbiK mechanism. Although they are not the most underexpressed genes in the analysis, the change is notable due to the detection of an increase in riboflavin biosynthesis during the normal infection and a decrease in pyrimidine biosynthesis in the AbiK infection. During a normal infection, lactococcal phage p2 hijacks the host cell's machinery and

overexpresses genes for proteins involved in pyrimidine ribonucleotide biosynthesis (33).

Another observation is the increase in riboflavin biosynthesis, which uses GTP as a substrate for the production of riboflavin (92). As previously mentioned, riboflavin is a precursor to molecules that facilitate many important processes in the cell related to cell survival (92).

During the AbiK mechanism, if pyrimidine ribonucleotide biosynthesis is reduced or inhibited, then that would cause an inhibition of phage DNA replication due to the lack of substrates and the lag in gene transcription. In addition, due to the lack of substrates, the host cell would die due to key processes being shut down because of decreased riboflavin synthesis. In cells containing AbiK that were not infected by the phage, these processes are still reduced but not enough to kill the cell. Upon phage infection, the resources are more limited due to the phage's hijacking of the machinery, inducing cell death. The mechanism by which AbiK could reduce or inhibit pyrimidine biosynthesis is unknown, and further replicates are required to confirm or deny these findings. In addition, the Sak3 protein encoded on the phage genome is known to be involved, but its role in the system remains an enigma.

3.5 Methods and Materials

3.5.1 General Protocols

Strains, plasmids, growth conditions, and protocols are described in General Protocols of Chapter 2 (2.5.1).

3.5.2 RT-qPCR

3.5.2.1 *Sample collection and preparation*

Overnight cultures made from single colonies of *L. lactis* were inoculated 1:100 into GM17 supplemented with 10 mM CaCl₂. Medium was supplemented with chloramphenicol (Cm) at 25 µg/mL. Cultures were grown at 30°C until an optical density (600 nm) of 0.150 was achieved in 10 mL of culture. The culture was centrifuged at 5 000 x g for 5 minutes at 4°C, and the pellet resuspended in 9 mL of fresh medium. Phages were diluted in fresh medium to a titer of 1 x 10⁵ PFU/mL and added to the culture, mixed gently, and then incubated at 30°C for 10 minutes to allow phages to adsorb to host cells. Cultures were centrifuged at 5 000 x g for 5 minutes at 4°C to remove unadsorbed phages, and pellets were resuspended in 1 mL of fresh medium then added to a flask containing 19 mL of fresh medium which was separated into 1 mL aliquots. Aliquots were incubated at 30°C, with an aliquot withdrawn every 5 minutes for a total of 50 minutes. Control cultures where sterile medium was added instead of phage to mimic a phage infection were withdrawn at initial and final time points. Samples were frozen at -80°C before RNA extraction using the RiboPure™ RNA Purification Kit, bacteria (Invitrogen™) (93). RNA was extracted according to the manufacturer's protocols, eluting with 50 µL of RNase-free water at the elution step. Multiplicity of infection ranged from 0.001 – 0.002.

3.5.2.2 Preparation of standards for RT-qPCR

Standards were prepared from genomic DNA extracted from lactococcal phage p2 according to section 2.5.1.4. DNA was quantified using the Nanodrop spectrophotometer. The number of genome copies in samples was calculated, and samples were diluted to create a series of standards with different genome copy numbers (30, 300, 3 000, 30 000, and 300 000). Ct values ranged from 11 – 31 for standards during qPCR reactions.

3.5.2.3 Primer design

Five genes were targeted for RT-qPCR analysis: the capsid, the baseplate gene, the DNA polymerase gene, the HNH endonuclease gene, and the *sak3* gene. All genes in the lactococcal phage p2 genome are present as single copies in the genome, so genome copy numbers obtained from analysis would be equal to the number of copies of the genome. Primer sets were designed using the PrimerQuest™ tool from IDT™ (Integrated DNA Technologies) with a desired amplicon length between 75 - 150 bp, GC content between 40 - 60%, and an optimal primer melting temperature of 62°C. The primers were between 18 - 25 bp long (Table 3-7).

Table 3-7: Primer sequences for RT-qPCR.

Primer	Sequence (5' - 3') *	Length (bp)	Size of amplicon (bp)
Capsid_F	TGACTTTGTTTCGCCCTACTG	20	109
Capsid_R	GCGAACGTTAGCATTTGCAG	20	
Baseplate_F	TATGGAGGAACCGCACCA	18	96
Baseplate_R	ATCCCAACGGCTTAAACG	18	
Sak3_F	CCCTCTGTTGCTTTCCAAGT	20	107
Sak3_R	GCGCTAAATCGAGCTGAAGA	20	
DNAPol_F	CCATTGCCTGCGCTAAATC	19	118
DNAPol_R	GCAGGAGGTTTGCTTTGG	18	
HNHEndo_F	TCCAAAGTGTTCTGCCATTTCT	22	108
HNHEndo_R	GGAGGTTCTTTATACGAAAGAGCAA	25	

* Compatible primers are named as F (forward) and R (reverse). Primers purchased from IDT™.

3.5.2.4 RT-qPCR

RT-qPCR was performed on the Qiagen Rotor-Gene Q platform with the QuantiNova SYBR Green RT-PCR Kit according to the manufacturer's protocol (94). Each experiment was performed in duplicate with 1 μ L of the RNA extraction used as the template. A control lacking the reverse transcriptase was done to detect residual DNA in the sample (**Supplementary Figures 5-7**). A melt-curve analysis was also performed to check for nonspecific amplifications. Ct values for measured samples fell within ranges of the standard samples.

3.5.3 RNA-Sequencing

3.5.3.1 Sample collection and preparation

Samples were collected similarly to RT-qPCR experiments (**3.5.2.1**) with a change of adding phages with a titer of 1×10^8 PFU/mL. Aliquots were incubated at 30°C, with an aliquot withdrawn every 10 minutes for a total of 30 minutes. Control cultures where sterile medium was added instead of phage to mimic a phage infection were withdrawn at initial and final time points. Samples were frozen at -80°C before RNA extraction using the RNAprotect Bacteria Reagent and RNeasy Mini Kit with the on-column DNase digest (Qiagen) (82, 95). RNA was extracted according to the manufacturer's protocols, eluting with 50 μ L of RNase-free water at the elution step. Multiplicity of infection was 1.0. Eluted RNA samples were then to the University of Regina (Dr. Christopher Yost's laboratory) for further processing.

3.5.3.2 Preparation of samples for RNA-Sequencing

The RNA concentration in the samples was quantified with a Qubit 2.0 fluorometer with a Qubit RNA Broad Range Assay Kit. Sample quality was then observed using the Agilent Bioanalyzer 2100 with the Agilent RNA 6000 Nano Kit, and an RNA integrity number was obtained for each sample. The NEBNext rRNA Depletion Kit (Bacteria) was then used to deplete

rRNA. RNA fragmentation, first and second strand cDNA synthesis, end prep, and sequencing adapter ligation (unique dual indexes) was then done using the NEBNext Ultra II Direction RNA Library Prep Kit (Illumina). The samples were then pooled and sent to the BC Genome Science Centre for sequencing on a NovaSeq instrument (Illumina).

3.5.3.3 Analysis of RNA-Sequencing data

RNA-sequencing reads were aligned to the *L. lactis* MG1363 genome (NC_009004), the lactococcal phage p2 genome (NC_042024) and the plasmid sequence (pSRQ823) using Geneious software (96). Following this, the NOIseq R package was used to generate simulated RNA-Seq replicates and reads were normalized across all samples using edgeR and the TMM method of normalization to generate normalized counts for all samples (97). Pairwise differential expression analyses between conditions were done using the NOIseq R package, and results were filtered for further analysis to contain only genes with over 95% probability of being differentially expressed (97). Assignment of all genes to a COG category was done by querying genes against the COG database using the COGclassifier tool, which categorized 78% of the genes (89). The remaining genes were categorized manually, into existing categories and new categories (numbered) specific to this study

Chapter 4 : Biochemistry of AbiK

4.1 Introduction

The AbiK mechanism is brought about by a single gene, *abiK*, which encodes a protein of the same name (24). AbiK has reverse transcriptase motifs, and was found to have polymerase activity when tested *in vitro* (1). AbiK is unique among reverse transcriptase homologs as it uses untemplated polymerization to make a ssDNA of random sequence (1). This ssDNA is covalently attached to the protein, as polymerization products were lost by phenol extraction (1). In addition, when the AbiK protein is resolved on SDS-PAGE gels, the protein band was also observed to have a retarded migration after a label-chase assay, further proving a covalent bond between AbiK and its polymerization product (1).

Many years of studies have gone into determining which amino acid residue on AbiK acts as the priming site for the ssDNA product (2). The carboxy-terminal portion of the AbiK protein was known to be required for the abortive infection phenotype. Abolishment of 46 amino acids from the carboxy terminal removed the Abi phenotype, therefore initial studies looked at possible priming residues in this region. Conserved serine, threonine and tyrosine residues were identified as potential targets due to their hydroxyl group. Five conserved tyrosine residues on the carboxy-terminal region of AbiK were found from a sequence alignment with AbiK and 16 related proteins (2). Mutants that converted the tyrosine residues to phenylalanine residues were constructed to remove the hydroxyl group and then checked for polymerization activity. All mutant constructs retained polymerization activity, indicating that none of the five conserved tyrosine residues act as the priming site (**Figure 4-1**). Further methods involved sending fragments of the AbiK protein that was proteolytically cleaved by trypsin to mass spectrometry to detect if any fragments were larger than expected, indicating a covalently attached group (2).

From these studies, a phosphate group was detected in a fragment on the amino-terminal region of AbiK, indicating that the priming site could instead be in the amino-terminal region of AbiK.

Robetta and AlphaFold were released in 2021 and are free, open access databases that predict protein structures based on the primary amino acid sequences of proteins (98). The protein model of AbiK was generated using Robetta and studied to help elucidate AbiK's DNA binding site and where AbiK's active site is. The model was also analyzed to see what role the carboxy terminus of AbiK could play in the AbiK mechanism.

In 2022, the AbiK structure was published, revealing the active site, and that Y44 serves as the DNA attachment site (57). A mutant, Y44F, was purified and crystallized showing AbiK's state before DNA polymerization and the consequences of this mutation (57). Interestingly, AbiK was found to oligomerize, forming a hexamer, which is unexpected for a reverse transcriptase (57). This thesis chapter contains biochemical and *in vivo* studies to determine the location of the DNA attachment site, in addition to an analysis of the AbiK model generated by Robetta and comparisons to the published structure.

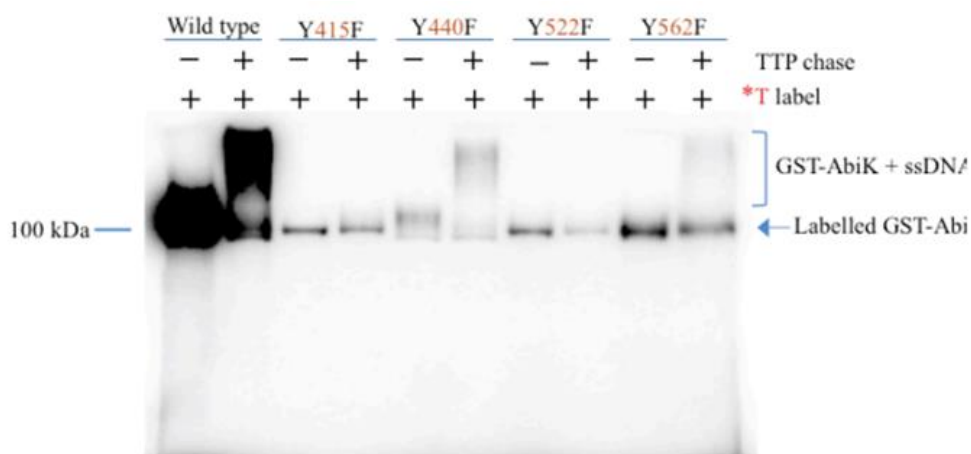


Figure 4-1: Label-chase assay for AbiK and mutant proteins.

Wild-type AbiK and mutant (Y415F, Y440F, Y522F and Y562F) AbiK proteins assayed for self-labeling and polymerization. Successful labeling activity is indicated by a band being present around 100 kDa, where GST-AbiK migrates. A successful chasing activity is indicated by a slower migrating band. Figure from B. Soufi's thesis, copied with permission (2).

4.2 Aims

One aim of this study involves the determination of the DNA attachment site on AbiK. Using a sequence alignment of AbiK and related proteins, six conserved tyrosines in the amino-terminal region of AbiK were chosen. Mutagenesis to convert the tyrosines into phenylalanine was done to remove the hydroxyl group that could act as the primer. This was done for two different studies: *in vivo* studies to look at the consequences of the mutations in *L. lactis* during the AbiK mechanism, and *in vitro* studies to see the consequences of the mutations on AbiK's catalytic activity. Together, these studies confirm the location of the DNA attachment site on the AbiK protein and reveal the *in vivo* consequences when AbiK lacks its priming site.

The second aim of this study was to analyze the Robetta-generated model of AbiK. This model was analyzed for AbiK's priming site, and to detect structural similarities between AbiK and proteins with known functions. A structural analysis and comparison to other proteins can help elucidate the function of the carboxy-terminus and how it facilitates the AbiK mechanism. The Robetta-generated model for Sak3 was also generated and analyzed.

4.3 Results and Discussion

4.3.1 Sequence Alignment of AbiK and Close Relatives

A sequence alignment of AbiK and 16 close relatives was performed at the start of the project to determine the conserved serine, threonine, or tyrosine residues in the amino-terminal region of AbiK (**Supplementary Figure 8**). Six residues, Y9, Y21, Y23, Y24, Y44 and Y51, were identified to have high sequence conservation, and were chosen for these studies (**Figure 4-2**). An updated protein BLAST search was performed in late 2022, and an updated alignment was done with AbiK and 99 of its close relatives which confirmed the 6 tyrosine residues with high conservation (**Supplementary Figure 9**). This updated alignment was done due to an increase of related sequences in the database, although no known functions were uncovered.

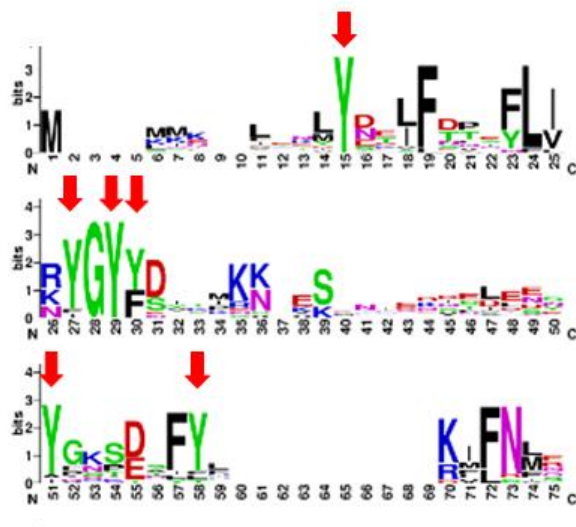


Figure 4-2: WebLogo of conserved tyrosines in the amino-terminal region of AbiK.

WebLogo of amino terminus of AbiK and 16 closely related protein sequences. Conserved tyrosine residues are indicated (red arrow). Note that numbers correspond to the sequence alignment and not amino acid positions for AbiK. Sequence logo was generated using WebLogo.

4.3.2 Making Y to F mutants of AbiK

4.3.2.1 *Escherichia coli* constructs

For *in vitro* studies, AbiK was expressed and purified as a GST-AbiK fusion protein from *E. coli* cells, with the GST-tag on the amino terminus. This fusion protein was expressed using the pGEX4T1-AbiK plasmid (**Supplementary Figure 10**). Recombinant PCR was used to make single nucleotide mutations to mutate conserved tyrosines into phenylalanine. Since phenylalanine residues lack the hydroxyl group, AbiK should be unable to use the mutated residues as a DNA attachment site. Six mutants were successfully made and confirmed by sequencing: Y9F AbiK, Y21F AbiK, Y23F AbiK, Y24F AbiK, Y44F AbiK, and Y51F AbiK (**Figure 4-3**). Y51F AbiK was made later than the others and was not used in protein assays.

4.3.2.2 *Lactococcus lactis* constructs

To see the *in vivo* effects of the AbiK mutants, the same mutations were introduced into the pSRQ823 plasmid using QuikChange Lightning mutagenesis. With these mutations made in the pSRQ823 plasmid, the mutant AbiK protein was expressed *in vivo* in *L. lactis* cells to see how the mutations affect the AbiK mechanism and to detect if the mutant AbiK protein continued to impede phage infections. Six mutants were successfully made and confirmed by sequencing: Y9F AbiK, Y21F AbiK, Y23F AbiK, Y24F AbiK, Y44F AbiK, and Y51F AbiK (**Figure 4-4**).

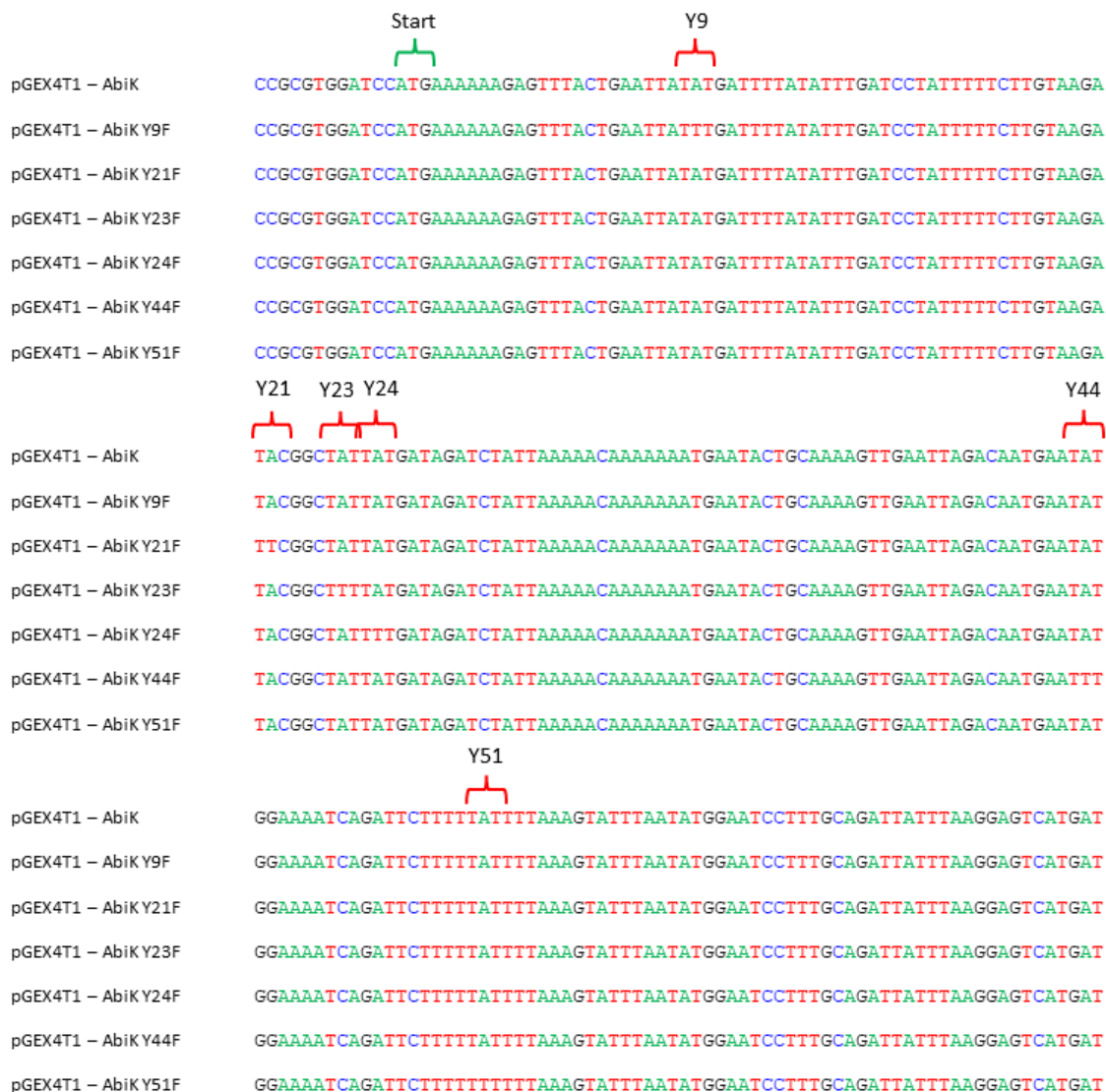


Figure 4-3: Nucleotide sequence alignment of pGEX4T1-AbiK and tyrosine to phenylalanine AbiK mutants.

4.3.3 Protein Purification of AbiK

The AbiK and mutant AbiK proteins were expressed in *E. coli* BL21(DE3) cells and then purified using affinity purification. In these constructs, a GST-tag was fused to the amino-terminus of AbiK, generating a 97 kDa fusion protein (GST-tag 26 kDa, AbiK 71 kDa). The WT and mutant fusion proteins migrate slightly above the 100 kDa protein marker (**Figure 4-5**). The slower than expected migration is due to AbiK being found covalently attached to polynucleotides in cells, which are varying in size. This variation in size also leads to multiple GST-AbiK bands which are detected in the gel (**Figure 4-5**). From silver stain analysis, GST-AbiK, GST-Y9F AbiK, GST-Y21F AbiK, GST-Y23F AbiK, and GST-Y24F AbiK were detected on the gel (**Figure 4-5**). GST-Y44F AbiK could not be detected with confidence.

Overall, the purification was messy as many other bands were detected in the silver-stained gel. A large amount of GST-tag was observed (26 kDa), which indicates the degradation of AbiK in the GST-AbiK fusion protein *in vivo*. The overexpression of AbiK in *E. coli* resulted in a large amount of degraded protein due to difficulties with producing properly folded protein (1). From the recent structure of AbiK, which reveals that AbiK preferably forms an oligomer, it is likely that the GST-tag inhibits this oligomer-formation, thus causing the difficulties with folding (57).

A western blot was performed to detect the GST-tag in the samples from the purification of GST-AbiK and its mutants. A band corresponding to GST-AbiK was confidently detected in the WT and Y21F mutant form of AbiK (**Figure 4-6**). From a longer exposure, a band corresponding to GST-AbiK was detected in Y9F and Y23F (**Figure 4-6**). GST-Y24F AbiK was unable to be detected despite a clear presence of the band in the silver stain. Unfortunately, GST-Y44F AbiK still could not be detected in the western blot.

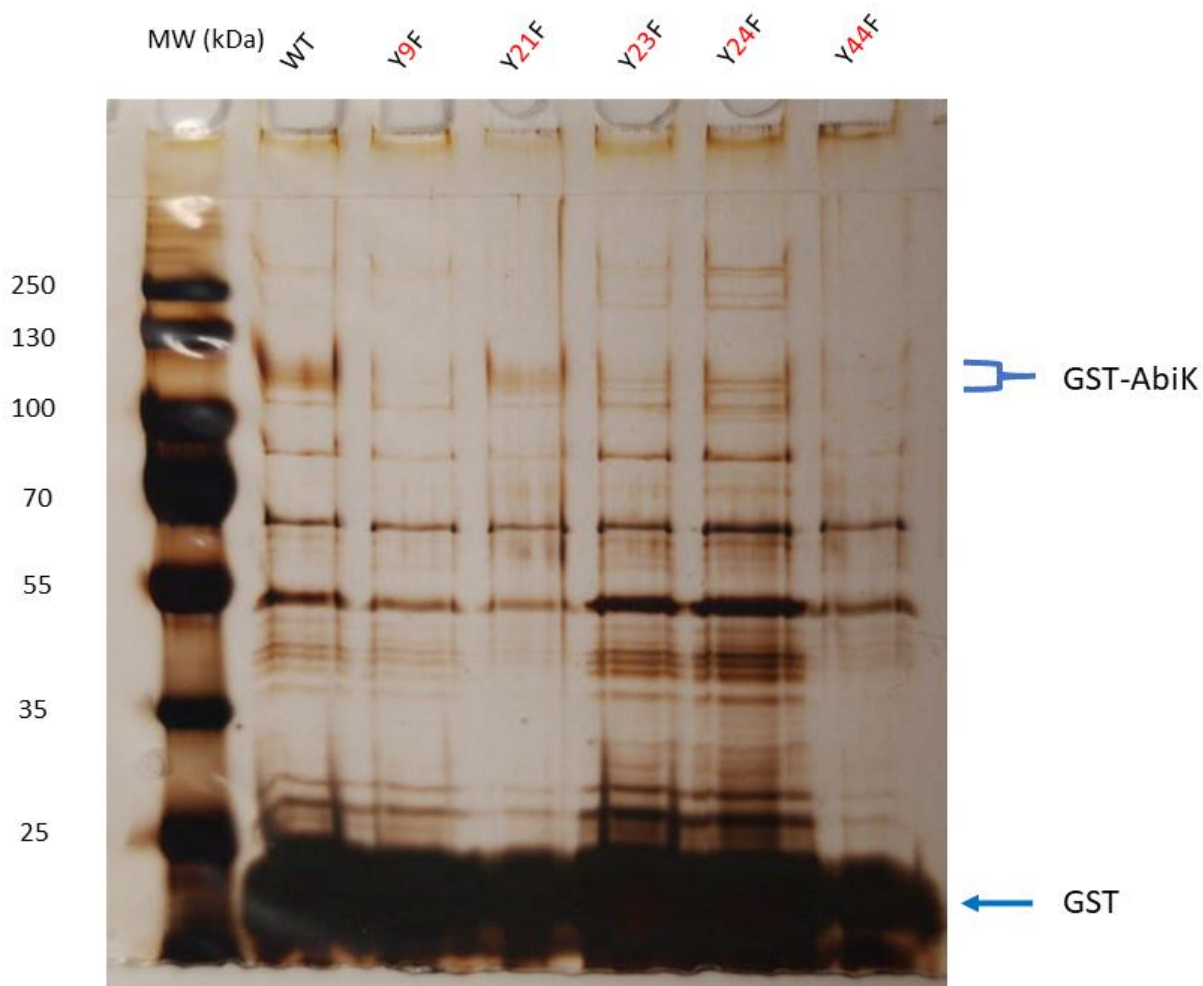


Figure 4-5: Silver stain of GST-AbiK and mutant purifications.

10% SDS-PAGE gel with elutions for the purification GST - AbiK and GST – Y to F AbiK mutants. Silver stain was used to visualize proteins. Lane one contains the PageRuler Plus Stained protein ladder (ThermoFisher) with sizes shown. Lanes 2-7 show the elutions from the purification of the wild-type GST-AbiK construct and the GST – Y to F mutants. The expected migration of the GST tag and fusion proteins is indicated.

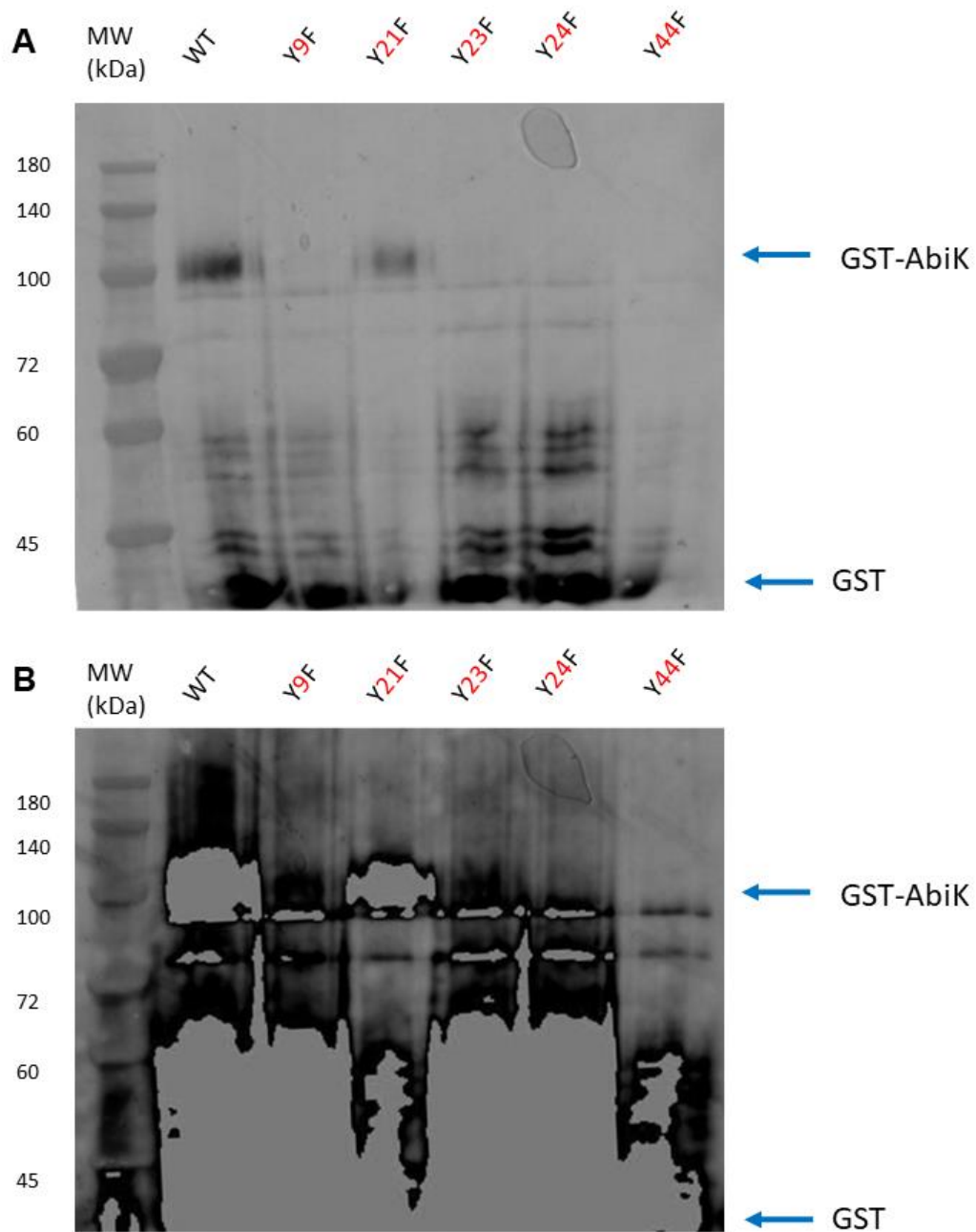


Figure 4-6: Western blot of GST-AbiK and mutant purifications.

A: Western blot of the elutions for the purification GST - AbiK and GST - Y to F AbiK mutants. An anti-GST antibody from rat was used to bind the GST-tag. Rabbit anti-rat HRP conjugate antibodies were used for chemiluminescent detection. Lane one contains the BlueAQUA pre-stained protein ladder (GeneDirex, Inc) with sizes shown. Lanes 2-7 show the elutions from the purification of the wild-type GST-AbiK construct and the GST - Y to F mutants. The expected migration of the GST tag and fusion proteins is indicated. **B:** A longer exposure of the same blot is shown.

4.3.4 Label-Chase Assay

Elutions from the GST affinity purification of WT-AbiK and the mutant AbiK's were tested for activity using a radioactive label-chase assay. The radioactive label-chase assay is described in **Figure 4-7A**. Labelled and chased assay reactions were then resolved on SDS-PAGE gels, where the labelled reaction produces a band that comigrates with GST-AbiK and the chase reaction produces a slower migrating band, corresponding to GST-AbiK with a polynucleotide chain.

From the label-chase assay of GST-AbiK and the GST-AbiK Y to F mutants, all constructs except for Y44F AbiK incorporated the radioactive nucleotide in the label reaction and polymerized a longer strand in the chase reaction (**Figure 4-7**). Since Y44F was unable to incorporate a radioactive nucleotide in the label reaction, it was suggestive of Y44 being the priming site. However, GST-Y44F was unable to be detected from either silver staining or western blotting, therefore the results could be due to the protein not being properly produced and purified, making it difficult to say with certainty that Y44 is the priming site.

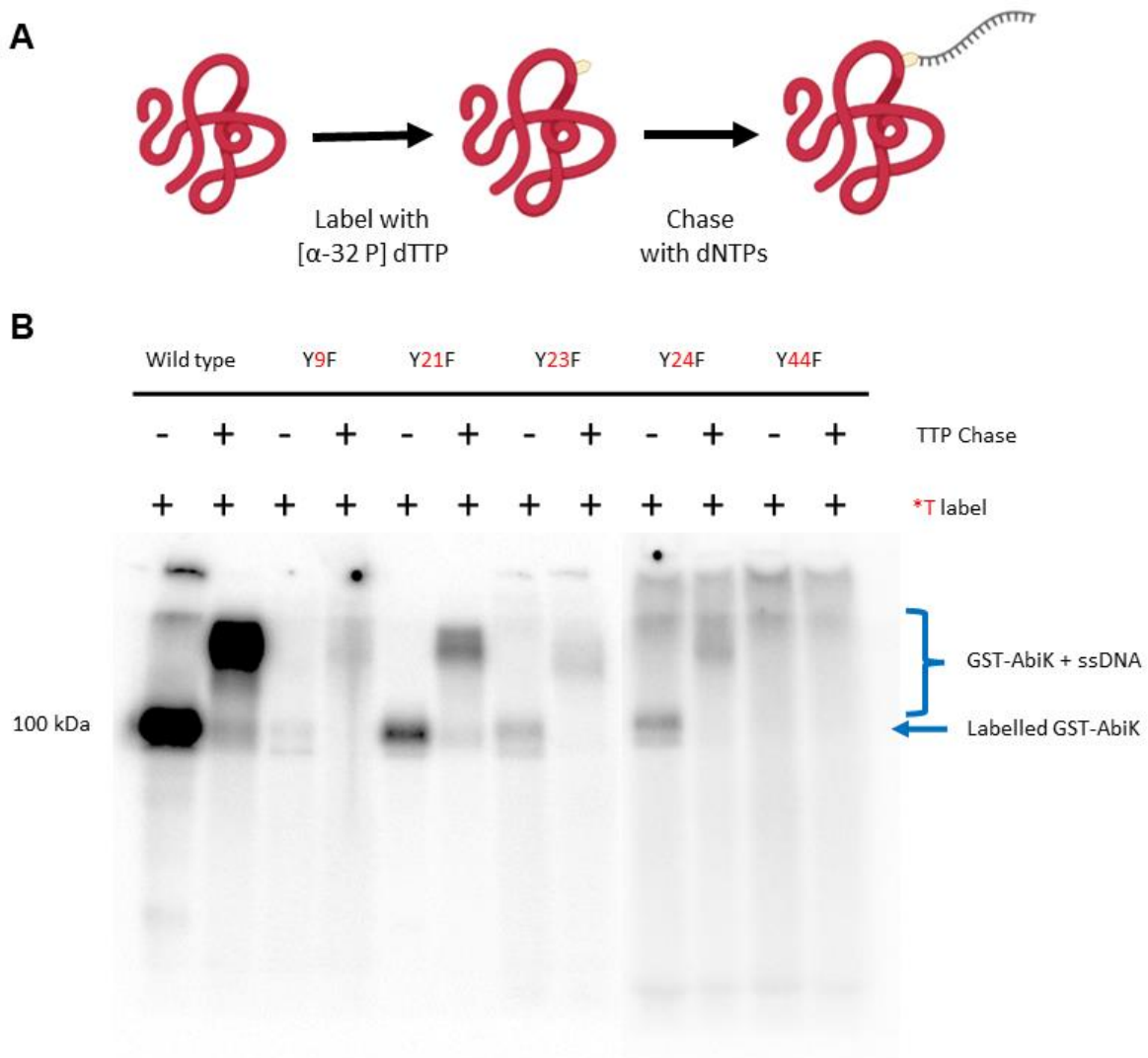


Figure 4-7: Label-Chase Assay.

A: Schematic of the label-chase assay. AbiK protein (red) was labelled with $[\alpha\text{-}^{32}\text{P}]$ dTTP which gets covalently attached to AbiK, followed by a chase with dNTPs that elongates the ssDNA on AbiK. **B:** Label-chase assay of wild-type GST-AbiK protein and GST – Y to F AbiK mutants. Assay products were resolved on a 10% SDS-PAGE gel and visualized by phosphorimaging. The products of the labelling reaction co-migrate with GST-AbiK, and the label-chase reaction produces a slower migrating band. The expected migration of products is indicated.

4.3.5 *In vivo* effects of Y to F AbiK mutants

To observe the *in vivo* effects of the AbiK mutants, mutant proteins were constitutively expressed in *L. lactis* cells which were then challenged by lactococcal phage p2 and the mutant *sak3* (M90I) lactococcal phage p2. All mutants except for Y44F AbiK showed the same phenotype as *L. lactis* containing the pAbiK plasmid as they were resistant to lactococcal phage p2, meaning that those mutations did not affect the AbiK mechanism (**Figure 4-8**). Interestingly, Y44F showed the same phenotype as *L. lactis* containing the p Δ AbiK plasmid, showing that this mutation was detrimental to the AbiK mechanism, rendering the *L. lactis* cells sensitive to lactococcal phage p2 infection (**Figure 4-8**). All constructs were sensitive to infection by the mutant *sak3* (M90I) lactococcal phage p2 (**Figure 4-8**).

Construction of the Y44F mutant proved difficult in comparison to the other 5 mutants. Transformants in *L. lactis* with the Y44F AbiK plasmid did not appear and grow at the same frequency as the wild-type pSRQ823 plasmid or the other mutants. A typical transformation with 50 - 100 ng of DNA and 100 μ L of the transformation being plated would yield 200 - 300 colonies with the wild-type plasmid. However, no colonies formed with transformation of the Y44F AbiK plasmid. When the quantity of DNA was increased to 300 ng with 1 mL of the transformation plated, 10 colonies formed on *L. lactis* transformation plates.

Due to the difficulty to obtain Y44F AbiK transformants, additional colonies were tested to see if all Y44F AbiK transformants were sensitive to lactococcal phage p2 infection, which all 10 were found to be (**Figure 4-9**). These colonies were also checked for plasmid integrity, and all of them were found to have insertions, deletions, or mutations (**Table 4-1, Supplementary Figures 11-12**). The fact that a mutation was found in all the colonies that formed, suggests that the Y44F AbiK mutant is toxic to *L. lactis*. For the cell to survive, it had to mutate the Y44F

AbiK plasmid to produce inactive protein. This is an interesting development, as the AbiK mechanism, likely leading to cell death, is mediated by this protein, and knowing that a mutant form of the protein is toxic to cells even without a phage infection is intriguing.

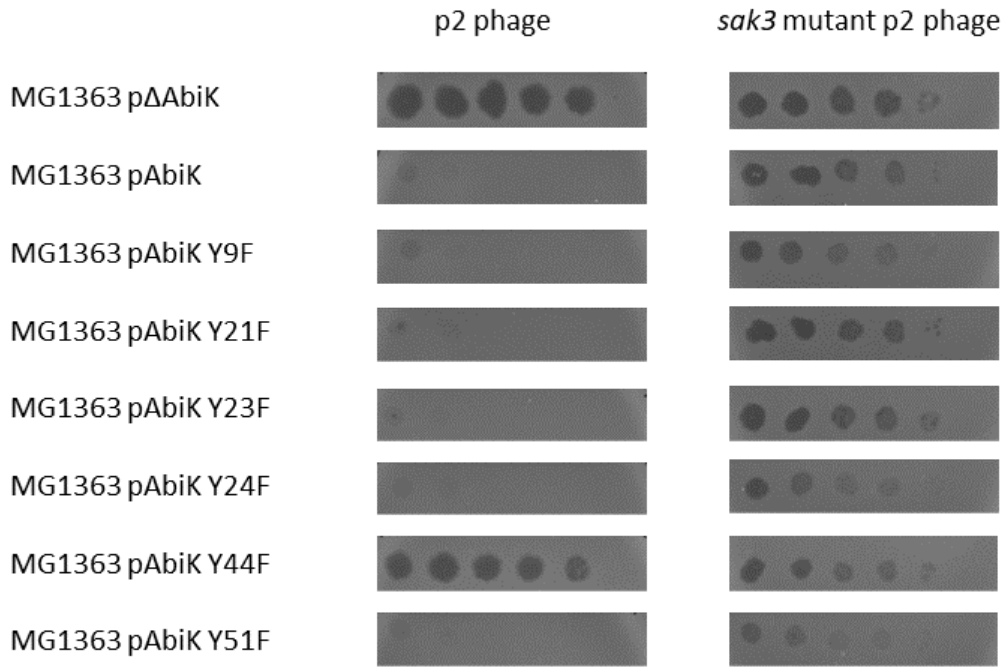


Figure 4-8: Effects of Y to F AbiK mutations in vivo.

Serial dilutions of lactococcal phage p2 and *sak3* mutant lactococcal phage p2 were spotted onto bacterial lawns of *L. lactis* strain MG1363 pΔAbiK (AbiK⁻ cells), MG1363 pAbiK (AbiK⁺ cells), or MG1363 pAbiK with Y to F mutants of AbiK.

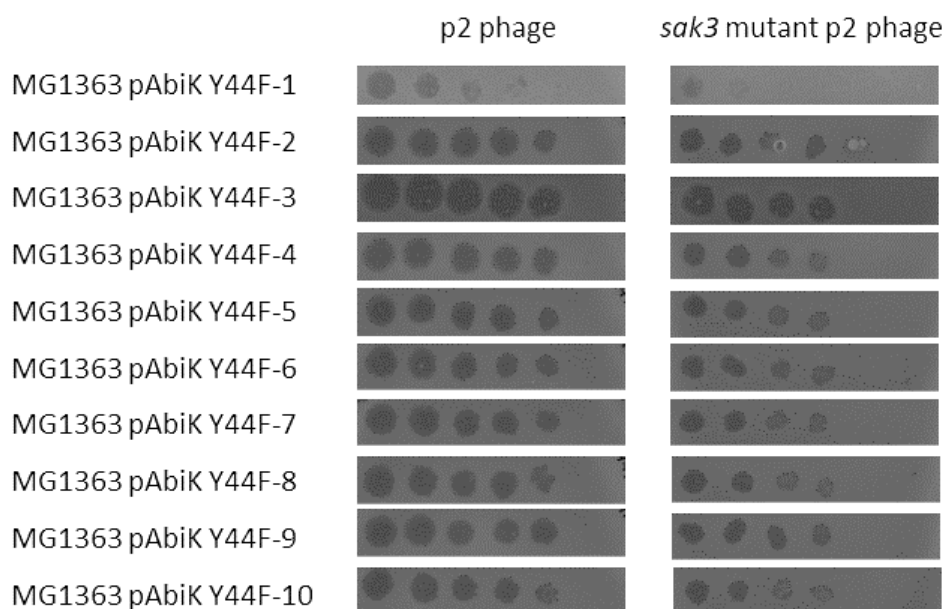


Figure 4-9: Effects of Y44F AbiK mutations in vivo.

Phage spot assay testing different colonies of *L. lactis* strain MG1363 pAbiK with the Y44F mutation. Serial dilutions of lactococcal phage p2 and *sak3* mutant lactococcal phage p2 were spotted onto bacterial lawns of *L. lactis* strain MG1363 pAbiK Y44F.

Table 4-1: Summary of mutations found in pAbiK Y44F plasmids.

Plasmid	Mutation Found
pAbiK Y44F – 1	~ 1000 bp deletion
pAbiK Y44F – 2	Single nucleotide deletion at positions 908 and 1058
pAbiK Y44F – 3	16 bp insertion in <i>abiK</i>
pAbiK Y44F – 4	Single nucleotide deletion at position 1058
pAbiK Y44F – 5	345 bp deletion in <i>abiK</i>
pAbiK Y44F – 6	~ 1000 bp deletion
pAbiK Y44F – 7	~ 2 000 bp insertion
pAbiK Y44F – 8	95 bp deletion in <i>abiK</i>
pAbiK Y44F – 9	~ 2 000 bp insertion
pAbiK Y44F – 10	Single nucleotide insertion after position 97

4.3.6 Structural Analysis of AbiK model

4.3.6.1 Analysis of AbiK domains

The model for AbiK was generated by inputting the entire amino acid sequence of AbiK into Robetta's structure prediction query (99). The output was five monomeric models with slight variations, with the largest discrepancy being a flexible region from positions 1 - 60 in the protein models. For simplicity, model 1 was chosen for analysis as it was the one with the least variation in error estimates in each position.

When looking at the model, two discrete domains for AbiK are visually identified, but three domains are assigned. The priming region of AbiK is known to be on the amino-terminal region of the AbiK protein, and this domain spans amino acids 1 – 80. The reverse transcriptase domain, containing the reverse transcriptase motifs, spans amino acids 81 – 292. The carboxy-terminal region of AbiK spans amino acids 292 – 599. These three domains are named the priming domain (positions 1 - 80), the reverse transcriptase domain (positions 81 - 292), and the α -Rep domain (positions 293 - 599) (**Figure 4-10**).

4.3.6.2 Analysis of AbiK's RT domain

AbiK contains RT motifs that are essential for abortive infection as mutations of key catalytic residues eliminate phage resistance (47). AbiK's RT domain from the Robetta model was superposed with a group II intron reverse transcriptase (6AR1) to compare the polymerase domains of the proteins (100). The group II intron reverse transcriptase was chosen for superposition because it is a bacterial reverse transcriptase, making it suitable for comparison with the bacterial protein AbiK, and there is 55% sequence similarity in the reverse transcriptase regions of the proteins. One of the published structures of the group II intron reverse

transcriptase was crystallized with its primer-template, allowing the superposition to suggest how the nascent DNA will bind to AbiK during polymerization.

AbiK's RT domain (residues 81 - 292) aligns well with the RT domain in the group II intron reverse transcriptase (residues 60-273) structure, with an RMSD of 2.043 Å (calculated using C α pairs) (**Figure 4-11**). The amino-terminal region of AbiK contains more loops compared to the group II intron reverse transcriptase. The large loop (residues 13 - 56) in the N-terminal region of AbiK sits where the primer-template does in the group II intron reverse transcriptase, indicating that the priming site of the AbiK protein should reside in this loop (**Figure 4-12**). The carboxy-terminal region of AbiK does not superpose with the maturase domain of the group II intron reverse transcriptase (**Figure 4-11**).

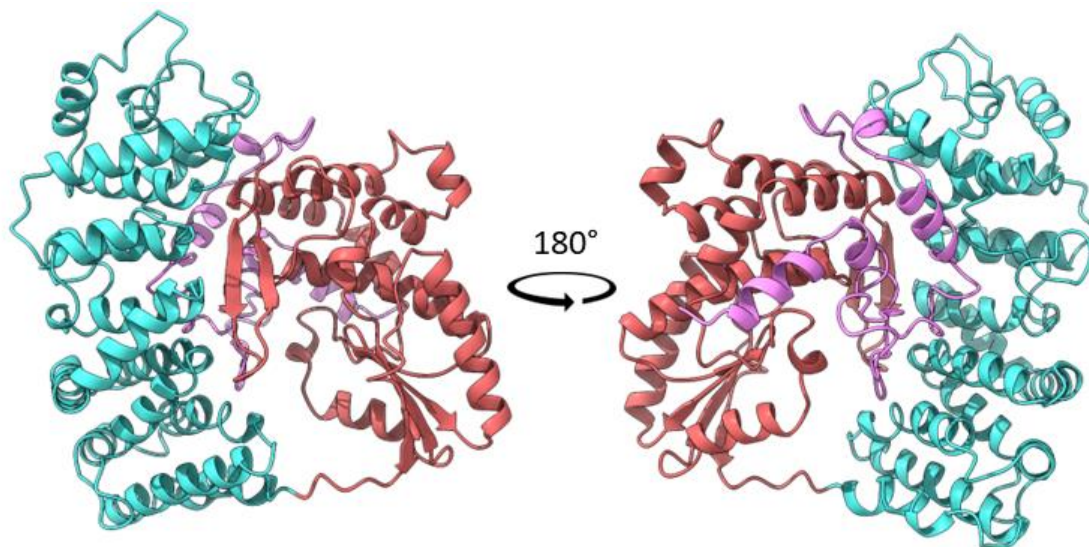


Figure 4-10: Ribbon diagram of AbiK model.

Ribbon diagram of AbiK model generated by Robetta. The priming domain is coloured in violet, with the reverse transcriptase domains in red and the carboxy terminal (α -Rep) domain in turquoise. Figure made using UCSF Chimera X (58).

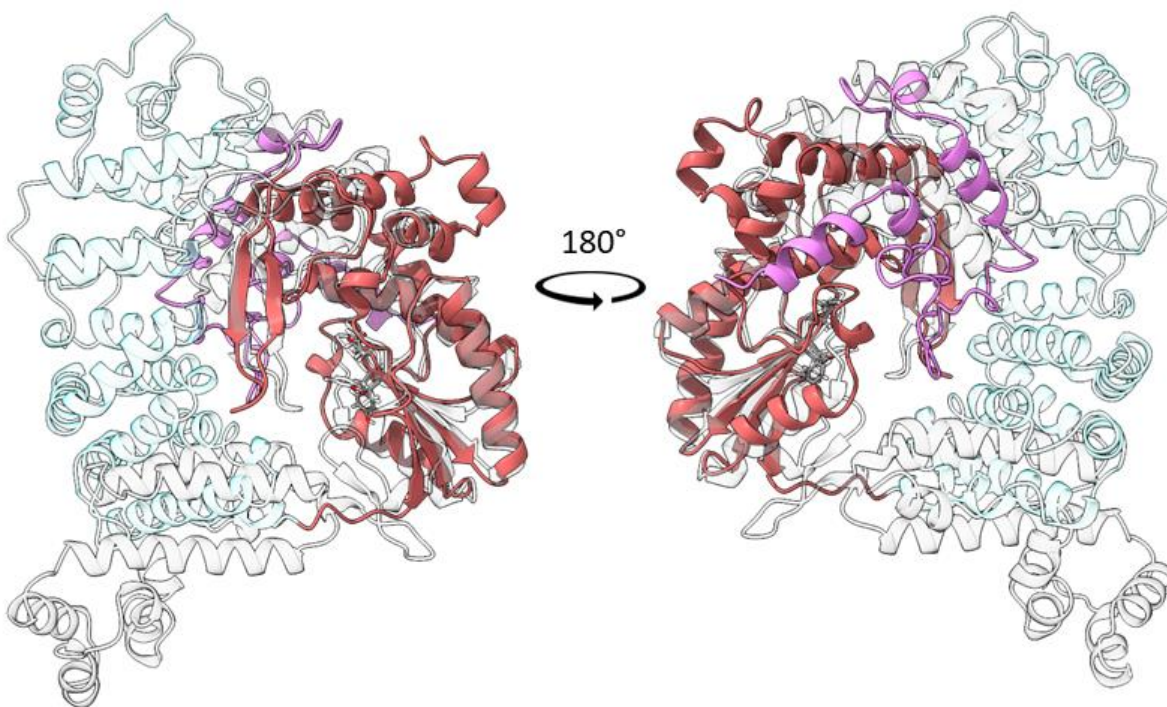


Figure 4-11: Superposition of AbiK model with group II intron reverse transcriptase.

Superposition of AbiK model with group II intron reverse transcriptase (6AR1). The priming domain of AbiK is coloured in violet, with the reverse transcriptase domain in red and the α -Rep domain in transparent turquoise. The group II intron reverse transcriptase is coloured in white. Figure made using UCSF Chimera X (58).

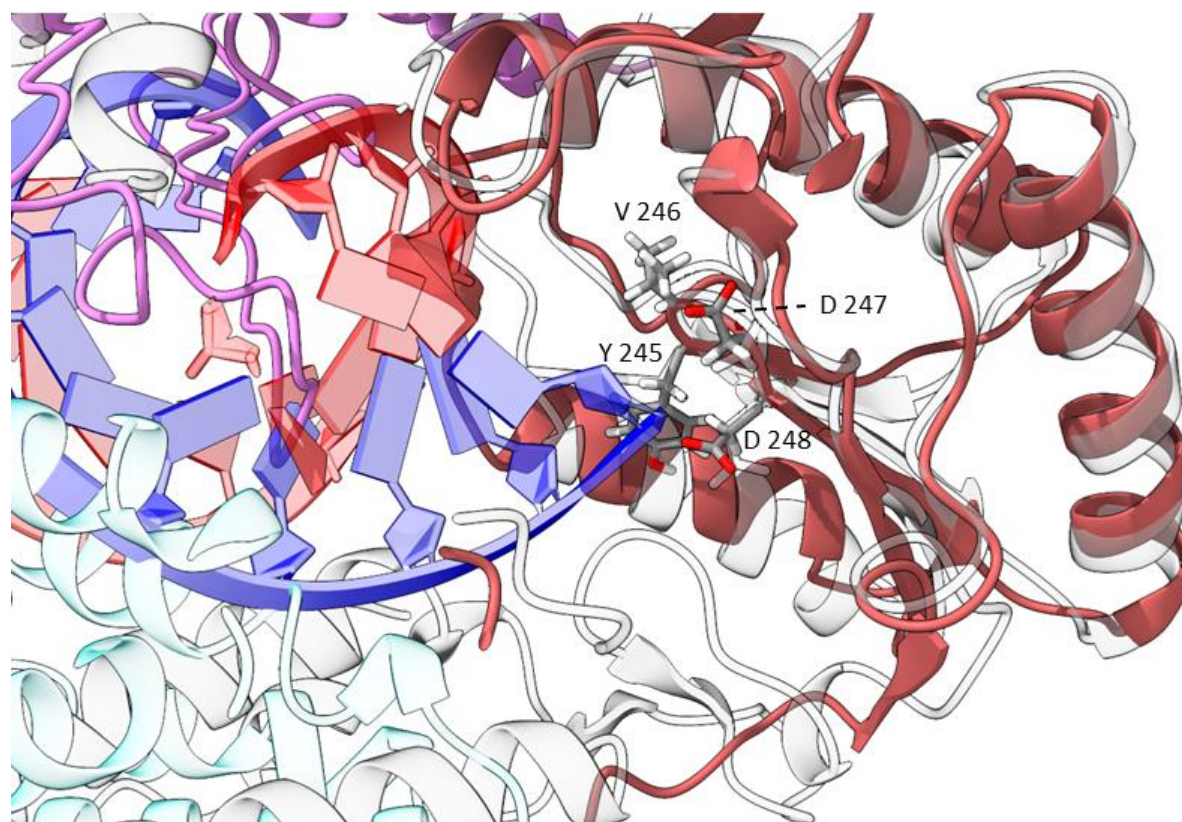


Figure 4-12: Superposition of AbiK model active site with 6AR1.

Superposition of AbiK model active site with group II intron reverse transcriptase (6AR1) active site. The priming domain of AbiK is coloured in violet, with the reverse transcriptase domains in red and the α -Rep domain in transparent turquoise. The group II intron reverse transcriptase is coloured in white. The RNA template is coloured red, and the DNA substrate is coloured blue. Key catalytic residues of AbiK are shown as sticks and labeled. Figure made using UCSF Chimera X (58).

4.3.6.3 Analysis of AbiK's carboxy terminal domain

The function of the carboxy terminal region of AbiK has remained elusive for over two decades (1). Initial hypotheses about its function stemmed from other reverse transcriptases, putatively indicating that the carboxy terminus could contain a maturase as seen in group II intron reverse transcriptases, a thumb domain of a polymerase, or an endonuclease (47). Experiments were performed to test for enzymatic activities in the carboxy terminal domain of AbiK, specifically for RNase activity, with no conclusions formed (2). Although the amino acid sequence for this domain of AbiK does not align to proteins with known functions, the model can lead to hypotheses about its function (101). In the model for AbiK, residues 293-599 form a domain that contains many alpha helices that pack antiparallel to each other.

The helices fold in a right-handed twist, allowing the domain to wrap around AbiK's active site and the location of the nascent DNA strand (**Figure 4-13**). The bundle of alpha helices is similar to other nucleotide binding domains, such as the HEAT repeat, the pentatricopeptide repeat, or the armadillo repeat domain (**Figure 4-13**) (101). The carboxy terminal region of AbiK was superposed with the structure of an engineered pentatricopeptide repeat that was bound to ssDNA (**Figure 4-14**). From this superposition, the ssDNA can be seen to sit along the carboxy terminal region of AbiK, implying that the carboxy terminal region of AbiK can have a structural function to stabilize the ssDNA, which is prone to digestion by nucleases within cells. This is further supported by experimental data, as AbiK is known to have short ssDNA sequences covalently attached to it, even following nuclease digestion (1, 57). The carboxy terminus is therefore hypothesized to be involved in stabilizing the nascent DNA strand that AbiK polymerizes.

A systematic analysis of reverse transcriptases identified and classified several prokaryotic reverse transcriptases involved in viral defense mechanisms (54). The RTs were grouped into four different classes, the largest of which is a class of RTs that contain repeat-containing domains (54). AbiK was classified to be part of this class of RTs due to its alpha-helix HEAT-like repeat in its carboxy terminal region, which was determined through structural modeling (54). This structural motif was dubbed the α Rep domain, differentiating it from the HEAT repeat as there is no sequence similarity (54). Although many other prokaryotic reverse transcriptases were found to have the α Rep domain, its function remains unknown but it is hypothesized to have an accessory role (54). Several members of this RT class were found to be multi-domain and multi-gene systems, being fused to or functioning with other effector domains that are involved in the defense mechanisms, making the α Rep domain involved in the recruitment of the effectors or stabilization of the protein structure (54).

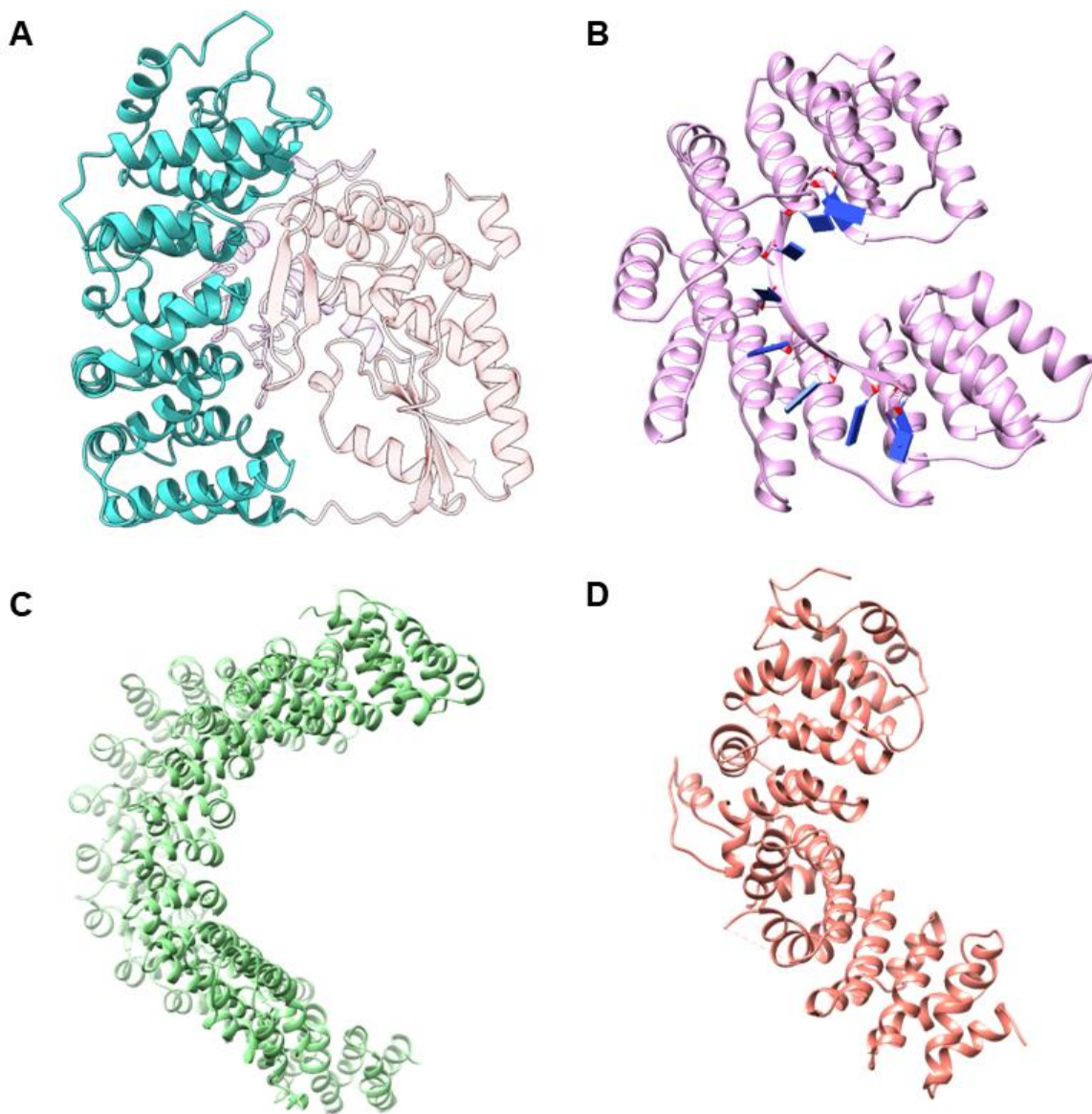


Figure 4-13: Comparison of AbiK α Rep domain and other alpha helical repeat domains.

Comparison of AbiK model's carboxy-terminal domain (A) with other alpha helical repeat domains: Pentatricopeptide repeat domain with ssDNA (B, 50RQ), HEAT repeat in PP2A (C, 1B3U), and the Armadillo repeat domain (D, 1XM9) (102–104). Figure made using UCSF Chimera X (58).

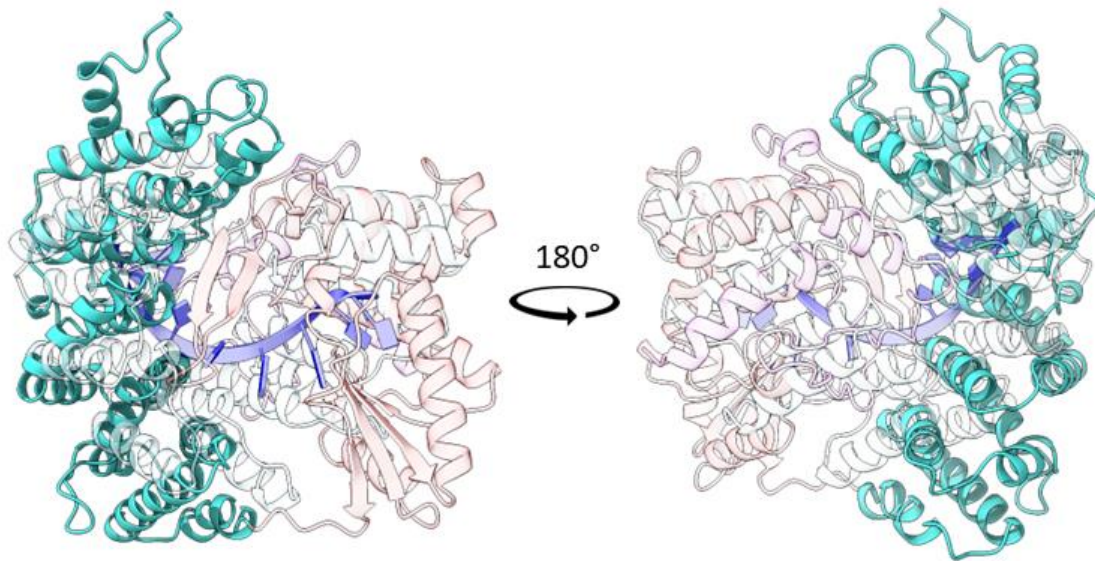


Figure 4-14: Superposition of AbiK model with pentatricopeptide repeat.

Superposition of AbiK model with pentatricopeptide repeat domain (50RQ) (102). The amino-terminal domain of AbiK is coloured in transparent violet, with the reverse transcriptase domains in transparent red and the carboxy-terminal domain in turquoise. The pentatricopeptide repeat domain is coloured in white. The ssDNA is coloured in dark blue. Figure made using UCSF Chimera X (58).

4.3.6.4 Analysis of AbiK's active site and DNA attachment site

The catalytic residues of the reverse transcriptase portion of AbiK are YVDD in positions 245 - 248 and were confirmed when mutations of these residues rendered the AbiK mechanism ineffective (1). The catalytic residues of AbiK sit in a pocket of the protein, which acts as the active site where polymerization occurs (**Figure 4-15**). The pocket has a channel, acting as an exit site for the nascent DNA strand (57). A large loop (residues 20 - 57) that contains the proposed DNA attachment site in the amino terminal region of AbiK sits within this pocket, supporting that an amino acid within this region is the covalent attachment site for the nascent DNA.

The previously proposed DNA attachment sites were examined. Tyrosine 9 (Y9) is not close to the active site and instead is part of an alpha helix that is exposed on the surface of AbiK (**Figure 4-15**). The hydroxyl groups of Y23, Y24, and Y51 all point away from the active site residues. Y21 and Y44 are the most likely candidates for the DNA attachment site, with the hydroxyls of Y21 and Y44 sitting 17.0 and 17.4 Å away from the catalytic aspartate (D248), respectively. However, Y21 sits closer to alpha helices in the RT domain, making van der Waals interactions with them. Furthermore, Y44 sits on the most flexible region of the loop and does not appear to make any interactions, making it the most likely candidate for the priming site. This was an exciting revelation as it supported the experimental data.

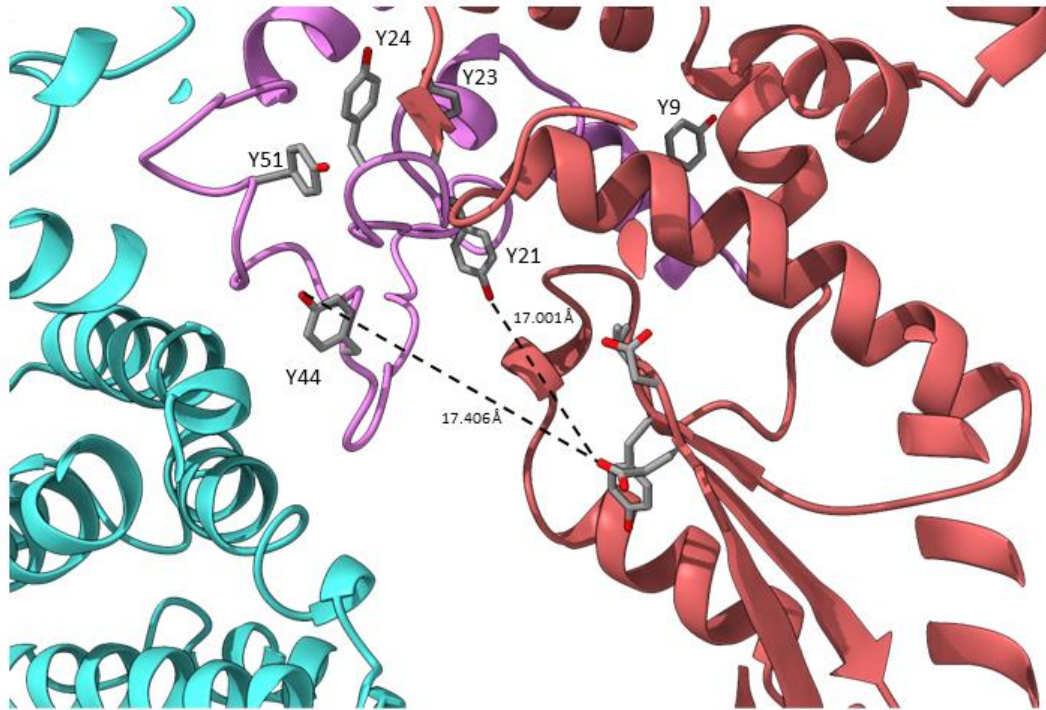


Figure 4-15: Active site of AbiK with proposed DNA attachment sites.

The amino terminal domain of AbiK is coloured in violet, with the reverse transcriptase domains in red and the carboxy terminal domain in turquoise. Key catalytic residues of AbiK are shown as sticks. Hypothesized priming site residues are shown as sticks and labeled. Distance between catalytic residues (residues 245-248) and closest hypothesized priming site residues is indicated with a black dashed line. Figure made using UCSF Chimera X (58).

4.3.6.5 Comparison of AbiK model to published structures

Three different crystal structures of AbiK were submitted into the Protein Data Bank in September 2022 by Figiel et al, showing that AbiK is an oligomer that forms a homohexamer (**Figure 4-16**) (57). One structure of AbiK has a polyC DNA strand and a magnesium ligand that diffracted to 3.1 Å (7R07), one has the polyC strand of DNA that diffracted to 2.27 angstroms (7R06), and the last structure is the Y44F mutant variant of AbiK that diffracted to 2.68 angstroms (7Z0Z). The Y44F variant lacks the DNA attachment site, and therefore the DNA strand, giving insight into the structure of the AbiK before any polymerization has occurred.

In the Y44F variant of AbiK, amino acids 32 - 42 were not modeled in the structure. However, F44 can be seen and is positioned close to the active site residues, interpreted as the position Y44 would take before DNA synthesis (**Figure 4-17**). In the wild-type AbiK structure, the loop with Y44 is displaced to the outer surface of the protein and is covalently attached to the nascent DNA strand (**Figure 4-17**). The nascent DNA strand is seen to continue outwards, before being cut off in the structure. The DNA strand loops back to the active site through a channel in the protein to the site where DNA synthesis occurs (**Figure 4-17**). The superposition of the model generated by Robetta and the crystal structure of the Y44F variant structure shows that the two are nearly identical (RMSD across 584 C α pairs is 3.475 Å), making interpretations generated from the model valid (**Figure 4-17**).

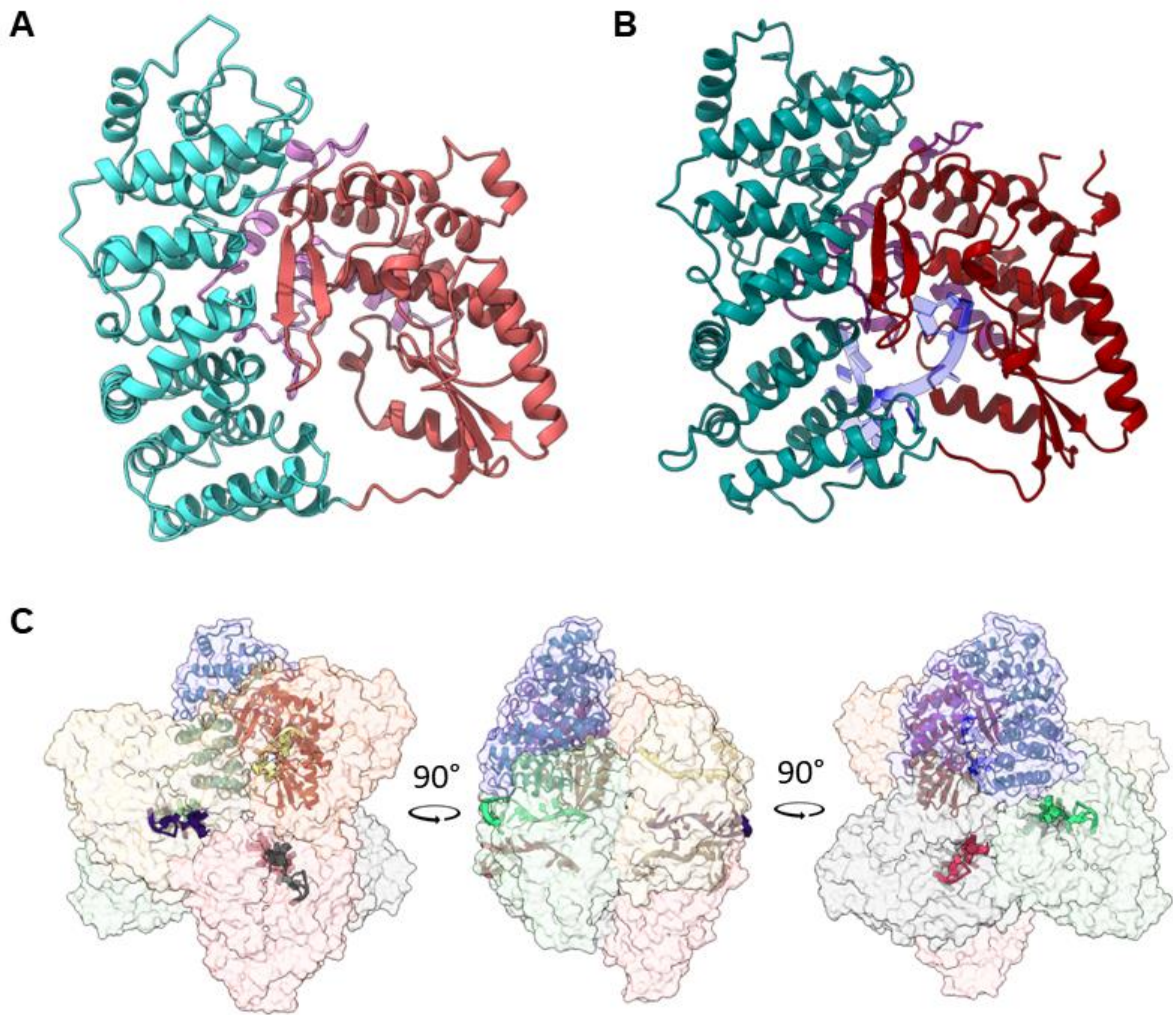


Figure 4-16: Comparison of AbiK model and the crystal structure.

A: Ribbon diagram of AbiK model generated by Robetta. The amino-terminal domain is coloured in violet, with the reverse transcriptase domain in red and the carboxy-terminal domain in turquoise. **B:** Ribbon diagram of one protomer of AbiK structure (7R06). The amino-terminal domain is coloured in dark violet, with the reverse transcriptase domains in dark red and the carboxy-terminal domain in dark turquoise. DNA strand is shown in blue. **C:** Space filling model of AbiK's oligomeric structure (7R06), with a ribbon diagram for one protomer. DNA strands are shown. Figure made using UCSF Chimera X (58).

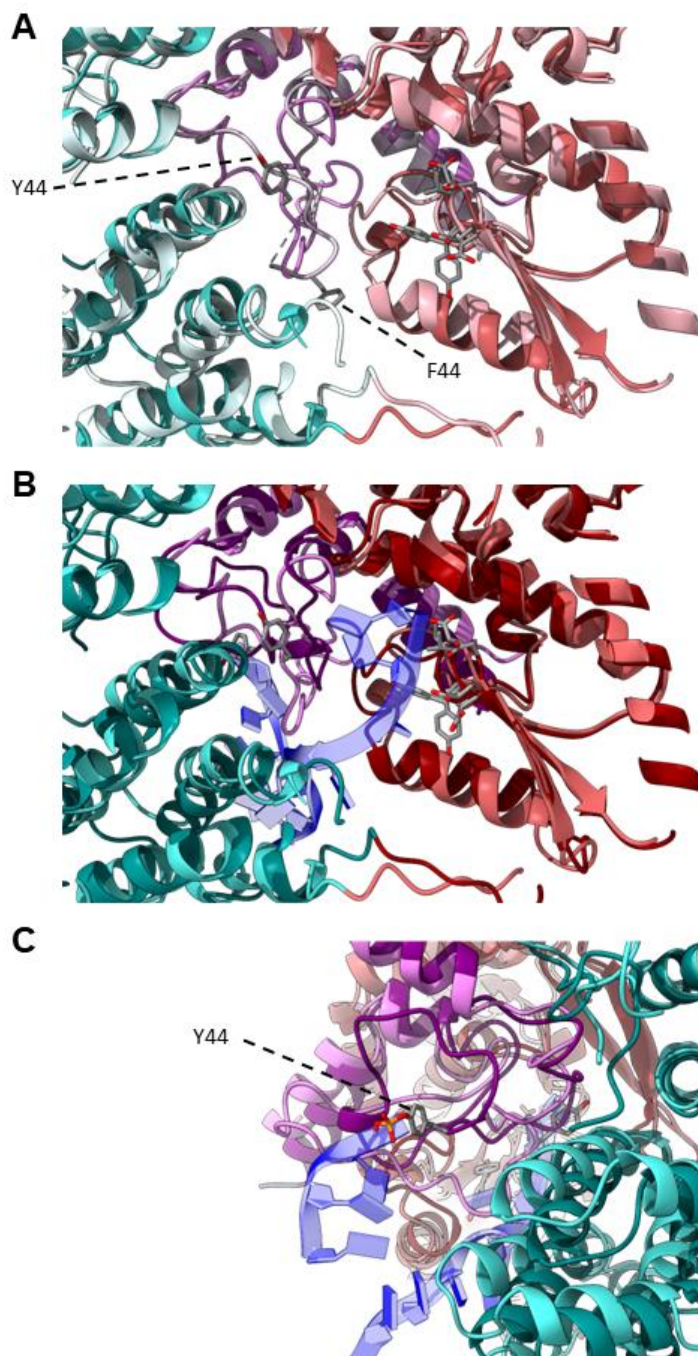


Figure 4-17: Active site of AbiK.

A: Superposition of AbiK model active site with AbiK Y44F mutant (7Z0Z) active site. The amino-terminal domain of AbiK is coloured in violet, with the reverse transcriptase domains in red and the carboxy-terminal domain in turquoise. The structure of the AbiK Y44F mutant is shown in lighter colours. Tyrosine 44 of the AbiK model and phenylalanine 44 of the AbiK Y44F mutant structure are indicated. **B:** Superposition of AbiK model active site with AbiK structure (7R06) active site. The amino-terminal domain of AbiK is coloured in violet, with the reverse transcriptase domains in red and the carboxy-terminal domain in turquoise. The structure of the solved AbiK structure is shown in darker colours. Catalytic residues are shown as sticks. **C:** Position of Y44 in structure of AbiK (7R06) is shown. DNA is shown in blue. Figure made using UCSF Chimera X (58).

4.3.7 Analysis of Sak3 model

After challenging four different phages against AbiK containing hosts, resistant phages were found to have mutations in the *sak* gene, which were numbered according to the phage they were identified in (59). The four *sak* genes, named *sak*, *sak2*, *sak3*, and *sak4*, were all found to be non-homologous to each other in sequence, but were found to have homology to single-strand annealing proteins (59). Sak was found to possess a conserved DNA binding domain like that of RAD52 (59). Sak3 was chosen for model analysis since it is encoded on ORF35 of the lactococcal phage p2 genome. Sak3 was biochemically studied and found to bind both ss- and dsDNA, hydrolyze ATP, stimulate RecA's DNA strand exchange, and anneal single strands of DNA together (3).

The model for Sak3 was generated by inputting the entire amino acid sequence of Sak3 into Robetta's structure prediction query. Like AbiK, five monomeric models with slight variations were generated and model 1 was chosen for analysis as it was the one with the least variation in error estimates in each position. (**Figure 4-18B**). When Sak3 is superposed with a single subunit of human RAD52 (1KN0), the amino-terminal regions of the two proteins (residues 1-144 of Sak3 and residues 36-167 of RAD52) align well with an RMSD of 1.835 Å (calculated using C α pairs), despite not having sequence homology (**Figure 4-18D**) (105). The carboxy-terminal regions of the proteins differ. Where RAD52's carboxy-terminus inserts into the adjacent protomer to form the oligomeric structure, Sak3's carboxy-terminal region sticks outwards and does not contact the adjacent protomer. Using RAD52's oligomeric unit (11-mer), a model of Sak3 as an 11-mer was generated (**Figure 4-18C**).

The oligomeric structure of Sak3 was analyzed via transmission electron microscopy and was found to make a donut-like shape with an outer diameter of 150 Å and an inner diameter of

60 Å (**Figure 4-18A**) (3). The best symmetry from class averages of the electron microscopy images was threefold or sixfold, showing that Sak3 adopts a sixfold symmetry (3). With the model generated using RAD52, Sak3 forms an 11-mer like RAD52, and the Sak3 model has an outer diameter of 180 Å and an inner diameter of 60 Å, suggesting that Sak3 likely forms an 11- or 12-mer. The discrepancy of the outer diameter could be explained by the flexible carboxy terminus of Sak3, which is also seen in the EM class averages. According to Blue-native PAGE, Sak3 migrated at a very high molecular weight (> 480 kDa), but MALS/UV/RI analysis detects Sak3 at a mass around 350 kDa (3). This mass is larger than the predicted mass of 250 kDa for Sak3's 11-mer, but the increase in mass is explained by saturating amounts of ssDNA that are bound to Sak3 (3). According to the mass and the diameter and the evidence given, Sak3 is likely an 11- or 12-mer, like RAD52, making the estimations of the model valid.

Three single-point mutations (V16A, M90I, and S144Y) found in Sak3 gave lactococcal phage p2 resistance to the AbiK mechanism (59). These mutations were mapped onto the model for Sak3 to suggest effects of the mutations on Sak3's structure (**Figure 4-18E-G**). Valine 16 is located in the amino terminal end of Sak3 and is seen to make many van der Waal interactions within the Sak3 monomer (**Figure 4-18E**). Serine 144 is located at the interface between two protomers and is likely promoting oligomerization of the protein through hydrogen bonding (**Figure 4-18G**). When the Sak3 model is superposed with the RAD52 structure, methionine 90 is seen to be at the interface where DNA binds to the protein, possibly making this mutation detrimental to Sak3's ability to bind DNA (**Figure 4-18F**). Sak3 is necessary for the AbiK mechanism, as an inactive Sak3 leads to an ineffective AbiK mechanism (59). It remains elusive what role Sak3 plays biologically, what role Sak3 plays during the AbiK mechanism, and how a mutation of the *sak3* gene allows the phage to bypass the AbiK mechanism.

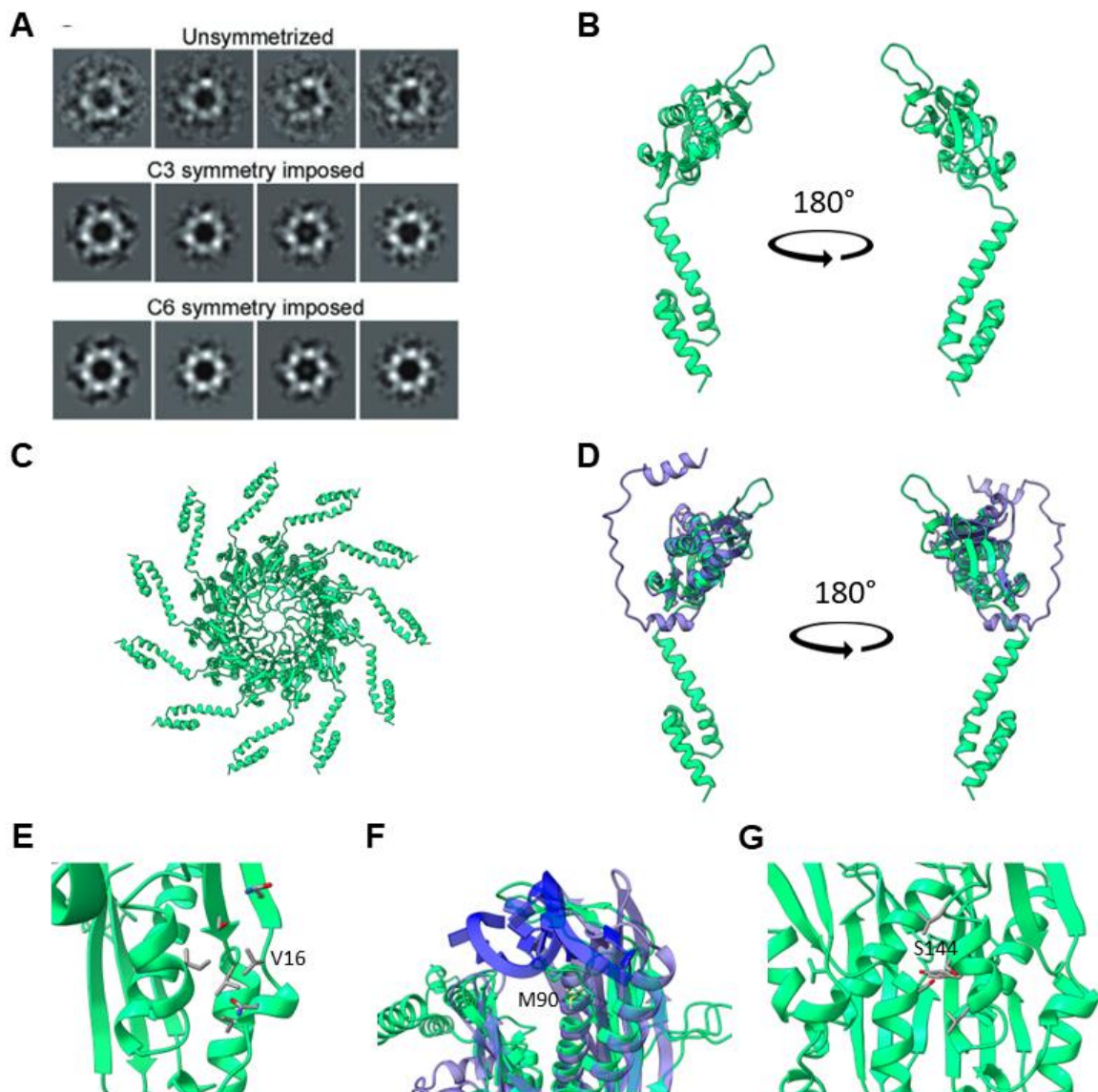


Figure 4-18: Structure of Sak3.

A: Electron micrograph photo of Sak3 (3). **B:** Model of Sak3 monomer generated by Robetta. **C:** Model of Sak3 oligomer (11-mer) generated by Robetta. **D:** Superposition of Sak3 monomer with RAD52 monomer (1KN0, purple). **E, F, G:** Position of single amino acid mutations in Sak3 that result in an escape of the AbiK phenotype. Residues of interest are labeled. Image of position of M90 is superposed with RAD52 to show proximity to binding site of DNA. DNA is shown in blue. Figure made using UCSF Chimera X (58).

4.4 Conclusions

The suspected DNA attachment site is tyrosine 44, from both *in vitro* and *in vivo* experiments. For *in vitro* experiments, there was no concrete evidence that the Y44F mutant form of AbiK was successfully expressed in *E. coli* as it could not be detected by silver-stained gels or by western blotting. For *in vivo* experiments in *L. lactis*, all colonies of Y44F AbiK that were tested were found to have mutations in the *abiK* gene, implying Y44F AbiK is toxic to the cells. Analysis of the AbiK model also suggests that tyrosine 44 is the priming site, as it sits on a flexible loop near the active site residues. The published structure of AbiK confirms our suspicions that tyrosine 44 is the priming site as the nascent DNA is covalently bound to AbiK on this residue.

Analyses of the model were found to be valid, as a structural alignment of AbiK's model generated by Robetta and AbiK's solved structure are similar. AbiK's active site and reverse transcriptase domain aligns well to known reverse transcriptases. Contrary to previous hypotheses, the carboxy terminal region of AbiK does not fold into a domain that is known to possess a catalytic activity. Instead, it folds into a repetitive alpha helical structure seen in other motifs, like the HEAT repeat and pentatricopeptide repeat. A study done looking at reverse transcriptases involved in defense systems has detected this domain in many prokaryotic reverse transcriptases and named this domain the α Rep domain that is hypothesized to bind nucleotides or other proteins (54).

It remains unknown what role AbiK's polymerase activity and potential binding activities have in the AbiK mechanism. Sak3 is also known to be involved in the AbiK mechanism, as mutations that appear to disrupt its oligomeric structure and binding activities render the phage resistant to the AbiK mechanism. Interestingly, experiments performed imply that the Y44F

mutant of AbiK is toxic to cells in the absence of Sak3 or a phage infection, as the only viable colonies have additional mutations in this gene that render the gene inactive in *L. lactis*. The Y44F mutant of AbiK is not toxic to *E. coli*, however, as the protein was able to be produced, purified, and crystallized by Figiel et al., but it is important to note that the majority of the protein that was expressed was monomeric, rather than hexameric (57). In addition, attempts to clone the *sak3* gene into *L. lactis* (**Chapter 2**) imply that Sak3 is either toxic to cells or slows their growth in the absence of AbiK. This leads to beliefs that although Sak3 may be activating AbiK, Sak3 may also have a synergistic effect leading to cell death.

4.5 Methods and Materials

4.5.1 General Protocols

4.5.1.1 Bacterial strains, plasmids, and growth conditions

Bacterial strains of *L. lactis* and *E. coli* used in this study are listed (**Table 4-2**). Refer to section **2.5.1.1** for methods.

4.5.1.2 DNA isolation and manipulation

Refer to section **2.5.1.3** for methods. Sequencing of DNA samples was done by the University of Calgary Core DNA Services or Plasmidsaurus (<https://www.plasmidsaurus.com/>).

4.5.1.3 Recombinant PCR

When using recombinant PCR cloning to get a single nucleotide mutation, two pairs of primers were designed. One primer pair consisted of a forward primer upstream of the desired mutation containing a restriction site, and a reverse primer containing the desired mutation. The second primer pair consisted of one forward primer containing the desired mutation, and a reverse primer downstream of the desired mutation with a restriction site. Two separate PCR reactions were performed, and then the PCR products were combined in a third PCR reaction containing the forward upstream and reverse downstream primers. The resulting product is a PCR product with restriction sites on both ends with the desired mutation in the middle. Restriction enzyme subcloning can then be done to insert the new mutation into the target plasmid through restriction enzyme sites (See **2.5.1.6**).

4.5.1.4 Quikchange lightning cloning

In Quikchange lightning cloning, forward and reverse primers were designed to contain the single nucleotide mutation and to amplify the entire plasmid. After PCR, the template is degraded using the DpnI enzyme, which targets methylated DNA, and the PCR product is

transformed into competent cells for nick repair. Experiments were done using Agilent's QuikChange Lightning Site-Directed Mutagenesis Kit or QuikChange II Site-Directed Mutagenesis Kit according to the manufacturer's protocol (106).

Table 4-2: Strains and plasmids used in this study.

Strain, Plasmid, or Phage	Relevant Characteristics *	Source
<i>E. coli</i>		
DH5 α	<i>lacZ</i> Δ M15 <i>recA1 endA1 hsdR17</i>	Invitrogen
BL21 (DE3)	F ⁻ <i>ompT hsdS_B</i> (<i>r_B</i> ⁻ , <i>m_B</i> ⁻) <i>gal dcm</i> (DE3)	Invitrogen
<i>L. lactis</i>		
MG1363	Plasmid-free host for phage p2	(47)
MG1363 <i>AbiK</i> ⁻	MG1363 (p Δ <i>AbiK</i>), Cm ^R , <i>AbiK</i> ⁻	This study
MG1363 <i>AbiK</i> ⁺	MG1363 (p <i>AbiK</i>), Cm ^R , <i>AbiK</i> ⁺	This study
Plasmids		
pGEX4T1- <i>AbiK</i>	<i>abiK</i> gene in expression vector with GST-tag, Amp ^R	(1)
pGEX4T1- <i>AbiK</i> Y9F	Y9F mutant <i>abiK</i> gene in expression vector with GST-tag, Amp ^R	This study
pGEX4T1- <i>AbiK</i> Y21F	Y21F mutant <i>abiK</i> gene in expression vector with GST-tag, Amp ^R	This study
pGEX4T1- <i>AbiK</i> Y23F	Y23F mutant <i>abiK</i> gene in expression vector with GST-tag, Amp ^R	This study
pGEX4T1- <i>AbiK</i> Y24F	Y24F mutant <i>abiK</i> gene in expression vector with GST-tag, Amp ^R	This study
pGEX4T1- <i>AbiK</i> Y44F	Y44F mutant <i>abiK</i> gene in expression vector with GST-tag, Amp ^R	This study
pGEX4T1- <i>AbiK</i> Y51F	Y51F mutant <i>abiK</i> gene in expression vector with GST-tag, Amp ^R	This study
pSRQ823- <i>AbiK</i> Cut (p Δ <i>AbiK</i>)	pSRQ823 with <i>abiK</i> deletion, Cm ^R , <i>AbiK</i> ⁻	This study
pSRQ823 (p <i>AbiK</i>)	<i>abiK</i> encoded in pNZ123, Cm ^R , <i>AbiK</i> ⁺	(1)
p <i>AbiK</i> Y9F	Y9F mutant <i>abiK</i> gene in pSRQ823, Cm ^R	This study
p <i>AbiK</i> Y21F	Y21F mutant <i>abiK</i> gene in pSRQ823, Cm ^R	This study
p <i>AbiK</i> Y23F	Y23F mutant <i>abiK</i> gene in pSRQ823, Cm ^R	This study
p <i>AbiK</i> Y24F	Y24F mutant <i>abiK</i> gene in pSRQ823, Cm ^R	This study
p <i>AbiK</i> Y44F	Y44F mutant <i>abiK</i> gene in pSRQ823, Cm ^R	This study
p <i>AbiK</i> Y51F	Y51F mutant <i>abiK</i> gene in pSRQ823, Cm ^R	This study

* *lacZ* Δ M15, partial deletion of *lacZ* that allows α -complementation; *recA1*, mutation in recombination gene; *endA1*, mutation in endonuclease gene; *hsdR17* and *hsdS_B*, mutation in methylation and restriction system genes; F⁻, strain does not contain F episome; *gal*, mutation in the galactokinase gene; *dcm*, mutation in the DNA cytosine methylase gene; (DE3), λ lysogen that encodes T7 RNA polymerase; Cm^R, chloramphenicol resistance; Amp^R, ampicillin resistance; *AbiK*⁻, lacking *AbiK* mechanism; *AbiK*⁺, *AbiK* mechanism present.

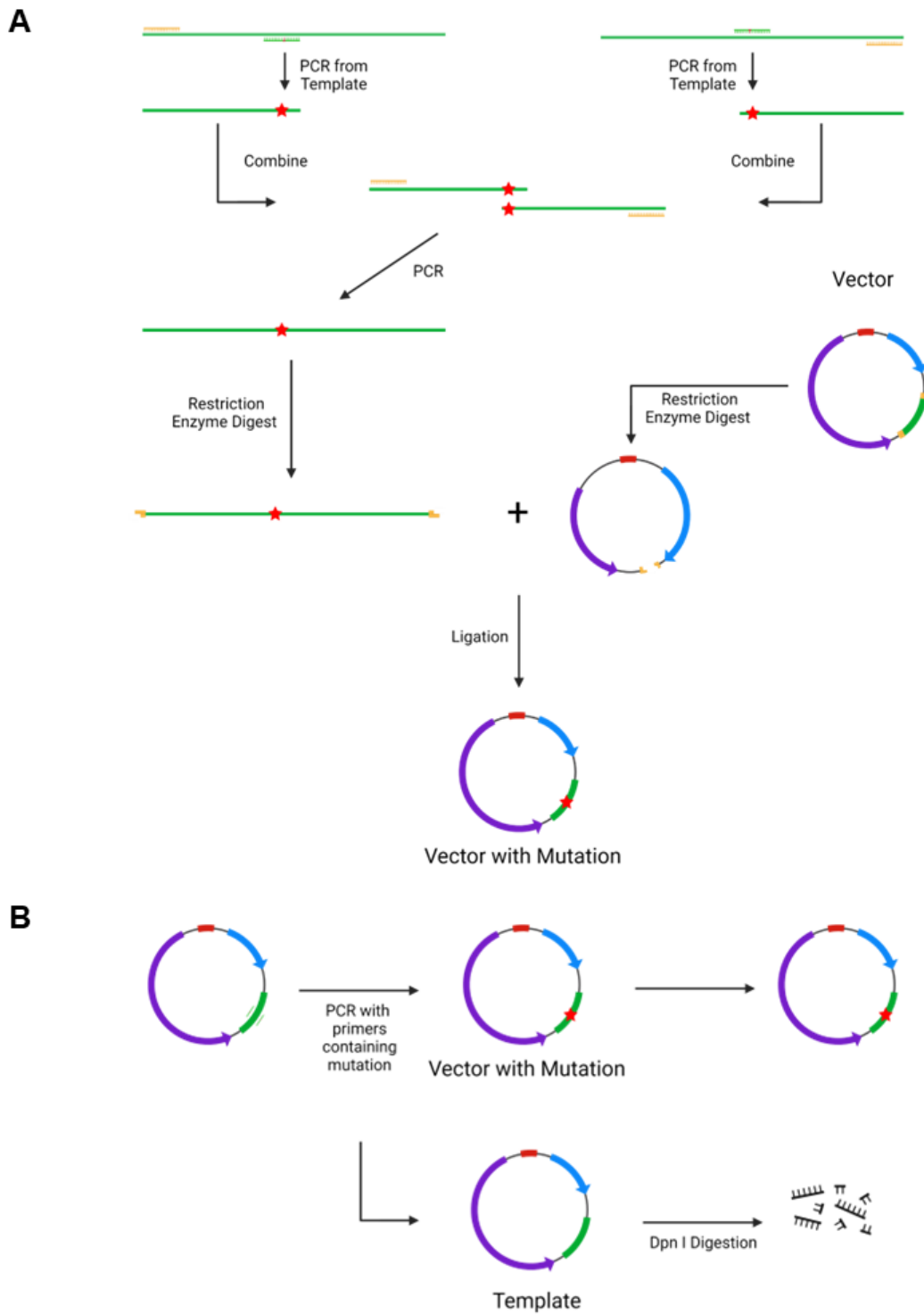


Figure 4-19: Schematic of cloning methods.

A: A schematic representation of recombinant PCR resulting in a vector with a single nucleotide mutation. **B:** A Schematic representation of Quikchange lightning cloning from Agilent. Created with BioRender.com.

4.5.2 Sequence Alignment

A protein blast search was done using AbiK's protein sequence looking at the standard databases and non-redundant protein sequences (107). The query looked up a maximum of 100 target sequences. The COBALT (Constraint-based Multiple Alignment Tool) was used to do a multiple alignment of the 100 sequences, which was downloaded from the server for analysis. A WebLogo (using Berkeley's WebLogo tool) was made using the multiple sequence alignment, to find and detect conserved tyrosines in the amino terminal region and to detect the reverse transcriptase domains. Search, alignment, and analysis was done on November 26, 2022. Sequence alignment of AbiK with 16 closely related sequences was performed previously (2).

4.5.3 Plasmid Construction

4.5.3.1 Construction of mutants in *E. coli*

To make Y to F mutants of AbiK for expression in *E. coli*, pGEX4T1-AbiK was used as a template for either recombinant PCR or Quikchange lightning cloning using described methods (4.5.1.3 and 4.5.1.4) (106). Six mutants were created: Y9F, Y21F, Y23F, Y24F, Y44F, and Y51F. Single nucleotide mutations were confirmed via DNA sequencing.

4.5.3.2 Construction of mutants in *L. lactis*

To make Y to F mutants of AbiK for expression in *L. lactis*, pSRQ823 (pAbiK) was used as a template for Quikchange lightning cloning using described methods (4.5.1.4). A total of six mutants were created: Y9F, Y21F, Y23F, Y24F, Y44F, and Y51F. Single nucleotide mutations were confirmed via DNA sequencing. Initial cloning of these mutants was performed in *E. coli* DH5 α , then the plasmid was electroporated into *L. lactis* strain MG1363.

Table 4-3: Primers used in cloning and sequencing.

Primer *	Sequence (5' - 3')
Y9F_Forward	GAGTTTACTGAATTATTTGATTTTATATTTGATCCTATTTTTCTT G
Y9F_Reverse	CAAGAAAATAGGATCAAATATAAAATCAAATAATTCAGTAAA CTC
Y21F_Forward	CCTATTTTTCTTGTAAGATTCGGCTATTATGATAGATCTATT
Y21F_Reverse	AATAGATCTATCATAATAGCCGAATCTTACAAGAAAAATAGG
Y23F_Forward	CCTATTTTTCTTGTAAGATACGGCTTTTATGATAGATCTATT
Y23F_Reverse	AATAGATCTATCATAAAAAGCCGTATCTTACAAGAAAAATAGG
Y24F_Forward	CCTATTTTTCTTGTAAGATACGGCTATTTTGATAGATCTATT
Y24F_Reverse	AATAGATCTATCAAATAGCCGTATCTTACAAGAAAAATAGG
Y44F_Forward	GCAAAAGTTGAATTAGACAATGAATTTGGAAAATCAGATTC
Y44F_Reverse	GAATCTGATTTTCCAAATTCATTGTCTAATTCAACTTTTGC
Y51F_Forward	GGAAAATCAGATTCTTTTTTTTTTAAAGTATTTAATATGGAATC CTTTGC
Y51F_Reverse	GCAAAGGATTCCATATTAATACTTTAAAAAAAAAAGAATCTG ATTTTCC
AllYF_S	CACAACATGTTGGGTGG
AllYF_AS	ACATATATAGTTCGGTAATAATCCTAGAC
Y9F_S	GAATTATTTGATTTTATATTTGATCCTATTTTTCTTG
Y9F_AS	TCAAATAATTCAGTAAACTCTTTTTTCATGG
Y21F_S	GATTCGGCTATTATGATAGATCTATTA AAAAC
Y21F_AS	CTATCATAATAGCCGAATCTTACAAG
Y23F_S	GATACGGCTTTTATGATAGATCTATTA AAAAC
Y23F_AS	CTATCATAAAAAGCCGTATCTTACAAG
Y24F_S	GATACGGCTATTTTGATAGATCTATTA AAAAC
Y24F_AS	CTATCAAATAGCCGTATCTTACAAG
Y44F_S	GACAATGAATTTGGAAAATCAGATTCTTT
Y44F_AS	TTTTCCAAATTCATTGTCTAATTCAAC
pNZ123 (354-R)	GGTTATCATGCAGGATTGTT

* Compatible primers are named as S (sense) and AS (antisense) or Forward and Reverse. Primers purchased from IDT™.

4.5.4 Protein Purification

4.5.4.1 Protein purification protocol

Protein purification of WT GST-AbiK and Y to F mutant GST-AbiK proteins were done according to a protocol listed elsewhere with slight modifications (1). Overnight cultures in LB (supplemented with 100 µg/mL of ampicillin) made from single colonies of *E. coli* BL21(DE3) harboring the pGEX4T1-AbiK plasmid were inoculated 1:100 into 2xYT medium (**Appendix A**) supplemented with 100 µg/mL of ampicillin. The cultures were grown at 37°C until an OD₆₀₀ between 0.4 - 0.6 was achieved. Cells were then induced with 0.1 mM IPTG for three hours at 30°C, harvested via centrifugation at 4 500 x g for 15 minutes at 4°C and then stored at -80°C. Thawed cells were resuspended in 20 mL of lysis buffer (16 mM Na₂HPO₄, 4 mM NaH₂PO₄, 150 mM NaCl, 1% Triton X-100, 5 mM DTT and 1 mM PMSF, pH 7.3) then cells were lysed with a French pressure cell. The lysate was clarified by centrifugation at 13 000 x g for 25 minutes at 4°C, then the supernatant was diluted in lysis buffer to a total volume of 35 mL. 3.5 mL of 10 x ATP buffer was added (final concentrations: 16 mM Na₂HPO₄, 4 mM NaH₂PO₄, 150 mM NaCl, 5 mM DTT, 10mM ATP pH 7.3, 50 mM KCl, 20 mM MgCl₂) to the clarified lysate, which was incubated at 37°C for 10 minutes, followed by an addition of 200 µL of *E. coli* denatured cell lysate, and then incubated at 30°C for 10 minutes. The denatured cell lysate was used to bait heat shock proteins, that often elute with AbiK in this purification.

The lysate was centrifuged at 7 000 x g at 4°C for 15 minutes, then the supernatant was removed and kept on ice. Glutathione Sepharose 4B beads (GE healthcare) were prepared by washing 300 µL of beads with three volumes of lysis buffer for a total of three washes, and then 10 volumes of lysis buffer were added to beads, which were kept on ice before addition of the beads to the lysate. The lysate was allowed to incubate with the beads with shaking for one hour

at 4°C. After incubation with the beads, the cell lysate was added to a gravity column and the flowthrough was discarded. The column was washed with 10 mL of wash buffer 1 (16 mM Na₂HPO₄, 4 mM NaH₂PO₄, 150 mM NaCl, 1% Triton X-100, 5 mM DTT, 10mM ATP pH 7.3, 50 mM KCl, and 20 mM MgCl₂) and then washed with 5 mL of wash buffer 2 (16 mM Na₂HPO₄, 4 mM NaH₂PO₄, 150 mM NaCl, 5 mM DTT, 5 mM ATP pH 7.3, 50 mM KCl, and 20 mM MgCl₂) before elution of the fusion protein with 5 mL of elution buffer (50 mM Tris-HCl pH 8.0 and 10 mM reduced glutathione). The eluted protein sample was stored in 25 mM Tris-HCl pH 8.0, 5 mM reduced glutathione, 50 mM NaCl, 5 mM DTT and 50% glycerol at -20°C.

4.5.4.2 E. coli denatured cell lysate preparation

Denatured *E. coli* cell lysate was prepared for the protein purification of GST-AbiK. Overnight cultures in LB made from single colonies of *E. coli* BL21 (DE3) were inoculated 1:100 into 400 mL of LB medium and grown to an OD₆₀₀ of 0.8 at 37°C with shaking. Cells were pelleted by centrifugation at 4 000 x g for 15 minutes at 4°C, and then cells were resuspended in 20 mL lysate buffer (140 mM NaCl, 2.7 mM KCl, 10 mM Na₂HPO₄, 1.8 mM KH₂PO₄, 1% Triton X-100, and 1 mM PMSF). Cells were lysed via sonication, and the lysate was frozen at -80°C. The frozen lysate was lyophilized, and the lyophilized cell lysate was resuspended in 1.5 mL of 8M Urea, then split into 200 µL aliquots for storage at -20°C.

4.5.4.3 SDS-PAGE gel electrophoresis and visualization

SDS-PAGE gel electrophoresis was performed as previously described using 8 - 12% (v/v) of polyacrylamide for the resolving gel and gels were electrophoresed at 200 V for 1 hour using 1 x Laemmli buffer (**Appendix A**) (73). Protein gels were stained using either Coomassie staining or silver staining using previously described methods (73).

4.5.4.4 Western blot

When needed, a western blot was performed using previously described methods (73). Gels were equilibrated in transfer buffer (25 mM Tris, 192 mM glycine, and 20% methanol) and then assembled in a transfer cassette to transfer proteins to a nitrocellulose membrane in a cassette at 100 V for 2 hours. After transfer, the membrane was stained with Ponceau solution (**Appendix A**) for 5 mins, and then rinsed with deionized water three times before imaging.

Following the Ponceau stain, the membrane was blocked with 10% skim milk powder in TBS buffer (**Appendix A**), overnight with shaking at 4°C. The following day, the membrane was washed three times with TBS buffer, then the primary α -GST 1:1000 antibody (Immunology Consultant Laboratory) from rat (in 5% skim milk powder in TBS buffer) was allowed to bind by incubation for 2 hours at room temperature. Following the incubation with the primary antibody, the membrane was washed three times for 5 minutes each with TBS-T buffer (TBS + 0.1% Tween-20) before incubation with the secondary rabbit anti-rat HRP conjugate 1:5000 antibody (Immunology Consultant Laboratory) (in 5% skim milk powder in TBS buffer) for 1.5 hours at room temperature. The membrane was washed three times for 5 minutes each with TBS-T buffer (TBS + 0.1% Tween-20) and then visualized using the ECL Western Blot Substrate (GE Healthcare Amersham) using the manufacturer's protocol on an Amersham Imager (108).

4.5.5 Label-chase Assay

Purified GST-AbiK (2 μ L) was incubated with 0.5 μ L [α -³²P] dTTP (Perkin-Elmer, 3000 Ci/mmol) in reverse transcriptase buffer (100 mM KCl, 2 mM MgCl₂, 10 mM DTT, and 50 mM Tris-HCl pH 8.5) for 10 minutes at 37°C for the labelling reaction. The reaction was stopped with the addition of 1.1 μ L ddH₂O and incubating the reaction on ice. For the chase reaction, 1.1 μ L of 5 mM dATP was added to the labeling reaction for incubation at 37°C for an

additional 10 minutes. The reaction was stopped by placing the samples on ice. For resolution by SDS-PAGE, samples were mixed with SDS-PAGE loading dye (**Appendix A**) and then boiled for 10 minutes before samples were loaded and run on a gel. Completed gels were then exposed to phosphor plates, and the autoradiograms were imaged using ImageQuant software.

4.5.6 *In vivo* Effects of AbiK Mutants

Overnight cultures were made from single colonies of *L. lactis* strain MG1363 pAbiK or pAbiK mutants in GM17 supplemented with 10 mM CaCl₂ and chloramphenicol at 25 µg/mL. Serial dilutions of lactococcal phage p2 and *sak3* mutant (M90I) lactococcal phage p2 were made in fresh medium. Phages were titered by plaque assays using the agar double-layer technique to detect if mutant forms of AbiK are susceptible to phage infection (76). Controls were done with *L. lactis* strain MG1363 pSRQ823-AbiKCut and pSRQ823 (pAbiK).

4.5.7 Protein Model Generation and Analysis

Protein models for AbiK and Sak3 were generated using the Robetta protein structure prediction service by inputting their primary amino acid sequences as a query (99). Five monomeric models were output for each query, and model 1 was chosen for analysis due to the least variation in ångstrom error estimates in each position. Analysis, superposition, and imaging was done on ChimeraX (58). Analysis for AbiK was performed in July and August 2021 and analysis for Sak3 was performed in May 2022.

Chapter 5 : Conclusions and Future Directions

5.1 Principal Conclusions of the Research

The primary goal of this research was to uncover the mechanism of AbiK, and to see what happens in the host cell that prevents phage infection and causes cell death. Over the years, hypotheses for the AbiK mechanism were formed but as more research was done on the AbiK protein, they were disproven. Before the AbiK protein was studied to test its polymerization activity, the AbiK protein was proposed to produce a cDNA using an unknown template, which would be readily degraded in cells by nucleases (55). Upon phage infection, the Sak protein would bind to the cDNA, which can sequester phage mRNA to prevent protein production (55). It is now known that this is not the mechanism by which AbiK acts, as the protein was proven to have untemplated polymerization (1). The second hypothesis was based on the lack of knowledge about the function for the carboxy terminal region of the AbiK protein. This region was proposed to have a nuclease activity that is normally sterically hindered by the protein itself, but upon phage infection, Sak binds onto the ssDNA and causes a conformational change to expose the nuclease region (2). It is now proposed that the carboxy terminal region of AbiK has an accessory role rather than a catalytic function, disproving this proposed mechanism (57).

In this research, both *in vivo* and *in vitro* strategies were adopted to formulate a hypothesis for the mechanism and propose how cell death occurs. *In vivo* strategies involved analyzing the DNA and RNA kinetics during the AbiK mechanism and seeing what changed as a result. A mutant form of the phage that is resistant to the AbiK mechanism was also studied, to see how the phage mutant bypassed the system. *In vitro* studies looked at the biochemistry of the AbiK protein, and analysis of the models for the AbiK and Sak3 proteins. Information from the

in vitro studies gives light into the activities that these proteins have, enabling the elucidation of their roles during the mechanism.

5.1.1 *In vivo* Effects of the AbiK Mechanism

During a typical wild-type phage infection where lactococcal phage p2 infects *L. lactis* strain MG1363, the phage adsorbs to the host cell and injects its DNA into the host cell (12). The phage then hijacks the cellular machinery to transcribe its genes and replicate its genome, before creating phage progeny which can then be released from the cell through lysis (12). This study has confirmed, through RNA-Seq, that the phage is indeed hijacking the cellular machinery to make its own transcripts. During the AbiK infection, this still occurs but transcription is delayed, occurring later than during the wild-type phage infection. In addition, a slow down of the transcription of early and middle genes which is typical in the wild-type phage infection is not seen during the AbiK infection. The full details of the mutant phage's transcription during the escape of AbiK infection have not yet been revealed, but RT-qPCR showed that transcription of the phage genes either match or is lower than transcription during the AbiK infection.

Next, the AbiK mechanism has been seen to inhibit phage DNA replication, shown via Southern blots and qPCR of samples taken during infection. This study used both Southern blotting and qPCR, along with multiple biological replicates to produce the results seen. There is a discrepancy between the results shown in this study and previously published findings, where phage DNA replication was detected in 936-group phages, which lactococcal phage p2 is a member of (30).

The *sak3* mutant phage (M90I) can overcome the inhibition of phage DNA replication, but the packaging of the phage DNA into phage progeny appears to be hindered and not as effective as what is seen during the wild-type phage infection. There is further evidence of this in

the one-step growth curves, which showed that the *sak3* mutant phage (M90I) was less efficient at producing phage progeny compared to the wild-type phage, with even fewer progeny produced when the AbiK mechanism is active.

From preliminary RNA-Seq experiments, the differential gene expression between the wild-type phage infection and the AbiK infection was analyzed. The most notable observations were changes in the expression of pyrimidine ribonucleotide biosynthesis and in riboflavin biosynthesis. During the wild-type phage infection, lactococcal phage p2 causes an overexpression of proteins involved in riboflavin biosynthesis, an important precursor for key processes in the cell. During the AbiK mechanism, this overexpression of proteins involved in riboflavin biosynthesis is no longer seen, but there is also an underexpression of genes involved in pyrimidine ribonucleotide biosynthesis over the course of the infection. When looking at the differential gene expression between the normal infection and the AbiK infection, an underexpression of riboflavin biosynthesis can be seen in the AbiK infection compared to the wild-type infection, indicating a decreased production of the molecule.

5.1.2 *In vitro* Revelations about the AbiK Protein

Previous studies have shown that AbiK is a DNA polymerase that synthesizes a ssDNA product that is covalently bound to the protein itself, attached to tyrosine 44 (1, 57). This polymerization activity is untemplated and random, and the AbiK protein will polymerize the strand using any available deoxyribonucleotides as a substrate (1). The structure for the AbiK protein has been solved, and it was determined to be a homohexamer, with six active sites capable of polymerization activity on one molecule (57). When the tyrosine is mutated into a phenylalanine, the protein's ability to oligomerize is hindered and experiments for this study imply that this mutant AbiK protein is toxic to *L. lactis* cells (57). The carboxy terminal region

of the AbiK protein folds into a repetitive alpha helical structure and is hypothesized to bind nucleotides or other proteins (57).

Sak3, a protein encoded on the phage genome, is known to be involved in the AbiK mechanism. This is due to mutations in the *sak3* gene rendering the phage immune to the AbiK mechanism, allowing the development of phage progeny (59). Sak3 has many biochemical activities, including binding both ss- and dsDNA, ATP hydrolysis, the stimulation of RecA's DNA strand exchange and the ability to anneal single strands of DNA (3). The location of mutations on a Sak3 model leads to the belief that the mutations either inhibit Sak3's ability to oligomerize into its functional oligomer or inhibit Sak3's ability to bind DNA. The exact biological role of Sak3 in the phage infection has not been confirmed, but based on its activities it has been hypothesized to be involved in DNA replication or in packaging of the phage DNA.

5.2 Proposed Mechanism for AbiK

Using the evidence provided, a hypothesis for the mechanism of AbiK can be formulated. In cells containing AbiK, the AbiK protein is known to polymerize an untemplated ssDNA (1). I propose that AbiK does this indiscriminately using any deoxyribonucleotides it has access to. A consequence of this is a monopoly on the resource pool of ribonucleotides, limiting what can be used for other processes in the cell (**Figure 5-1**). Further evidence is the reduction of genes involved in pyrimidine ribonucleotide biosynthesis in RNA-Seq experiments. Although this hinders cell processes, the cell contains nucleases which can cleave the product to replenish the ribonucleotide resources in an uninfected cell (**Figure 5-1**).

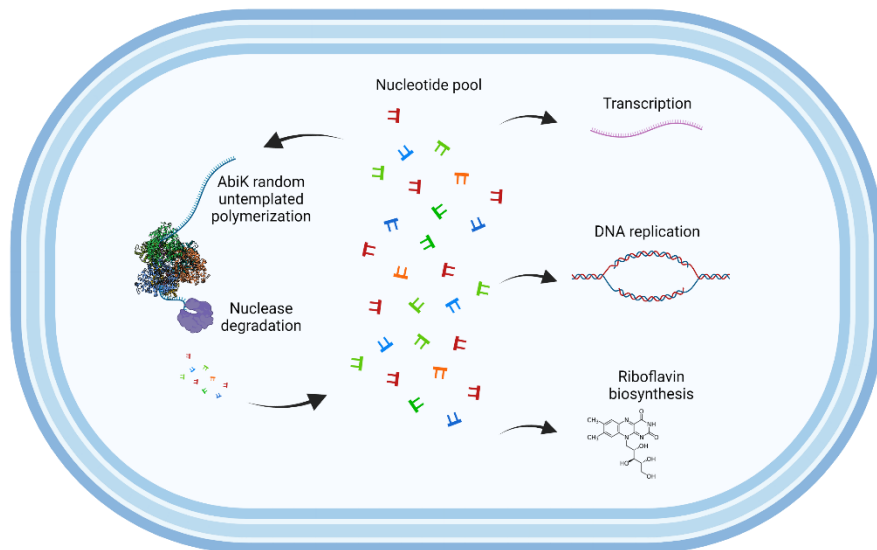


Figure 5-1: AbiK in an uninfected cell.

A schematic representation of AbiK in an uninfected cell. AbiK randomly incorporates deoxyribonucleotides in a ssDNA that is covalently attached to itself, draining the cell's nucleotide pool. Nucleases present in the cell degrade the ssDNA that AbiK generates, replenishing the nucleotide pool. The nucleotide pool can be used for cellular processes including transcription, DNA replication and riboflavin biosynthesis. Created with BioRender.com.

During an infection, the Sak3 protein is quickly produced. The Sak3 protein then protects the ssDNA tail on AbiK, allowing AbiK to continue to polymerize a very long strand and consume the deoxyribonucleotides in the cell (**Figure 5-2**). As a result, transcription of phage genes is delayed due to the limited resources, and phage DNA replication is inhibited as deoxyribonucleotides are monopolized by AbiK (**Figure 5-2**). One downstream effect is a reduced expression of the genes for riboflavin biosynthesis. Riboflavin is a molecule that acts as a precursor to many molecules that facilitate important processes in the cell necessary for cell survival. Without the production of riboflavin, several cell processes shut down and the cell dies (**Figure 5-2**). When the Sak3 protein is mutated and no longer functional, then cellular nucleases have access to and can cleave the ssDNA on AbiK, allowing the phage to be able to use the cellular resources (**Figure 5-3**).

The mutant form of AbiK (Y44F) was found to be toxic in *L. lactis* cells. This mutant lacks the priming site for the ssDNA and is unable to polymerize its ssDNA (57). It has been shown that the ssDNA makes interactions with the carboxy terminal region of AbiK, likely stabilizing the structure and assisting with AbiK's oligomerization (57). In the absence of the DNA, the mutant AbiK exists primarily as a monomer, with the majority unfolded, and this might be the cause of toxicity to cells.

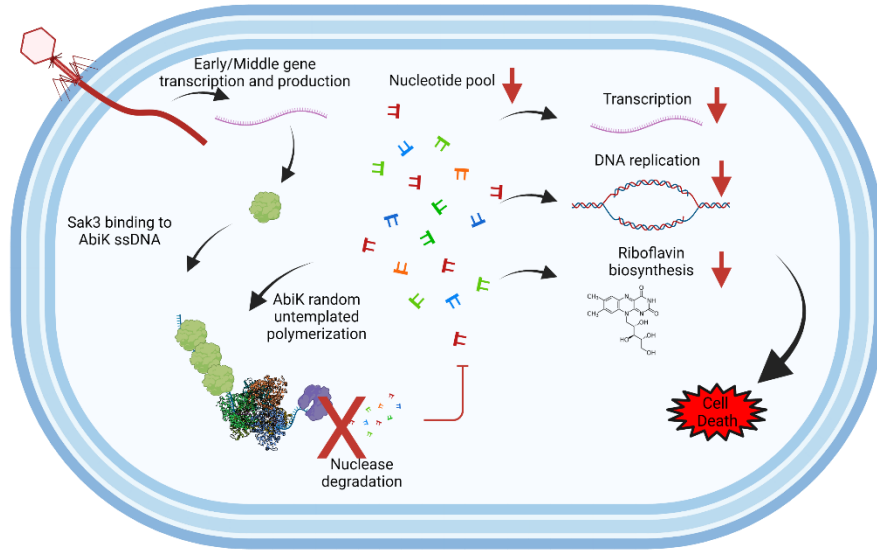


Figure 5-2: AbiK mechanism during a phage infection.

A schematic representation of the AbiK mechanism during a phage infection. AbiK randomly incorporates deoxyribonucleotides in a ssDNA that is covalently attached to itself, draining the cells nucleotide pool. Upon phage infection, the Sak3 protein is made and binds to the ssDNA attached to AbiK. Nucleases present in the cell are unable to degrade the ssDNA that AbiK generates, inhibiting the replenishment of the nucleotide pool. Downstream cellular processes are suppressed, eventually causing cell death. Created with BioRender.com.

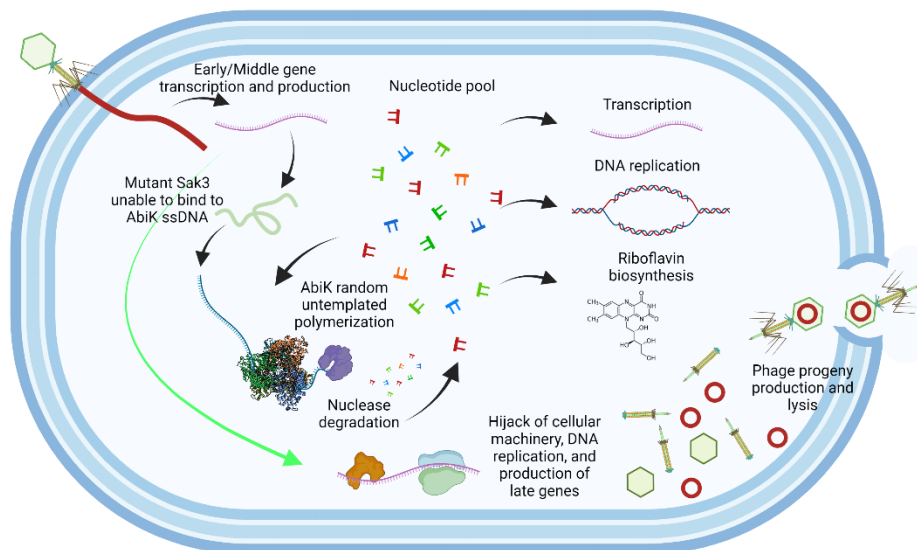


Figure 5-3: Sak3 mutant phage's bypass of AbiK mechanism.

A schematic representation of a Sak3 mutant phage bypassing the AbiK mechanism. AbiK randomly incorporates deoxyribonucleotides in a ssDNA that is covalently attached to itself, draining the cells nucleotide pool. Upon phage infection, a non-functional mutant Sak3 protein is unable to bind to the ssDNA attached to AbiK. Nucleases present in the cell degrade the ssDNA that AbiK generates, replenishing the nucleotide pool. The nucleotide pool can be used for cellular processes including transcription, DNA replication and riboflavin biosynthesis. The mutant phage bypasses the AbiK mechanism entirely (green arrow) and can hijack the cellular machinery and make phage progeny that ultimately lyse the cell. Created with BioRender.com.

5.3 Future Directions

Many clues have been obtained for how the AbiK mechanism works and what is happening within cells to prevent phage propagation, but many questions remain on the exact mechanism. A good start to reveal more about what is occurring in this mechanism is to send the complete set of samples for RNA-Seq analysis. With the completed time set and a total of 3 biological replicates, the data will be more statistically relevant and ensure which genes are being differentially expressed.

Next, electron microscopy has been previously adopted to look at cells post-infection during the AbiK infection and see what phenotypes they adopt (30). These images showed empty phage capsid surrounding a network of DNA during the AbiK mechanism, hypothesized to be concatemers of the phage DNA (30). However, it is now known that the phage DNA is not replicated during this mechanism. With current improved technology, it would be good to repeat this and see if the phenotype can be replicated, or if the cell's morphology changes during the AbiK mechanism. Additionally, experiments to identify the origin of the DNA network would be interesting. For example, to test if the DNA network was generated by AbiK, the localization of AbiK could be detected in the cell by using a fluorescent tag or other marker to see if this localizes with the DNA network. The proposed mechanism for AbiK is based on AbiK's ability to generate a long ssDNA in the presence of the Sak3 protein. Using electron microscopy during the AbiK infection, a long ssDNA with Sak3 molecules bound could be detected to confirm if this is occurring.

AbiK is suspected to interact with Sak3 during its mechanism, but further experiments need to be conducted to prove this interaction. A pull-down assay with AbiK as the target will reveal all interactions that AbiK makes. From these data, how AbiK signals to downregulate or

upregulate other genes in the system can also be inferred. It would also be interesting to do a pull-down assay during an infection with the *sak3* mutant phage, to see if any interactions are changed in this system due to the mutant Sak3 protein. In addition, to confirm if metabolites are depleted when AbiK is present in the cell and during the AbiK mechanism, metabolomics can be done to follow these pathways.

Lastly, a lot remains unknown about the exact mechanisms by which lactococcal phage p2 replicates. Most of its early and middle genes remain unannotated with unknown functions, and the exact process the phage uses to hijack the cellular machinery remains unknown. In addition to this, the Sak3 protein is involved in lactococcal phage p2's development, but it is unknown what role it plays and if AbiK disrupts its role. Furthermore, when the *sak3* gene is mutated, how the phage can bypass a mutation of one of its genes and continue to replicate remains an enigma. Further experiments to characterize many of the hypothetical genes in lactococcal phage p2 will add clarity to how the phage replicates, making it easier to discern the exact mechanism of how AbiK aborts its infection

References

1. Wang, C., Villion, M., Semper, C., Coros, C., Moineau, S., and Zimmerly, S. (2011) A reverse transcriptase-related protein mediates phage resistance and polymerizes untemplated DNA *in vitro*. *Nucleic Acids Res.* **39**, 7620–9
2. Soufi, B. (2019) AbiK: A novel polymerase that confers resistance to phage infection. *M.Sc. thesis*
3. Scaltriti, E., Launay, H., Genoix, M.-M., Bron, P., Rivetti, C., Grolli, S., Ploquin, M., Campanacci, V., Tegoni, M., Cambillau, C., Moineau, S., and Masson, J.-Y. (2011) Lactococcal phage p2 ORF35-Sak3 is an ATPase involved in DNA recombination and AbiK mechanism. *Mol. Microbiol.* **80**, 102–116
4. Pellett, P. E., Mitra, S., and Holland, T. C. (2014) Basics of virology. *Handb. Clin. Neurol.* **123**, 45–66
5. Meyer, H., Ehmann, R., and Smith, G. L. (2020) Smallpox in the post-eradication era. *Viruses.* 10.3390/v12020138
6. Eisinger, R. W., and Fauci, A. S. (2018) Ending the HIV/AIDS Pandemic1. *Emerg. Infect. Dis.* **24**, 413–416
7. Global HIV & AIDS statistics — Fact sheet (2022)
8. Raman, R., Patel, K. J., and Ranjan, K. (2021) Covid-19: Unmasking emerging SARS-CoV-2 variants, vaccines and therapeutic strategies. *Biomolecules.* 10.3390/biom11070993
9. Spackman, E. (2020) A brief introduction to avian influenza virus. *Methods Mol. Biol.* **2123**, 83–92
10. Lycett, S. J., Duchatel, F., and Digard, P. (2019) A brief history of bird flu. *Philos. Trans. R. Soc. B Biol. Sci.* 10.1098/rstb.2018.0257
11. Dion, M. B., Oechslin, F., and Moineau, S. (2020) Phage diversity, genomics and phylogeny. *Nat. Rev. Microbiol.* **18**, 125–138
12. Sharma, S., Chatterjee, S., Datta, S., Prasad, R., Dubey, D., Prasad, R. K., and Vairale, M. G. (2017) Bacteriophages and its applications: an overview. *Folia Microbiol. (Praha).* **62**, 17–55
13. Clokie, M. R. J., Millard, A. D., Letarov, A. V., and Heaphy, S. (2011) Phages in nature. *Bacteriophage.* **1**, 31–45
14. Ackermann, H. W. (2009) Phage classification and characterization. *Methods Mol. Biol.* **501**, 127–140
15. Bradley D. (1967) Ultrastructure of bacteriophages and bacteriocins. *Bacteriol. Rev.*
16. King, A. M. Q., Adams, M. J., Carstens, E. B., and Lefkowitz, E. J. (2011) *Virus taxonomy: Ninth report of the international committee on taxonomy of viruses*
17. (ICTV), I. C. on T. of V. (2022) *Virus Taxonomy: 2022 Release*
18. Zhu, Y., Shang, J., Peng, C., and Sun, Y. (2022) Phage family classification under *Caudoviricetes*: A review of current tools using the latest ICTV classification framework. *Front. Microbiol.* 10.3389/fmicb.2022.1032186
19. Salmond, G. P. C., and Fineran, P. C. (2015) A century of the phage: past, present and future. *Nat. Rev. Microbiol.* **13**, 777–786
20. Hitchcock, N. M., Devequi Gomes Nunes, D., Shiach, J., Valeria Saraiva Hodel, K., Dantas Viana Barbosa, J., Alencar Pereira Rodrigues, L., Coler, B. S., Botelho Pereira Soares, M., and Badaró, R. (2023) Current clinical landscape and global potential of

- bacteriophage therapy. *Viruses*. 10.3390/v15041020
21. Bolsan, A. C., Rodrigues, H. C., Abilhôa, H. C. Z., Hollas, C. E., Venturin, B., Gabiatti, N. C., Bortoli, M., Kunz, A., and De Prá, M. C. (2022) Bacteriophages in wastewater treatment: can they be an approach to optimize biological treatment processes? *Environ. Sci. Pollut. Res.* **29**, 89889–89898
 22. Zakrzewska, M., and Burmistrz, M. (2023) Mechanisms regulating the CRISPR-Cas systems. *Front. Microbiol.* 10.3389/fmicb.2023.1060337
 23. Chopin, M.-C., Chopin, A., and Bidnenko, E. (2005) Phage abortive infection in lactococci: variations on a theme. *Curr. Opin. Microbiol.* **8**, 473–9
 24. Emond, E., Holler, B. J., Boucher, I., Vandenberg, P. A., Vedamuthu, E. R., Kondo, J. K., and Moineau, S. (1997) Phenotypic and genetic characterization of the bacteriophage abortive infection mechanism AbiK from *Lactococcus lactis*. *Appl. Environ. Microbiol.* **63**, 1274–83
 25. Fortier, L. C., Bransi, A., and Moineau, S. (2006) Genome sequence and global gene expression of Q54, a new phage species linking the 936 and c2 phage species of *Lactococcus lactis*. *J. Bacteriol.* **188**, 6101–6114
 26. Deveau, H., Labrie, S. J., Chopin, M. C., and Moineau, S. (2006) Biodiversity and classification of lactococcal phages. *Appl. Environ. Microbiol.* **72**, 4338–4346
 27. Jarvis, A. W., Fitzgerald, G. F., Mata, M., Mercenier, A., Neve, H., Powell, I. B., Ronda, C., Saxelin, M., and Teuber, M. (1991) Species and type phages of lactococcal bacteriophages. *Intervirology.* **32**, 2–9
 28. Braun, V., Hertwig, S., Neve, H., Geis, A., and Teuber, M. (1989) Taxonomic differentiation of bacteriophages of *Lactococcus lactis* by electron microscopy, DNA-DNA hybridization, and protein profiles. *J. Gen. Microbiol.* **135**, 2551–2560
 29. Oliveira, J., Mahony, J., Hanemaaijer, L., Kouwen, T. R. H. M., and van Sinderen, D. (2018) Biodiversity of bacteriophages infecting *Lactococcus lactis* starter cultures. *J. Dairy Sci.* **101**, 96–105
 30. Boucher, I., Emond, E., Dion, E., Montpetit, D., and Moineau, S. (2000) Microbiological and molecular impacts of AbiK on the lytic cycle of *Lactococcus lactis* phages of the 936 and P335 species. *Microbiology.* **146** (Pt 2, 445–53
 31. Millen, A. M., and Romero, D. A. (2016) Genetic determinants of lactococcal C2 viruses for host infection and their role in phage evolution. *J. Gen. Virol.* **97**, 1998–2007
 32. Labrie, S. J., Josephsen, J., Neve, H., Vogensen, F. K., and Moineau, S. (2008) Morphology, genome sequence, and structural proteome of type phage P335 from *Lactococcus lactis*. *Appl. Environ. Microbiol.* **74**, 4636–4644
 33. Lemay, M. L., Otto, A., Maaß, S., Plate, K., Becher, D., and Moineau, S. (2019) Investigating *Lactococcus lactis* MG1363 response to phage p2 infection at the proteome level. *Mol. Cell. Proteomics.* **18**, 704–714
 34. Samson, J. E., and Moineau, S. (2010) Characterization of *Lactococcus lactis* phage 949 and comparison with other lactococcal phages. *Appl. Environ. Microbiol.* **76**, 6843–6852
 35. Egido, J. E., Costa, A. R., Aparicio-Maldonado, C., Haas, P. J., and Brouns, S. J. J. (2022) Mechanisms and clinical importance of bacteriophage resistance. *FEMS Microbiol. Rev.* 10.1093/femsre/fuab048
 36. Doron, S., Melamed, S., Ofir, G., Leavitt, A., Lopatina, A., Keren, M., Amitai, G., and Sorek, R. (2018) Systematic discovery of antiphage defense systems in the microbial pangenome. *Science* (80-.). 10.1126/science.aar4120

37. Payne, L. J., Meaden, S., Mestre, M. R., Palmer, C., Toro, N., Fineran, P. C., and Jackson, S. A. (2022) PADLOC: a web server for the identification of antiviral defence systems in microbial genomes. *Nucleic Acids Res.* **50**, W541–W550
38. Samson, J. E., Magadán, A. H., Sabri, M., and Moineau, S. (2013) Revenge of the phages: defeating bacterial defences. *Nat. Rev. Microbiol.* **11**, 675–687
39. Mojica, F. J. M., Díez-Villaseñor, C., García-Martínez, J., and Soria, E. (2005) Intervening sequences of regularly spaced prokaryotic repeats derive from foreign genetic elements. *J. Mol. Evol.* **60**, 174–182
40. Ofir, G., Melamed, S., Sberro, H., Mukamel, Z., Silverman, S., Yaakov, G., Doron, S., and Sorek, R. (2018) DISARM is a widespread bacterial defence system with broad anti-phage activities. *Nat. Microbiol.* **3**, 90–98
41. Goldfarb, T., Sberro, H., Weinstock, E., Cohen, O., Doron, S., Charpak-Amikam, Y., Afik, S., Ofir, G., and Sorek, R. (2015) BREX is a novel phage resistance system widespread in microbial genomes. *EMBO J.* **34**, 169–183
42. Kronheim, S., Daniel-Ivad, M., Duan, Z., Hwang, S., Wong, A. I., Mantel, I., Nodwell, J. R., and Maxwell, K. L. (2018) A chemical defence against phage infection. *Nature.* **564**, 283–286
43. Pedruzzi, I., Rosenbusch, J. P., and Locher, K. P. (1998) Inactivation *in vitro* of the *Escherichia coli* outer membrane protein FhuA by a phage T5-encoded lipoprotein. *FEMS Microbiol. Lett.* **168**, 119–125
44. Labrie, S. J., Samson, J. E., and Moineau, S. (2010) Bacteriophage resistance mechanisms. *Nat. Rev. Microbiol.* **8**, 317–327
45. Lopatina, A., Tal, N., and Sorek, R. (2020) Abortive infection: bacterial suicide as an antiviral immune strategy. *Annu. Rev. Virol.* **7**, 371–384
46. Makarova, K. S., Wolf, Y. I., and Koonin, E. V. (2013) Comparative genomics of defense systems in archaea and bacteria. *Nucleic Acids Res.* **41**, 4360–4377
47. Fortier, L.-C., Bouchard, J. D., and Moineau, S. (2005) Expression and site-directed mutagenesis of the lactococcal abortive phage infection protein AbiK. *J. Bacteriol.* **187**, 3721–3730
48. Haaber, J., Samson, J. E., Labrie, S. J., Campanacci, V., Cambillau, C., Moineau, S., and Hammer, K. (2010) Lactococcal abortive infection protein AbiV interacts directly with the phage protein SaV and prevents translation of phage proteins. *Appl. Environ. Microbiol.* **76**, 7085–92
49. Short, F. L., Akusobi, C., Broadhurst, W. R., and Salmond, G. P. C. (2018) The bacterial Type III toxin-antitoxin system, ToxIN, is a dynamic protein-RNA complex with stability-dependent antiviral abortive infection activity. *Sci. Rep.* 10.1038/s41598-017-18696-x
50. Samson, J. E., Bélanger, M., and Moineau, S. (2013) Effect of the abortive infection mechanism and type III toxin/antitoxin system AbiQ on the lytic cycle of *Lactococcus lactis* Phages. *J. Bacteriol.* **195**, 3947–3956
51. Lau, R. K., Ye, Q., Birkholz, E. A., Berg, K. R., Patel, L., Mathews, I. T., Watrous, J. D., Ego, K., Whiteley, A. T., Lowey, B., Mekalanos, J. J., Kranzusch, P. J., Jain, M., Pogliano, J., and Corbett, K. D. (2020) Structure and mechanism of a cyclic trinucleotide-activated bacterial endonuclease mediating bacteriophage immunity. *Mol. Cell.* **77**, 723-733.e6
52. Cohen, D., Melamed, S., Millman, A., Shulman, G., Oppenheimer-Shaanan, Y., Kacem, A., Doron, S., Amitai, G., and Sorek, R. (2019) Cyclic GMP–AMP signalling protects

- bacteria against viral infection. *Nature*. **574**, 691–695
53. Durmaz, E., and Klaenhammer, T. R. (2007) Abortive phage resistance mechanism AbiZ speeds the lysis clock to cause premature lysis of phage-infected *Lactococcus lactis*. *J. Bacteriol.* **189**, 1417–1425
 54. González-Delgado, A., Mestre, M. R., Martínez-Abarca, F., and Toro, N. (2021) Prokaryotic reverse transcriptases: from retroelements to specialized defense systems. *FEMS Microbiol. Rev.* **45**, 1–19
 55. Bouchard, J. D. (2004) Mode d’action du système de résistance aux phages AbiK de *Lactococcus lactis*. *Ph.D. thesis*
 56. Robbins, D. J., Barkley, M. D., and Coleman, M. S. (1987) Interaction of terminal transferase with single-stranded DNA. *J. Biol. Chem.* **262**, 9494–502
 57. Figiel, M., Gapinska, M., Czarnocki-Cieciura, M., Zajko, W., Sroka, M., Skowronek, K., and Nowotny, M. (2022) Mechanism of protein-primed template-independent DNA synthesis by Abi polymerases. *Nucleic Acids Res.* **50**, 10026–10040
 58. Pettersen, E., Goddard, T., Huang, C., Meng, E., Couch, G., Croll, T., Morris, J., and Ferrin, T. (2021) UCSF ChimeraX: structure visualization for researchers, educators, and developers. *Protein Sci.* **30**, 70–82
 59. Bouchard, J. D., and Moineau, S. (2004) Lactococcal phage genes involved in sensitivity to AbiK and their relation to single-strand annealing proteins. *J. Bacteriol.* **186**, 3649–3652
 60. Lopes, A., Amarir-Bouhram, J., Faure, G., Petit, M.-A., and Guerois, R. (2010) Detection of novel recombinases in bacteriophage genomes unveils Rad52, Rad51 and Gp2.5 remote homologs. *Nucleic Acids Res.* **38**, 3952–3962
 61. Ploquin, M., Bransi, A., Paquet, E. R., Stasiak, A. Z., Stasiak, A., Yu, X., Cieslinska, A. M., Egelman, E. H., Moineau, S., and Masson, J.-Y. (2008) Functional and structural basis for a bacteriophage homolog of human RAD52. *Curr. Biol.* **18**, 1142–1146
 62. Zimmerly, S., and Wu, L. (2015) An unexplored diversity of reverse transcriptases in bacteria. *Mob. DNA III*. 10.1128/9781555819217.ch54
 63. Storms, Z. J., and Sauvageau, D. (2015) Modeling tailed bacteriophage adsorption: Insight into mechanisms. *Virology*. **485**, 355–362
 64. Maginnis, M. S. (2018) Virus-receptor interactions: the key to cellular invasion. *J. Mol. Biol.* **430**, 2590–2611
 65. Clokie, M. R. J., and Kropinski, A. M. (2009) *Bacteriophages: Methods and Protocols Volume 1: Isolation, Characterization, and Interactions*
 66. Sciara, G., Bebeacua, C., Bron, P., Tremblay, D., Ortiz-Lombardia, M., Lichiere, J., van Heel, M., Campanacci, V., Moineau, S., and Cambillau, C. (2010) Structure of lactococcal phage p2 baseplate and its mechanism of activation. *Proc. Natl. Acad. Sci.* **107**, 6852–6857
 67. Nava, A. R., Mauricio, N., Sanca, A. J., and Domínguez, D. C. (2020) Evidence of calcium signaling and modulation of the LmrS multidrug resistant efflux pump activity by Ca²⁺ ions in *S. aureus*. *Front. Microbiol.* 10.3389/fmicb.2020.573388
 68. Hayes, P. C., Wolf, C. R., and Hayes, J. D. (1989) Blotting techniques for the study of DNA, RNA, and proteins. *BMJ*. **299**, 965–968
 69. Mackay, I. M., Arden, K. E., and Nitsche, A. (2002) Real-time PCR in virology. *Nucleic Acids Res.* **30**, 1292–1305
 70. Lemay, M. L., Maaß, S., Otto, A., Hamel, J., Plante, P. L., Rousseau, G. M., Tremblay, D.

- M., Shi, R., Corbeil, J., Gagné, S. M., Becher, D., and Moineau, S. (2020) A lactococcal phage protein promotes viral propagation and alters the host proteomic response during infection. *Viruses*. 10.3390/v12080797
71. Terzaghi, B., and Sandine, W. (1975) Improved medium for lactic streptococci and their bacteriophages. *Appl. Microbiol.* **30**, 341–341
 72. Mahoney, J., Tremblay, D. M., Labrie, S. J., Moineau, S., van Sinderen, D., Mahony, J., Tremblay, D. M., Labrie, S. J., Moineau, S., and van Sinderen, D. (2015) Investigating the requirement for calcium during lactococcal phage infection. *Int. J. Food Microbiol.* **201**, 47–51
 73. Sambrook, J. F., and Russell, D. (2001) *Molecular Cloning: a Laboratory Manual (3rd ed.)*, Cold Spring Harbor Laboratory Press
 74. Holo, H., and Nes, I. F. (1989) High-frequency transformation, by electroporation, of *Lactococcus lactis* subsp. *cremoris* grown with glycine in osmotically stabilized media. *Appl. Environ. Microbiol.* **55**, 3119–3123
 75. Moineau, S., Fortier, J., Ackermann, H.-W., and Pandian, S. (1992) Characterization of lactococcal phages from Quebec cheese plants. *Can. J. Microbiol.* **38**, 875–882
 76. Kropinski, A. M., Mazzocco, A., Waddell, T. E., Lingohr, E., and Johnson, R. P. (2009) Enumeration of bacteriophages by double agar overlay plaque assay. *Methods Mol. Biol.* **501**, 69–76
 77. O’Sullivan, D., and Klaenhammer, T. (1993) High- and low-copy-number *Lactococcus* shuttle cloning vectors with features for clone screening. *Gene*. **137**, 227–231
 78. Bio Basic (2021) EZ-10 spin column genomic DNA minipreps kit handbook
 79. Bio Basic (2019) EZ-10 spin column plasmid DNA miniprep kit, EZ-10 spin column PCR products purification kit, EZ-10 spin column DNA gel extraction kit
 80. Geneaid (2017) High-speed plasmid mini kit
 81. Norgen Biotek (2014) Phage DNA isolation kit
 82. Qiagen (2015) RNAprotect® bacteria reagent handbook
 83. GE Healthcare (2006) Amersham Hybond-XL
 84. Abràmoff, M. D., Magalhães, P. J., and Ram, S. J. (2004) Image processing with imageJ. *Biophotonics Int.* **11**, 36–41
 85. Qiagen (2014) Rotor-Gene® SYBR® green handbook
 86. Qiagen (2013) QuantiNova™ SYBR® green PCR handbook
 87. Stark, R., Grzelak, M., and Hadfield, J. (2019) RNA sequencing: the teenage years. *Nat. Rev. Genet.* **20**, 631–656
 88. Maier, R. M., and Pepper, I. L. (2015) Bacterial Growth. in *Environmental Microbiology: Third Edition*, pp. 37–56, 10.1016/B978-0-12-394626-3.00003-X
 89. Shimoyama, Y. (2022) COGclassifier: A tool for classifying prokaryote protein sequences into COG functional category [Computer software].
 90. Tabib-Salazar, A., Liu, B., Barker, D., Burchell, L., Qimron, U., Matthews, S. J., and Wigneshweraraj, S. (2018) T7 phage factor required for managing RpoS in *Escherichia coli*. *Proc. Natl. Acad. Sci. U. S. A.* **115**, E5353–E5362
 91. Darwin, A. J. (2005) The phage-shock-protein response. *Mol. Microbiol.* **57**, 621–628
 92. Lei, J., Xin, C., Xiao, W., Chen, W., and Song, Z. (2021) The promise of endogenous and exogenous riboflavin in anti-infection. *Virulence*. **12**, 2314–2326
 93. Invitrogen (2011) Invitrogen™ RiboPure™ RNA purification kit, bacteria
 94. Qiagen (2015) QuantiNova™ SYBR green RT-PCR kit

95. Qiagen (2019) RNeasy® mini handbook
96. Sturrock, S., Buxton, S., Cooper, A., Markowitz, S., Duran, S., Thierer, T., Ashton, B., Meintjes, P., and Drummond, A. (2012) Geneious Basic: An integrated and extendable desktop software platform for the organization and analysis of sequence data. *Bioinformatics*. **28**, 1647–1649
97. Tarazona, S., Furió-Tarí, P., Turrà, D., Di Pietro, A., Nueda, M. J., Ferrer, A., and Conesa, A. (2015) Data quality aware analysis of differential expression in RNA-seq with NOISeq R/Bioc package. *Nucleic Acids Res.* 10.1093/nar/gkv711
98. Tunyasuvunakool, K., Adler, J., Wu, Z., Green, T., Zielinski, M., Zidek, A., Bridgland, A., Cowie, A., Meyer, C., Laydon, A., Velankar, S., Kleywegt, G. J., Bateman, A., Evans, R., Pritzel, A., Figurnov, M., Ronneberger, O., Bates, R., Kohl, S. A. A., Potapenko, A., Ballard, A. J., Romero-Paredes, B., Nikolov, S., Jain, R., and Hassabis, D. (2021) Highly accurate protein structure prediction for the human proteome. *Nature*. **596**, 590–596
99. Baek, M., DiMaio, F., Anishchenko, I., Dauparas, J., Ovchinnikov, S., Lee, G. R., Wang, J., Cong, Q., Kinch, L. N., Dustin Schaeffer, R., Millán, C., Park, H., Adams, C., Glassman, C. R., DeGiovanni, A., Pereira, J. H., Rodrigues, A. V., Van Dijk, A. A., Ebrecht, A. C., Opperman, D. J., Sagmeister, T., Buhlheller, C., Pavkov-Keller, T., Rathinaswamy, M. K., Dalwadi, U., Yip, C. K., Burke, J. E., Christopher Garcia, K., Grishin, N. V., Adams, P. D., Read, R. J., and Baker, D. (2021) Accurate prediction of protein structures and interactions using a three-track neural network. *Science (80-.)*. **373**, 871–876
100. Stamos, J. L., Lentzsch, A. M., and Lambowitz, A. M. (2017) Structure of a thermostable group II intron reverse transcriptase with template-primer and its functional and evolutionary implications. *Mol. Cell*. **68**, 926-939.e4
101. Sun, P. D., Foster, C. E., and Boyington, J. C. (2004) Overview of protein structural and functional folds. *Curr. Protoc. Protein Sci.* **35**, 1711–171189
102. Spåhr, H., Chia, T., Lingford, J. P., Siira, S. J., Cohen, S. B., Filipovska, A., and Rackham, O. (2018) Modular ssDNA binding and inhibition of telomerase activity by designer PPR proteins. *Nat. Commun.* 10.1038/s41467-018-04388-1
103. Barford, D., Hemmings, B. A., Groves, M. R., Turowski, P., and Hanlon, N. (1999) The structure of the protein phosphatase 2A PR65/A subunit reveals the conformation of its 15 tandemly repeated HEAT motifs. *Cell*. **96**, 99–110
104. Choi, H. J., and Weis, W. I. (2005) Structure of the armadillo repeat domain of plakophilin 1. *J. Mol. Biol.* **346**, 367–376
105. Kagawa, W., Kurumizaka, H., Ishitani, R., Fukai, S., Nureki, O., Shibata, T., and Yokoyama, S. (2002) Crystal structure of the homologous-pairing domain from the human Rad52 recombinase in the undecameric form. *Mol. Cell*. **10**, 359–371
106. Agilent Technologies (2011) Quikchange lightning site-directed mutagenesis kit. *Instr. Man.*
107. Altschul, S. F., Gish, W., Miller, W., Myers, E. W., and Lipman, D. J. (1990) Basic local alignment search tool. *J. Mol. Biol.* **215**, 403–410
108. GE Healthcare (2006) Amersham ECL Western blotting detection reagents and analysis system

Appendices

Appendix A: Common Media and Buffers

GM17 (M17 supplemented with 0.5% glucose)

Tryptone	5.00 g
Soy peptone	5.00 g
Beef extract	5.00 g
Yeast extract	2.50 g
Ascorbic acid	0.50 g
Magnesium sulfate	0.25 g
Disodium- β -glycerophosphate	19.00 g
Distilled water up to	1.00 L

Autoclave to sterilize.

Add 25 mL of sterilized 20% glucose solution and mix well.

For solid media, add 10.0 g of agar per 1 L of broth.

LB (Lysogeny Broth)

Tryptone	10.00 g
Yeast extract	5.00 g
NaCl	10.00 g
Distilled water up to	1.00 L

Autoclave to sterilize.

For solid media, add 10.0 g of agar per 1 L of broth.

2xYT

Tryptone	16.00 g
Yeast extract	10.00 g
NaCl	5.00 g
Distilled water up to	1.00 L

Autoclave to sterilize.

1 M, Tris-HCl

Tris base	121.10 g
HCl to desired pH	~42 mL for pH 8.0
Distilled water up to	1.00 L

Autoclave to sterilize.

0.5 M, EDTA (Ethylenediaminetetraacetic Acid)

EDTA · 2H ₂ O	186.10 g
NaOH to desired pH	~20 g for pH 8.0
Distilled water up to	1.00 L

Autoclave to sterilize.

1xTAE (Tris-acetate-EDTA Buffer)

Tris base	4.85 g
Glacial acetic acid	1.21 mL
0.5 M EDTA (pH 8.0)	2.00 mL
Distilled water up to	1.00 L

1xTBE (Tris-borate-EDTA Buffer)

Tris base	5.40 g
Boric acid	5.50 g
0.5 M EDTA (pH 8.0)	4.00 mL
Distilled water up to	1.00 L

20xSSC (Saline-sodium citrate Buffer)

NaCl	175.30 g
Sodium citrate	77.40 g
Distilled water up to	1.00 L

Adjust to pH 7.0 with HCl.

10xLaemmli Electrophoresis Running Buffer

Tris base	30.00 g
Glycine	144.00 g
SDS	10.00 g
Distilled water up to	1.00 L

4xSDS-PAGE Loading Dye

Tris-HCl, 1.0 M, pH 6.8	10.00 mL
SDS	4.00 g
Glycerol	20.00 mL
β -mercaptoethanol	10.00 mL
Bromophenol blue	0.10 g
Distilled water up to	50.00 mL

Ponceau S Staining Solution

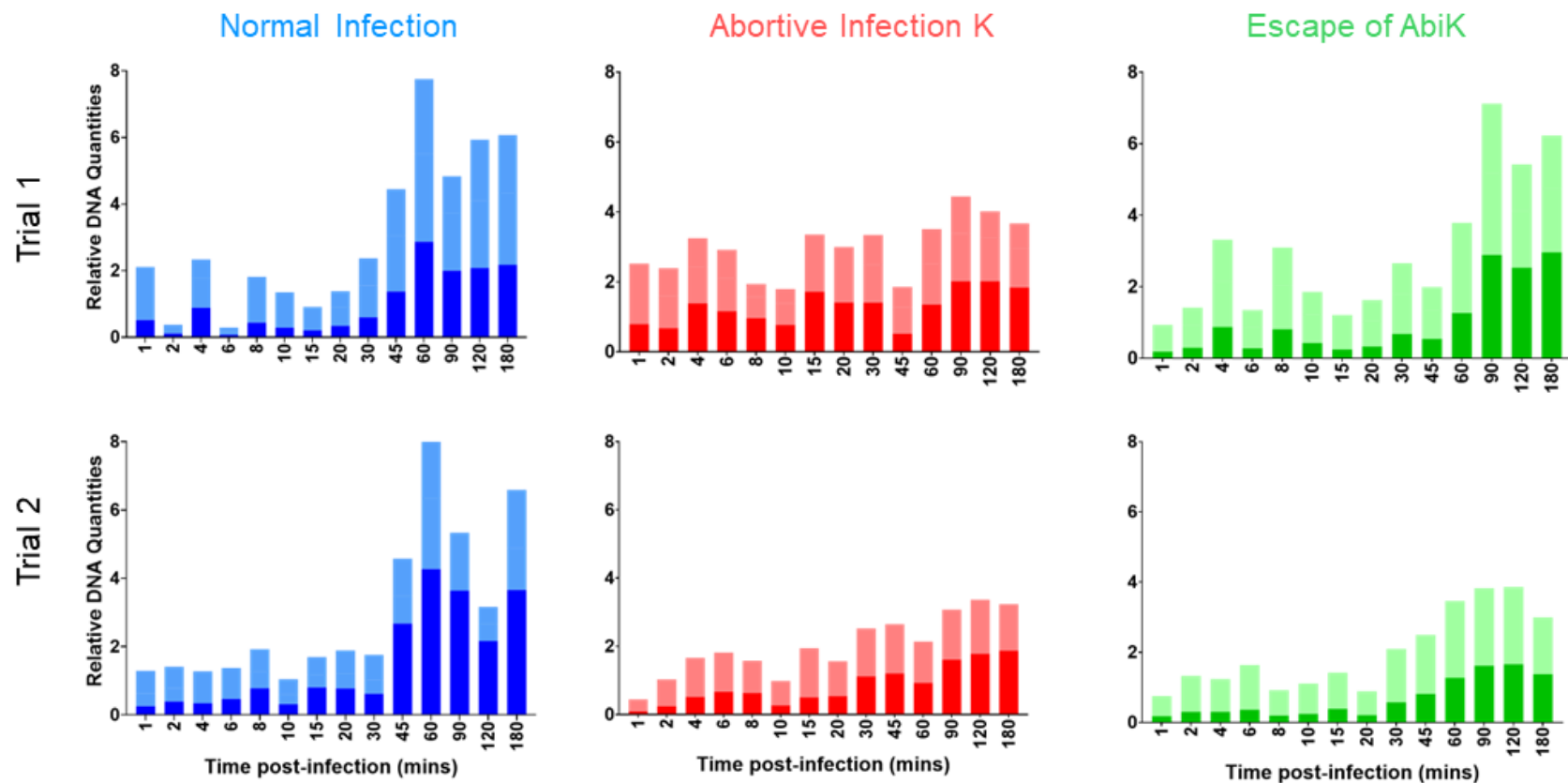
Ponceau S	1.00 g
Glacial acetic acid	50.00 mL
Distilled water up to	1.00 L

10xTBS Buffer (Tris-Buffered Saline)

Tris base	24.00 g
NaCl	88.00 g
Distilled water up to	1.00 L

Adjust to pH 7.6 with HCl.

Appendix B: Supplementary Data



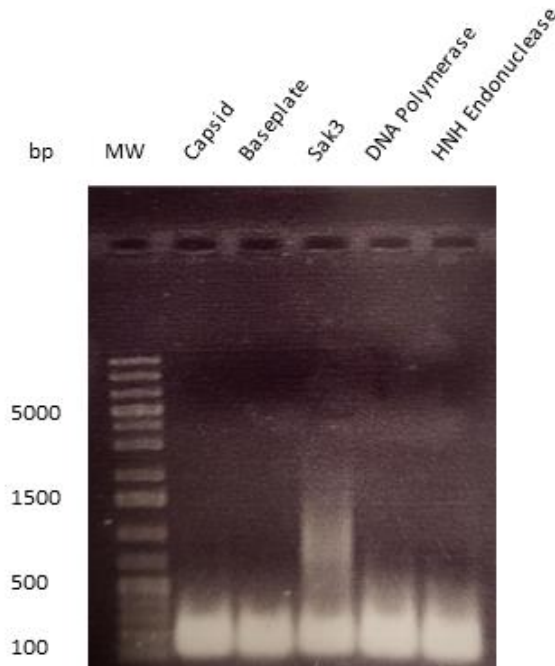
Supplementary Figure 1: Densitometry analysis of Southern blots with probe 7-1.

Bar graph of the relative DNA quantities from time points post-infection. Values were obtained by densitometry analysis of Southern blots probed by probe 7-1, where the band intensity was divided by the average of all band intensities. Mature (light) and immature (dark) forms of phage DNA are shown.



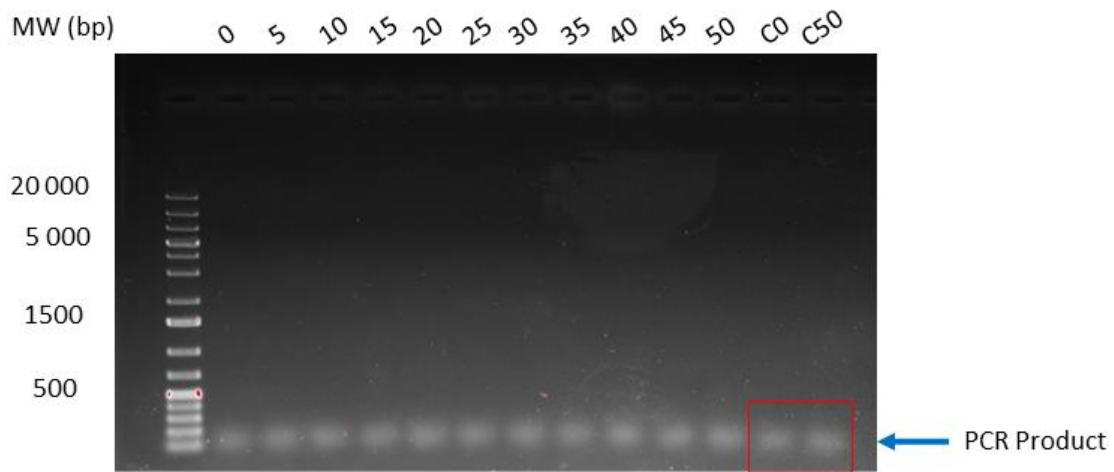
Supplementary Figure 2: Southern blot of samples pretreated at 65°C.

Southern blot hybridization of the normal infection, where DNA is extracted from time points post-infection. DNA samples were double digested with EcoRI and HindIII restriction enzymes then treated at 65°C before electrophoresis and transfer to a Hybond-XL (Amersham) membrane, followed by hybridization by probe 7-1. For the normal infection, lactococcal phage p2 infected AbiK⁻ cells. Negative controls without phages (time = 0 minutes) were performed. Undigested and single digestion (EcoRI and HindIII) controls were performed.



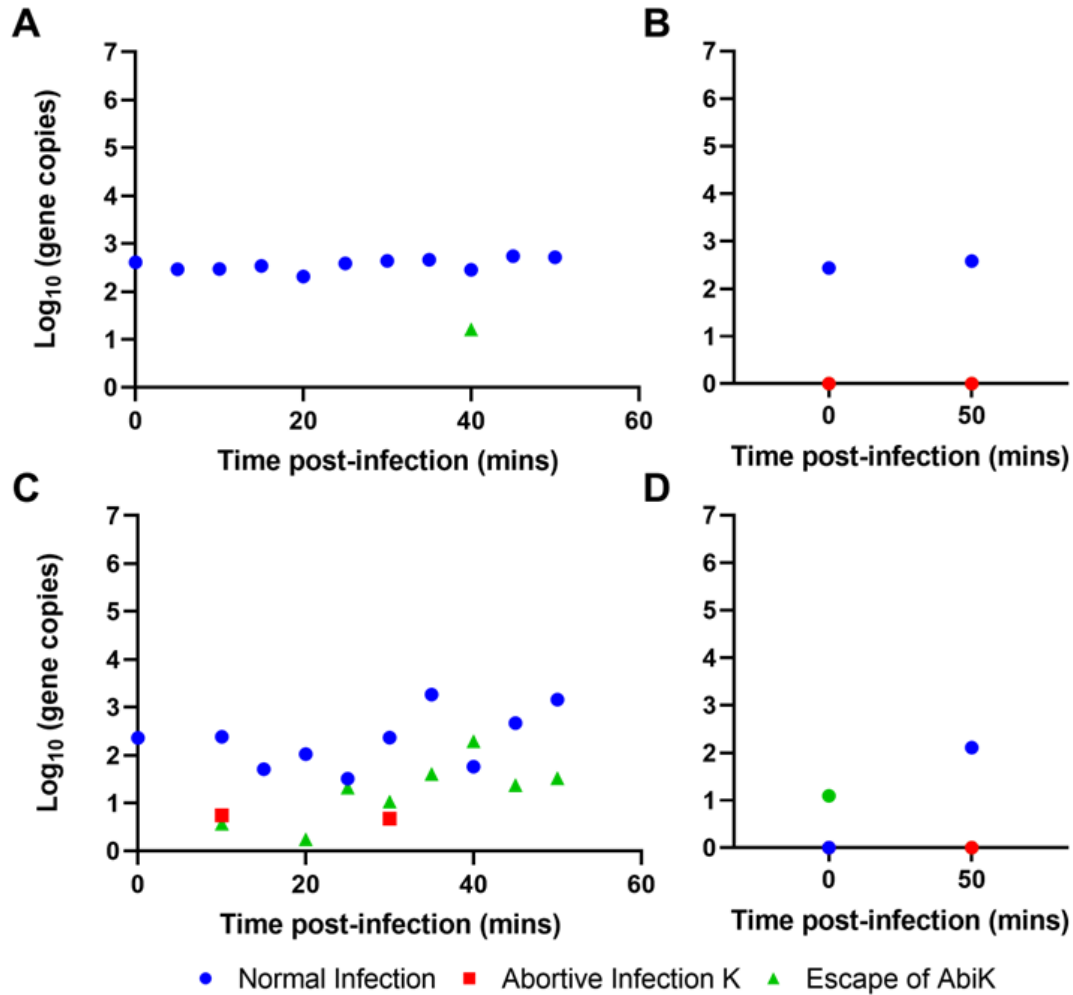
Supplementary Figure 3: PCR products of primers designed for RT-qPCR.

PCR products of primers designed for RT-qPCR using the lactococcal phage p2 DNA as a template were run on a 1.0% agarose gel at 90 V for 1 hour and then stained with ethidium bromide for visualization.



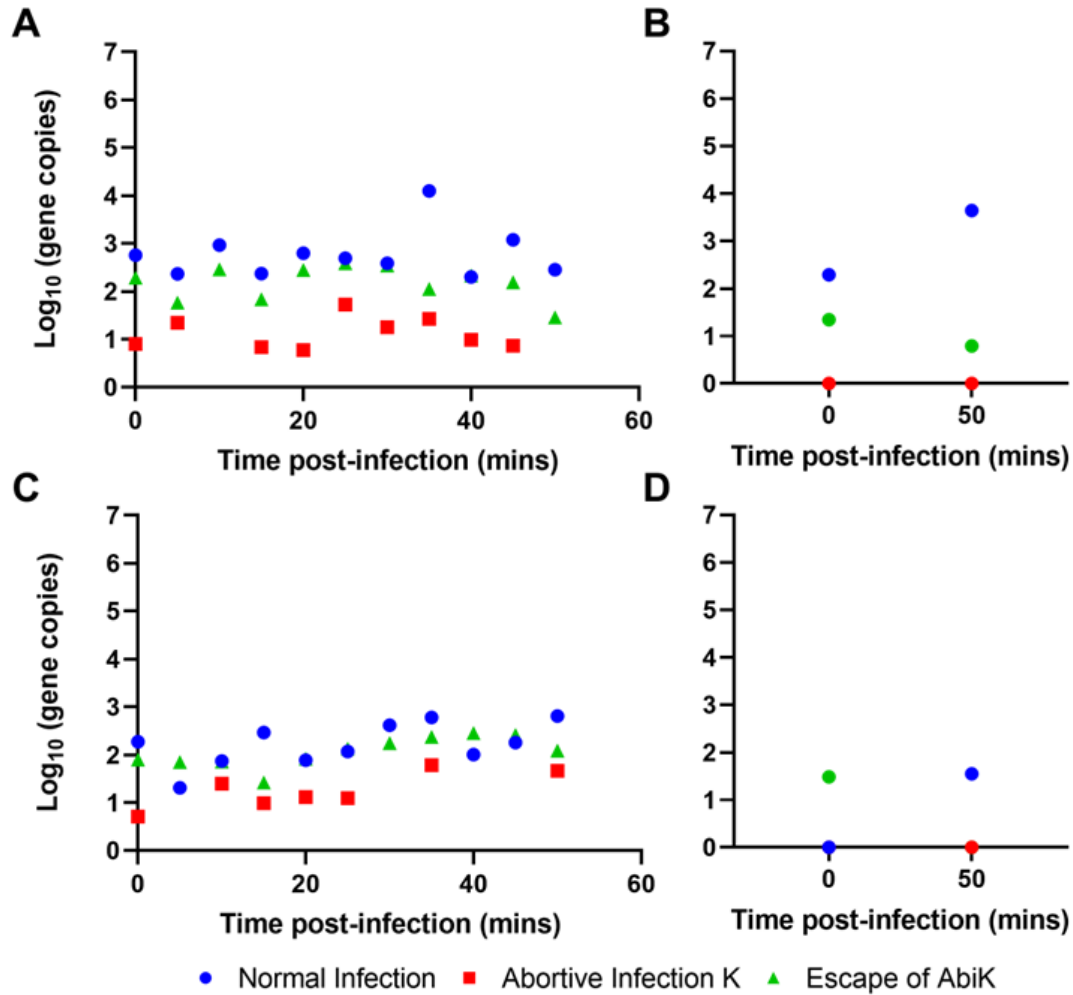
Supplementary Figure 4: RT-qPCR Products.

RT-qPCR products from primers targeting the DNA polymerase gene from samples taken post-infection of the AbiK mechanism. Lanes 2 – 12 contain time points post-infection. Lanes 13-14 contain no-phage control samples at 0 and 50 minutes. Red box indicates PCR product detected in no-phage controls. Samples were run on a 1.0% agarose gel at 90 V for 1 hour and then stained with ethidium bromide for visualization.



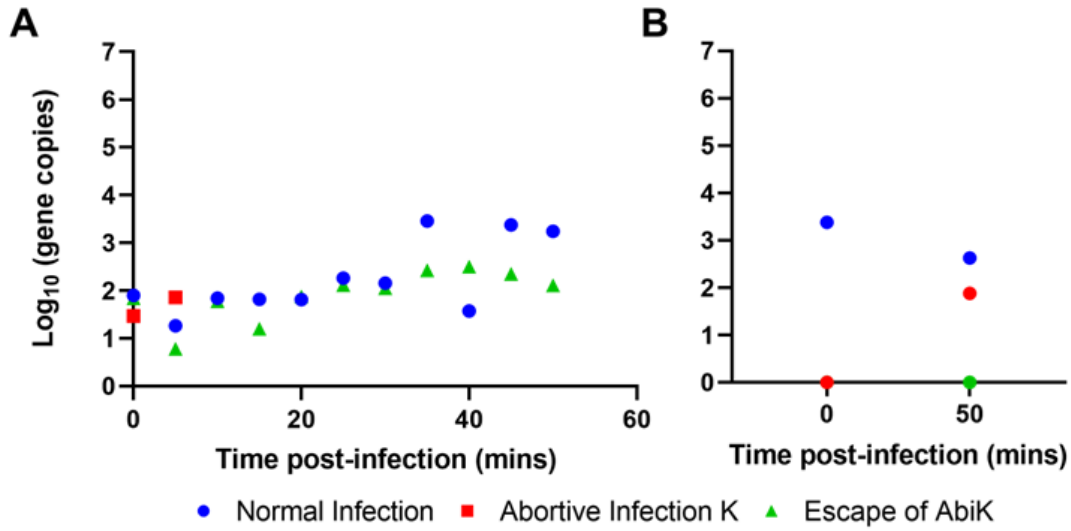
Supplementary Figure 5: DNA Control of Figure 3-1.

The log of gene copies of DNA present in samples from time points post-infection analyzed by RT-qPCR primers targeting the DNA polymerase gene (A) and primers targeting the HNH endonuclease gene (C). Negative controls without phages were performed at time points 0 minutes and 50 minutes using primers targeting the DNA polymerase gene (B) and primers targeting the HNH endonuclease gene (D). Values represent a single replicate. Missing data points represent values > 1.



Supplementary Figure 6: DNA Control of Figure 3-2.

The log of gene copies of DNA present in samples from time points post-infection analyzed by RT-qPCR primers targeting the capsid gene (A) and primers targeting the baseplate gene (C). Negative controls without phages were performed at time points 0 minutes and 50 minutes using primers targeting the capsid gene (B) and primers targeting the baseplate gene (D). Values represent a single replicate. Missing data points represent values > 1.

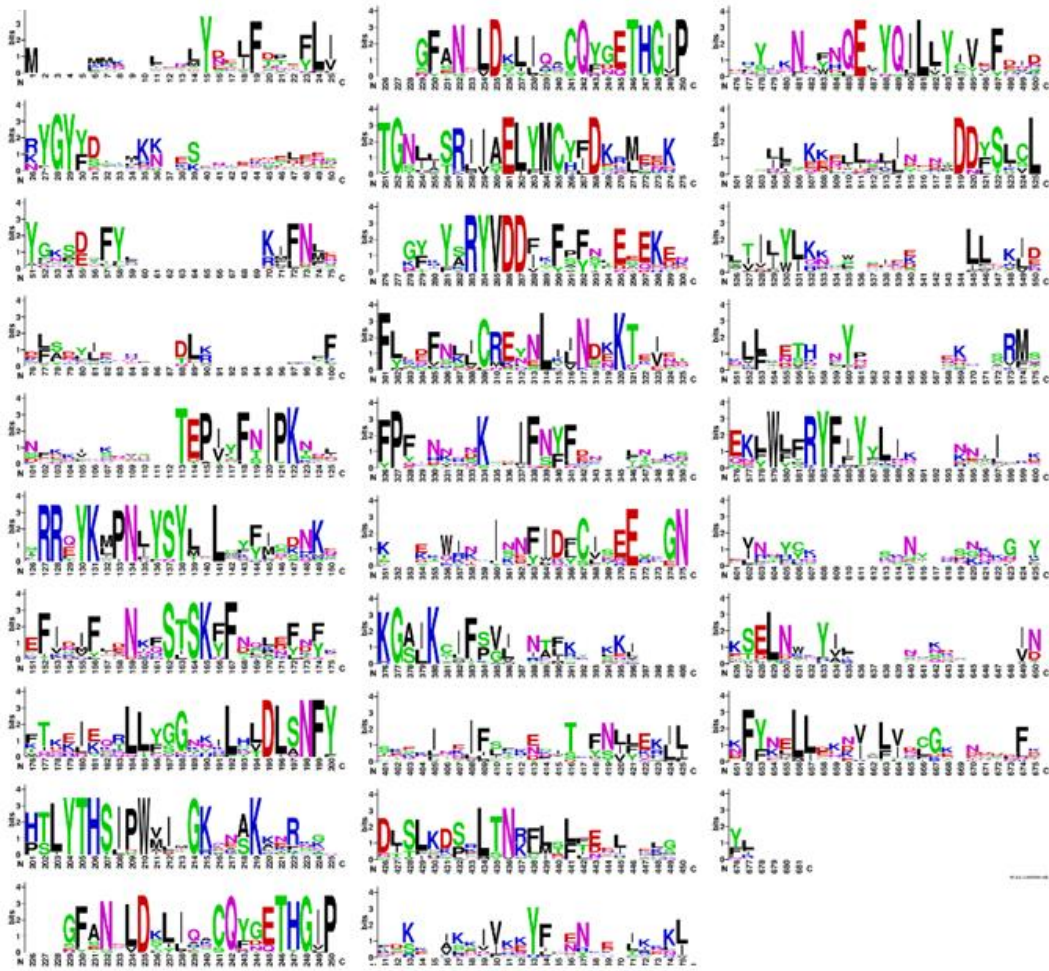


Supplementary Figure 7: DNA Control of Figure 3-3.

The log of gene copies of DNA present in samples from time points post-infection analyzed by RT-qPCR primers targeting the sak3 gene (A). Negative controls without phages were performed at time points 0 minutes and 50 minutes using primers targeting the sak3 gene (B). Values represent a single replicate. Missing data points represent values > 1.

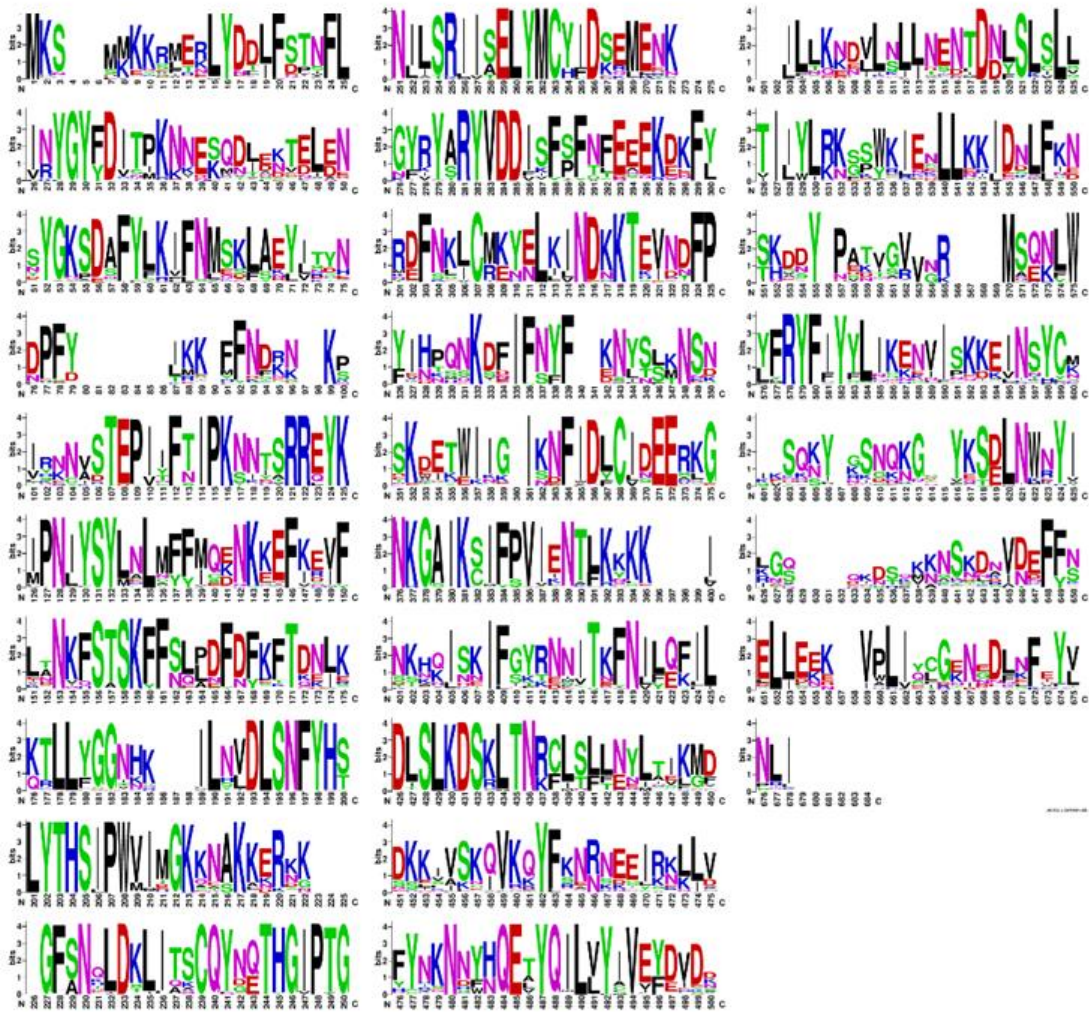
Supplementary Table 1: Percentage of transcript counts in COG categories for RNA-Seq.

COG	WT_C0	WT_C30	AbiK_C0	AbiK_C30	WT_0	WT_10	WT_30	AbiK_0	AbiK_10	AbiK_30
A	0.00	0.00	0.00	0.00	0.00	0.00	0.00	0.00	0.00	0.00
B	0.00	0.00	0.00	0.00	0.00	0.00	0.00	0.00	0.00	0.00
C	8.07	9.72	4.58	5.09	7.76	7.32	7.67	4.29	3.87	3.84
D	1.83	1.50	1.75	1.55	1.78	1.65	1.51	1.73	1.64	1.40
E	5.77	5.51	5.80	5.18	5.05	4.44	4.67	5.20	4.57	4.34
F	2.41	2.57	2.51	2.70	2.56	2.41	2.22	2.70	2.66	2.55
G	11.32	12.93	11.35	11.43	10.89	10.90	10.79	11.06	10.84	9.86
H	2.32	1.68	2.23	1.79	2.28	1.92	1.61	2.20	1.98	1.70
I	2.19	1.95	2.08	1.72	2.20	1.90	1.56	2.03	1.77	1.38
J	32.02	35.03	35.92	40.55	32.63	32.37	30.14	36.59	37.77	34.39
K	5.20	5.05	5.18	5.28	5.18	4.72	4.34	5.23	5.21	4.53
L	4.47	3.55	4.76	4.23	4.50	4.22	3.76	4.81	4.61	3.94
M	3.81	3.31	3.68	3.43	3.70	3.28	3.09	3.62	3.36	2.96
N	0.08	0.05	0.08	0.05	0.08	0.07	0.06	0.07	0.06	0.05
O	3.23	2.74	3.31	2.73	3.22	2.81	2.55	3.25	2.98	2.49
P	2.56	1.87	2.50	1.90	2.47	2.28	2.00	2.40	2.21	1.83
Q	0.22	0.17	0.18	0.15	0.22	0.15	0.13	0.17	0.14	0.12
R	2.63	2.20	2.69	2.36	2.59	2.27	2.02	2.66	2.44	2.11
S	5.03	3.81	4.93	4.14	4.95	4.17	3.51	4.89	4.42	3.59
T	2.48	2.23	2.41	2.17	2.40	2.08	1.96	2.38	2.16	1.86
U	0.66	0.58	0.74	0.65	0.63	0.58	0.52	0.72	0.66	0.55
V	1.21	0.97	1.12	1.00	1.14	0.90	0.87	1.06	0.90	0.86
W	0.00	0.00	0.00	0.00	0.00	0.00	0.00	0.00	0.00	0.00
X	0.51	0.44	0.43	0.40	0.51	0.42	0.38	0.44	0.41	0.35
Y	0.00	0.00	0.00	0.00	0.00	0.00	0.00	0.00	0.00	0.00
Z	0.00	0.00	0.00	0.00	0.00	0.00	0.00	0.00	0.00	0.00
1	0.04	0.11	0.13	0.05	0.06	0.04	0.05	0.04	0.05	0.03
2	0.17	0.09	0.19	0.11	0.16	0.13	0.10	0.18	0.14	0.10
3	0.79	0.73	0.71	0.65	0.75	0.91	0.86	0.74	0.76	0.66
4	0.00	0.00	0.00	0.00	0.80	1.07	0.51	0.61	0.99	1.09
5	0.00	0.00	0.00	0.00	0.20	1.01	0.69	0.11	0.88	2.54
6	0.00	0.00	0.00	0.00	0.42	5.29	11.74	0.16	1.88	10.38
7	0.97	1.21	0.72	0.70	0.87	0.71	0.70	0.65	0.64	0.51



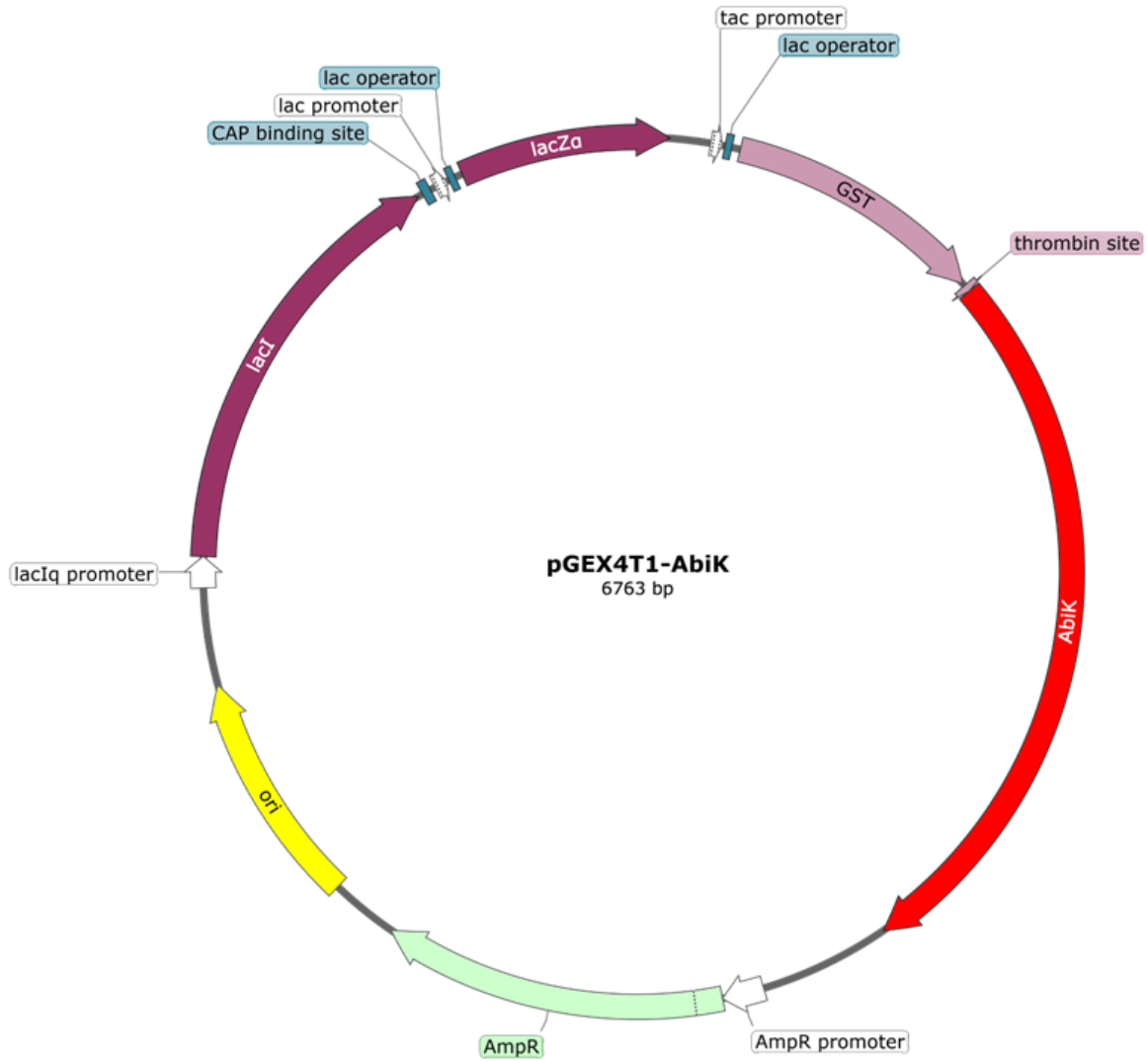
Supplementary Figure 8: WebLogo of AbiK and 16 related protein sequences.

Note that numbers correspond to the sequence alignment and not amino acid positions for AbiK. Sequence logo was generated using WebLogo.



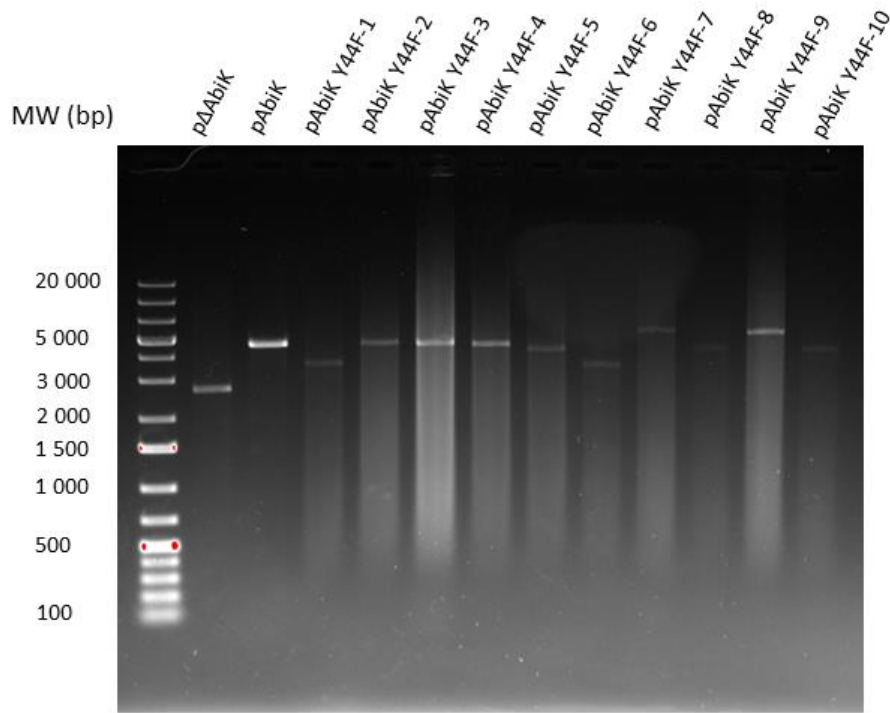
Supplementary Figure 9: WebLogo of AbiK and 99 related protein sequences.

Note that numbers correspond to the sequence alignment and not amino acid positions for AbiK. Sequence logo was generated using WebLogo.



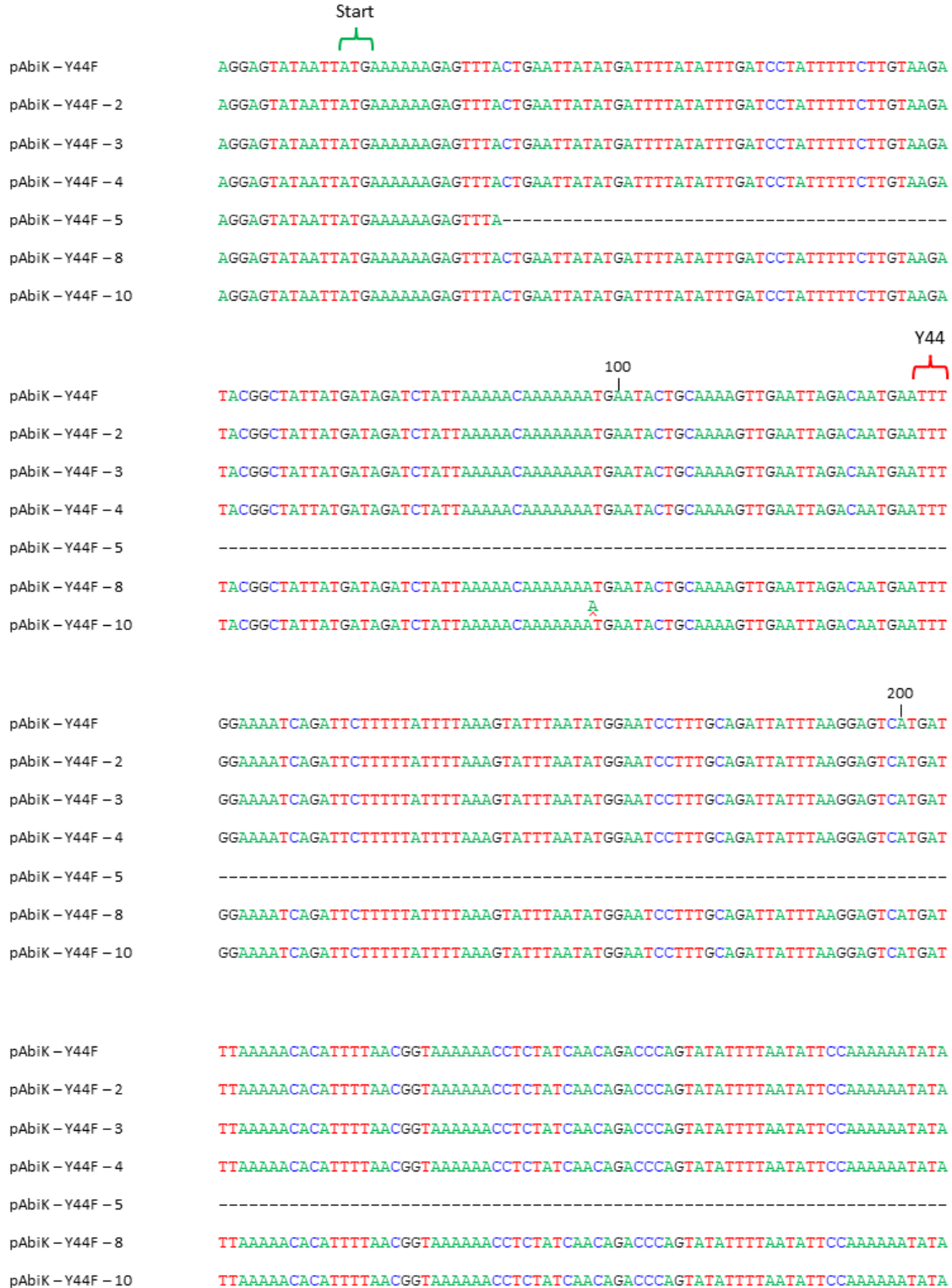
Supplementary Figure 10: Plasmid map for pGEX4T1-AbiK.

The *abiK* gene is coloured red, promoters in white, operators in blue, *lac* genes in magenta, GST in pink, ori in yellow, and the ampicillin resistance gene in green. Plasmid map was generated using Snapgene.



Supplementary Figure 11: Plasmid sizes of pAbiK Y44F.

Plasmids were purified from *L. lactis* strain MG1363 and then digested with single-cutter enzyme EcoRI before being run on a 1.0% agarose gel at 90 V for 1 hour and then stained with ethidium bromide for visualization.



Supplementary Figure 12: Alignment of the nucleotide sequences of AbiK mutants (1/7).

Nucleotide sequence alignment of the AbiK sequence of pAbiK Y44F and pAbiK Y44F plasmids purified from colonies of MG1363. Nucleotides are numbered according to the location in the *abiK* gene and the start and stop codons are indicated. Deletions are denoted by a dash (-) and insertions are denoted with a circumflex (^).

300
|

pAbiK – Y44F GAAGCTAGAAGACAATATAAGATGCCCAATTTATACAGTTATATGGCATTAAATTTATTATATATGTGACAAAT

pAbiK – Y44F – 2 GAAGCTAGAAGACAATATAAGATGCCCAATTTATACAGTTATATGGCATTAAATTTATTATATATGTGACAAAT

pAbiK – Y44F – 3 GAAGCTAGAAGACAATATAAGATGCCCAATTTATACAGTTATATGGCATTAAATTTATTATATATGTGACAAAT

pAbiK – Y44F – 4 GAAGCTAGAAGACAATATAAGATGCCCAATTTATACAGTTATATGGCATTAAATTTATTATATATGTGACAAAT

pAbiK – Y44F – 5 -----

pAbiK – Y44F – 8 GAAGCTAGAAGACAATATAAGATGCCCAATTTATACAGTTATATGGCATTAAATTTATTATATATGTGACAAAT

pAbiK – Y44F – 10 GAAGCTAGAAGACAATATAAGATGCCCAATTTATACAGTTATATGGCATTAAATTTATTATATATGTGACAAAT

400
|

pAbiK – Y44F AAAAAAGAGTTTATAGAAGTATTTATTGATAACAAATTTTCAACGTCAAAAATTTTTAATCAATTGAATTTT

pAbiK – Y44F – 2 AAAAAAGAGTTTATAGAAGTATTTATTGATAACAAATTTTCAACGTCAAAAATTTTTAATCAATTGAATTTT

pAbiK – Y44F – 3 AAAAAAGAGTTTATAGAAGTATTTATTGATAACAAATTTTCAACGTCAAAAATTTTTAATCAATTGAATTTT

pAbiK – Y44F – 4 AAAAAAGAGTTTATAGAAGTATTTATTGATAACAAATTTTCAACGTCAAAAATTTTTAATCAATTGAATTTT

pAbiK – Y44F – 5 -----TAGAAGTATTTATTGATAACAAATTTTCAACGTCAAAAATTTTTAATCAATTGAATTTT

pAbiK – Y44F – 8 AAAAAAGAGTTTATAGAAGTATTTATTGATAACAAATTTTCAACGTCAAAAATTTTTAATCAATTGAATTTT

pAbiK – Y44F – 10 AAAAAAGAGTTTATAGAAGTATTTATTGATAACAAATTTTCAACGTCAAAAATTTTTAATCAATTGAATTTT

pAbiK – Y44F GATTATCCTAAGACACAAGAAATTAACACAAACATTATTATATGGAGGAATAAAGAAATTTACATTTAGATTTA

pAbiK – Y44F – 2 GATTATCCTAAGACACAAGAAATTAACACAAACATTATTATATGGAGGAATAAAGAAATTTACATTTAGATTTA

pAbiK – Y44F – 3 GATTATCCTAAGACACAAGAAATTAACACAAACATTATTATATGGAGGAATAAAGAAATTTACATTTAGATTTA

pAbiK – Y44F – 4 GATTATCCTAAGACACAAGAAATTAACACAAACATTATTATATGGAGGAATAAAGAAATTTACATTTAGATTTA

pAbiK – Y44F – 5 GATTATCCTAAGACACAAGAAATTAACACAAACATTATTATATGGAGGAATAAAGAAATTTACATTTAGATTTA

pAbiK – Y44F – 8 GATTATCCTAAGACACAAGAAATTAACACAAACATTATTATATGGAGGAATAAAGAAATTTACATTTAGATTTA

pAbiK – Y44F – 10 GATTATCCTAAGACACAAGAAATTAACACAAACATTATTATATGGAGGAATAAAGAAATTTACATTTAGATTTA

500
|

pAbiK – Y44F TCTAATTTTTATCATACTTTATATACACATAGTATACCATGGATGATTGATGGAAAACTGCATCTAAACAA

pAbiK – Y44F – 2 TCTAATTTTTATCATACTTTATATACACATAGTATACCATGGATGATTGATGGAAAACTGCATCTAAACAA

pAbiK – Y44F – 3 TCTAATTTTTATCATACTTTATATACACATAGTATACCATGGATGATTGATGGAAAACTGCATCTAAACAA

pAbiK – Y44F – 4 TCTAATTTTTATCATACTTTATATACACATAGTATACCATGGATGATTGATGGAAAACTGCATCTAAACAA

pAbiK – Y44F – 5 TCTAATTTTTATCATACTTTATATACACATAGTATACCATGGATGATTGATGGAAAACTGCATCTAAACAA

pAbiK – Y44F – 8 TCTAATTTTTATCATACTTTATATACACATAGTATACCATGGATGATTGATGGAAAACTGCATCTAAACAA

pAbiK – Y44F – 10 TCTAATTTTTATCATACTTTATATACACATAGTATACCATGGATGATTGATGGAAAACTGCATCTAAACAA

Supplementary Figure 12 continued (2/7).

600
|

pAbiK – Y44F AATAGAAAAAAGGGTTTTCTAATACATTAGATACTTTGATTACAGCTTGTCAATACGACGAAACACATGGC

pAbiK – Y44F – 2 AATAGAAAAAAGGGTTTTCTAATACATTAGATACTTTGATTACAGCTTGTCAATACGACGAAACACATGGC

pAbiK – Y44F – 3 AATAGAAAAAAGGGTTTTCTAATACATTAGATACTTTGATTACAGCTTGTCAATACGACGAAACACATGGC

pAbiK – Y44F – 4 AATAGAAAAAAGGGTTTTCTAATACATTAGATACTTTGATTACAGCTTGTCAATACGACGAAACACATGGC

pAbiK – Y44F – 5 AATAGAAAAAAGGGTTTTCTAATACATTAGATACTTTGATTACAGCTTGTCAATACGACGAAACACATGGC

pAbiK – Y44F – 8 AATAGAAAAAAGGGTTTTCTAATACATTAGATACTTTGATTACAGCTTGTCAATACGACGAAACACATGGC

pAbiK – Y44F – 10 AATAGAAAAAAGGGTTTTCTAATACATTAGATACTTTGATTACAGCTTGTCAATACGACGAAACACATGGC

700
|

pAbiK – Y44F ATTCCAACCTGGAATCTATTGTCTAGGATTATTACCGAACTATATATGTGCCATTTTGATAAACAAATGGAA

pAbiK – Y44F – 2 ATTCCAACCTGGAATCTATTGTCTAGGATTATTACCGAACTATATATGTGCCATTTTGATAAACAAATGGAA

pAbiK – Y44F – 3 ATTCCAACCTGGAATCTATTGTCTAGGATTATTACCGAACTATATATGTGCCATTTTGATAAACAAATGGAA

pAbiK – Y44F – 4 ATTCCAACCTGGAATCTATTGTCTAGGATTATTACCGAACTATATATGTGCCATTTTGATAAACAAATGGAA

pAbiK – Y44F – 5 ATTCCAACCTGGAATCTATTGTCTAGGATTATTACCGAACTATATATGTGCCATTTTGATAAACAAATGGAA

pAbiK – Y44F – 8 ATTCCAACCTGGAATCTATTGTCTAGGATTATTACCGAACTATATATGTGCCATTTTGATAAACAAATGGAA

pAbiK – Y44F – 10 ATTCCAACCTGGAATCTATTGTCTAGGATTATTACCGAACTATATATGTGCCATTTTGATAAACAAATGGAA

pAbiK – Y44F TATAAGAACTTTGTGATTCAAGATATGTAGATGATTTTATATTTCCGTTTACTTTTGAGAATGAAAAGCAA

pAbiK – Y44F – 2 TATAAGAACTTTGTGATTCAAGATATGTAGATGATTTTATATTTCCGTTTACTTTTGAGAATGAAAAGCAA

pAbiK – Y44F – 3 TATAAGAACTTTGTGATTCAAGATATGTAGATGATTTTATATTTCCGTTTACTTTTGAGAATGAAAAGCAA

pAbiK – Y44F – 4 TATAAGAACTTTGTGATTCAAGATATGTAGATGATTTTATATTTCCGTTTACTTTTGAGAATGAAAAGCAA

pAbiK – Y44F – 5 TATAAGAACTTTGTGATTCAAGATATGTAGATGATTTTATATTTCCGTTTACTTTTGAGAATGAAAAGCAA

pAbiK – Y44F – 8 TATAAGAACTTTGTGATTCAAGATATGTAGATGATTTTATATTTCCGTTTACTTTTGAGAATGAAAAGCAA

pAbiK – Y44F – 10 TATAAGAACTTTGTGATTCAAGATATGTAGATGATTTTATATTTCCGTTTACTTTTGAGAATGAAAAGCAA

800
|

pAbiK – Y44F GAATTTTTAAATGAATTTAACTAATCTGTCGAGAAAAAATCTTAATTATTAATGATAATAAAACGAAAGTT

pAbiK – Y44F – 2 GAATTTTTAAATGAATTTAACTAATCTGTCGAGAAAAAATCTTAATTATTAATGATAATAAAACGAAAGTT

pAbiK – Y44F – 3 GAATTTTTAAATGAATTTAACTAATCTGTCGAGAAAAAATCTTAATTATTAATGATAATAAAACGAAAGTT

pAbiK – Y44F – 4 GAATTTTTAAATGAATTTAACTAATCTGTCGAGAAAAAATCTTAATTATTAATGATAATAAAACGAAAGTT

pAbiK – Y44F – 5 GAATTTTTAAATGAATTTAACTAATCTGTCGAGAAAAAATCTTAATTATTAATGATAATAAAACGAAAGTT

pAbiK – Y44F – 8 GAATTTTTAAATGAATTTAACTAATCTGTCGAGAAAAAATCTTAATTATTAATGATAATAAAACGAAAGTT

pAbiK – Y44F – 10 GAATTTTTAAATGAATTTAACTAATCTGTCGAGAAAAAATCTTAATTATTAATGATAATAAAACGAAAGTT

Supplementary Figure 12 continued (3/7).

900
|

pAbiK – Y44F GACAAATTTCCCGTTTGTGATAAAATCGAGTAAATCGGATAATTTTTCTTTTTTAAAAATATTACTTCAACT

pAbiK – Y44F – 2 GACAAATTTCCCGTTTGTGATAAAATCGAGTAAATCGGATAATTTTTCTTTTTT–GAAAAATATTACTTCAACT

pAbiK – Y44F – 3 GACAAATTTCCCGTTTGTGATAAAATCGAGTAAATCGGATAATTTTTCTTTTTTAAAAATATTACTTCAACT

pAbiK – Y44F – 4 GACAAATTTCCCGTTTGTGATAAAATCGAGTAAATCGGATAATTTTTCTTTTTTAAAAATATTACTTCAACT

pAbiK – Y44F – 5 GACAAATTTCCCGTTTGTGATAAAATCGAGTAAATCGGATAATTTTTCTTTTTTAAAAATATTACTTCAACT

pAbiK – Y44F – 8 GACAAATTTCCCGTTTGTGATAAAATCGAGTAAATCGGATAATTTTTCTTTTTTAAAAATATTACTTCAACT

pAbiK – Y44F – 10 GACAAATTTCCCGTTTGTGATAAAATCGAGTAAATCGGATAATTTTTCTTTTTTAAAAATATTACTTCAACT

pAbiK – Y44F AATTCCAACGACAAGTGGATTAAAGAAATAAGCAATTTTATAGATTATTGTGTGAATGAAGAACATTTAGGG

pAbiK – Y44F – 2 AATTCCAACGACAAGTGGATTAAAGAAATAAGCAATTTTATAGATTATTGTGTGAATGAAGAACATTTAGGG

pAbiK – Y44F – 3 AATTCCAACGACAAGTGGATTAAAGAAATAAGCAATTTTATAGATTATTGTGTGAATGAAGAACATTTAGGG

pAbiK – Y44F – 4 AATTCCAACGACAAGTGGATTAAAGAAATAAGCAATTTTATAGATTATTGTGTGAATGAAGAACATTTAGGG

pAbiK – Y44F – 5 AATTCCAACGACAAGTGGATTAAAGAAATAAGCAATTTTATAGATTATTGTGTGAATGAAGAACATTTAGGG

pAbiK – Y44F – 8 AATTCCAACGACAAGTGGATTAAAGAAATAAGCAATTTTATAGATTATTGTGTGAATGAAGAACATTTAGGG

pAbiK – Y44F – 10 AATTCCAACGACAAGTGGATTAAAGAAATAAGCAATTTTATAGATTATTGTGTGAATGAAGAACATTTAGGG

1000
|

pAbiK – Y44F AATAAGGGAGCTATAAAATGATTTTTCCCGTTATAACAAATACATTGAAACAAAAAAAAGTAGATACTAAA

pAbiK – Y44F – 2 AATAAGGGAGCTATAAAATGATTTTTCCCGTTATAACAAATACATTGAAACAAAAAAA–GTAGATACTAAA

pAbiK – Y44F – 3 AATAAGGGAGCTATAAAATGATTTTTCCCGTTATAACAAATACATTGAAACAAAAAAAAGTAGATACTAAA

pAbiK – Y44F – 4 AATAAGGGAGCTATAAAATGATTTTTCCCGTTATAACAAATACATTGAAACAAAAAAA–GTAGATACTAAA

pAbiK – Y44F – 5 AATAAGGGAGCTATAAAATGATTTTTCCCGTTATAACAAATACATTGAAACAAAAAAAAGTAGATACTAAA

pAbiK – Y44F – 8 AATAAGGGAGCTATAAAATGATTTTTCCCGTTATAACAAATACATTGAAACAAAAAAAAGTAGATACTAAA

pAbiK – Y44F – 10 AATAAGGGAGCTATAAAATGATTTTTCCCGTTATAACAAATACATTGAAACAAAAAAAAGTAGATACTAAA

1100
|

pAbiK – Y44F AATATAGACAATATCTTTTCGAAAAGAAACATGGTTACCAATTTTAATGTTTTCGAAAAAATATTAGATTTA

pAbiK – Y44F – 2 AATATAGACAATATCTTTTCGAAAAGAAACATGGTTACCAATTTTAATGTTTTCGAAAAAATATTAGATTTA

pAbiK – Y44F – 3 AATATAGACAATATCTTTTCGAAAAGAAACATGGTTACCAATTTTAATGTTTTCGAAAAAATATTAGATTTA

pAbiK – Y44F – 4 AATATAGACAATATCTTTTCGAAAAGAAACATGGTTACCAATTTTAATGTTTTCGAAAAAATATTAGATTTA

pAbiK – Y44F – 5 AATATAGACAATATCTTTTCGAAAAGAAACATGGTTACCAATTTTAATGTTTTCGAAAAAATATTAGATTTA

pAbiK – Y44F – 8 AATATAGACAATATCTTTTCGAAAAGAAACATGGTTACCAATTTTAATGTTTTCGAAAAAATATTAGATTTA

pAbiK – Y44F – 10 AATATAGACAATATCTTTTCGAAAAGAAACATGGTTACCAATTTTAATGTTTTCGAAAAAATATTAGATTTA

Supplementary Figure 12 continued (4/7).

1200
|

pAbiK – Y44F TCATTAAAAGATTCAAGATTAACTAATAAGTTTTTGACTTTCCTTGAAAAATATTAATGAATTTGGATTTTCA

pAbiK – Y44F – 2 TCATTAAAAGATTCAAGATTAACTAATAAGTTTTTGACTTTCCTTGAAAAATATTAATGAATTTGGATTTTCA

pAbiK – Y44F – 3 TCATTAAAAGATTCAAGATTAACTAATAAGTTTTTGACTTTCCTTGAAAAATATTAATGAATTTGGATTTTCA

pAbiK – Y44F – 4 TCATTAAAAGATTCAAGATTAACTAATAAGTTTTTGACTTTCCTTGAAAAATATTAATGAATTTGGATTTTCA

pAbiK – Y44F – 5 TCATTAAAAGATTCAAGATTAACTAATAAGTTTTTGACTTTCCTTGAAAAATATTAATGAATTTGGATTTTCA

pAbiK – Y44F – 8 TCATTAAAAGATTCAAGATTAACTAATAAGTTTTTGACTTTCCTTGAAAAATATTAATGAATTTGGATTTTCA

pAbiK – Y44F – 10 TCATTAAAAGATTCAAGATTAACTAATAAGTTTTTGACTTTCCTTGAAAAATATTAATGAATTTGGATTTTCA

pAbiK – Y44F AGTTTATCAGCTTCAAATATTGTAAAAAATATTTTAGTAATAATTCAAAGGGCTTAAAAGAAAAAATAGAC

pAbiK – Y44F – 2 AGTTTATCAGCTTCAAATATTGTAAAAAATATTTTAGTAATAATTCAAAGGGCTTAAAAGAAAAAATAGAC

pAbiK – Y44F – 3 AGTTTATCAGCTTCAAATATTGTAAAAAATATTTTAGTAATAATTCAAAGGGCTTAAAAGAAAAAATAGAC

pAbiK – Y44F – 4 AGTTTATCAGCTTCAAATATTGTAAAAAATATTTTAGTAATAATTCAAAGGGCTTAAAAGAAAAAATAGAC

pAbiK – Y44F – 5 AGTTTATCAGCTTCAAATATTGTAAAAAATATTTTAGTAATAATTCAAAGGGCTTAAAAGAAAAAATAGAC

pAbiK – Y44F – 8 AGTTTATCAGCTTCAAATATTGT-----

pAbiK – Y44F – 10 AGTTTATCAGCTTCAAATATTGTAAAAAATATTTTAGTAATAATTCAAAGGGCTTAAAAGAAAAAATAGAC

1300
|

pAbiK – Y44F CACTATCGTAAAAATAATTTTAATCAAGAATTATATCAAATATTGTTGTATATGGTTGCTTTGAAATAGAT

pAbiK – Y44F – 2 CACTATCGTAAAAATAATTTTAATCAAGAATTATATCAAATATTGTTGTATATGGTTGCTTTGAAATAGAT

pAbiK – Y44F – 3 CACTATCGTAAAAATAATTTTAATCAAGAATTATATCAAATATTGTTGTATATGGTTGCTTTGAAATAGAT

pAbiK – Y44F – 4 CACTATCGTAAAAATAATTTTAATCAAGAATTATATCAAATATTGTTGTATATGGTTGCTTTGAAATAGAT

pAbiK – Y44F – 5 CACTATCGTAAAAATAATTTTAATCAAGAATTATATCAAATATTGTTGTATATGGTTGCTTTGAAATAGAT

pAbiK – Y44F – 8 -----TGTATATGGTTGCTTTGAAATAGAT

pAbiK – Y44F – 10 CACTATCGTAAAAATAATTTTAATCAAGAATTATATCAAATATTGTTGTATATGGTTGCTTTGAAATAGAT

1400
|

pAbiK – Y44F GATTTATTAAATCAAGAAGAATTACTAAACTTAATTGATTTAAATATTGATGATTATTCTTTAATTTTAGGG

pAbiK – Y44F – 2 GATTTATTAAATCAAGAAGAATTACTAAACTTAATTGATTTAAATATTGATGATTATTCTTTAATTTTAGGG

pAbiK – Y44F – 3 GATTTATTAAATCAAGAAGAATTACTAAACTTAATTGATTTAAATATTGATGATTATTCTTTAATTTTAGGG

pAbiK – Y44F – 4 GATTTATTAAATCAAGAAGAATTACTAAACTTAATTGATTTAAATATTGATGATTATTCTTTAATTTTAGGG

pAbiK – Y44F – 5 GATTTATTAAATCAAGAAGAATTACTAAACTTAATTGATTTAAATATTGATGATTATTCTTTAATTTTAGGG

pAbiK – Y44F – 8 GATTTATTAAATCAAGAAGAATTACTAAACTTAATTGATTTAAATATTGATGATTATTCTTTAATTTTAGGG

pAbiK – Y44F – 10 GATTTATTAAATCAAGAAGAATTACTAAACTTAATTGATTTAAATATTGATGATTATTCTTTAATTTTAGGG

Supplementary Figure 12 continued (5/7).

1500
|

pAbiK – Y44F ACGATTTTATACCTAAAGAATAGTTCATATAAATTGGAAAAATTATTAATAAAAAATAGATCAATTATTTATT

pAbiK – Y44F – 2 ACGATTTTATACCTAAAGAATAGTTCATATAAATTGGAAAAATTATTAATAAAAAATAGATCAATTATTTATT

pAbiK – Y44F – 3 ACGATTTTATACCTAAAGAATAGTTCATATAAATTGGAAAAATTATTAATAAAAAATAGATCAATTATTTATT

pAbiK – Y44F – 4 ACGATTTTATACCTAAAGAATAGTTCATATAAATTGGAAAAATTATTAATAAAAAATAGATCAATTATTTATT

pAbiK – Y44F – 5 ACGATTTTATACCTAAAGAATAGTTCATATAAATTGGAAAAATTATTAATAAAAAATAGATCAATTATTTATT

pAbiK – Y44F – 8 ACGATTTTATACCTAAAGAATAGTTCATATAAATTGGAAAAATTATTAATAAAAAATAGATCAATTATTTATT

pAbiK – Y44F – 10 ACGATTTTATACCTAAAGAATAGTTCATATAAATTGGAAAAATTATTAATAAAAAATAGATCAATTATTTATT

pAbiK – Y44F AATACTCATGCCAACTACGACGTTAAAACCTTCTCGTATGGCAGAAAAATTATGGCTATTTTCGTTATTTCTTT

pAbiK – Y44F – 2 AATACTCATGCCAACTACGACGTTAAAACCTTCTCGTATGGCAGAAAAATTATGGCTATTTTCGTTATTTCTTT
ACGTTAAAACCTTCTCG

pAbiK – Y44F – 3 AATACTCATGCCAACTACGACGTTAAAACCTTCTCGTATGGCAGAAAAATTATGGCTATTTTCGTTATTTCTTT

pAbiK – Y44F – 4 AATACTCATGCCAACTACGACGTTAAAACCTTCTCGTATGGCAGAAAAATTATGGCTATTTTCGTTATTTCTTT

pAbiK – Y44F – 5 AATACTCATGCCAACTACGACGTTAAAACCTTCTCGTATGGCAGAAAAATTATGGCTATTTTCGTTATTTCTTT

pAbiK – Y44F – 8 AATACTCATGCCAACTACGACGTTAAAACCTTCTCGTATGGCAGAAAAATTATGGCTATTTTCGTTATTTCTTT

pAbiK – Y44F – 10 AATACTCATGCCAACTACGACGTTAAAACCTTCTCGTATGGCAGAAAAATTATGGCTATTTTCGTTATTTCTTT

1600
|

pAbiK – Y44F TATTTTTTAAATTGTAAGAATATTTTTAGTCAAAAAGAGATAAATAGTTATTGTCAATCTCAAAACTATAAT

pAbiK – Y44F – 2 TATTTTTTAAATTGTAAGAATATTTTTAGTCAAAAAGAGATAAATAGTTATTGTCAATCTCAAAACTATAAT

pAbiK – Y44F – 3 TATTTTTTAAATTGTAAGAATATTTTTAGTCAAAAAGAGATAAATAGTTATTGTCAATCTCAAAACTATAAT

pAbiK – Y44F – 4 TATTTTTTAAATTGTAAGAATATTTTTAGTCAAAAAGAGATAAATAGTTATTGTCAATCTCAAAACTATAAT

pAbiK – Y44F – 5 TATTTTTTAAATTGTAAGAATATTTTTAGTCAAAAAGAGATAAATAGTTATTGTCAATCTCAAAACTATAAT

pAbiK – Y44F – 8 TATTTTTTAAATTGTAAGAATATTTTTAGTCAAAAAGAGATAAATAGTTATTGTCAATCTCAAAACTATAAT

pAbiK – Y44F – 10 TATTTTTTAAATTGTAAGAATATTTTTAGTCAAAAAGAGATAAATAGTTATTGTCAATCTCAAAACTATAAT

1700
|

pAbiK – Y44F TCAGGACAGAACGGATATCAAACAGAACCTTAATTGGAATTATATTTAAAGGTC AAGGGAAGGATCTTAGAGCG

pAbiK – Y44F – 2 TCAGGACAGAACGGATATCAAACAGAACCTTAATTGGAATTATATTTAAAGGTC AAGGGAAGGATCTTAGAGCG

pAbiK – Y44F – 3 TCAGGACAGAACGGATATCAAACAGAACCTTAATTGGAATTATATTTAAAGGTC AAGGGAAGGATCTTAGAGCG

pAbiK – Y44F – 4 TCAGGACAGAACGGATATCAAACAGAACCTTAATTGGAATTATATTTAAAGGTC AAGGGAAGGATCTTAGAGCG

pAbiK – Y44F – 5 TCAGGACAGAACGGATATCAAACAGAACCTTAATTGGAATTATATTTAAAGGTC AAGGGAAGGATCTTAGAGCG

pAbiK – Y44F – 8 TCAGGACAGAACGGATATCAAACAGAACCTTAATTGGAATTATATTTAAAGGTC AAGGGAAGGATCTTAGAGCG

pAbiK – Y44F – 10 TCAGGACAGAACGGATATCAAACAGAACCTTAATTGGAATTATATTTAAAGGTC AAGGGAAGGATCTTAGAGCG

Supplementary Figure 12 continued (6/7).

pAbiK – Y44F AATAACTTTTTAATGAATTGATAGTAAAAGAAAGTTTGGTTAATTTCTTGTGGTGAGAACGAAGATTTCAA

pAbiK – Y44F – 2 AATAACTTTTTAATGAATTGATAGTAAAAGAAAGTTTGGTTAATTTCTTGTGGTGAGAACGAAGATTTCAA

pAbiK – Y44F – 3 AATAACTTTTTAATGAATTGATAGTAAAAGAAAGTTTGGTTAATTTCTTGTGGTGAGAACGAAGATTTCAA

pAbiK – Y44F – 4 AATAACTTTTTAATGAATTGATAGTAAAAGAAAGTTTGGTTAATTTCTTGTGGTGAGAACGAAGATTTCAA

pAbiK – Y44F – 5 AATAACTTTTTAATGAATTGATAGTAAAAGAAAGTTTGGTTAATTTCTTGTGGTGAGAACGAAGATTTCAA

pAbiK – Y44F – 8 AATAACTTTTTAATGAATTGATAGTAAAAGAAAGTTTGGTTAATTTCTTGTGGTGAGAACGAAGATTTCAA

pAbiK – Y44F – 10 AATAACTTTTTAATGAATTGATAGTAAAAGAAAGTTTGGTTAATTTCTTGTGGTGAGAACGAAGATTTCAA

Stop



pAbiK – Y44F TATTTAAATTGATAAGTATTTGAAATCTATTATTAGTTCCTGAAAAATAGCTGTGTCTTGTCAATATAAAT

pAbiK – Y44F – 2 TATTTAAATTGATAAGTATTTGAAATCTATTATTAGTTCCTGAAAAATAGCTGTGTCTTGTCAATATAAAT

pAbiK – Y44F – 3 TATTTAAATTGATAAGTATTTGAAATCTATTATTAGTTCCTGAAAAATAGCTGTGTCTTGTCAATATAAAT

pAbiK – Y44F – 4 TATTTAAATTGATAAGTATTTGAAATCTATTATTAGTTCCTGAAAAATAGCTGTGTCTTGTCAATATAAAT

pAbiK – Y44F – 5 TATTTAAATTGATAAGTATTTGAAATCTATTATTAGTTCCTGAAAAATAGCTGTGTCTTGTCAATATAAAT

pAbiK – Y44F – 8 TATTTAAATTGATAAGTATTTGAAATCTATTATTAGTTCCTGAAAAATAGCTGTGTCTTGTCAATATAAAT

pAbiK – Y44F – 10 TATTTAAATTGATAAGTATTTGAAATCTATTATTAGTTCCTGAAAAATAGCTGTGTCTTGTCAATATAAAT

Supplementary Figure 12 continued (7/7).

Appendix C: Reuse Permissions

Permissions for Figure 1-8:

[Nucleic Acids Res.](#) 2011 Sep; 39(17): 7620–7629.
Published online 2011 Jun 15. doi: [10.1093/nar/gkr397](https://doi.org/10.1093/nar/gkr397)

PMCID: PMC3177184
PMID: [21676997](https://pubmed.ncbi.nlm.nih.gov/21676997/)

A reverse transcriptase-related protein mediates phage resistance and polymerizes untemplated DNA *in vitro*

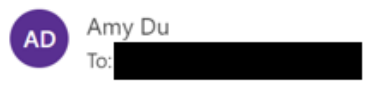
[Chen Wang](#),¹ [Manuela Villion](#),² [Cameron Semper](#),¹ [Colin Coros](#),¹ [Sylvain Moineau](#),^{2,3} and [Steven Zimmerly](#),^{1,*}

► [Author information](#) ► [Article notes](#) ▼ [Copyright and License information](#) [Disclaimer](#)

[Copyright](#) © The Author(s) 2011. Published by Oxford University Press.

This is an Open Access article distributed under the terms of the Creative Commons Attribution Non-Commercial License (<http://creativecommons.org/licenses/by-nc/3.0/>), which permits unrestricted non-commercial use, distribution, and reproduction in any medium, provided the original work is properly cited.

Permissions for Figure 4-1:


 AD Amy Du
To: [REDACTED] Thu 2023-05-18 12:51 PM

Hello Bahar,

According to the copyright guidelines of the University of Calgary, I need your approval to use one of the figures (Figure 3.2.3) from your thesis "[AbiK: A Novel Polymerase That Confers Resistance to Phage Infection](#)" in my thesis.

Please reply to the email with acknowledgement and permission if you agree. Let me know if you have any questions.

Thank you,
Amy Du

 BS Bahar Soufi [REDACTED]
To: Amy Du Thu 2023-05-18 1:03 PM

[△EXTERNAL]

Hi Amy,

Thank you for reaching out to me.

You have my permission to use this figure on your thesis.

Kind Regards,
Bahar Soufi

Permissions for Figure 4-18:



This is a License Agreement between Amy Du ("User") and Copyright Clearance Center, Inc. ("CCC") on behalf of the Rightsholder identified in the order details below. The license consists of the order details, the Marketplace Permissions General Terms and Conditions below, and any Rightsholder Terms and Conditions which are included below. All payments must be made in full to CCC in accordance with the Marketplace Permissions General Terms and Conditions below.

Order Date	17-May-2023	Type of Use	Republish in a thesis/dissertation
Order License ID	1356176-1	Publisher	BLACKWELL PUBLISHING LTD.
ISSN	0950-382X	Portion	Image/photo/illustration

LICENSED CONTENT

Publication Title	Molecular microbiology	Rightsholder	John Wiley & Sons - Books
Article Title	Lactococcal phage p2 ORF35-Sak3 is an ATPase involved in DNA recombination and AbiK mechanism.	Publication Type	Journal
Author/Editor	INTERNATIONAL UNION OF MICROBIOLOGICAL SOCIETIES.	Start Page	102
Date	01/01/1987	End Page	116
Language	English	Issue	1
Country	United Kingdom of Great Britain and Northern Ireland	Volume	80

REQUEST DETAILS

Portion Type	Image/photo/illustration	Distribution	Canada
Number of Images / Photos / Illustrations	1	Translation	Original language of publication
Format (select all that apply)	Print, Electronic	Copies for the Disabled?	Yes
Who Will Republish the Content?	Academic institution	Minor Editing Privileges?	Yes
Duration of Use	Life of current edition	Incidental Promotional Use?	No
Lifetime Unit Quantity	Up to 499	Currency	CAD
Rights Requested	Main product		

NEW WORK DETAILS

Title	The Virus Resistance Mechanism of Abortive Infection K in Lactococcus lactis	Institution Name	University of Calgary
Instructor Name	Michael Hynes	Expected Presentation Date	2023-05-24

ADDITIONAL DETAILS

The Requesting Person/Organization to Appear on the License	Amy Du
---	--------

REQUESTED CONTENT DETAILS

Title, Description or Numeric Reference of the Portion(s)	Figure 3C	Title of the Article/Chapter the Portion Is From	Lactococcal phage p2 ORF35-Sak3 is an ATPase involved in DNA recombination and AbiK mechanism.
Editor of Portion(s)	Scaltriti, Erika; Launay, H?l?ne; Genois, Marie?Michelle; Bron, Patrick; Rivetti, Claudio; Grolli, Stefano; Ploquin, Mickael; Campanacci, Val?rie; Tegoni, Mariella; Cambillau, Christian; Moineau, Sylvain; Masson, Jean?Yves	Author of Portion(s)	Scaltriti, Erika; Launay, H?l?ne; Genois, Marie?Michelle; Bron, Patrick; Rivetti, Claudio; Grolli, Stefano; Ploquin, Mickael; Campanacci, Val?rie; Tegoni, Mariella; Cambillau, Christian; Moineau, Sylvain; Masson, Jean?Yves
Volume of Serial or Monograph	80	Publication Date of Portion	2011-03-31
Page or Page Range of Portion	102-116		

RIGHTSHOLDER TERMS AND CONDITIONS

No right, license or interest to any trademark, trade name, service mark or other branding ("Marks") of WILEY or its licensors is granted hereunder, and you agree that you shall not assert any such right, license or interest with respect thereto. You may not alter, remove or suppress in any manner any copyright, trademark or other notices displayed by the Wiley material. This Agreement will be void if the Type of Use, Format, Circulation, or Requestor Type was misrepresented during the licensing process. In no instance may the total amount of Wiley Materials used in any Main Product, Compilation or Collective work comprise more than 5% (if figures/tables) or 15% (if full articles/chapters) of the (entirety of the) Main Product. Compilation or Collective Work. Some titles may be available under an Open Access license. It is the Licensors' responsibility to identify the type of Open Access license on which the requested material was published, and comply fully with the terms of that license for the type of use specified Further details can be found on Wiley Online Library <http://olabout.wiley.com/WileyCDA/Section/id-410895.html>.